Biopharmaceutic Prediction of Oral Absorption from Immediate Release Dosage Forms

Dissertation

zur Erlangung des Grades

„Doktor der Naturwissenschaften“

im Promotionsfach Pharmazie

am Fachbereich Chemie, Pharmazie, Geographie und Geowissenschaften

der Johannes Gutenberg-Universität Mainz

Mauricio Andrés García Alcalde

geb. in Santiago, Chile

Mainz, den 19.05.2022

Dekanin: Univ.-Prof. Dr. Tanja Schirmeister

1. Berichterstatter: Univ.-Prof. Dr. Peter Langguth

2. Berichterstatter: PD Dr. Thomas Nawroth

Tag der mündlichen Prüfung: 20.06.22

ABSTRACT

Characterization of the efficacy and safety of pharmaceuticals is typically carried out by the pharmaceutical industry through assessment of pharmacokinetics in clinical trials performed in humans. However, outcomes of those studies do not depend only on the active pharmaceutical ingredient (API) but also on the whole pharmaceutical product. Therefore, even though two different products contain the same API at the same dose in the same dosage form, they may still showcase different efficacy/safety profiles. This situation can even occur after post-approval changes in the manufacturing/formulation of the same product. Considering the infeasibility of performing clinical trials every time a new formulation needs to be tested, the development of surrogate *in vitro* and *in silico* biopredictive methods becomes increasingly relevant. The aim of this dissertation is to discuss the development and implementation of biopharmaceutic methods to predict oral drug absorption from immediate release (IR) dosage forms.

Carbamazepine (neutral) and ibuprofen (weak acid) were used as model drugs of the biopharmaceutic classification system (BCS) class II (highly permeable and poorly soluble), while acyclovir served as an example of the BCS class III (poorly permeable and highly soluble). Regarding carbamazepine, a high level of agreement between *in vivo* observations and the dissolution of tablets under compendial dissolution conditions (900 ml, 1% sodium lauryl sulfate media, apparatus II, 50 rpm) was found, as shown in Publication 1. For the second case, a biopredictive *in vitro* dissolution methodology for two ibuprofen suspensions was developed using bicarbonate buffer at physiological concentrations and compared to their *in vivo* equivalent dissolution. Moreover, the concept of surface pH and mechanistic mass transfer analysis were employed to successfully develop a surrogate media utilizing phosphate buffer (Publication 2). Conversely, for a BCS class III drug, as acyclovir, the pharmacokinetic profiles in subjects are determined by the permeability rather than the solubility in gastrointestinal fluids. The effect of the excipient chitosan on acyclovir permeability was better predicted by mucus-secreting *ex-vivo* models, such as rat jejunum mounted on an Ussing-chamber set-up (Publication 3). Furthermore, the variability in acyclovir oral pharmacokinetics seems to rely on physiological variables rather than formulation aspects related to tablet dissolution. In fact, the input of the *in vitro* dissolution of acyclovir tablets into a physiologically-based pharmacokinetic (PBPK) model resulted in the correct prediction of their bioequivalence, in spite of their different dissolution rates (Publication 4).

In conclusion, biopharmaceutic prediction of oral absorption is possible for IR dosage forms, provided the surrogate methodology is rationally selected. The consideration of both the drug's physical-chemical parameters and the interaction between the pharmaceuticals and gastrointestinal contents are critical. The implementation of predictive surrogate methods in the pharmaceutical industry, as well as their acceptance from regulatory agencies, may result in the acceleration of drug development, while also reducing the number of clinical trials.

ZUSAMMENFASSUNG

Die Charakterisierung der Wirksamkeit und Sicherheit von Pharmazeutika wird in der pharmazeutischen Industrie üblicherweise durch Erhebung pharmakokinetischer Daten in klinischen Studien im Menschen durchgeführt. Das Ergebnis dieser Studien hängt dabei nicht nur von dem untersuchten Wirkstoff alleine ab, sondern vor allem von dem eingesetzten pharmazeutischen Produkt. Daher kann es dazu kommen, dass zwei Produkte, die den identischen Wirkstoff enthalten, unterschiedliche Wirksamkeits- und Sicherheitsprofile aufweisen. Basierend auf der Annahme, dass die erneute Durchführung klinischer Studien bei geringfügigen Änderungen in der Formulierung oder im Herstellprozess dasselbe Produkt nicht praktikabel ist, zeigt, dass die Entwicklung bio-prädiktiver Surrogat in vivo und in silico Methoden von zunehmender Bedeutung ist. Zier dieser Dissertation ist es, die Entwicklung und Etablierung biopharmazeutischer Methoden für die Voraussage der oralen Resorption aus schnellfreisetzenden Formen (immediate release, IR) zu diskutieren.

Carbamazepin (neutral) und Ibuprofen (schwache Säuere) wurden dabei als Modellsubstanzen des biopharmazeutischen Klassifikationssystems (BCS) Klasse II (hochpermeabel und schwerlöslich) ausgewählt. Aciclovir dient als Beispiel für eine Substanz der BCS Klasse III (schlecht permeabel, hochlöslich). Für Carbamazepin wurde eine gute Übereinstimmung zwischen den in vivo beobachteten Parametern und den nach Arzneibuchbedingungen durchgeführten Freisetzungsversuchen aus den Tabletten (900 ml, 1% Natriumdodecylsulfat Medium, Apparatur II, 50 rpm), wie in Publikation 1 gezeigt, gefunden. Für Iburpofen wurde eine bioprädiktive in vitro Freisetzungsmethode unter Verwendung eines physiologischen Bicarbonatpuffersystems entwickelt. Dabei wurde das Freisetzungsverhalten von zwei Ibuprofen Suspensionen in vitro unter Verwendung der entwickelten Methode mit dem Freisetzungsverhalten in vivo verglichen. Außerdem wurde das Konzept des Oberflächen pH-Werts und der mechanistischen Massentransferanalyse angewendet um ein Phosphat-Surrogatpuffersystem zu entwickeln (Publikation 2). Für die BCS Klasse III Substanz Aciclovir ist die Permeabilität der entscheidende Faktor, der das pharmakokinetische Profil der Substanz in vivo bestimmt. Die Löslichkeit in den Medien des Gastrointestinaltrakts spielt hierbei eine untergeordnete Rolle. Der Effekt von Chitosan auf die Permeabilität von Aciclovir konnte mithilfe eines ex-vivo Mukussekretionsmodells vorausgesagt werden. Dabei wurde Ratten Jejunum auf einem Ussing-Kammer Setup fixiert (Publikation 3). Darüber hinaus konnte gezeigt werden, dass die physiologische Variabilität einen größeren Einfluss auf das pharmakokinetische Profil von Aciclovir hat, als die Freisetzungsgeschwindigkeit von Aciclovir aus den unterschiedlichen Tablettenformulierungen. Das Einsetzen von Eingangsvariablen aus den Freisetzungsdaten von Aciclovir Tabletten in ein physiologisch-basiertes pharmakokinetisches (PBPK) Modell resultierte in der korrekten Voraussage der Bioäquivalenz, trotz unterschiedlicher Freisetzungsgeschwindigkeiten in vitro (Publikation 4).

Zusammenfassend kann festgehalten werden, dass die biopharmazeutische Voraussage der oralen Absorption von IR Darreichungsformen möglich ist, wenn die Surrogat Methode rational ausgewählt wird. Dabei müssen sowohl die physikochemischen Parameter des Wirkstoffs als auch die Interkation zwischen den Pharmazeutika und den Inhaltsstoffen des Gastrointestinaltrakts berücksichtigt werden. Die Implementierung von Surrogat Methoden in der Pharmazeutischen Industrie, sowie deren

Akzeptanz von regulatorischen Behörden, könnte zu einer Beschleunigung der Arzneimittelentwicklung beitragen und gleichzeitig die Anzahl an klinischen Studien reduzieren.

TABLE OF CONTENTS

Chapter 1. Introduction

The development of oral drug products with intended systemic therapeutic effect demands the characterization of pharmacokinetics during early stages of development. This depiction is key to screen the likelihood of success for a given product. In these trials, healthy subjects are administered with the product and plasma samples are collected over time. And since formulation variables typically affect only the pre-systemic processes involving the drug, then the impact of those formulation variables on plasma concentration levels is a reliable indicator of their impact on the pharmacodynamic response. Therefore, these studies can be considered a good surrogate for assessing clinical efficacy and safety, as it allows the determination of drug concentrations in the bloodstream over time.

With the time and cost of these studies limiting the drug development process, [1,2] the improvement of *in vitro* and *in silico* tools capable to predict the outcomes of such a study is of major importance for pharmaceutical industry. Moreover, predictive methodologies may further reduce the number of clinical trials needed for a given product, because they can be used as screening tools before coming to pivotal studies.

In order to predict drug pharmacokinetics, it is critical to understand that drug concentrations in plasma are a consequence of the gastrointestinal (GI) absorption process. Hence, the understanding of biopharmaceutics is key to achieve accurate predictions. Biopharmaceutics has been defined as the “interdependence of biological aspects of the living organism (the patient) and the physical-chemical principles that govern the preparation and behavior of the medicinal agent or drug product”.[3] Therefore, the introduction section of this dissertation includes a detailed literature review on the state of the art for both gastrointestinal physiology and physical-chemical processes governing drug absorption, namely dissolution and permeation. The knowledge in these areas would form the basis to developing surrogate methodologies that successfully predict the absorption from immediate release (IR) solid oral dosage forms.

Considering their physical-chemical characteristics, drugs can be classified into four different classes according to their solubility and permeability features.[4] In this dissertation, four case studies are presented for drugs belonging to BCS classes II (high permeability/low solubility) and III (low permeability/high solubility). The results of this work consist of four peer-reviewed publications that the reader can find at the appendix section. Overall, this dissertation shows examples of biopharmaceutic predictive (biopredicitve) methods successfully developed. Further, the implications and opportunities attached to these findings are also discussed.

1. Bioavailability and bioequivalence

After oral administration, the drug must transit through the gastrointestinal tract where its absorption takes place prior to reaching the bloodstream (see sections below for details). Thereupon, the amount of drug that reaches the systemic circulation is subsequently eliminated by one or several mechanisms until all drug is eventually cleared from the system. The drug concentrations in plasma *versus* time profile can be plotted for a drug administered by the oral route. In this case, it is expected that drug levels in plasma initially rise, followed by a decrease at later times, as a consequence of drug elimination. In this regard, the concept of bioavailability was introduced to make reference to the drug biologically available to exert its pharmacological effect, i.e., drug that reached systemic circulation. According to the Food and Drug Administration (FDA) of the United States, bioavailability is defined as: "the rate and extent to which the active ingredient or active moiety is absorbed from a drug product and becomes available at the site of action".[5] From this definition, the area under the curve (AUC) becomes an important parameter as it represents the extent of absorption into the bloodstream. As such, the maximum concentration (C_{max}) is another relevant parameter, which additionally accounts for the rate of absorption.

Bioavailability studies are widely used not only for investigational new drugs, but also for the development of generic products. Although generics contain drugs with "known" efficacy and safety, these latter factors may differ from those initially reported for the original product. This will happen if differences in the formulation and/or manufacturing processes have an effect on the absorption of the drug. Thus, a comparative bioavailability study (bioequivalence study) is needed to assess potential discrepancies between plasma profiles generated by the original (reference) product and the generic (test). In case of absence of statistical differences between the reference and test products, the formulations are deemed bioequivalent, provided they share the same active compound, dose and dosage form. Furthermore, changes in bioavailability (and therefore in efficacy and safety) can also occur for products already in the market if raw materials, manufacturing equipment and/or processes are altered post-approval. Comparative bioavailability studies may also be required in this type of scenarios to verify that efficacy and safety remain the same.

Bioavailability studies in many cases require human healthy volunteers to be carried out. This means that ethical concerns are given considering all different scenarios where a bioavailability study might be required (bioequivalence, post-approval changes, testing of new formulations, batch-to-batch uniformity, assessing the effect of food on absorption, among many others). Furthermore, they are costly in terms of time and finances for pharmaceutical industry. Moreover, the possibility of an unsatisfactory result is always real, which may further increase the cost, time and number of subjects used for experimentation. The consequences of this

may impact not only the manufacturer, but also patients, whose access to efficacious and safe medicines is disrupted. In this scenario, the development of predictive surrogate methodologies may provide a solution in order to reduce the monetary and time costs related to pharmacokinetic trials, as well as, to reduce the number of in-human studies. Therefore, there is a need for developing/improving the state of the art with respect to surrogate tools for *in vivo* testing. In this manner, the number of bioavailability studies can be decreased to a minimum or even waived, if scientifically justified. Furthermore, surrogate methodologies with high predictive power can be used in early stages of development to screen the most promising formulations with higher probabilities of succeeding in bioavailability trials.

2. The oral route of administration

2.1 Common oral dosage forms

The word “drug” is often utilized in everyday life to make reference to any sort of medicine. However, the administration of a therapeutic agent needs for a vehicle (dosage form), such that the drug, also called active pharmaceutical ingredient (API), is carried by the dosage form to the site of absorption or targeted tissue. Oral solutions are the simplest dosage form to enable oral drug administration. In this dosage form, the API is dissolved in a proper solvent (typically water). Inactive pharmaceutical ingredients (excipients) can be added to this formulation in order to improve, for instance, drug solubilization, stability or ease of administration. As for less water-soluble APIs, oral solution formulations may not be the first choice, since their manufacturing will be limited by the poor solubility of the drug solid material and the dose required. This issue may be overcome by formulating the product as a pharmaceutical suspension. According to European Pharmacopeia, this latter type of formulation is considered a liquid dosage form.[6] However, and unlike solutions, suspensions also contain a solid phase dispersed in the external liquid phase. Most of the amount of the poorly soluble API is contained in the dispersed particles, whereas a minor fraction of the dose is dissolved in the external phase at a concentration equal to drug solubility. Here, excipients, such as surfactant additives, are critical to decrease the internal energy of the system and stabilize the dispersion. Dispersed solid particles make the difference between solution and suspensions not only in terms of manufacturing, but also in their clinical performance. While all the amount of drug is immediately available to be absorbed in case of solutions, drug absorption from suspensions requires previous API dissolution. Hence, dissolution rate may affect not only drug absorption, but also plasma concentrations and, therefore, its pharmacological effects.

On the other hand, solid oral dosage forms are perhaps the most common among oral drug products. In fact, they are preferred by both users and physicians in many countries around

the world.[7,8] Moreover, the manufacturing process for solid dosage forms also displays several advantages, for instance longer drug stability, taste-masking, cost-effectiveness, large-scale production, as well as the possibility to control the release (e.g. through enteric coating). Unlike liquid dosage forms such as solutions or suspensions, the release from solid dosage forms involves disintegration as step prior to dissolution. In the case of immediate release (IR) dosage forms, the API is rapidly released upon disintegration of the vehicle. Hence, these dosage forms are preferred in cases when rapid therapeutic effect is desired (e.g., instantaneous pain relief, antiinflammation), whenever high plasma concentrations are needed, or for APIs with wide therapeutic range (e.g., some antibiotics/antivirals).[3] Typical examples of IR solid oral dosage forms encompass tablets, hard-shell capsules, granules, among many others. These types of dosage forms commonly use excipients, such as fillers, disintegrants, lubricants and binders. Even though excipients are “inactive” ingredients (due to the lack of intrinsic pharmacological activity), they might be able to impact the clinical performance of the therapeutic agent. The reason for that is the role they could play on the physico-chemical processes and interactions occurring in the gastrointestinal tract, such as disintegration, dissolution and/or absorption.[9] Similarly, manufacturing parameters could also have an impact on the final clinical outcome of the product (e.g. particle size effect on dissolution).[10] The basis for these interactions are explained in the following sections.

2.2 Physiology of the oral route

The oral route offers several advantages, such as non-invasiveness, patient compliance, convenience for repeated and prolonged use, safety, among others.[3] In spite of its convenience, this route of administration sometimes results in irregular, unpredictable and/or suboptimal clinical outcomes. As for two different products containing the same API in the same dosage form, at the same strength, potential differences in their clinical performance are most likely caused by pre-systemic events involving disintegration, dissolution and/or absorption. Hence, interactions between formulation variables and gastrointestinal (GI) features are key to understand and anticipate these differences. Accordingly, the development of predictive surrogate (*in vitro* and *in silico*) tests that account for relevant physiological aspects has captured the attention of pharmaceutical industry, regulatory agencies and academia. The importance of these tests lies on their potential to detect an early failure of the product in clinical trials, to understand unsatisfactory clinical outcomes in patients treated with an existing product and to rationally guide the (re)formulation of drug products (i.e., generics for which bioequivalence needs to be demonstrated). However, the success of these techniques relies on their ability to correctly simulate the critical physiological feature for that given product. In the following sections, the physiology of the oral route is described. Further,

it is important to consider that critical physiological conditions and luminal contents may change depending on the fasted/fed state of the subject. As for oral bioavailability/bioequivalence purposes, the performance of single dose trials under fasted conditions typically represents the most discriminative conditions. Hence, gastrointestinal physiology under fasted conditions is specially emphasized throughout this section.

i. Gastrointestinal transit

Gastric transit. Pharmaceutical products orally ingested follow the GI transit. Thus, the ingested material may undergo absorption into the systemic circulation, biotransformation (metabolism) and/or may be excreted with the feces. After being swallowed, the drug product reaches the stomach within few seconds.[11] The basal water of volume in fasted subjects has been determined between 25 and 45 ml by magnetic resonance imagining (MRI) techniques, which rapidly increases after drinking water.[12–14] Likewise, emptying of gastric water occurs relatively fast, with an apparent first-order emptying half-life of around 11 – 15 min.[13,15] Functionally, the stomach can be divided in three anatomical regions namely fundus, body (corpus) and antrum, from proximal to distal.[16] While the first two parts carry out storage functions, the antrum works as a mill for the ingested material.[17] The dynamics for gastric contents under fasted conditions depends on phases of the inter-digestive migrating motor complex (IMMC). Phase I is characterized by long periods (approx. 90 min) with reduced contractile activity.[18] During phase II (10 – 20 min), contractions become stronger, which has been evidenced by an increase in stomach pressures measured by high-resolution manometry.[19] Lastly, stomach contraction reaches the strongest peristaltic contractions under phase III (also known as housekeeping waves). This contractile phase lasts approximately 10 – 15 min and propagates from proximal to distal.[18] Gastric emptying into the duodenum requires materials to pass through the pyloric sphincter, which acts as a gastric sieve. Accordingly, the rapid gastric emptying of water and dissolved compounds would be a consequence of limited pyloric resistance to these fluids. Conversely, for non-digested solid materials (>1 mm), their gastric emptying may take place during phase III of the IMMC under fasted conditions.[18] Therefore, the gastric residence of pharmaceuticals under fasted conditions relies on their disintegration/dissolution in stomach fluids, as well as on the IMMC phase they are ingested. On the other hand, the IMMC pattern is disrupted upon food ingestion. Gastric emptying becomes slower under these conditions and the mechanical shear is increased.[20] This physiological change is beneficial for nutrition, since it provides the food with longer gastric times and larger fluid volumes to allow its digestion and dissolution in the stomach prior to nutrient absorption in the small bowel.[18] However, this alteration also exemplifies how fed conditions may reduce discrimination between two immediate release products. With gastric emptying being slower, the pre-absorptive time for dissolution becomes longer and clinical differences due to dissolution may be overlooked under these conditions.

Small intestinal transit. Luminal contents that leave the stomach reach the small intestine. From proximal to distal, the small bowel is divided into three segments, namely duodenum, jejunum and ileum. The duodenum receives fluids not only from the stomach, but also from pancreas and liver. These latter organs secrete pancreatic juice and bile, respectively, into the duodenum through the coledocus.[16] The duodenal segment ends at the duodenojejunal flexure, a bit distal to the the ligament of Treitz, around 25 to 30 cm after the pylorus.[21] Transit of material along the duodenum seems to be fast, as even large non-disintegratable tablets and capsules left the duodenum in less than 5 min.[11,18]

The jejunal segment is well-known for its pivotal role on nutrient absorption. The enhanced surface area in this region is key to favor the absorption process. Even though the intestine has been geometrically modeled as a cylinder, the luminal surface of the intestinal wall is not smooth.[22] Instead, it shows different folds that houses the villi and crypts. The villus is mainly formed by epithelial and goblet cells, while other types of differentiated and undifferentiated cells can be found in the bottom of crypts.[22] Furthermore, the surface of the luminal (apical) membrane of epithelial enterocytes is additionally folded due to microvilli, thus enhancing the intestinal surface. Currently, there is still a debate on the actual small intestinal effective area for permeation, although there is agreement that it may be several square meters (estimated between 32 – 140 m^2).[23,24] Moreover, epithelial cells at the jejunum level are joined by tight-junctions, which are Ca^{2+}-chelating proteins that keeps epithelial cells connected.[22] Accordingly, tight-junctions create inter-cellular (paracellular) pores that also contribute to absorption of small molecules. The jejuno-ileal segment is the longest portion of the small intestine, with a mean length of around 630 cm measured in *post-mortem* humans.[21] Likewise, transit in this segment is also longer than duodenal transit, such that total small intestine transit time (SITT) was in average 3.5±1.0 h.[25] The SITT seems to be very consistent, which can be evidenced by the relatively low variability compared to gastric residence. Furthermore, similar SITT were shown for different materials, including food, tablets, pellets and fluids.[26,27] Interestingly, transit through the small intestine was a discrete process that does not occur at constant velocity.[28] This may have to do with the different GI pressure patterns, and probably also with the discrete distribution of luminal water in several small pockets. The volume of water in the small intestine ranged from 43 to 105 ml,[13,14] suggesting that only a minor portion of the intestinal volume is filled with liquid water. Taken together, all these features maximize the absorption process in this segment.

ii. Luminal contents

Gastric Fluids. The contents in the stomach, as well as the physico-chemical characteristics of the gastric fluid strongly depend on the fasted/fed conditions and the type of food taken in.[29] Electrolyte concentrations of chloride, sodium, potassium and calcium, were 102, 68, 13.4 and

0.6 mM in aspirates of fasted gastric fluid.[30] This data is consistent with the reported ionic strength of 100 mM.[30] In addition, the stomach is well-known for its acidic environment. Parietal cells in the stomach wall secrete hydrochloric acid due to action of both the H^+/K^+ APTase and chloride channels. The mean gastric pH has been determined in different studies to range between 1.6 and 2.7,[15,31,32] such that hydrogen ion concentration is around 10 mM in stomach. However, large intra- and inter-subject pH variability has been observed in fasted conditions, with pH reaching values over 4.0 in some subjects.[29,33] Poor mixing of gastric fluid during resting phases of the IMMC and hypochlorhydria may be among the explanations for this large variability.[18,29]

Digestive enzymes are also secreted by gastric chief cells into the gastric lumen to support the disintegration/dissolution of food in acidic gastric fluids (chyme formation). The main protein secreted is the pepsinogen, which is activated into pepsin at acidic pH. This latter enzyme exhibits endopeptidase activity. Protein concentration in gastric aspirates under fasted conditions was quantified at 1.8 mg/ml, corresponding mainly to digestive enzymes.[29]

Both, the acidic nature of gastric fluids and digestive enzymes have the potential to damage the stomach wall. Protection is provided by mucus, a viscoelastic hydrophilic gel composed of 90 – 95% water, 2 – 5% mucin proteins and traces of lipids, proteins, DNA and electrolytes.[34] Its gel properties are mainly a consequence of the cross-linked and entangled network created by mucins. Chemically, mucins are high molecular weight (MW) glycoproteins containing high percentages of glycans (50 – 80% of MW) and non-glycosylated cysteine-rich domains.[35,36] Among their glycans, sialic acid is one of the most abundant, conferring the mucus with rather acidic properties, due to its low pKa of 2.6.[37] In this manner, the mucus layer slows acid diffusion, aiding continuously secreted bicarbonate to neutralize the protons and maintain microclimate at the epithelium surface.[38] Concentration of mucin in gastric mucus is around 20 mg/ml (2%),[39] while mucus layer thickness is 180 µm (among the thickest along the human gastrointestinal tract).[38,40]

Small intestinal contents.

Upon gastric emptying, the acidic gastric fluid is neutralized in the duodenum by action of the bicarbonate secreted with the bile and from Brunner's glands.[41] Moreover, constant bicarbonate supply is provided by epithelial cells through the highly expressed chloride-bicarbonate ($Cl^-/HCO3^-$) exchanger.[22,42,43] Bicarbonate concentrations in duodenum and jejunum were determined at 6.7 and 8.2 mM, respectively.[44,45] These values rise from proximal to distal small intestine, as bicarbonate concentration was measured to be 30 mM at the ileal level.[26,45] In the intestinal lumen, bicarbonate neutralizes hydrogen ions (H^+) forming carbonic acid, which is next dehydrated into carbon dioxide and water. Given the lipophilicity of carbon dioxide, this molecule rapidly permeates across epithelia and is excreted

through the breath.[46] Further insights on bicarbonate activity, chemistry and pharmaceutical implications can be found in Section 3.3 of the present chapter. As a consequence of bicarbonate buffering, proximal to distal luminal pH increases from around 6.8 in jejunum to 7.4 in ileum.[32,47] However, luminal pH drops after reaching the ascending colon as action of colonic microbiota. Metabolism of colonic bacteria generates high concentrations of short chain fatty acids (30 mM),[48] such as acetate, reducing bulk pH to approx. 6.5.[47] Buffer capacity of intestinal fluids was determined potentiometrically between 3.2 and 5.6 mmol/l/ΔpH in duodenal and jejunal fluids,[49] while it increased up to 21.4 mmol/l/ΔpH in ileum.[50] Nonetheless, enhanced buffer capacity under physiological conditions is expected, due to both the continuous bicarbonate secretion and rapid permeation of CO_2, the conjugate acid in bulk.[51]

In addition to bicarbonate, duodenal fluids are also supplemented with pancreatic and liver secretions to further support the digestion. On the one hand, bile salts are secreted from the gall bladder, through the coledocus, into the duodenal lumen. These compounds are surfactants that reduce the surface tension of small intestinal fluids to 32.3 mN/m.[29] Concentration of bile salts in fasted jejunum and distal duodenum have been determined, respectively, around 2.6 and 2.9 mM.[29,30] However, concentrations may be greater near the site of secretion, since concentrations of 4.3 – 6.4 mM have also been reported in duodenal fluid from fasted subjects. The main bile acids in small intestinal fluids are taurocholic and glycolic acids, accounting for 14 – 45 and 17 – 31% of total bile salts in small intestinal aspirates.[52,53] Owing to their surfactants properties, bile acids can form micelles with values for critical micelle concentration (CMC) ranging between 2.8 and 12 mM. Micellar aggregation and concentrations depend also on the chemical nature of the bile acid, ionic strength and presence of other amphipathic compounds, as lecithin. [52] Luminal micelles created by bile salts aid in the solubilization of fat-rich meals. Likewise, they can also enhance the solubility of poorly soluble drugs.[53,54] On the other hand, juice secreted from the pancreas further supports the digestion process. Pancreatic juices consist of a pool of enzymes including amylases, lipases and proteases.[26] Protein contents in the fasted duodenum and jejunum were measured at 3.1 and 2.1 mg/ml, respectively.[29,30] These luminal enzymes can also impact the performance of pharmaceuticals (stability, bioactivation and/or biodegradation).

Similar to gastric tissue, the intestinal wall is also covered by a mucus layer. At this level, covering mucus layer is thinner than stomach and it can be divided in two types of layers, namely tightly-attached and loosely- adhered. After being secreted by goblet cells, mucus can either form the former type of layer (by adhering to epithelial cells) or create the latter type (by continuous secretion).[40] Unlike the tightly-attached layer, the loose mucus is shed, following the intestinal transit, such that it works as a preventive mechanism for macromolecules to

reach the epithelium. Thus, the thickness of the loosely-adhered layer is regulated by continuous secretion, on one hand, and degradation/shedding, on the other. In turn, the tightly-attached mucus forms a viscoelastic pseudoplastic gel layer that poses an additional resistance to radial mass transport.[38,40]

3. Basis for drug absorption

3.1 Biopharmaceutic classification system

As mentioned earlier, small intestinal conditions are ideal for absorption of small compounds from the lumen into the systemic circulation. Mass transport analysis can be applied to this phenomenon to allow for a better understanding of this overall process. The radial mass transport that the drug undergoes during absorption can be modeled as a serial resistance process (Fig. 1.1). Solubilized drug in the lumen permeates, first, across an unstirred water layer from the bulk to the surface of the intestinal wall (intestinal epithelia). Next, a second mass transfer step takes place at the intestinal wall, where the drug permeates across the intestinal epithelia. From this theoretical analysis, it can be inferred that the reciprocate of total absorption rate is equal to the sum of reciprocates for the rate of mass transport across each of these two barriers, namely the boundary aqueous layer and epithelial wall.[4] Conversely, drug absorption from solid particles requires for a previous step. Their absorption may, then, be influenced by drug release/dissolution, which is ultimately a function of its solubility.

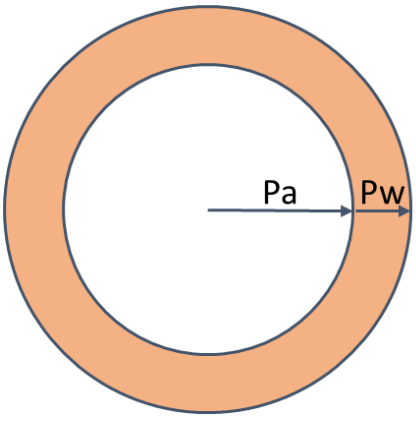

Figure 1.1. Scheme representing radial mass transport from intestinal lumen. Permeation through aqueous layer (Pa) and through intestinal wall (Pw) are processes disposed in series, meaning that the slowest step would limit the mass transport rate from the lumen (i.e., drug absorption). Adapted from reference [23].

With the small intestine offering the main time window for drug absorption (absorption window), the relevance of these two kinetic processes (aqueous and wall permeation, Pa and Pw, respectively) is greatest within the small intestinal residence time (around 3 h). Taking this into account, Amidon et al. [4] proposed three dimensionless numbers (absorption number, dose number and dissolution number, named An, Do and Dn, respectively) to identify the rate

limiting step upon oral drug absorption. Briefly, An was defined as the ratio of the residence to the absorption time, with this latter parameter being inversely proportional to the effective permeability (P_{eff}, cm/s). In turn, both Do and Dn are respectively known as dose and dissolution number, both of them refer to drug thermodynamic solubility (C_s, mg/ml).[4] Hence, a given API might be classified based on its permeability and solubility, according to the biopharmaceutics classification system (BCS, Table 1.1). This classification sheds light on predicting the oral absorption of such an API, as it is discussed below.

Table 1.1. Biopharmaceutics classification system (BCS), adapted from reference [4].

BCS class	Permeability	Solubility	Limiting step for absorption
I	High	High	Gastric emptying
II	High	Low	Drug dissolution and/or solubility
III	Low	High	Permeation across intestinal wall
IV	Low	Low	Difficult to predict (case-dependent)

To exemplify this, one might think about metoprolol, as a model BCS class I compound. For this drug, both the permeability and solubility are sufficiently high to be considered as rate limiting steps in its oral absorption. Hence, the rate and extent of metoprolol absorption only depend on the rate and extent of release from the dosage form. If metoprolol is formulated as immediate release solid oral dosage form (e.g., IR tablet) and it is rapidly released from the dosage form, its absorption rate relies exclusively on gastric emptying and the extent of absorption is expected to be 100% of the dose. This means that, if two different solid IR drug products contain qualitatively and quantitatively the same API and they exhibit rapidly similar release from the dosage form, they will display comparable bioavailability profiles and, hence, they will be most likely bioequivalent. This theoretical scenario becomes less straightforward for other BCS classes, as shown below.

The absorption of a BCS class II drug is limited by its solubility, which affects not only the Do, but also the Dn. Hence, unless the drug is extremely poorly soluble (Do>>>1), the rate and extent of absorption will be given by the intraluminal dissolution of the API. In this scenario, the drug-releasing character of the excipient composition (i.e., tablet disintegration) does not correlate with the absorption anymore, such that drug dissolution becomes the major limitation to intestinal absorption. Thus, manufacturing parameters with potential impact on *in vivo* dissolution (e.g., particle size) become relevant in this case. Further, *in vitro-in vivo* correlations (IVIVC) are expected for dosage forms containing this type of compounds. This means dissolution profiles in an *in vitro* experimental set-up may correlate to *in vivo* absorption and/or plasma profiles. However, the predictive power of *in vitro* dissolution methods may be limited if physiological aspects are not appropriately considered.

Given the physiological gradient of pH along the gastrointestinal tract, it is expected that class II compounds behave differently according to their acid-base properties. Therefore, three different sub-classes were suggested for BCS II compounds, where the BCS class IIa, IIb and IIc corresponded to poorly soluble weak acids, bases and neutral molecules, respectively.[55] This sub-classification may have regulatory consequences. For instance, the biowaiver of a BCS IIa (e.g. ibuprofen) may be theoretically possible, because of the pH shift upon reaching the small intestine to values above its pKa of 4.4,[56] which would increase the ionized fraction of ibuprofen. Its anionic form exhibits enhanced solubility, such that ibuprofen would theoretically behave as a “pseudo-BCS I”. However, bio-inequivalence has been observed for IR ibuprofen tablets as a consequence of non-discriminating *in vitro* tests.[57,58]

The BCS class III encompasses APIs whose absorption is limited by their permeation through the intestinal wall. If the permeation time is slower than the residence time within the absorption window (typically around 3 h for the small bowel), the An will be <1 and drug absorption will be incomplete. In absence of active carrier-mediated transport, drug passive permeability across intestinal mucosa follows Fickian diffusional kinetics and it depends on concentration gradient and drug diffusion through the intestinal epithelium (See section 3.4 for details). Similar to BCS I case, it can be expected that oral absorption is not affected by drug dissolution, provided the release is very fast.[4] However, class III compounds are more sensitive to little variations of intestinal permeability and/or the role of membrane transporters. These physiological factors may have an impact on the clinical performance and, thus, they may contribute to subject-to-subject variability. Consequently, the presence of any “inactive” ingredient in the formulation with potential effect on the residence time (e.g. polyols such as mannitol or sorbitol),[59] intestinal permeability (e.g. sodium lauryl sulfate or chitosan),[60,61] or carrier-mediated active transport (e.g. surfactants, such as polysorbates, PEO castor oil or macrogol derivatives),[62–64] may cause bio-inequivalence for pharmaceutical equivalents containing BCS III drugs. On the other hand, if drug dissolution is considerably slower than permeability, it is theoretically possible that *in vitro* release profiles correlates to *in vivo* observations, provided the absence of any critical excipient in the formulation.[65]

Finally, given their poor solubility and permeability, the intestinal absorption of the BCS class IV drugs is usually problematic and difficult to predict. This is because the rate limiting step to the absorption of these drugs is not obvious and cannot be generalized. Furthermore, low systemic exposure is expected for this BCS class. This explains why the proper selection of excipients and drug delivery system (e.g., complexation or nanoparticles) has become a growing research topic for formulating these molecules.[66]

3.2 BCS-based biowaivers

Regulatory agencies worldwide have used the BCS framework to make regulatory decisions in terms of waiving from clinical trials (biowaivers).[67,68] Biowaiver were implemented by the Food and Drug Administration (FDA) in the United States (US) in the early 2000s, and there upon followed by several agencies around the world. Recently, the international council for harmonization (ICH) issued the M09 guideline on biowaivers based on the biopharmaceutics classification system.[69] According to this guidance, IR solid oral dosage forms containing BCS class I and/or III are eligible for biowaivers. However, BCS classification is not the only requirement, since the drug products should also fulfill dissolution requirements related to the release of the drug. Dissolution experiment should be performed in pharmacopeial buffers at pH 1.2, 4.5, 6.8 and at the pH of the lowest solubility, if applies.[69] As for a BCS class I, the requirement is that ≥ 85% of the dose is dissolved ≤15 min (very rapid dissolution). Alternatively, drug product dissolution may be ≥ 85% of the dose in ≤30 min (rapid dissolution), provided that test product dissolution is similar to the reference. Dissolution similarity can be assessed by the calculation of the similarity factor (f_2), whose value becomes lower than 50 if the average difference between curves is higher than 10%.[70] By contrast, requirements for BCS class III APIs are stricter than for class I, due to their permeability limitations. Accordingly, biowaiver for BCS III drugs is only possible if products show very rapid dissolution. Likewise, the presence of critical excipients that may affect the absorption is of higher concern for class III, as well. Hence, excipients in test product should be qualitatively the same and quantitatively similar (less than 10%) to those in the reference formulation.[69]

3.3 Dissolution

i. General principles for dissolution

As previously mentioned, dissolution of small molecules is a critical attribute for predicting the performance *in vivo* of poorly soluble drugs (BCS II). Upon dissolution, solid material is transferred from solid to liquid phase. Molecules are dissolved in the liquid phase, forming a saturated solution at the solid surface. Drug concentration at this region is equal to the saturation solubility of the compound (C_s). At steady-state, the dissolved drug diffuses from the concentrated region near the solid surface to the bulk of the solution following the first Fick's law:

$$J = -D \frac{\partial C}{dx} \tag{1.1}$$

Where J is the flux (μmol/cm^2*s), D is the diffusivity constant (cm^2/s) and ∂C/dx is the driving force for the flux, which depends on the chemical gradient, ∂C (mM), and the position x (cm) across the diffusional pathway.[71] In dissolution, this latter distance is denoted as the

theoretical length between the solid surface and the bulk solution, also known as the stagnant diffusion layer or boundary layer (h). Meanwhile, the concentration gradient is consequence of the difference between the saturation concentration (C_s) near the solid surface and the concentration in the bulk (C), such that:

$$J = D\frac{(C_s - C)}{h} \tag{1.2}$$

Combining equation 1.1 and 1.2 (considering the surface area of the particle "A", in cm^2) and rearranging, the mass transport rate from the solid surface into the bulk (dM/dt, in µmol/s) across the diffusional layer is described as follows:

$$\frac{dM}{dt} = \frac{DA}{h}(C_s - C) \tag{1.3}$$

The equation 1.3 is also known as the Nernst-Brunner equation, which describes the overall dissolution rate.[72] The Figure 1.2 shows a schematic representation of the diffusional layer model.

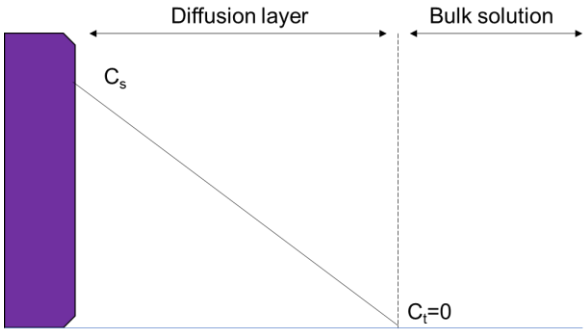

Figure 1.2. Schematic representation of the diffusional layer dissolution model at steady-state. Solid state API is represented in purple. Fickian diffusion takes place across the diffusion layer according to the concentration gradient. Adapted from reference [3].

ii. Dissolution of small ionizable molecules

Unlike neutral compounds, dissolution modeling for ionizable drugs demands the consideration of the acid-base reactions between drug and either water or buffering species present in the media.[73] A model that accounts for diffusional fluxes and chemical reactions of all species was deduced by Mooney et al. (Fig 1.3, panel A).[74] Given that chemical reactions are much faster than diffusional fluxes, the authors assumed that under steady-state conditions, acid-base reactions occur at any point within the diffusion layer, such that any equilibrium is reached instantaneously (much faster than diffusion of the chemical species).[74] The example in Fig 1.3, panel A, shows an acidic drug (HA, in purple) which is ionized into its more soluble anionic

form (A^-, green line) on the solid surface, as shown by the higher concentrations of this latter species.

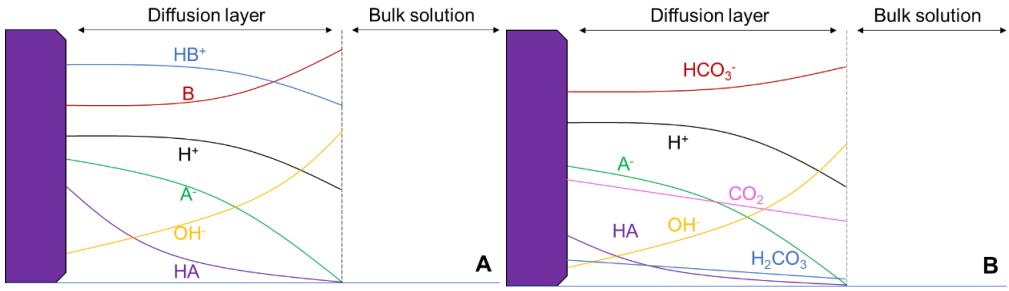

Figure 1.3. Schematic representation of species concentrations (y-axis) versus position (x-axis) proposed by Mooney et al. for conventional buffers (A) or Al-Gousous et al. for bicarbonate buffer (B). Solid state weak acid drug is shown in purple while color lines show theoretical species concentrations along the boundary layer under sink conditions. Models adapted from references [74,75].

The degree of ionization at the solid surface is dependent on the acidity (equilibrium) constant, Ka, according to the equilibrium shown in eqn 1.4.

$$HA \overset{Ka}{\rightleftharpoons} H^+ + A^- \tag{1.4}$$

In presence of a buffered media, the conjugate base species (B^-) will diffuse towards the solid following the concentration gradient (Fig. 1A, red line). As B^- is fluxing into the boundary layer, it reacts with the less soluble neutral form (HA), according the equilibrium in eqn 1.5.

$$HA + B^- \rightleftharpoons HB + A^- \tag{1.5}$$

Therefore, greater concentrations of A^- and H^+ are formed within the diffusion layer and near the solid surface for buffer containing media. Under sink conditions, this acid-base reaction boosts the concentration of the ionic species, hence increasing the chemical gradient across the diffusion layer.[74] Thus, this model implies that the higher the concentration of the buffer conjugate base, the faster the dissolution of acidic drugs. An additional consequence of this reaction is the higher formation of H^+ on the solid surface ($[H^+]_0$), which in turn may lower the surface pH (pH_0). Calculation of pH_0 is possible with this model by solving a triple polynomial equation derived from the mass transport and chemical reaction analysis. This equation was reported by Mooney and coauthors,[74] and it states that $[H^+]_0$ is a function of known parameters, involving diffusional rates for different species, acidity constants, buffer concentrations in the bulk and intrinsic solubility of the drug.[74] By knowing the value of $[H^+]_0$, it is possible to known not only the fraction of drug ionized at the surface, but also the calculation of the total drug flux (J_{drug}) under sink conditions across a diffusion layer with

thickness=h is possible. In this scenario, proton generation at the solid surface is equal to formation of ionized drug for a monoprotic acid, such that total drug flux is:

$$J_{drug} = -D_{HA}\frac{[HA]_0}{h}\left(1 + \frac{K_a}{[H^+]_0}\right) \quad (1.6)$$

Where the diffusion coefficient, D, is assumed to be the same for both ionized and deionized species. Similar to the term pH_0, sub-index makes reference to the position with 0 and h being the solid surface and the bulk, respectively, as shown in the fig 1.3.

The mentioned model can be applied to most of buffers. However, it does not capture the picture for the *in vivo* buffering species in intestinal fluid, i.e., bicarbonate. Unlike typical buffers, bicarbonate displays a unique equilibrium due to the subsequent dehydration of carbonic acid into carbon dioxide (eqn 1.7).

$$HCO_3^- + H^+ \underset{Ka}{\rightleftharpoons} H_2CO_3 \overset{Kd}{\underset{Kh}{\rightleftharpoons}} H_2O + CO_{2(aq)} \quad (1.7)$$

The apparent pKa (pKa_{app}) of bicarbonate has been potentiometrically determined 6.04, although the true pKa (bicarbonate protonation to form carbonic acid) at 37 ^oC and ionic strength=150 mM would be equal to 3.30.[75] Potentiometric titration is a slow process which provides bicarbonate equilibrium with enough time to equilibrate; hence carbon dioxide behaves as the apparent conjugate acid in this scenario. In the context of dissolution, both hydration and dehydration reactions occur in time-scales more comparable to diffusional times within the boundary layer (mean process time 10^{-2} – 10^1 s) much slower than the acid-base proton transfer reaction (mean reaction time ~10^{-7} s).[75] Thus, slow hydration/dehydration reactions prevent the system to reach equilibrium during dissolution, implying that the equilibrium condition assumed by Mooney et al.[74] does not stand anymore.

Recently, Al-Gousous et al. proposed a “reversible non-equilibrium” (RNE) model to calculate both $[H^+]_0$ and J_{drug} in bicarbonate-buffered media under non-equilibrium conditions.[75] Similar to Mooney’s model, calculation of pH_0 is function of diffusion constants and concentrations of different species, as well as equilibrium constants of reactions involved. Although in this case, diffusion of products from hydration/dehydration reactions, as well as CO_2/H_2CO_3 interconversion, are of major relevance. Given that this interconversion occurs in time-scales comparable to diffusion in boundary layer, the pKa of bicarbonate to ionize the acidic drug at the solid surface (effective pKa, pKa_{eff}) depends on the time to allow such an interconversion.[75] By applying mass balance analysis to RNE model, Al-Gousous et al.[75] deduced the equation 1.8, which can be used to calculate the effective pKa as a function of the timeframe for interconversion.

$$pKa_{eff} = 3.3 + \log(1 + \frac{D_{CO_2}}{D_{H_2CO_3}} \times \frac{k_d}{k_h + \frac{1}{t_D^{CO_2}}}) \quad (1.8)$$

Where $t_D^{CO_2}$ is time for carbon dioxide diffusion through the boundary layer, which is equal to 0.5* h^2/D_{CO2}. From this equation, it can be seen that the shorter the thickness of the diffusion layer, the shorter the time for diffusion of CO_2, hence the [kd/(kh + $(t_D^{CO_2})^{-1}$)] term becomes negligible in the absence of a diffusional layer. In this theoretical scenario, pKa_{eff} tends to 3.30, only accounting for the proton transfer reaction. Conversely, when the length of diffusional layer tends to infinity, the logarithmic term increases the value for the pKa_{eff}, according to CO_2-H_2CO_3 interconversion and diffusional constants.

iii. Considerations for in vitro and in vivo dissolution

Experimental conditions and standard apparatuses to investigate dissolution of oral dosage forms *in vitro* are thoroughly described in the European and United States pharmacopeias (USP).[6,76] The USP type I and II apparatus consist of a 1000 ml vessel coupled to either a rotational basket or paddle, respectively, which provide hydrodynamics to media. With dissolution being a function of solubility, the temperature during the experiment needs to be controlled, as well. Values of 37 ^oC are preferred to mimic physiological conditions. When testing dosage form dissolution, the vessel is filled with compendial media prior the experiment and the dosage form is submerged into media. From Nernst-Brunner equation (eqn 1.3), it is clear that dissolution slows down when the concentration in the bulk at time=t, C_t becomes closer to C_s. Therefore, the large volume used in this setting aims at maintaining sink conditions throughout the experiment (i.e., C_t is no more than 0.1 – 0.3 the C_s). Under *in vivo* situation, sink conditions are provided by intestinal transepithelial absorption, such that drug dissolved is transferred from the lumen into systemic circulation.[4] In addition, enhanced solubility by action of luminal bile salts may also contribute to the physiological sink in the lumen. Even though sink conditions are considered in the *in vitro* testing, this may differ from *in vivo* sink, especially for BCS II drugs. While luminal saturation for BCS class II is prevented by rapid drug absorption, compendial saturation due to poor aqueous solubility is not. In this regard, *in vitro* resemblance of *in vivo* dissolution can be improved by adding co-solvents, surfactants or even an organic phase to the *in vitro* dissolution media.[77–80]

Concerning to media composition, compendial buffers are typically well described in different pharmacopeias.[6,76] Even though the pH for these media can be adjusted in order to match the physiological pH range, sections above demonstrated the importance of accounting for buffer concentrations and physical-chemical interactions during drug dissolution. Buffer concentrations in compendial media are typically around 50 mM of the buffering salts,[76] which are enormous compared to luminal bicarbonate concentrations of around 5 – 15 mM in upper small intestine.[26,45] According to Mooney's model, higher buffer concentrations can

accelerate *in vitro* dissolution of weak ionizable drugs,[74] to a point where the *in vitro* testing becomes insensitive to detect any potential discrepancy between the clinical performance of two different products.[81] Moreover, given that solid dissolution is a function of bicarbonate pKa_{eff}, [75] matching the very same molarities in luminal bulk without matching the same buffer species is not sufficient. The equation 1.7 depicts that neutralized bicarbonate is converted in CO_2, which, leaves the small bowel by permeating through the intestinal wall, under *in vivo* conditions. While *in vivo* buffer capacity in the bulk is maintained by constant bicarbonate secretion, this is extremely difficult to be replicated in standard pharamacoepial apparatuses. This results in a rise in the bulk pH due to bicarbonate neutralization.[82] Maintenance of bulk pH requires, then, for an improvement of the dissolution apparatus. One of the most successful approaches has been the introduction of constant sparging of a mixture of an inert gas (e.g. N_2 or He) and carbon dioxide gas into the media.[81,83–85] Since the partial pressure of $CO_{2(g)}$ is proportional to the concentration of $CO_{2(aq)}$, this latter parameter can be controlled by adjusting the sparging flow rates of the mixture of gases.[86] Then, bicarbonate consumption throughout the experiment is replenished by the constant carbon dioxide sparging, such that the pH and the enhanced buffer capacity in the bulk are maintained.[51] A shortcoming of this method is the altered hydrodynamics resultant from bubbles generated while sparging. Even though this may be a major concern in stablishing bicarbonate media for quality control purposes, $CO_{2(g)}$ sparging has a great potential in guiding the development of orally administered drug products.

As explained, it is clear that pKa values are of major importance to account for the effect of buffers on dissolution of weak ionizable drugs. Hence, it is also important to consider any other variable with potential impact on the ionization. With the ionic strength (IS) in upper gastrointestinal fluids ranging between 100 – 150 mM, [30] its effect on the acidity constants cannot be neglected. In this regard, the extended Debye-Hückel equation (eqn 1.9) can be used to account for the activity of different species in equilibria for ionic strength values up to 300 mM.[87] Hence, the pKa at the ionic strength (IS, mol/l) of luminal fluids (pKa') can be calculated as:

$$pKa' = pKa + \frac{0.51\,(2z-1)\sqrt{IS}}{1+\sqrt{IS}} \qquad (1.9)$$

Where z is the charge of the conjugate acid species. Therefore, the development of biopredictive *in vitro* media requires the consideration of the ionic strength to increase the predictivity of *in vivo* dissolution. Experimentally, this parameter can be controlled by adding appropriate concentrations of sodium chloride to dissolution media.

3.4 Permeability

i. General principles for permeability

While the comprehension of dissolution is important for BCS class II drugs, the understanding of the permeability (P, cm/s) process is highly relevant, especially for the BCS class III. Once in solution, drug permeation is the result of a serial rate process. Mass of drug is firstly transported from the bulk to the intestinal wall, such that an aqueous resistance needs to be overcome. This aqueous resistance is otherwise known as the stagnant unstirred water layer (UWL). Secondly, the drug at the intestinal wall is partitioned into epithelial cells forming the intestinal wall and transported toward systemic circulation following the concentration gradient. In other words, total drug permeation rate can be either limited by the permeability through an aqueous unstirred layer (P_a) or the permeability across the epithelial wall (P_w), as shown in eqn 1.10.[4]

$$\frac{1}{P} = \frac{1}{P_w} + \frac{1}{P_a} \tag{1.10}$$

In turn, permeability through intestinal epithelia (P_w) can occur through different parallel mechanisms, such as passive diffusion (P_{pass}), active transport (P_{actv}) and passive paracellular absorption (P_{para}), among others (Fig. 1.4). Likewise, total mass transport at the absorption site will be the sum of all concurrent parallel flux mechanisms for each given drug, as following:

$$J_w = J_t = J_{pass} + J_{actv} + J_{para} \tag{1.11}$$

Where J are the fluxes of drug (nmol/cm^2*s) through each different mechanistic route. Similar to dissolution, the passive diffusion process follows Fickian diffusion kinetics at steady-state. Hence, passive flux rate (J_{pass}) is directly proportional to the chemical potential, with the proportionality constant being defined as passive permeability coefficient (P_{pass}). This relation is shown in equation 1.12, as follows:

$$J_{pass} = \frac{dM_r}{A \times t} = P_{pass} \times (C_w - C) \tag{1.12}$$

Where dM_r is the change of mass in the receiver compartment (nmol) and C_w the concentration at the surface of intestinal wall (µM). Similar as dissolution equations, the concentration in receiver compartment (C) at time=t can be neglected under physiological sink conditions.

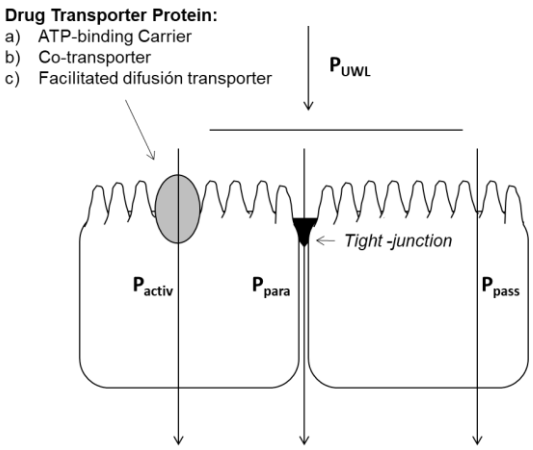

Figure 1.4. Resistances to mass transport during gastrointestinal absorption of drugs. Adapted from reference [22].

Given their high solubility in water, it is expected that BCS class III compounds undergo little resistance to reach the surface of epithelia. However, their absorption is limited by their slow transport across the lipidic cell membrane. Thus, additional transport mechanisms, as those described below, may have greater contribution for this type of drugs.

ii. Carrier-mediated transport

Drug transport through biological barriers may be affected by the presence of membrane-transporter proteins or carriers. These proteins can mediate the transport of substrates provided an appropriate drug-transporter affinity. Unlike Fickian kinetics, active carrier mediated transport usually utilizes driving forces different from purely concentration gradient. That means that they can either improve or hinder drug absorption, through either uptake-mediated or efflux-mediated transport mechanisms, respectively. In these cases, the maximum velocity of this process will be limited by the saturation of the transporter proteins mediating the active mass transport of the substrate. Therefore, Michaelis-Menten saturation kinetics better describes the active carrier-mediated transport (eqn 1.13),[23] where maximum mass transport rate (nmol/cm^2*s) and the Michaelis-Menten affinity constant (μM) are represented by the parameters J_{max} and K_m, respectively.

$$J_{actv} = \frac{J_{max} \times C_d}{K_m + C_d} \tag{1.13}$$

Several drug transporters have been found to be expressed in intestinal epithelia. From eqn 1.11 becomes clear that the lower the passive flux, the more relevant the contribution of transport-mediated active processes. This latter point is true not only for intestinal drug absorption, but also for any other distribution/elimination process in which transmembrane transport is required. Thus, carrier-mediated active transport may provide one possible

explanation for overall non-linearity in pharmacokinetics, as well as, inter-subject differences related to poorly permeable compounds.[88]

iii. Paracellular transport

Furthermore, epithelial cells form a monolayer with cellular junction being maintained by the presence of tight-junction proteins, as explained in section 2 of the present chapter. These junctions create intercellular pores that contributes to the absorption of small molecules (paracellular pathway). Permeability through paracellular pore was modeled by Adson et al.,[89] as following:

$$P_{para} = \frac{\varepsilon D[F_{(r/R)}]}{\delta}\left(\frac{k}{1-\varepsilon^{-k}}\right) \quad (1.14)$$

Where ε is the porosity, δ is the length of the paracellular pore (cm) and D is the diffusion coefficient through the pore (cm^2/s). The right side of the equation (in brackets) accounts for the electrochemical preference of the paracellular route for cationic compounds due to the negative potential inside the pore as a consequence of the negatively charged amino acids (mainly glutamate) forming the tight-junction. In this regard, k is the electrochemical energy parameter. On the other hand, the $F_{(r/R)}$ term (Renkin function) is a dimensionless parameter to describe the diffusion of a molecule with radius, r (Å), across a molecular sieve with pore radius, R (Å).[89,90]

iv. Considerations for in vitro and in vivo permeability and excipient effect

Determination of intestinal permeability under *in vivo* conditions is very challenging. Hence, both FDA and ICH guidances recommend to assess *in vivo* drug permeability via surrogate parameters, such as absolute bioavailability or mass balance for oral solutions. Permeability measurements have been carried out by applying different techniques, with the double balloon approach being the most used to report P_{eff} values in humans.[91] Shortly, this method consists of intubating volunteers with two balloons, which can be inflated in order to isolate a segment of the GI tract. Subsequently, a drug solution is perfused and luminal samples are collected overtime to determine the rate of disappearance. The equation 1.15 is, thereafter, used to calculate the effective permeability (P_{eff}, cm/s), assuming a well-stirred model.

$$P_{eff} = Q_{in} \times \frac{(C_{in}-C_{out})}{(C_{out}\times A)} \quad (1.15)$$

Where C_{in} and C_{out} are the entering and leaving concentrations, Q_{in} is the perfusion rate (ml/min) and A is the available surface to absorption equals to $2\pi rl$ (cm^2), for a cylinder with radius=r and length=l.[92]

Even though human P_{eff} determination played a key role in the development of the BCS, the complexity of this experiment makes it unfeasible for it to be applied to each new drug candidate. Therefore, *in vitro* surrogate methods have been developed.[93,94] The use of cell monolayers utilizing the colorectal carcinoma cell line Caco-2 have been accepted by regulatory guidelines.[68,69] In this set-up, Caco-2 cells are seeded onto porous polycarbonate membranes, such that they create an epithelial monolayer that resembles intestinal wall. A donor solution is placed on the luminal (apical) compartment, and samples are withdrawn overtime from the acceptor (basal) chamber. From this experiment, the apparent permeability (P_{app}, cm/s) can then be calculated using the equation 1.16:

$$J = \frac{dM_r}{A \times t} = P_{app} \times (C_d - C_t) \quad (1.16)$$

Where the flux (J) is equal to the drug appearance in the basal chamber (dMr, nmol) over the area (A, cm^2) and time (t, s). This is, in turn, equals to P_{app} multiplied by the concentration gradient, which is equal to the initial concentration in the donor chamber (Cd, µM) under sink conditions.

Similarly, the Ussing-type chamber is another experimental set-up, where separation between donor and basal compartments by a membrane is also possible. Unlike polycarbonate Transwells® used for Caco-2 studies, this apparatus allows the fixation of animal tissue (i.e., rat jejunum) in order to be used as biological membrane. This may be advantageous in resembling the absorption site for some drugs, because tightly-grown Caco-2 cells may sometimes underestimate the paracellular contribution due to their colonic origin.[95] In addition, the complexity of animal intestinal tissue may secrete biorelevant luminal contents, such as mucus, throughout the experiment.[96]

In vitro systems may help to not only assess drug permeability in early stages of development, but also to understand potential differences between two drug products.[97] As explained above, excipients in formulations may affect drug permeability by one or several mechanisms. Therefore, *in vitro* testing may help to assess those potential effects in a very cost/efficient fashion, because early detection of these issues would warn the manufacturer to make changes in the formulation before going to more expensive *in vivo* trials. In this regard, the predictability of an excipient effect could increase with enhancing the resemblance of the gastrointestinal conditions at the absorption site. For instance, the protective effect provided by luminal mucus may be a critical factor that needs to be considered to reduce the risk of false positives for permeability enhancer effects.[98]

4. Pharmacokinetic modeling

The kinetic processes explained in previous sections describe relatively simple and ideal scenarios, where all experimental conditions can be controlled. However, the complexity of the *in vivo* scenario makes it extremely difficult to stablish 100% mechanistic modeling. However, kinetic processes that a drug undergoes *in vivo* (pharmacokinetics) can be lumped and simplified in the following macro-processes: liberation, absorption, distribution, metabolism and excretion (LADME). In most cases, pharmacological therapy aims at achieving a systemic effect. Therefore, quantification of drug concentrations in bloodstream over time in a clinical trial is a good surrogate of drug concentrations at the site of action. Moreover, applying modeling techniques to plasma-time profiles experimentally obtained, the pharmacokinetics in complex living beings, such as humans, can be studied and predicted. Classical compartmental models and, more recently developed, physiologically-based pharmacokinetic models (PBPK) are briefly described below.

4.1 Compartmental models

The simplest model to study the pharmacokinetics of a given compound is to assume that the whole body can be treated as a lumped-single compartment. After an intravenous bolus dose, the complete dose reaches the bloodstream instantaneously and the experimental maximum drug concentration in plasma (C_{max}) will correspond to the first data point measured. If distribution into tissues is fast, the relatively slower elimination coefficient can be estimated from a one compartment model, which typically follows a first-order elimination kinetic (eqn 1.17).

$$-\frac{dX_c}{dt} = K_e X_c \tag{1.17}$$

Where X_c and t are the amount of drug in the compartment and the time, respectively, and K_e is the first order elimination coefficient. Integrating, dividing through volume (V) and applying natural logarithm on the equation 1.17, the linear form can be obtained (eqn 1.18) to account for plasma concentrations, C_c.

$$lnC_c = lnC_0 - K_e t \tag{1.18}$$

Fitting experimental data to this model allows the estimation of the elimination constant rate (slope). In addition, the intercept allows the calculation of the plasma concentration at times=0 (C_0), which is equal to the dose (X_0) over the volume in which the drug was distributed (volume of distribution=Vd).

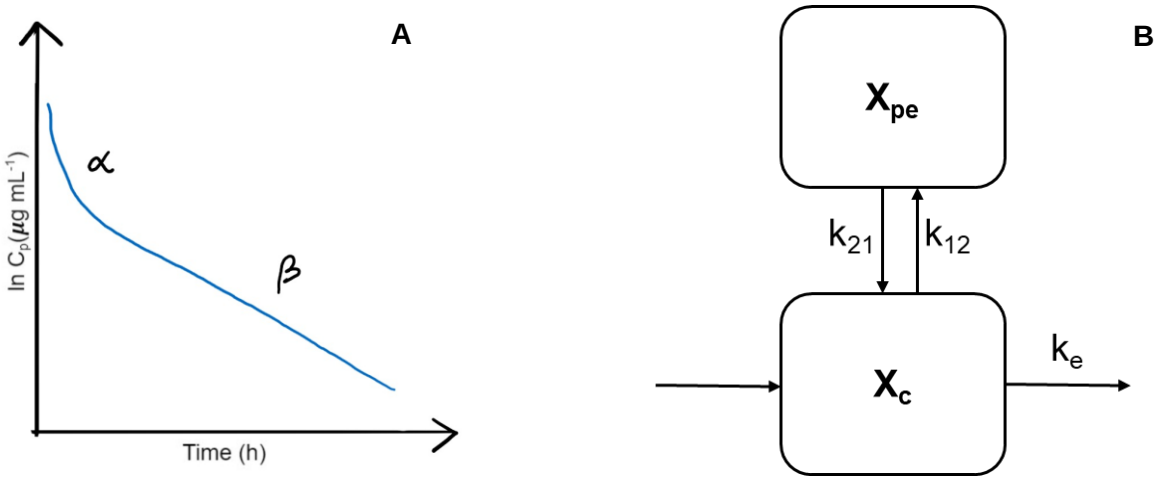

Figure 1.5. Intravenous drug disposition profile for two-compartmental distribution. The α and β phases display the distribution and elimination macro-processes, respectively (Panel A). Compartmental model for two compartment drug disposition (Panel B). The terms X_c, X_{pe}, k_{12}, k_{21} and k_e parameters are explained in the text. Adapted from reference [88].

In spite of its simplicity, the mono-compartmental model may not fit all cases, as some drugs show biphasic (Fig 1.5), or even triphasic. These profiles are seen when distribution is slower relative to elimination, such that the former process becomes visible when monitoring plasma concentrations. For instance, a biphasic distribution can be modeled in a two-compartmental system, where sampled plasma concentrations correspond to the central compartment (Fig 1.5).

In this case, the change of mass of drug in plasma over time can be written as:

$$\frac{dX_c}{dt} = X_{pe}k_{21} - X_c k_{12} - X_c k_e \tag{1.19}$$

Where X_c and X_{pe} are drug amounts the central (typically plasma) and peripheral compartment, respectively. Kinetic rate coefficients, k_{12} and k_{21}, are the distribution rate microconstants and k_e is the elimination rate microconstant. Solving this equation and fitting to intravenous plasma data allow estimation of distribution constants, as well as the estimation of the volume of distribution in central compartment (V_c).

As for extravascular administration (i.e., through the oral route), a previous input rate process must be considered which relates to drug absorption before reaching systemic circulation. Assuming mono-compartmental distribution, the following general equation describes the drug exposure in presence of an absorption process with k_a being the absorption rate coefficient.

$$\frac{dX_c}{dt} = X_c K_a - X_c K_e \tag{1.20}$$

Therefore, knowing the elimination/distribution parameters, for instance from intravenous plasma profiles, absorption rate coefficient can be obtained by fitting plasma profiles to this

model. Compartmental analysis can be further utilized for other applications, for example to model intraluminal dissolution.

4.2 Deconvolution and convolution

From a biopharmaceutic perspective, the understanding of kinetic processes taking place at the absorption site (i.e., gastrointestinal lumen) is key to stablish a meaningful relation between one characteristic determined *in vitro* and its corresponding *in vivo* response. With intraluminal sampling being too complex to perform, ethically questionable and time/money-costly, plasma profiles may offer an indirect route to assess the absorption phenomenon. In this regard, additional mathematical treatment on data obtained *in vivo* and/or *in vitro* is needed. As explained, the plasma-time concentration profile is function of other functions namely, drug release, absorption, distribution, metabolism and excretion. This means that plasma profiles observed after oral administration of a dosage form can be considered a convoluted process, where the plasma profile (output function, $H_{(t)}$) depends on an impulse function ($G_{(t)}$) described by distribution/metabolism/elimination and an input function ($X_{(t)}$) for the overall dissolution/absorption process.[3] This is shown in eqn. 1.21, with * representing the convolution operator.

$$H_{(t)} = G_{(t)} * X_{(t)} \tag{1.21}$$

Knowing the parameters that describe the impulse function $G_{(t)}$, for instance from intravenous data, the input function can be numerically assessed by deconvolution methods. For drugs having well characterized disposition, model-dependent approaches can offer simpler, yet effective, methods to calculate the fraction absorbed over time. On the one hand, the Wagner-Nelson method can be used for drugs with mono-compartmental distribution. This method is based on a mass balance where the amount of drug absorbed at infinity (total amount absorbed=$X_{a(inf)}$) is assumed to be equal to the amount eliminated at t=infinity ($X_{e(inf)}$). Meanwhile, the amount absorbed at time=t ($X_{a(t)}$) will be the sum of the amount in the plasma compartment (X_c) plus the amount already absorbed at that time, which is equal to the amount already eliminated during that period of time ($X_{e(t)}$).[99] Therefore, the Wagner-Nelson approach can be represented as:

$$Fa_{(t)} = \frac{X_{a\,(t)}}{X_{a\,(inf)}} = \frac{X_c + X_{e(t)}}{X_{e(\mathrm{inf})}} = \frac{C_{c(t)} + K_e AUC_{0-t}}{K_e AUC_{0-inf}} \tag{1.22}$$

Hence, the calculation of the fraction absorbed at time=t ($Fa_{(t)}$) is possible. Likewise, Loo and Riegelmann proposed a similar mass balance approach to calculate $Fa_{(t)}$ in the case of a drug with bi-compartmental distribution.[100]

$$Fa_{(t)} = \frac{X_{a\,(t)}}{X_{a\,(inf)}} = \frac{X_{c(t)}+X_{pe(t)}+X_{e(t)}}{X_{e(\mathrm{inf})}} \quad (1.23)$$

Where the amount of drug in the peripheral compartment at time=t ($X_{pe(t)}$) needs to be estimated with intravenous data, as explained above for two-compartmental pharmacokinetics. Furthermore, deconvolution approaches can also be applied for multi-compartmental models (i.e., physiologically-based pharmacokinetic models, also known as PBPK, described below) by setting the proper set of differential equations.

On the other hand, data obtained from an *in vitro* set-up can be convoluted with an impulse function describing the distribution/metabolism/elimination of the drug in order to predict plasma-time profiles. The success of this mathematical approach lies on the accuracy of the *in vitro* experiment to represent appropriately the *in vivo* liberation/absorption process for a given drug product. For that purpose, the experimental data obtained *in vitro* requires to be described as an input function. In this regard, the Weibull distribution offers great flexibility, such that a wide spectrum of dissolution curves can be fitted to this function.[101]

$$F_{(t)} = F_{(inf)}\left(1 - e^{-\left(\frac{(t-t_0)^{\alpha}}{\beta}\right)}\right) \quad (1.24)$$

The $F_{(t)}$ and $F_{(inf)}$ are the fractions dissolved/absorbed at time=t and infinity, respectively. While β represents the time at which $F_{(t)}$ is equal to 0.632, α is a shape parameter, which modifies the form of the input function at values either higher or lower than unity.[3,101] Meanwhile, the t_0 parameter accounts for any possible lag time, which can be useful, for instance, to describe the dissolution process of an enteric coated dosage form. In contrast, the dissolution of an immediate release dosage usually has an exponential shape, on the one hand, and no significant lag time, on the other.

4.3 Physiologically-based pharmacokinetic models

More recently, pharmacokinetic models based on physiological knowledge have been developed to account for tissue distribution of drugs. These types of models are known as physiologically-based pharmacokinetic (PBPK) models due to their ability of include more physiological aspects in their calculations. Semi empirical equations proposed by Poulin and Thiel were pivotal to their development, given that they allow the calculation of the volume of distribution at steady-state (V_{ss}) as a sum of volumes of distribution into tissues (extracellular interstitial spaces for less permeable drugs), erythrocytes and plasma.[102] Distribution into these compartments can be calculated from physico-chemical drug parameters (*n*-octanol:buffer partition and olive oil:buffer partition), biochemical parameters (erythrocyte:plasma ratio, fraction unbound in plasma, fraction unbound in tissues) and physiological volumes (tissues, extracellular, plasma). As mentioned, diffusion of less

permeable compounds from extracellular fluid into tissues may assumed to be slower than perfusion, such that tissue distribution will be limited by their permeability.

As for the GI tract, this has been modeled in PBPK software packages as a multicompartmental system with first-order kinetic mass transfer among compartments. This approach was based on the work of Yu et al. on developing a compartmental absorption and transit model. Here, the small intestine was described by seven fictious compartments disposed in series.[103] This model allowed to successfully predict the plasma profiles for 10 different compounds orally administered.[104] This work was the starting point for some PBPK model software manufacturers, who further optimized this model to account for other physiological variables, such as pH gradient in the bulk and regional absorption, among others.

5. Overall introduction to the publications

As showcased throughout this introduction, drug absorption from IR oral pharmaceutical products is highly dependent on physico-chemical characteristics of the API and the dosage form. Therefore, prediction of oral absorption of drugs demands a case-by-case analysis. In this dissertation, four cases were studied and discussed. An introduction on each of these cases is presented below.

5.1 Case I: Risk assessment of biowaiver for Carbamazepine IR oral products and insights on predictive *in vitro* methods

Carbamazepine is a neutral active molecule used to palliatively control seizure episodes in epilepsy treatment and relieve neuropathic pain in trigeminal neuralgia. Since carbamazepine is included in both adults and children lists of essential medicines (EML) issued by the World Health Organization (WHO),[105] it is important to correctly classify this API under the BCS framework in the light of existing evidence. As for extensively characterized drugs with large amount of evidence published on their physical-chemistry, pharmacokinetics and dosage form performance, a systematic review on available data in literature is a reasonable approach to correctly classify the API. Furthermore, this approach enables the researcher to perform a risk assessment of waiving *in vivo* bioequivalence studies for carbamazepine, considering not only its BCS classification, but also further evidence on the usage of surrogate *in vitro* methods and/or the clinical performance of carbamazepine products.

On the one hand, safety concerns might arise for carbamazepine products due to observation of adverse effects at plasma levels similar to therapeutic concentrations.[106] On the other hand, successful IVIVCs have been developed for IR carbamazepine tablets by our working

group. The findings reported suggests that the pharmacopeial dissolution method (using 900 ml of 1% SLS in type II apparatus at 75 rpm) may be sufficiently discriminating to detect bio-inequivalencies between IR oral carbamazepine products.[79,80] These two factors need to be taken into account to assess whether the benefits of a biowaiver overweigh any potential risk related to carbamazepine clinical performance. A systematic review of relevant literature on carbamazepine would enable to draw conclusions in these regards.

5.2 Case II: Development of a biopredictive dissolution method for ibuprofen oral suspensions

Ibuprofen is a well-known non-steroidal anti-inflammatory drug usually formulated as IR oral dosage forms. Chemically, this molecule is a weak acid BCS class II drug (BCS IIa) with a pKa= 4.4.[56] Hence, it may be expected that the enhanced solubility at small intestinal pH provides ibuprofen with ideal conditions to behave as a “pseudo-BCS I”. However, *in vitro* dissolution of ibuprofen 600 mg IR tablets was shown under-discriminating compared to *in vivo* pharmacokinetics of same products, where differences in C_{max} were observed.[57] In spite of matching *in vivo* relevant pHs in the design of the *in vitro* experiment, dissolution conditions in that study largely over-estimated the luminal situation for concentrations of buffer species and ionic strength. This resulted in a lack of discrimination with the *in vitro* dissolution being extremely faster than *in vivo*, most likely, as a consequence of enormous buffer capacity of the media.[57] Moreover, differences in chemical nature between pharmacopeial buffers and luminal bicarbonate also impact dissolution kinetics of ionizable molecules and, hence, need to be taken into account.

In order to stablish a fair comparison between *in vivo* and *in vitro* dissolution, reliable data of intra-intestinal dissolution rate is needed. Recently, a novel approach to enable intraduodenal administration of ibuprofen suspensions to healthy volunteers was published by our working group.[107] Briefly, a small-bore smooth tube was nasally introduced in healthy subjects, retrieved from the pharynx and supplemented with telemetric and administration capsules. The whole device was swallowed and both the tube length and pH were monitored in order to guide the placement of the capsule at the duodenum. A peristaltic pump was used to administer either ibuprofen solution or suspensions through the tube. Subjects received the following treatments: A: Ibuprofen solution infused at fasted gastric emptying rate (half-life, 12 min); B: Small particle size suspension (Suspension A) at fasted gastric emptying rate; C: Large particle size suspension (Suspension B) at fasted gastric emptying rate; and D: Suspension B infused at slower rate (half-life, 20 min).[107] With this experimental design, the dissolution rate of suspensions with controlled particle size in the small intestine can be assessed by contrasting plasma concentration-time profiles from each suspension treatment against the profile

obtained with the solution. In addition, both potential effects of early gastric exposure and variable gastric residence times can be controlled, as well. The authors observed differences in plasma-time profiles among the treatments, (Fig. 1.6) suggesting that ibuprofen absorption depends on particle size dissolution in small intestinal fluid. Hence, the controlled conditions applied to that study can be further used to develop and evaluate a biopredictive dissolution method for ibuprofen as a model BCS class IIa API.

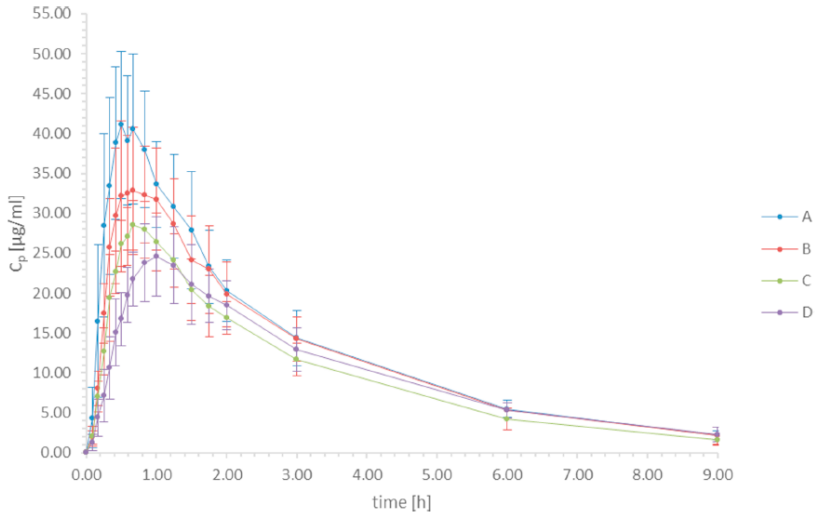

Figure 1.6. Ibuprofen plasma profiles after intraduodenal administration of: an oral solution (A), oral suspension with small particle size (B), oral suspension with large particle size (C) and the latter suspension pumped with a slower infusion rate (D). Reprinted with permission from reference [107].

5.3 Case III: Assessing the effect of chitosan on acyclovir absorption through bioaccessibility and permeability *in vitro* methods

The absorption of drugs belonging to the BCS class III is limited by their permeability, such that they are the class most sensitive to the effects of excipients on drug absorption. On the one hand, chitosan is a polycationic polysaccharide currently used in food industry, but with a great potential in pharmaceutical industry, due to its promising properties as excipient.[108] However, one promising feature for this excipient is its absorption enhancer property. In fact, several studies have shown that chitosan enhances the permeability of different low permeability model compounds using diverse experimental models (Table 2). The underlying mechanism for this effect seems to be associated with its polycationic status at physiological pH. The positive charges would allow the interaction with epithelial cell membrane, causing a conformational disruption in zonula occludens-1 (ZO-1) protein, a major contributor of the tight-junctions that creates the paracellular pore. The final result of this effect would be a reduction in the resistant to paracellular transport.[109]

Motivated by this evidence, the permeability enhancer potential of chitosan was assessed in healthy subjects using acyclovir (BCS III, Fa= 10 – 30%) as a model drug (Fig. 1.7).[60] The apparent linearity in acyclovir's oral pharmacokinetic at lower strengths (200 – 400 mg),[110] the lack of evidence on any potential carrier-mediated transport mediating intestinal absorption,[111] and its expected paracellular permeability, further supported the selection of this model compound. In the mentioned study, Zovirax® IR tablets (acyclovir 200 mg) were dissolved in absence or presence of chitosan at two concentration levels prior administration to healthy volunteers in fasted conditions. Unexpectedly, plasma concentrations with chitosan treatments were lower than the control, suggesting an unanticipated negative excipient effect (Fig. 1.7).[60] With alterations in GI transit times due to chitosan being unlikely, two hypotheses emerged from that work to explain the findings. Firstly, an interaction between positively charged chitosan and luminal bile acids is possible, which may result in a reduction of luminal concentrations of bile salts and, therefore, reduced solubility of acyclovir at small intestine. Secondly, polyanionic mucin proteins present intestinal mucus may also interact with chitosan, such that acyclovir absorption is either prevented or delayed by chitosan-mucus binding at the absorption site and/or increasing the viscosity of mucus microclimate.[60] These hypotheses need to be challenged in order to better understand the mechanisms underlying this *in vivo* observation and to develop surrogate methodologies with better biopredictability of this phenomenon.

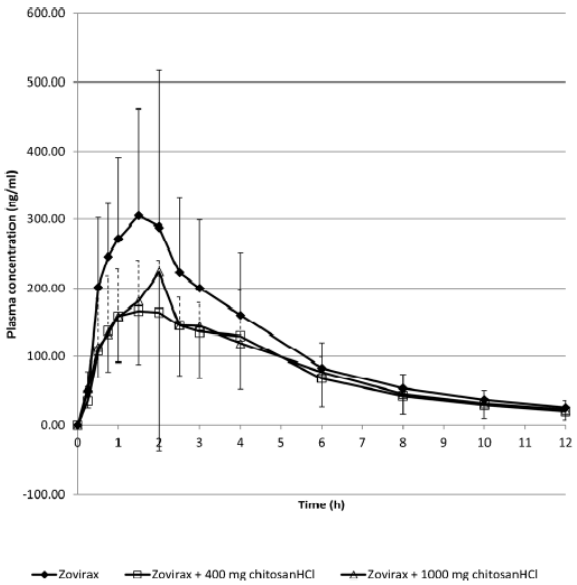

Figure 1.7. Acyclovir plasma profiles after administering Zovirax ® tablets 200 mg, previously dissolved in absence (black) or presence of 400 mg (white squares) or 1000 mg of chitosan (white triangles). Reprinted with permission from reference [60].

Table 1.2. Summary of studies on the effect of chitosan on the permeability/absorption of low permeable molecules.

Drug	Chitosan (Ch) type		Experimental design	Concentration of Ch	Results	
	DD (%)	MW (kDa)			Ratio Test/control (Parameter)*	Others Observations
Acyclovir oral solution [60]	93.05	30-400	*In vivo*, healthy humans	1.6 g/l 4.0 g/l	• 0.56 (C_{max}) • 0.63 (C_{max}) • 0.70 (AUC_{0-12})	-
Acyclovir solution (pH 5.5) [112]	16.7	Different MW tested. Range: 10-150	*Ex vivo*, rat jejunum.	3 g/l 10 g/l	• ~ 2.5 (C_{max})# • ~ 1.6 (AUC_{0-3}) # • ~ 6.0 (C_{max}) # • ~ 2.4 (AUC_{0-3}) #	**i)** Ch 1.0 % below 10-14 kDa had no effect on AUC 0-3h. **ii)** PEG at the same Cs viscosity had no effect on acyclovir absorption.
Acyclovir solution (pH 6.2) [113]	NR	NR	*In situ* perfusion, different Rats intestine segments.	1 g/l	• 3.00 (P_{eff} Ileum)	**i)** Ratios from jejunum and colon were 2.02 and 1.05, both not significant.
Acyclovir and Mannitol (oral) solutions (pH 5.5) [114]	75-90	200-600	*In vitro* Caco-2. *In vivo* in Rats§.	10 g/l 30 g/l	• 4.08 (P_{app}) • 1.57 (AUC_{0-20}) • 1.57 (F) • 3.43 (P_{app}) • 2.02 (AUC_{0-20}) • 3 (F)	**i)** P_{app} ratios comparable to mannitol ratio. **ii)** C_{max} ratios at 1 and 3% were 1.17 and 1.10, both not significant. **iii)** Ch increased C_{max} variability.
Acyclovir and Mannitol Solutions (pH 6.3) [115]	85	20	*In vitro* Caco-2 *In vitro* MDCK	1 g/l 5 g/l 1 g/l 5 g/l	• 5.80 (P_{app}) • 10.2 (P_{app}) • 7.17 (P_{app}) • 13.8 (P_{app})	**i)** P_{app} ratios comparable to mannitol ratio.
Mannitol Solutions (pH 5.5) [109]	**Ch1:** 65%-170 kDa **Ch2:** 99%-31 kDa		*In vitro* Caco-2	0.05 g/l 0.05 g/l	• 11.2 (P_{app} mannitol) • 3.11 (P_{app} mannitol)	**i)** Cs 51%-22 kDa (also tested) had no effect. **ii)** Heparin (polyanion) inhibited and reversed Ch effect (30 and 70% reverse for Ch1 and Ch2, respectively).

Ch: Chitosan.
NR: Not reported.
*: Acyclovir unless it is specified.
#: Results obtained by using chitosan MW 150 kDa.
§: Different subjects used to perform control and test experiments.

5.4 Case IV: Development of a PBPK model to predict the variable absorption of acyclovir IR tablets

Even though dosage forms containing lower strengths of acyclovir display linear pharmacokinetics, high within-study variability has been observed (as depicted by the large standard deviations in the Figure 1.7). This variability does not seem to be explained by dissolution processes, since de Miranda et al. found overlapping AUC and C_{max} between acyclovir oral solutions and IR capsules administered to fasted subjects in a cross-over design.[116] Conversely, oral administration of the same product to different populations resulted in divergent pharmacokinetic parameters. For instance, the reference product (Zovirax® 400 mg) was administered to fasted healthy subjects in two single-dose comparative bioavailability trials to Saudi Arabians and Europeans, respectively.[110,117] Interestingly, both AUC and C_{max} were around 35 – 44% lower in the former compared to the latter population.

Acyclovir absorption is governed by passive non-saturable diffusion. However, the presence of post-absorptive active processes (affecting disposition/elimination) may explain the population-related discrepancies in plasma curves. The use of two-compartments to describe acyclovir's intravenous disposition profiles supports this hypothesis.[118] Furthermore, acyclovir is rapidly excreted into urine with its clearance (Cl) being higher than creatinine's. Therefore, acyclovir plasma profiles are most likely a result of a combination of one or more distribution and elimination mechanism. In fact, acyclovir uptake has been characterized in overexpressing *in vitro* systems as a substrate of the human isoform of the organic anion transporters (hOATs), multidrug and toxin extrusion transporters (hMATE1) and organic cation transporter (OCT1).[119–121] The high polymorphism on the latter protein has been associated with population-related differences on pharmacokinetics of another BCS class III model compound, i.e., metformin.[122] The OCT1 is mainly expressed at sinusoidal membrane of hepatocytes, mediating liver uptake of organic substances prior their metabolism.[123] Hence, OCT1 polymorphism may also affect acyclovir hepatic uptake, resulting in despair plasma profiles across populations. In this regard, PBPK models are a powerful *in silico* tools that can be used to test this hypothesis and also to develop a computational method to predict the effect of the interplay between physiological and formulation variables on the oral disposition of acyclovir IR dosage forms.

Chapter 2. Objectives

Taken together, it can be hypothesized that the correct application of *in vitro* and/or *in silico* surrogate methodologies that account for relevant luminal interactions between physiological and pharmaceutical aspects would allow to accurately predict the absorption of drugs from immediate release oral dosage forms. Therefore, the aim of this dissertation is to investigate the potential of diverse surrogate biopharmaceutic methodologies to predict the oral absorption of pharmaceutical products of either BCS class II or III drugs. Four case studies are analyzed and discussed in this manuscript. Specific aims were drafted for each case study, as detailed below:

i. To assess the risk of biowaiver (by applying surrogate methods, such as IVIVCs under compendial conditions) for IR solid oral dosage forms containing carbamazepine (BCS IIc drug) through the revision of relevant literature available on carbamazepine.
ii. To rationally develop a biopredictive method for intestinal dissolution of ibuprofen (BCS class IIa) suspensions, considering relevant buffering species and concentrations in the design of the *in vitro* methodology.
iii. To study the negative effect of chitosan on the absorption dissolved acyclovir (BCS class III) by applying a set of *in vitro* surrogate experimental methodologies with biopredictive potential.
iv. To assess the hypothetical role of OCT1 polymorphism on the variable oral pharmacokinetics/biopharmaceutics of acyclovir multisource products (BCS class III) through coupling *in vitro* dissolution techniques to PBPK *in silico* modeling.

.

Chapter 3. Results

The results obtained in this dissertation are shown in four peer-reviewed publications, which the reader can find at the appendix section of this manuscript. Nonetheless, a brief summary for each publication is provided, including aims, a short description of methods utilized and the most relevant findings.

1. BIOWAIVER MONOGRAPH FOR IMMEDIATE-RELEASE SOLID ORAL DOSAGE FORMS: CARBAMAZEPINE

Original publication	Mauricio A. García, Rodrigo Cristofoletti, Bertil Abrahamsson, Dirk W. Groot, Alan Parr, James E. Polli, Mehul Mehta, Vinod P. Shah, Tajiri Tomakazu, Jennifer B. Dressman, Peter Langguth. **Biowaiver Monograph for Immediate-Release Solid Oral Dosage Forms: Carbamazepine.** *Journal of Pharmaceutical Sciences*. 2021;110(5): 1935-1947. DOI: *10.1016/j.xphs.2021.02.019*.
Authorship	First author
Author contribution	Investigation, Formal analysis, Data curation, Writing-original draft preparation.

Carbamazepine is an antiepileptic drug indexed in the 21st version of the Essential Medicines List (EML) issued by the World Health Organization (WHO). In such a list, carbamazepine 200 mg drug products formulated as solid oral IR dosage forms are recommended. This investigation aimed at assessing the risk of biowaiver for carbamazepine IR products. Literature on carbamazepine was collected from PubMed and International Pharmaceutical Abstracts databases using pertinent keywords, such as: “carbamazepine”, “indications”, “therapeutic index”, “solubility”, “polymorphs”,” “partition coefficient”, “permeability”, “absorption”, “metabolism”, “bioavailability”, “bioequivalence”, “dissolution”, “IVIVC” and “excipients”.

A full description on carbamazepine’s general characteristics was depicted, encompassing its therapeutic indication, therapeutic index, doses, dosage forms and strengths available in the market. Furthermore, information on carbamazepine’s physical-chemical characteristics, such as polymorphism, aqueous solubility and oil/water partition was provided, as well. In addition, pharmacokinetics for carbamazepine were described with special focus on gastrointestinal absorption and first pass metabolism. Finally, data collected on dosage form performance, including available bioequivalence trials, effect of polymorphism, effect of excipients and IVIVCs, was also depicted.

Concerning to carbamazepine general characteristics, literature revised showed an overlap between therapeutic and toxic concentrations with typical plasma concentrations in patients ranging between 2 – 17 µg/ml. A common therapeutic range between 4 and 12 µg/ml is often mentioned in literature, suggesting a therapeutic index of 3. However, such a number may be even lower in the light of the data collected. Therefore, carbamazepine should be considered a narrow therapeutic index (NTI) drug.

Overall, information available agreed on deeming carbamazepine as a low solubility compound under the frame of the BCS. For instance, carbamazepine aqueous solubility ranged from 0.24 – 0.36 mg/ml, regardless of the pH and/or composition of buffering salts in the media. This was consistent with the lack of ionizable groups in carbamazepine molecular structure within the physiological pH range. Considering the highest strength recommended by the EML, the Do for carbamazepine ranged from 2.22 – 3.33 for those solubility values. This interval increases two-fold if a dose of 400 mg is assumed, as this latter may represent the highest strength in the market in some countries. Of note, the presence of the surfactant sodium lauryl sulfate (SLS) enhanced the solubility in a concentration-dependent fashion up to values of 2.40 mg/ml at 1% SLS.

On the other hand, carbamazepine permeability was deemed high under the BCS. Although its absolute bioavailability lied between 70 – 78%, this value seems to be biased by the considerable first pass effect. Permeability measurements in humans ($4.3x10^{-4}$ cm/s), as well

as several *in vitro* assays, confirmed its classification. Taken together, carbamazepine was classified as a BCS class II compound.

Moreover, IVIVCs are expected for BCS class II products, provided the dissolution method is able to detect bio-inequivalences. Several examples of successful IVIVCs were found in literature on carbamazepine. In fact, nine out of ten publications utilized the pharmacopeial assay to discriminate between non-bioequivalent products (i.e. USP type II apparatus, SLS 1% media, 75 rpm, 37 ^{o}C). This key of the success underlying conditions appears to rely on the surfactant. In the intestinal lumen, carbamazepine is rapidly absorbed upon dissolution as a consequence of its high permeability. As mentioned, carbamazepine solubility is enhanced with increasing SLS concentrations. Hence, the presence of SLS 1% in media provides an enhanced sink during the dissolution experiment, such that it resembles better the *in vivo* sink for carbamazepine.

In spite of the promising detection potential of the mentioned *in vitro* testing conditions, there is still room for improvement, as several correlation parameters (Fa, Fd, Cmax, tmax, AUC) were explored in these publications. Hence, the lack of consensus on the appropriate correlation methodology may be considered a barrier to implement biowaivers for carbamazepine IR products.

In the light of these findings, data collected suggests a high risk of biowaiver for carbamazepine IR dosage forms. Firstly, BCS-biowaivers for products containing BCS class II drugs are not recommended in regulatory guidelines. Secondly, carbamazepine was found to be a NTI drug, hance a potential false positive biowaiver would represent a further risk for the patient. Finally, even though the compendial method seems to be a very promising tool to detect bio-inequivalences, agreement on what should be the best correlation parameters to successfully stablish an IVIVC is still demanded.

2. IN VITRO PREDICTION OF IN VIVO ABSORPTION OF IBUPROFEN FROM SUSPENSIONS THROUGH RATIONAL CHOICE OF DISSOLUTION CONDITIONS

Original publication	Michael Hofmann[1], Mauricio A. García[1], Jozef Al-Gousous, Alejandro Ruiz-Picazo, Florian Thieringer, Mai A. Nguyen, Wiking Månsson, Peter R. Galle, Peter Langguth. **In vitro prediction of in vivo absorption of ibuprofen from suspensions through rational choice of dissolution conditions**. *European Journal of Pharmaceutics and Biopharmaceutics*. 2020;149: 229-237. DOI: *10.1016/j.ejpb.2020.02.009*.
Authorship	First author
Author contribution	Investigation, Methodology, Formal analysis, Data curation, Writing-original draft preparation.

The *in vitro* dissolution testing has great biopredictive potential for drugs and/or drug products whose GI absorption is limited by their luminal dissolution, provided that intestinal factors governing the dissolution in the intestine are correctly mimicked (i.e. buffering species and concentrations). Hence, it can be inferred that a good understanding of intestinal dissolution is pivotal for this purpose. Recently, our working group developed a novel technique for intraduodenal administration of oral solutions and/or suspensions. Data obtained with this method has the advantage of being free of noise due to gastric transit/residence. Therefore, assessment of intra-intestinal dissolution may be possible through the application of pharmacokinetic modeling. In the mentioned study, one ibuprofen oral solution and two suspensions, i.e., suspension A (SA, particle diameter ~60 µm) and B (SB, particle diameter ~130 µm), were administered to fasted healthy volunteers and plasma profiles were followed over time. Plasma-time profiles became lower with increasing particle sizes, suggesting that ibuprofen absorption rate depended on intestinal dissolution rate. In this regard, the utilization of biorelevant *in vitro* media for ionizable solubility-limited drugs, such as bicarbonate-containing buffer, would lead to accurate predictions of *in vivo* dissolution. However, bicarbonate-containing media are difficult to handle due to the drop in bulk pH throughout the experiment. Nonetheless, the development of surrogate biopredicitive media may be possible by matching the drug surface ionization provoked by action of bicarbonate.

In this investigation, the same suspensions utilized in the *in vivo* trial were studied for *in vitro* dissolution. Both SA and SB were tested in three different buffers, namely phosphate, acetate and bicarbonate at pH 6.0. This latter buffer required constant CO_2/air sparging in order to maintain the desired concentrations of the conjugate acid (CO_2). Buffer molarities resembling physiological buffer concentrations in duodenum/jejunum segment (5 and 15 mM, based on the conjugate base) were chosen, meanwhile the ionic strength in the media was fixed to 0.154 M. Further, the possibility of using phosphate as a surrogate media was assessed by testing the dissolution at concentrations of phosphate equivalent to bicarbonate molarities (phosphate equivalent concentration). For that purpose, either the RNE or Mooney's et al. model was used to calculate the surface pH (pH_0) for each dissolution media. Phosphate equivalent molarity was back-calculated using the pH_0 in bicarbonate media as an input parameter. Finally, *in vitro* dissolution profiles were compared to deconvoluted *in vivo* dissolution profiles calculated from data obtained in the clinical trial. Impulse function parameters such as absorption, distribution and elimination coefficients were obtained from oral solution treatment, meanwhile dissolution coefficients for suspension dissolution were obtained by fitting data from either SA or SB treatment. A diphasic dissolution model was superior to the monophasic, as this latter underfitted the observed data. *In vivo* dissolution was finally calculated by solving the dissolution equation for the diphasic model using dissolution coefficients previously fitted as input.

Dissolution profiles for SA and SB overlapped between each other when phosphate either 5 or 15 mM was used as dissolution media. Conversely, bicarbonate-based media was able to detect differences in dissolution profiles between these formulations at both molarities, consistent with the previous *in vivo* findings. As for acetate buffer, while a concentration of 15 mM did not distinguish between formulations, the lower molarity allowed the separation of dissolution curves. The explanation for these results lies on the surface drug ionization, which directly relates not only to the dissolution rate but also to the pH_0. For instance, the pH_0 for bicarbonate buffer were calculated 5.09 and 5.31, at molarities of 5 and 15 mM, respectively. These values were largely overestimated by the pH_0 obtained with phosphate at either 5 or 15 mM. In fact, if the aforementioned pH_0 values were used to calculate the equivalent phosphate molarities in order to develop a surrogate buffer, phosphate concentrations of 1 and 2 mM (based on the conjugate base) can be respectively calculated. As expected, dissolution of SA and SB in these diluted phosphate media were considerably slower than both 5 and 15 mM. Furthermore, the closeness between dissolution curves in bicarbonate and equivalent phosphate media (overall f1=14.01%) confirmed that low molarity phosphate media (1 and 2 mM) are suitable surrogate buffers for either SA and SB formulations tested in this study.

Moreover, *in vivo* data previously reported by our working group was used to model the *in vivo* equivalent dissolution (IVED) profiles for the formulations used in this study. Pharmacokinetic coefficients for absorption (9.75 h^{-1}), distribution (2.98 and 2.31 h^{-1}) and elimination (0.90 h^{-1}), as well as volume of distribution (3.81 l), were all in good agreement with previous reports on ibuprofen. In fact, the model correctly predicted the profiles observed after administering the ibuprofen oral solution. In addition, the diphasic model also produced accurate simulations of plasma-time profiles after the respective treatments with ibuprofen suspensions, confirming the suitability of this modeling approach. As anticipated, IVED curves were different between SA and SB, with large particle size suspensions dissolving slower than their shorter counterpart. Remarkably, IVED profiles fell within the dissolution profiles in bicarbonate for the respective suspensions. Even though the limited sample size used in the clinical trial prevents any sound conclusion on this relationship, the findings of this work suggest that either bicarbonate or the surrogate media here developed may be useful as biopredictive methods for these formulations. Furthermore, this investigation highlights that mechanistic understanding of luminal dissolution process enhances the detection capacity of *in vitro* testing, leaving an open door to further discussion on implementing biowaivers for BCS class IIa compounds.

3. THE EFFECT OF CHITOSAN ON THE BIOACCESIBILITY AND INTESTINAL PERMEABILITY OF ACYCLOVIR

Original publication	Marlies Kubbinga, Patrick Augustijns, Mauricio A.García, Christian Heinen, Heleen M. Wortelboer, Miriam Verweie, Peter Langguth. **The effect of chitosan on the bioaccessibility and intestinal permeability of acyclovir**. *European Journal of Pharmaceutics and Biopharmaceutics*. 2019;136: 147-155. DOI: *10.1016/j.ejpb.2019.01.021*.
Authorship	Co-author
Author contribution	Formal analysis, Writing-original draft preparation.

One critical parameter for BCS class III IR oral solid dosage forms is the presence of excipients in the formulation with potential effect on their permeability, which is considered the rate limiting step for the absorption of these compounds. Several literatures have suggested the potential of chitosan, a polycationic polysaccharide, to be used in pharmaceutical formulations of BCS class III, due to their absorption enhancer properties. The absorption enhancer mechanism seems to be related to its positive charges, which bind epithelial cell membrane, resulting in a disbandment of the protein zonula occludens (ZO-1), otherwise known as tight junction-1 protein. The structural changes in this latter protein would disrupt the monolayer integrity and, hence, increase drug permeability through the paracellular pathway. Even though several publications suggest chitosan as a promising permeability enhancer, very few *in vivo* evidence has been generated in humans to further confirm the *in vitro* findings. In fact, our working group recently conducted an *in vivo* study on fasted healthy volunteers to test this effect. Subjects were administered with Zovirax ® tablets (acyclovir 200 mg) previously dissolved in absence or presence of chitosan 400 mg or 1600 mg. Surprisingly, chitosan did not enhance oral absorption of acyclovir. Instead, chitosan reduced acyclovir absorption in a concentration dependent fashion. Pharmacokinetic parameters affected were not only C_{max}, but also AUC.

Before developing a predictive method for this effect, it is critical to gain mechanistic understanding of the phenomenon. Consequently, alternative hypothesis emerged from that work in order to provide an explanation for the unexpected result. Typically, *in vitro* methods to assess permeability do not include other luminal contents, such as bile salts or intestinal mucus. However, an interaction between the positively charged chitosan and either of these anionic molecules cannot be ruled out. In this study, the effect of chitosan on acyclovir bioaccessability was studied in the TNO gastrointestinal tract model (TIM-1), a multicompartmental *in vitro* apparatus that allows the simulation of not only gastrointestinal transit, but also secretion of fluids containing bicarbonate, electrolytes, digestive enzymes and bile. Acyclovir and chitosan concentrations used in this study corresponded to the doses administered to volunteers in a glass of water (250 ml), following same instructions as in the clinical trial. These were acyclovir 0.8 g/l and chitosan at 1.6 or 4.0 g/l. At different timepoints, acyclovir in solution is withdrawn from the system through dialysis membranes. Therefore, the amount collected can be interpreted the amount of acyclovir available to be dissolved (bioaccessible). On the other hand, the chitosan effect on permeability was studied in diverse *in vitro* permeability models including i) Caco-2 monolayers, ii) Caco-2 monolayers supplemented with type III mucin from porcine stomach, iii) rat jejunum mounted on Ussing-type chamber, and iv) porcine excised jejunum mounted on the inTESTine™ apparatus. These experiments were controlled by measurement of transepithelial resistant and/or use of paracellular markers.

Acyclovir recovered in experiments performed in the TIM-1 apparatus was always greater than 90%, regardless of the concentration of chitosan. Furthermore, the bioaccessibility kinetics showed overlapping profiles for the control and two chitosan treatments. These results suggest that an interaction between chitosan and secretion fluids (including bile, among others) is unlikely to play a role on acyclovir oral absorption.

Concerning to acyclovir permeability in Caco-2 experimental set-up, both chitosan concentrations increased acyclovir permeability from 0.17 to 21 and 24, 10^{-6} cm/s, in good agreement with the evidence largely published in literature. As expected, such a permeability enhancement was accompanied by a reduction in the trans-epithelial resistant, evidencing the opening of tight-junction proteins. However, the presence of a mucus layer on top of the monolayer was able to prevent the permeability enhancer effect. Therefore, it is possible that loosely attached mucus in intestinal lumen prevents chitosan to exert its effect.

Unlike Caco-2 vitro experiments, the use of excised jejunal tissue better resemble the results obtained in the clinical trial. For instance, the presence of chitosan in the inTESTine™ (procine jejunum) slightly decreased the permeability of acyclovir, although this reduction was not statistically different. Notwithstanding, the rat jejunum mounted in the Ussing-type chamber resulted to be the most biopredictive method among those studied in this publication. Acyclovir permeability was reduced from 7.4 to 5.4 and 6.2, 10^{-6} cm/s in presence of chitosan 1.6 and 4 g/l, respectively. The success of jejunum tissue methods may be explained by the greater contribution of paracellular route to total transport compared to Caco-2, on the hand, and due to the constant mucus secretion, on the other. Moreover, enhanced hydrodynamics in Ussing-type chamber experiment (due to stirring) compared to Caco-2 (due to shaking) may also promote the interaction between mucus and chitosan. In fact, recent data generated in our lab suggests that coacervates created as a consequence of such an interaction would entrap part of acyclovir dose, reducing its bioaccesibility. These findings may provide a complete explanation that also includes the effect observed on acyclovir AUC (data not published). Overall, results of this study highlight the importance of accounting for critical luminal contents in diverse *in vitro* set-up in order to correctly predict the *in vivo* outcome. Furthermore, the Ussing-type chamber model using rat jejunum seems an appropriate model to assess a potential excipient effect during drug development stages.

4. PREDICTING PHARMACOKINETICS OF MULTISOURCE ACYCLOVIR ORAL PRODUCTS THROUGH PHYSIOLOGICALLY BASED BIOPHARMACEUTICS MODEL

Original publication	Mauricio A. García, Michael B. Bolger, Sandra Suarez-Sharp, Peter Langguth. **Predicting pharmacokinetics of multisource acyclovir oral products through physiologically based biopharmaceutics modeling**. *Journal of Pharmaceutical Sciences*. 2022;111(1): 262-273 DOI: *doi.org/10.1016/j.xphs.2021.10.013*.
Authorship	First author
Author contribution	Conceptualization, Investigation, Methodology, Formal analysis, Data curation, Writing-original draft preparation, Visualization.

Oral administration of acyclovir products has been associated with high intra-study and between-studies variability. Explanations for such a variability are still not entirely clear as they may be related to physiological aspects, manufacturing variables or both of them. Being a BCS class III, physiological aspects that play significant role on acyclovir oral disposition encompass permeability mechanisms (passive diffusion or paracellular transport), as well as, carrier-mediated transport through biological membranes. Meanwhile, critical manufacturing-related variables may include excipient composition and dissolution rate. This latter parameter is a requisite for biowaiver of BCS class III IR drug products, such that a biowaiver is only acceptable when the drug is very rapidly dissolved (more than 85% of the dose in less than 15 min).

Interestingly, the variability associated to acyclovir disposition does not seem to be greatly influenced by formulations, as indistinct C_{max} and AUC were observed between an oral solution and capsules. Moreover, differences of around 35 to 44% in AUC and C_{max} have been reported for the same product (Zovirax® 400 mg) tested in two different populations (Europeans *vs* Saudi Arabian subjects). Physiological features that explain this discrepancy can be related to expression of either transporters or enzymes involved in acyclovir disposition. Acyclovir is a substrate of several transporters, such as the hOATs sub-family (Km=94 µM, for OAT2), hMATE1 (Km=2640 µM) and hOCT1 (Km= 151 µM). Further, it is partially metabolized by the alcohol dehydrogenase (ADH1) enzyme, mainly expressed in the liver. While population variability of OATs and MATE1 transporters is expected to be low, single nucleotide polymorphism (SNP) of the OCT1 transporter has been previously shown to affect the pharmacokinetics of other BCS class III compound, i.e., metformin. With higher presence of less active OCT1 isoforms in Europeans than in other populations, it is possible that these differences explain acyclovir between studies variability. Moreover, the impact of population variability on acyclovir disposition from formulations with different dissolution profiles also need to be assessed.

In this study, physiologically-based pharmacokinetics (PBPK) modeling was utilized to investigate the interplay between physiological and manufacturing aspects and their effects on acyclovir oral pharmacokinetics. The disposition/elimination model include the ADH1 enzyme (liver and kidney), as well as the MATE1 (liver and kidney efflux), the OAT2 (kidney uptake) and the OCT1 (liver uptake) transporters. Meanwhile, the absorption model included both passive and paracellular diffusion mechanisms. Permeability coefficients were obtained from in-house *in vitro* measurements (Caco-2 and Ussing-type chamber) and converted into human permeabilities by using the respective calibration equation. Differences between populations with normal and reduced OCT1 activity (i.e., Europeans) were accounted by reducing the OCT1 V_{max} in the latter population by 55% (based on average expression of less active

isoforms). Predictability of the model was evaluated by comparing plasma curves predicted to observed clinical data reported in literature. Additionally, the interplay between population variability and differences in dissolution behavior was assessed, as well as its impact on the bioequivalence decision. For that purpose, the dissolution of Zovirax® (reference) and two *in vivo* bioequivalent products (generic A and B) was investigated in simulated stomach and intestinal fluids (SGF and SIF at pH 1.2 and 6.5, respectively). The model was, afterwards, feed with dissolution profiles and plasma curves were predicted for each formulation and population in virtual bioequivalence trials (n=36).

While acceptable prediction of intravenous plasma profiles validated the disposition/elimination model, the absorption model was validated against clinical data for acyclovir strengths of 200 and 400 mg. Permeability estimates calculated from different experimental set-ups were very close to each other (0.22 – 0.31, 10^{-4} cm/s). However, the high sensitivity to permeability parameter demanded for the model to use an intermediate value of 0.29, 10^{-4} cm/s for all simulations. With these parameters set, the influence of the OCT1 V_{max} on acyclovir disposition was assessed by varying the OCT1 V_{max}. In this manner, the model was able to predict the plasma curves of different populations, where a higher OCT1 V_{max} increased acyclovir uptake to the liver, enhanced the hepatobiliary excretion and, hence, reduced overall plasma levels. Therefore, the OCT1 polymorphism can be considered a plausible explanation for the physiologically-related variability.

On the other hand, the *in vitro* dissolution of acyclovir generics was comparatively slower than the reference in both media, such that neither of them fulfilled the regulatory criterion for BCS class III products. Although, both products were deemed bioequivalents after *in vivo* trials. The fastest dissolution profile was observed for Zovirax® in SGF, while the slowest was the generic A in SIF (85% dissolved around 45 min). Interestingly, virtual bioequivalence studies in a cross-over design resulted in bioequivalence in C_{max} and AUC for both generics, regardless of either the dissolution curves used as input or the OCT1 activity. Hence, simulations with this model were consistent with the regulatory decision made for these generic products. Furthermore, findings suggests that manufacturing changes leading to slower dissolution have little impact on acyclovir pharmacokinetics and oral variability. Nonetheless, virtual bioequivalence in a parallel design between normal and reduced-OCT1 activity populations led to a large discrepancy in both C_{max} and AUC, such that the reference product was not bioequivalent to itself. Therefore, the results from this study demonstrated limited relevance of the very-fast dissolution criterion for BCS class III compounds. Moreover, this article emphasizes the potential of PBPK modeling as a tool to assess the performance of formulations that may be erroneously deemed as unsuccessful candidates after not meeting the *in vitro* parameters for dissolution.

Chapter 4. Overall discussion

Pharmacokinetic clinical trials are mandatory at early stages of development in order to screen among different formulations. Since the aim of those studies is to determine the pharmacokinetics of new compounds and/or their safety in humans, healthy volunteers are typically recruited for this purpose. For pharmaceutical industry, clinical trials represent an unavoidable expenditure toward the development of new pharmaceutical products.[2,124] For instance, the time and monetary costs of Phase I trials (to assess pharmacokinetics and safety) for investigational new drugs were estimated to be 18 months and $ 10 million USD, respectively.[1] The exorbitant costs of clinical trials are problematic not only for innovator companies that research and develop new therapeutic agents, but also for generic companies. As stated, there may be several other reasons to conduct this type of studies in the development of generics, such as the bioequivalence testing between two formulations, the demonstration of efficacy/safety for products after post-approval modifications, the evaluation of the effect of food on the performance of the formulation, etc. Furthermore, ethical concerns may arise regarding the overuse of healthy volunteers in testing pharmaceutical products.[125] This point may be exemplified by situations such as, whenever a critical raw material is purchased from a different supplier or whenever a critical manufacturing operation/equipment is modified. In these scenarios, another bioequivalence trial may be requested to assure the efficacy/safety of the new formulation, although the performance of clinical studies after every single manufacturing change is ethically questionable. Therefore, the development of surrogate methodologies to assess the biopharmaceutics through *in vitro* and/or *in silico* methods becomes very attractive for different sectors of pharmaceutical industry in order to reduce the costs and overcome the ethical issues associated with clinical trials.

1. Biopharmaceutic prediction for BCS class II drugs: Carbamazepine and Ibuprofen

In this dissertation, four case studies of IR oral dosage forms were tackled and the possibilities to find biopredicitive methodologies for these products were explored. Two of those products belonged to the BCS class II, i.e., oral absorption is limited by their solubility. According to the Nernst-Brunner equation (eqn. 1.3), the solubility affects directly the dissolution rate, which becomes a rate limiting step toward the absorption for compounds in this BCS class. Consequently, dissolution testing apparatuses detailed in pharmacopeia might be suitable to predict the oral biopharmaceutics for these compounds, provided that dissolution conditions are properly designed to resemble critical *in vivo* features that govern the dissolution. These latter depend not only on the luminal contents, but also on the physical-chemical properties of

the drug (product). For instance, the absence or presence of ionizable groups in this type of molecules leads to different interactions according to the luminal gradient, such that a sub-classification has been previously proposed on basis of their acid/base properties.[55]

On the one hand, carbamazepine is classified as a BCS IIc compound. When designing an *in vivo* predictive dissolution method for this sub-class, it is allowed to overlook some aspects, such as the buffer capacity and pH, because their role on drug dissolution is expected to be negligible compared to other parameters. In fact, carbamazepine solubility demonstrated to be insensitive to different buffers/pH.[126,127] However, the interaction with other luminal contents, i.e., surfactants, becomes more relevant for this drug.[54,128] For instance, carbamazepine solubility increases in presence of bile salts and other surface agents like SLS. The latter agent is included in the pharmacopeial method for carbamazepine IR solid oral dosage forms at a concentration of 1%, suggesting the predictive potential of this method.[76] Interestingly, it was found that nine of out ten studies on IVIVC for carbamazepine products successfully utilized compendial conditions (i.e., SLS 1%). The predictive power of this method seems to rely not only on the increased carbamazepine solubility in SLS-media but also on to enhanced sink conditions. Carbamazepine's high permeability creates an *in vivo* sink where the drug dissolved is withdrawn from the lumen upon dissolution. This appears to be correctly mimicked by the pharmacopeial testing conditions.

On the other hand, ibuprofen is an acidic BCS class II (BCS IIa) drug, hence, the resemblance of luminal buffer capacity is pivotal. Unlike carbamazepine, the pharmacopeial testing conditions for both ibuprofen tablets and suspensions (phosphate buffer 50 mM, pH 7.2)[76] hardly mimic the *in vivo* interactions. Under compendial conditions, the enormous buffer molarity boosts the dissolution rate to a point where differences between products are not accountable. This was true even for lower phosphate molarity/lower pH media (5 – 15 mM, pH 6.0), such that it was not able to detect the differences in the *in vivo* dissolution between suspensions A and B. Conversely, different dissolution curves were observed in bicarbonate buffer (5 – 15 mM, pH 6.0), in very good agreement with the *in vivo* situation. When using *in vitro* bicarbonate media at physiological concentrations, the surface ionization of ibuprofen (which drives its dissolution rate) becomes similar to what occurs within the lumen, and, therefore, the *in vivo* dissolution is more accurately simulated. However, the use of bicarbonate media in the *in vitro* experiment is not straightforward, because of constant gas sparging that is needed to maintain the enhanced buffer capacity as in the bulk of the intestinal lumen.[51] However, the critical parameter to be mimicked is not the buffer composition itself, but the ionization of the drug at the solid surface, as a consequence of the physiological concentrations of bicarbonate.[75] Therefore, the implementation of a surrogate buffer that achieves the same surface ionization (pH_0) is possible. This concept was demonstrated by calculating the

phosphate equivalent molarities of 1 and 2 mM, which resembled bicarbonate concentrations of 5 and 15 mM, respectively. The close match between dissolution in bicarbonate and the surrogate media brings a new opportunity for the development of biopredicitive dissolution testing for low soluble ionizable drugs, with great potential for regulatory and industrial applications (See below).

2. Biopharmaceutic prediction for BCS class III drug products: Acyclovir

Compounds belonging to the BCS class III have an oral absorption limited by their permeability. As a consequence, a major contribution of the intestinal transit time, paracellular permeation and/or carrier-mediated transport to their absorption/disposition is expected. Even though they are mainly dependent on the physiology of each subject, there are still concerns on the impact of excipient/dosage form to drug disposition, if the formulation has any influence on the aforementioned processes.[9] In this manuscript, the interplay between physiological and formulation aspects was assessed using acyclovir as a BCS class III model compound. Likewise, the oral biopharmaceutics for acyclovir were predicted through *in vitro* and *in silico* methods for different scenarios, namely the effect of excipients, transporters and dissolution.

Some pharmaceutical excipients used commonly on IR oral solid dosage forms have significant effect on drug permeability across different experimental models.[64,129–131] However, *in vivo* experimentation is still required to correctly assess the true outcome in humans. Several research has been conducted on the excipient potential of chitosan, where it has shown to consistently enhance the permeability of low permeable compounds (Table 2). Notwithstanding, our working group recently demonstrated that chitosan actually reduced acyclovir bioavailability in humans.[60] In the present work, acyclovir permeability was assayed across different permeability experimental set-ups to simulate the *in vivo* findings in an *in vitro* test. While mucus free experiments completely mispredicted this effect, the mucus-containing set-up provided much better matches to the findings from the clinical trial. Because of the high sensitivity to permeability, typical permeability *in vitro* tests based on epithelial monolayers may exaggerate such an effect, with the experimental model overestimating the role of the excipient.[130,132] In the *in vivo* situation, the intestinal lumen is protected by two mucus layers that cover the intestinal wall and prevent it against possible damaging agents.[98] Therefore, supplementing the Caco-2 model with an artificial mucus layer neutralized the effect of chitosan. Furthermore, the Ussing-chamber model caused the most accurate predictions of the *in vivo* observations, most likely because of both the constant mucus secretion from rat jejunal tissue and the promoted interaction between chitosan and mucus under the testing conditions.

Sensitivity to permeability was not only an issue in the *in vitro* methodologies, but also in the *in silico* simulations. For instance, the PBPK model here constructed predicted large changes in acyclovir C_{max} when little variations were made on the initial permeability estimates Moreover, parameter sensitivity analysis also revealed the importance of this parameter to predict the pharmacokinetics of acyclovir IR dosage forms. Therefore, the results here presented throw some warnings about the extrapolation from *in vitro* permeability to *in vivo* predictions. On the one hand, the inclusion of mucus in the *in vitro* model appears to be key to correctly predict the change in permeability. Hence, data produced in mucus-containing set-ups may improve the predictability of PBPK models. On the other hand, the mucus layer has been overlooked by PBPK modeling software, thus mechanistic simulations for this phenomenon are still missing. Accounting for these points might expand the use of PBPK modeling towards successfully predicting the effect of excipients.

The pharmacokinetics of poorly permeable compounds might also be greatly altered by the role of drug transporters. In the case of acyclovir, large disposition variability has been reported even when the same product is administered to different populations.[110,117,133] The OCT1 transporter expressed in the basal membrane of the liver was hypothesized to play a major role on acyclovir disposition, such that population-related variability may be explained by changes in transporter activity (due to i.e., polymorphism and/or disease state). In fact, it was possible to predict these scenarios when modeling alterations in OCT1 V_{max} in a PBPK model. Although this factor was key to understand the population-related variability in acyclovir pharmacokinetics, the impact of OCT1 activity on the comparative bioavailability of two acyclovir multisource products (e.g. bioequivalence assessment) seems to be negligible, provided a cross-over designed is granted.

With permeability being the limiting factor for the absorption of BCS III drugs, the role of dissolution is limited when the release occurs much faster than permeability (provided the lack of dramatic segmental permeability variation).[4] This aspect was captured by the PBPK model here developed, where the bioequivalence of two multisource generics to the reference was correctly predicted, in spite of displaying statistical differences in dissolution curves ($f2<50$). This demonstrates the limited relevance of the dissolution criteria in predicting the performance of BCS III IR oral dosage forms.

3. Regulatory implications

Current guidelines do not recommend BCS-based biowaivers for the class II, unless an IVIVC is successfully developed.[68,69] The carbamazepine case discussed in this manuscript demonstrates that IVIVCs are possible if key processes, such as the *in vivo* sink, are accounted

in the *in vitro* method. However, this example may be difficult to generalize. Carbamazepine solubility depended on the SLS concentration in media in the range 0.1 – 1%,[128] suggesting that SLS concentration would play a role on the detection capacity of this method. Further, the more meaningful SLS concentrations might change from drug-to-drug, meaning that finding the more appropriate testing conditions would require a semi-empirical approach, such that *in vivo* testing is still mandatory.

On the other hand, the biowaivers for BCS class IIa has been previously suggested. The argument for this has been the “pseudo-BCS I” behavior for this sub-class after the drug reaches the intestinal environment. However, the shortcoming in detecting bio-inequivalences when using typical biowaiver media (based on compendial buffers) is a major concern.[57] Remarkably, a biopredictive method was developed in this work, utilizing bicarbonate as dissolution medium. Even though the gas sparging associated with the use of bicarbonate media carries some difficulties (i.e., incompatibility with surfactants and validation/reproducibility concerns), this can be solved if a surrogate buffer is appropriately designed. This was carried out by applying mechanistic modeling for both diffusion and ionization in either typical or bicarbonate-based buffers.[74,75] Unlike the biorelevant bicarbonate media, a surrogate buffer overcomes the aforementioned challenges, while mimicking bicarbonate biorelevance at the same time. Therefore, the mechanistic design of surrogate buffers with an appropriate discrimination capacity might play a role in re-opening the discussion on biowaivers for the BCS class IIa sub-class.

With respect to the BCS class III, biowaivers are possible if: i) the formulation is qualitatively the same as the reference and quantitatively similar (difference< 10%) and ii) the dosage forms is very rapidly dissolved (>85% in 15 min).[69] The first point relates directly to the sensitivity to permeability and the potential effect of excipients on this process, while the second is associated with the interplay between dissolution and permeation rate. The results obtained in this dissertation support the conservative spirit of regulators for the effect of excipients. The prediction of the effect of chitosan was not straightforward and demanded the performance of *in vitro* techniques that are not mentioned in the international guidelines (Rat jejunum mounted on an Ussing-type chamber). Conversely, the outcomes regarding to the dissolution of BCS class III drugs suggest that the current criteria may be still over-discriminative. For instance, the pharmacokinetics of the slowest dissolving acyclovir generic (>85% in 45 min) was predicted not to differ from the reference product (>85% in 15 min), which is in good agreement with the *in vivo* observation. The bioequivalence decision was not influenced by the effect of the potential OCT1 polymorphism on acyclovir pharmacokinetics. Taken together, these findings may expand the use of PBPK modeling in supporting BCS-biowaiver applications for BCS class III IR oral solid dosage forms. Moreover, the importance of conducting

bioequivalence studies in a cross-over design, instead of a parallel design, was also endorsed in the light of these results.

4. Opportunities for pharmaceutical industry

While this thesis has regulatory implications (as mentioned above), it also showcases some opportunities for the pharmaceutical industry. The prediction of oral biopharmaceutics for IR dosage forms has great potential, especially during early stages of drug development.[134] For instance, the rational choice of biopredictive conditions for predicting *in vivo* dissolution of ibuprofen suspensions applied in this work can be replicated for other BCS IIa drugs. Having a biopredictive dissolution method would allow to guide rationally the development processes, such that the formulation can be optimized in order to match the desired dissolution rate (e.g., by modifying the particle size). Furthermore, this shows utility also for the generic industry, because biopredictive methods may be used to screen formulations and select the most promising candidate before going to bioequivalence trials. One adversity of setting biopredictive media for this type of compounds is the handling of bicarbonate as *in vitro* dissolution media.[56] Bicarbonate dissolution system can be challenging to set for some generic companies and difficult to validate. However, a strategy to develop surrogate media was shown in this work, as well. It can be anticipated that the introduction of the concept of surrogate media in pharmaceutical industry may be an efficient pathway to reduce monetary and temporary costs related to drug development.

Conversely, the dissolution of BCS class III drugs is considerably less relevant than their permeability. Although, the regulatory criterion for dissolution is still restrictive. This disjunctive may produce a manufacturer risk, where the company might discard a truly successful formulation because it did not satisfy the regulatory requirement (false negative). In this regard, PBPK modeling and simulations can be useful to predict the impact of dissolution in the pharmacokinetics. Furthermore, PBPK modeling may be of great utility to predict the biopharmaceutics of drugs that need to be tested in patients (i.e., oral antineoplastic). For this type of drugs, the recruitment of subjects for experimentation is more problematic than healthy volunteers. Moreover, cancer patients may have altered protein expression due to their disease conditions (e.g., diminished OCT1-activity).[135] Therefore, the correct application of PBPK modeling, as it was shown in this manuscript, may be helpful in gaining confidence in the formulation that is going to be selected for clinical trials in special populations.

Lastly, the effect of critical excipients is an issue for the BCS class III. Even though Caco-2 cells are generally accepted for permeability classification,[68,69] the lack of protective mucus increases the sensitivity of this experimental set-up to the effect of some permeability

enhancers. This fact may mislead the pharmaceutical development of a given product by equivocally suggesting an enhanced drug bioavailability (false positive). Hence, a more biopredictive test may be needed to better predict the performance of the product before failing the clinical trial. It was depicted in the present work that mucus-containing permeability experiments not only attenuated the permeability enhancer effect, but also led to obtain greater predictions of the *in vivo* scenario (i.e., Rat jejunum mounted on a Ussing-type chamber). The use of this test at early stages of drug development could then prevent both money and time wasting toward the development of new oral formulations.

Chapter 5. Conclusion

The potential of different biopharmaceutic predictive methods for immediate release dosage forms was assessed. Case studies were analyzed and discussed on predicting the oral absorption for BCS class II (carbamazepine and ibuprofen) or III compounds (excipient effect and physiology/formulation interplay for acyclovir).

The risk of waiving the *in vivo* studies for carbamazepine IR products was deemed high, due to i) its BCS class II classification and ii) its narrow therapeutic index. However, sound evidence was found on the strength of the compendial method (USP apparatus II, 75 rpm, 900 ml of 1% SLS) to detect bio-inequivalences. These conditions were further successfully used to develop IVIVCs for carbamazepine IR products.

A biopredictive method for ibuprofen (where the compendial method is inappropriate) intestinal dissolution was successfully developed. *In vitro* bicarbonate media at physiologically relevant concentrations matched the deconvoluted *in vivo* dissolution. Moreover, mechanistic modeling of pH_0 enabled the development of surrogate media based on phosphate buffer at concentrations between 1 – 2 mM, which correctly predicted the *in vivo* observation.

The negative effect of chitosan on acyclovir bioavailability was investigated through *in vitro* methodologies. *In vivo* findings were mainly explained by luminal presence of mucus, such that it would interact with chitosan reducing acyclovir permeation. The Ussing-type chamber set-up mounted with excised rat jejunum was the most biopredictive method among those studies.

Pharmacokinetic variability observed with acyclovir multisource products was investigated from a physiological and technological perspective. The interaction between these aspects was studied with PBPK modeling techniques. The model suggests that OCT1 polymorphism is a plausible explanation for the observed variability rather than dissolution of the tablets. Moreover, the bioequivalence of the products was correctly predictive with this *in silico* method.

The case studies presented in this dissertation showcase possible approaches that may be used to advance towards biopredictive methodologies for immediate release dosage forms. Furthermore, these methods have great potential in pharmaceutical industry, which might ultimately result in saving time and money through reducing the number of clinical trials carried out during drug development stages.

References

1. Zivin JA. Understanding Clinical Trials. Sci Am. 2000;282:69–75.

2. Bentley C, Cressman S, van der Hoek K, Arts K, Dancey J, Peacock S. Conducting clinical trials—costs, impacts, and the value of clinical trials networks: A scoping review. Clin Trials. 2019;16:183–93.

3. Krishna R, Yu L. Biopharmaceutics Applications in Drug Development. Krishna R, Yu L, editors. Nwe York, NY: Springer US; 2008.

4. Amidon GL, Lennernäs H, Shah VP, Crison JR. A Theoretical Basis for a Biopharmaceutic Drug Classification: The Correlation of In Vitro Drug Product Dissolution and in Vivo Bioavailability. Pharm Res. 1995;12:413–20.

5. CDER/FDA. Guidance for Industry Bioavailability and Bioequivalence Studies for Orally Administered Drug Products — General Guidance for Industry Bioavailability and Bioequivalence. FDA Guid. 2002;1–24.

6. Ph. Eur., European directorate for the quality of Medicines & Health Care (EDQM). European Pharamcopeia. 9th Ed. Leipzig: C.H.Beck, Nördlingen; 2017.

7. MacKenzie-Smith L, Marchi P, Thorne H, Timeus S, Young R, Le Calvé P. Patient Preference and Physician Perceptions of Patient Preference for Oral Pharmaceutical Formulations: Results from a Real-Life Survey. Inflamm Intest Dis. 2018;3:43–51.

8. Kurczewska-michalak M, Kardas P, Czajkowski M. Patients' preferences and willingness to pay for solid forms of oral medications—results of the discrete choice experiment in polish outpatients. Pharmaceutics. 2020;12.

9. Flanagan T. Potential for pharmaceutical excipients to impact absorption : A mechanistic review for BCS Class 1 and 3 drugs. Eur J Pharm Biopharm. Elsevier; 2019;141:130–8.

10. Pepin XJH, Parrott N, Dressman J, Delvadia P, Mitra A, Zhang X, et al. Current State and Future Expectations of Translational Modeling Strategies to Support Drug Product Development, Manufacturing Changes and Controls: A Workshop Summary Report. J Pharm Sci. Elsevier Ltd; 2021;110:555–66.

11. Weitschies W, Cardini D, Karaus M, Trahms L, Semmler W. Magnetic marker monitoring of esophageal, gastric and duodenal transit of non-disintegrating capsules. Pharmazie. 1999;54:426–30.

12. Grimm M, Koziolek M, Kühn JP, Weitschies W. Interindividual and intraindividual variability of fasted state gastric fluid volume and gastric emptying of water. Eur J Pharm Biopharm.

2018;127:309–17.

13. Mudie DM, Murray K, Hoad CL, Pritchard SE, Garnett MC, Amidon GL, et al. Quantification of gastrointestinal liquid volumes and distribution following a 240 mL dose of water in the fasted state. Mol Pharm. 2014;11:3039–47.

14. Schiller C, Fröhlich CP, Giessmann T, Siegmund W, Mönnikes H, Hosten N, et al. Intestinal fluid volumes and transit of dosage forms as assessed by magnetic resonance imaging. Aliment Pharmacol Ther. 2005;22:971–9.

15. Vinarov Z, Abdallah M, Agundez JAG, Allegaert K, Basit AW, Braeckmans M, et al. Impact of gastrointestinal tract variability on oral drug absorption and pharmacokinetics: An UNGAP review. Eur J Pharm Sci. 2021;162.

16. Netter FH. Atlas of Human Anatomy. 4th Editio. Barcelona, España: Elsevier Doyma S.L.; 2007.

17. Sjögren E, Abrahamsson B, Augustijns P, Becker D, Bolger MB, Brewster M, et al. In vivo methods for drug absorption – Comparative physiologies, model selection, correlations with in vitro methods (IVIVC), and applications for formulation/API/excipient characterization including food effects. Eur J Pharm Sci. 2014;57:99–151.

18. Koziolek M, Grimm M, Schneider F, Jedamzik P, Sager M, Kühn JP, et al. Navigating the human gastrointestinal tract for oral drug delivery: Uncharted waters and new frontiers. Adv Drug Deliv Rev. Elsevier B.V.; 2016;101:75–88.

19. Deloose E, Janssen P, Depoortere I, Tack J. The migrating motor complex: Control mechanisms and its role in health and disease. Nat Rev Gastroenterol Hepatol. Nature Publishing Group; 2012;9:271–85.

20. Kostewicz ES, Abrahamsson B, Brewster M, Brouwers J, Butler J, Carlert S, et al. In vitro models for the prediction of in vivo performance of oral dosage forms. Eur J Pharm Sci. Elsevier B.V.; 2014;57:342–66.

21. Hounnou G, Destrieux C, Desmé J, Bertrand P, Velut S. Anatomical study of the length of the human intestine. Surg Radiol Anat. 2002;24:290–4.

22. Amidon GL, Lee PI, Topp EM. Transport processes in pharmaceutical systems. Transp. Process. Pharm. Syst. 1999.

23. Sugano K. Biopharmaceutics Modeling and Simulations. Biopharm. Model. Simulations. 2012.

24. Helander HF, Fändriks L. Surface area of the digestive tract-revisited. Scand J

Gastroenterol. 2014;49:681–9.

25. Abuhelwa AY, Foster DJR, Upton RN. A Quantitative Review and Meta-models of the Variability and Factors Affecting Oral Drug Absorption—Part II: Gastrointestinal Transit Time. AAPS J. 2016;18:1322–33.

26. McConnell EL, Fadda HM, Basit AW. Gut instincts: Explorations in intestinal physiology and drug delivery. Int J Pharm. 2008;364:213–26.

27. Davis SS, Hardy JG, Fara JW. Transit of pharmaceutical dosage forms through the small intestine. Gut. 1986;27:886–92.

28. Weitschies W, Kosch O, Mönnikes H, Trahms L. Magnetic Marker Monitoring: An application of biomagnetic measurement instrumentation and principles for the determination of the gastrointestinal behavior of magnetically marked solid dosage forms. Adv Drug Deliv Rev. 2005;57:1210–22.

29. Kalantzi L, Goumas K, Kalioras V, Abrahamsson B, Dressman JB, Reppas C. Characterization of the human upper gastrointestinal contents under conditions simulating bioavailability/bioequivalence studies. Pharm Res. 2006;23:165–76.

30. Lindahl A, Ungell AL, Knutson L, Lennernäs H. Characterization of fluids from the stomach and proximal jejunum in men and women. Pharm. Res. 1997. p. 497–502.

31. Dressman JB, Berardi RR, Dermentzoglou LC, Russell TL, Schmaltz SP, Barnett JL, et al. Upper Gastrointestinal (GI) pH in Young, Healthy Men and Women. Pharm. Res. An Off. J. Am. Assoc. Pharm. Sci. 1990. p. 756–61.

32. Koziolek M, Grimm M, Becker D, Iordanov V, Zou H, Shimizu J, et al. Investigation of pH and Temperature Profiles in the GI Tract of Fasted Human Subjects Using the Intellicap® System. J Pharm Sci. Elsevier Masson SAS; 2015;104:2855–63.

33. Karamanolis G, Theofanidou I, Yiasemidou M, Giannoulis E, Triantafyllou K, Ladas SD. A glass of water immediately increases gastric pH in healthy subjects. Dig Dis Sci. 2008;53:3128–32.

34. Larhed AW, Artursson P, Björk E. The influence of gastrointestinal mucus [Internet]. Pharm. Res. 1998. p. 66–71.

35. Hang HC, Bertozzi CR. The chemistry and biology of mucin-type O-linked glycosylation. Bioorganic Med Chem. 2005;13:5021–34.

36. Turner BS, Bhaskar KR, Hadzopoulou-Cladaras M, Lamont JT. Cysteine-rich regions of pig gastric mucin contain von Willebrand factor and cystine knot domains at the carboxyl

terminaL. Biochim Biophys Acta - Gene Struct Expr. 1999;1447:77–92.

37. Lemmens G, Van Camp A, Kourula S, Vanuytsel T, Augustijns P. Drug disposition in the lower gastrointestinal tract: Targeting and monitoring. Pharmaceutics. 2021;13.

38. Ensign LM, Cone R, Hanes J. Oral drug delivery with polymeric nanoparticles: The gastrointestinal mucus barriers. Adv Drug Deliv Rev. Elsevier B.V.; 2012;64:557–70.

39. Georgiades P, Pudney PDA, Thornton DJ, Waigh TA. Particle tracking microrheology of purified gastrointestinal mucins. Biopolymers. 2014;101:366–77.

40. Cone RA. Barrier properties of mucus. Adv Drug Deliv Rev. Elsevier B.V.; 2009;61:75–85.

41. Prieto S, Marti JM, Pen N. Assessment of Biliary Bicarbonate Secretion. 1999;167–72.

42. Wang Z, Petrovic S, Mann E, Soleimani M. Identification of an apical Cl-/HCO3- exchanger in the small intestine. Am J Physiol Liver. 2002;282:G573–9.

43. Gleeson D. Acid-base transport systems in gastrointestinal epithelia. Gut. 1992;33:1134–45.

44. Repishti M, Hogan DL, Pratha V, Davydova L, Donowitz M, Tse CM, et al. Human duodenal mucosal brush border Na+/H+ exchangers NHE2 and NHE3 alter net bicarbonate movement. Am J Physiol - Gastrointest Liver Physiol. 2001;281:159–63.

45. Banwell JG, Gorbach SL, Pierce NF, Mitra R, Mondal A. Acute undifferentiated human diarrhea in the tropics. II. Alterations in intestinal fluid and electrolyte movements. J Clin Invest. 1971;50:890–900.

46. Meineke I, De Mey C, Eggers R, Bauer FE. Evaluation of the 13CO2 kinetics in humans after oral application of sodium bicarbonate as a model for breath testing. Eur J Clin Invest. 1993;23:91–6.

47. Ibekwe VC, Fadda HM, McConnell EL, Khela MK, Evans DF, Basit AW. Interplay between intestinal pH, transit time and feed status on the in vivo performance of pH responsive ileo-colonic release systems. Pharm Res. 2008;25:1828–35.

48. Diakidou A, Vertzoni M, Goumas K, Söderlind E, Abrahamsson B, Dressman J, et al. Characterization of the contents of ascending colon to which drugs are exposed after oral administration to healthy adults. Pharm Res. 2009;26:2141–51.

49. Fadda HM, Basit AW. Dissolution of pH responsive formulations in media resembling intestinal fluids: Bicarbonate versus phosphate buffers. J Drug Deliv Sci Technol. Elsevier Masson SAS; 2005;15:273–9.

50. Reppas C, Karatza E, Goumas C, Markopoulos C, Vertzoni M. Characterization of Contents of Distal Ileum and Cecum to Which Drugs/Drug Products are Exposed during Bioavailability/Bioequivalence Studies in Healthy Adults. Pharm Res. 2015;32:3338–49.

51. Al-Gousous J, Sun KX, McNamara DP, Hens B, Salehi N, Langguth P, et al. Mass Transport Analysis of the Enhanced Buffer Capacity of the Bicarbonate-CO2 Buffer in a Phase-Heterogenous System: Physiological and Pharmaceutical Significance. Mol Pharm. 2018;15:5291–301.

52. Moreno MP de la C, Oth M, Deferme S, Lammert F, Tack J, Dressman J, et al. Characterization of fasted-state human intestinal fluids collected from duodenum and jejunum. J Pharm Pharmacol. 2010;58:1079–89.

53. Dahlgren D, Venczel M, Ridoux JP, Skjöld C, Müllertz A, Holm R, et al. Fasted and fed state human duodenal fluids: Characterization, drug solubility, and comparison to simulated fluids and with human bioavailability. Eur J Pharm Biopharm. 2021;163:240–51.

54. Söderlind E, Karlsson E, Carlsson A, Kong R, Lenz A, Lindborg S, et al. Simulating Fasted Human Intestinal Fluids. Mol Pharm. 2010;

55. Tsume Y, Mudie DM, Langguth P, Amidon GE, Amidon GL. The Biopharmaceutics Classification System: Subclasses for in vivo predictive dissolution (IPD) methodology and IVIVC. Eur J Pharm Sci. Elsevier B.V.; 2014;57:152–63.

56. Sheng JJ, McNamara DP, Amidon GL. Toward an In Vivo dissolution methodology: A comparison of phosphate and bicarbonate buffers. Mol Pharm. 2009;6:29–39.

57. Álvarez C, Núñez I, Torrado JJ, Gordon J, Potthast H, García-Arrieta A. Investigation on the Possibility of Biowaivers for Ibuprofen. J Pharm Sci. 2011;100:2343–9.

58. Shohin IE, Kulinich JI, Vasilenko GF, Ramenskaya G V. Interchangeability evaluation of multisource ibuprofen drug products using biowaiver procedure. Indian J Pharm Sci. 2011;73:443–6.

59. Vaithianathan S, Haidar SH, Zhang X, Jiang W, Avon C, Dowling TC, et al. Effect of Common Excipients on the Oral Drug Absorption of Biopharmaceutics Classification System Class 3 Drugs Cimetidine and Acyclovir. J Pharm Sci. Elsevier Ltd; 2016;105:996–1005.

60. Kubbinga M, Nguyen MA, Staubach P, Teerenstra S, Langguth P. The influence of chitosan on the oral bioavailability of acyclovir - A comparative bioavailability study in humans. Pharm Res. 2015;32:2241–9.

61. Dahlgren D, Roos C, Johansson P, Tannergren C, Lundqvist A, Langguth P, et al. The effects of three absorption-modifying critical excipients on the in vivo intestinal absorption of

six model compounds in rats and dogs. Int J Pharm. Elsevier; 2018;547:158–68.

62. Soodvilai S, Soodvilai S, Chatsudthipong V, Ngawhirunpat T, Rojanarata T, Opanasopit P. Interaction of pharmaceutical excipients with organic cation transporters. Int J Pharm. Elsevier B.V.; 2017;520:14–20.

63. Otter M, Oswald S, Siegmund W, Keiser M. Effects of frequently used pharmaceutical excipients on the organic cation transporters 1–3 and peptide transporters 1/2 stably expressed in MDCKII cells. Eur J Pharm Biopharm. Elsevier B.V.; 2017;112:187–95.

64. Gurjar R, Chan CYS, Curley P, Sharp J, Chiong J, Rannard S, et al. Inhibitory Effects of Commonly Used Excipients on P-Glycoprotein in Vitro. Mol Pharm. American Chemical Society; 2018;15:4835–42.

65. Jamei M, Abrahamsson B, Brown J, Bevernage J, Bolger MB, Heimbach T, et al. Current status and future opportunities for incorporation of dissolution data in PBPK modeling for pharmaceutical development and regulatory applications: OrBiTo consortium commentary. Eur J Pharm Biopharm. Elsevier; 2020;155:55–68.

66. Khoshakhlagh P, Johnson R, Langguth P, Nawroth T, Schmueser L, Hellmann N, et al. Fasted-State Simulated Intestinal Fluid “faSSIF-C”, a Cholesterol Containing Intestinal Model Medium for in Vitro Drug Delivery Development. J Pharm Sci. 2015;104:2213–24.

67. European Medicines Agency (EMA)., COMMITEE FOR MEDICINAL PRODUCTS FOR HuMAN USE (CHMP). GUIDELINE ON THE INVESTIGATION OF BIOEQUIVALENCE DISCUSSION. Guidel. Investig. BIOEQUIVALENCE Discuss. 2010.

68. U.S. Department of Health and Human Services Food and Drug Administration Center for Evaluation and Research (CDER). [Internet]. Guid. Ind. Waiv. Vivo Bioavailab. Bioequivalence Stud. Immed. Solid Oral Dos. Forms Based a Biopharm. Classif. Syst. 2017.

69. INTERNATIONAL COUNCIL FOR HARMONISATION OF TECHNICAL REQUIREMENTS FOR PHARMACEUTICALS FOR HUMAN USE (ICH). ICH HARMONISED GUIDELINE: BIOPHARMACEUTICS CLASSIFICATION SYSTEM-BASED BIOWAIVERS M9. 2019.

70. Moore JW, Flanner HH. Mathematical Comparison of Dissolution Profiles. Pharm Technol. 1996;June:64–74.

71. Fick A. On liquid diffusion (Reprint of the original 1855 article). J Memb Sci. 1995;100:33–8.

72. Nernst W. Theorie der Reaktionsgeschwindigkeit in heterogenen Systemen. Zeitschrift für Physiol Chemie. 1904;47:52–5.

73. Mooney KG, Mintun MA, Himmelstein KJ, Stella VJ. Dissolution kinetics of carboxylic acids I: Effect of pH under unbuffered conditions. J Pharm Sci. 1981;70:13–22.

74. Mooney KG, Mintun MA, Himmelstein KJ, Stella VJ. Dissolution kinetics of carboxylic acids II: Effect of Buffers. J Pharm Sci. 1981;70:22–32.

75. Al-Gousous J, Salehi N, Amidon GE, Zi RM, Langguth P, Amidon GL. Mass Transport Analysis of Bicarbonate Buffer: Effect of the CO2 − H2CO3 Hydration − Dehydration Kinetics in the Fluid Boundary Layer and the Apparent Effective pKa Controlling Dissolution of Acids and Bases. Mol Pharm. 2019;16:2626–35.

76. The U.S. Pharmacopeial Convention. U.S. Pharmacopeia National Formulary. USP 42 NF 37. 37th ed. Rockville, MD: The United States Pharmacopeial convention; 2019.

77. Silva DA, Al-Gousous J, Davies NM, Chacra NB, Webster GK, Lipka E, et al. Biphasic dissolution as an exploratory method during early drug product development. Pharmaceutics. 2020;12:1–17.

78. Bermejo M, Meulman J, Davanço MG, Carvalho P de O, Gonzalez-Alvarez I, Campos DR. In vivo predictive dissolution (Ipd) for carbamazepine formulations: Additional evidence regarding a biopredictive dissolution medium. Pharmaceutics. 2020;12:1–21.

79. González-García I, Mangas-Sanjuan V, Merino-Sanjuán M, Álvarez-Álvarez C, Díaz-Garzón Marco J, Rodrí-Guez-Bonnín MA, et al. IVIVC approach based on carbamazepine bioequivalence studies combination. Pharmazie. 2017;72:449–55.

80. Kovaĉević I, Parojĉić J, Homŝek I, Tubić-Grozdanis M, Langguth P. Justification of biowaiver for carbamazepine, a low soluble high permeable compound, in solid dosage forms based on IVIVC and gastrointestinal simulation. Mol Pharm. 2009;6:40–7.

81. Al-Gousous J, Amidon GL, Langguth P. Toward Biopredictive Dissolution for Enteric Coated Dosage Forms. Mol Pharm. 2016;13:1927–36.

82. Amaral Silva D, Davies NM, Doschak MR, Al-Gousous J, Bou-Chacra N, Löbenberg R. Mechanistic understanding of underperforming enteric coated products: Opportunities to add clinical relevance to the dissolution test. J Control Release. Elsevier; 2020;325:323–34.

83. Goyanes A, Hatton GB, Merchant HA, Basit AW. Gastrointestinal release behaviour of modified-release drug products: Dynamic dissolution testing of mesalazine formulations. Int J Pharm. Elsevier B.V.; 2015;484:103–8.

84. Garbacz G, Kołodziej B, Koziolek M, Weitschies W, Klein S. A dynamic system for the simulation of fasting luminal pH-gradients using hydrogen carbonate buffers for dissolution testing of ionisable compounds. Eur J Pharm Sci. Elsevier B.V.; 2014;51:224–31.

85. Al-Gousous J, Ruan H, Blechar JA, Sun KX, Salehi N, Langguth P, et al. Mechanistic analysis and experimental verification of bicarbonate-controlled enteric coat dissolution: Potential in vivo implications. Eur J Pharm Biopharm. Elsevier; 2019;139:47–58.

86. Krieg BJ, Taghavi SM, Amidon GL, Amidon GE. In Vivo Predictive Dissolution : Comparing the Effect of Bicarbonate and Phosphate Buffer on the Dissolution of Weak Acids and Weak Bases. J Pharm Sci. Elsevier Masson SAS; 2015;104:2894–904.

87. Sinko PJ, Singh Y. Martin's Physical Pharmacy and Pharmaceutical Sciences: physical chemical and biopharmaceutical principles in the pharmaceutical sciences. 6th Editio. Sinko PJ, Singh Y, editors. Baltimore, MD. Philadelphia, PA: Lippincott Williams & Wilkins, a Wolters Kluwer business; 2011.

88. Jamhekar SS, Breen PJ. Basic Pharmacokinetics. 1st ed. Padstow, Cornwall, Great Britain: Pharamceutical Press, RPS Publishing; 2009.

89. Adson A, Raub TJ, Burton PS, Barsuhn CL, Hilgers AR, Ho NFH, et al. Quantitative approaches to delineate paracellular diffusion in cultured epithelial cell monolayers. J Pharm Sci. 1994;83:1529–36.

90. He Z. Theoretical Effects of Molecular Dimension and Configuration on Effective Diffusion Coefficient of Macromolecules in Microporous Membranes. Trans Tianjin Univ. 1995;1:42–7.

91. Lennernäs H. Regional intestinal drug permeation: Biopharmaceutics and drug development. Eur J Pharm Sci. 2014;57:333–41.

92. Dahlgren D, Roos C, Sjögren E, Lennernäs H. Direct in Vivo Human Intestinal Permeability (Peff) Determined with Different Clinical Perfusion and Intubation Methods. J Pharm Sci. 2015;104:2702–26.

93. Irvine JD, Takahashi L, Lockhart K, Cheong J, Tolan JW, Selick HE, et al. MDCK (Madin-Darby canine kidney) cells: A tool for membrane permeability screening. J Pharm Sci. 1999;88:28–33.

94. Hidalgo IJ, Raub TJ, Borchardt RT. Characterization of the Human Colon Carcinoma Cell Line (Caco-2) as a Model System for Intestinal Epithelial Permeability. Gastroenterology. 1989;96:736–49.

95. Artursson P, Ungell A-L, Löfroth J-E. Selective Paracellular Permeability in Two Models of Intestinal Absorption: Cultured Monolayers of Human Intestinal Epithelial Cells and Rat Intestinal Segments. J Pharm Sci. 1993;10:1123–9.

96. Heinen C, Reuss S, Saaler-reinhardt S, Langguth P. Mechanistic basis for unexpected bioavailability enhancement of polyelectrolyte complexes incorporating BCS class III drugs and

carrageenans. Eur J Pharm Biopharm. Elsevier B.V.; 2013;85:26–33.

97. Ruiz-Picazo A, Colón-Useche S, Perez-Amorós B, González-álvarez M, Molina-Martínez I, González-álvarez I, et al. Investigation to explain bioequivalence failure in pravastatin immediate-release products. Pharmaceutics. 2019;11:1–10.

98. Schipper NGM, Vårum KM, Stenberg P, Ocklind G, Lennernäs H, Artursson P. Chitosans as absorption enhancers of poorly absorbable drugs. 3: Influence of mucus on absorption enhancement. Eur J Pharm Sci. 1999;8:335–43.

99. Wagner JG, Nelson E. Per cent absorbed time plots derived from blood level and/or urinary excretion data. J Pharm Sci. 1963;52:610–1.

100. Loo JCK, Riegelman S. New Method for Calculating the Intrinsic Absorption Rate of Drugs. J Pharm Sci. 1968;57:918–28.

101. Langenbucher F. Linearization of dissolution rate curves by the Weibull distribution. J Pharm Pharmacol. 1972;24:979–81.

102. Poulin P, Theil FP. Prediction of pharmacokinetics prior to in vivo studies. 1. Mechanism-based prediction of volume of distribution. J Pharm Sci. 2002;91:129–56.

103. Yu LX, Crison JR, Amidon GL. Compartmental transit and dispersion model analysis of small intestinal transit flow in humans. Int J Pharm. 1996;140:111–8.

104. Yu LX, Amidon GL. A compartmental absorption and transit model for estimating oral drug absorption. Int J Pharm. 1999;186:119–25.

105. World Health Orgnization. WHO Model List of Essential Medicines. twentieth ed. World Health Organization. 21st Ed. World Heal. Organ. 2019. p. https://www.who.int/medicines/publications/essent.

106. Bialer M, Levy R, Perucca E. Does carbamazepine have a narrow therapeutic plasma concentration range? Ther Drug Monit. 1998;20:56–9.

107. Hofmann M, Thieringer F, Ahn M, Månsson W, Robert P, Langguth P. A novel technique for intraduodenal administration of drug suspensions/solutions with concurrent pH monitoring applied to ibuprofen formulations. Eur J Pharm Biopharm. Elsevier; 2019;136:192–202.

108. Józef Synowiecki, Nadia Ali Al-Khateeb. Production, Properties, and Some New Applications of Chitin and Its Derivatives. Crit Rev Food Sci Nutr. 2003;43:27.

109. Schipper NGM, Olson S, Hoogstraate JA, DeBoer AG, Vårum KM, Artursson P. Chitosans as Absorption Enhancers for Poorly Absorbable Drugs 2: Mechanism of Absorption Enhancement. Pharm Res. 1997;14:923–9.

110. Vergin H, Kikuta C, Mascher H, Metz R. Pharmacokinetics and bioavailability of different formulations of aciclovir. Arzneimittelforschung. 1995;45:508–15.

111. Meadows KC, Dressman JB. Mechanism of Acylovir Uptake in Rat Jejunum. Pharm Res. 1990;7:299–303.

112. Masuda A, Goto Y, Kurosaki Y, Aiba T. In Vivo Application of Chitosan to Facilitate Intestinal Acyclovir Absorption in Rats. J Pharm Sci. 2012;101:2449–56.

113. Ates M, Kaynak MS, Sahin S. Effect of permeability enhancers on paracellular permeability of acyclovir. J Pharm Pharmacol. 2016;68:781–90.

114. Merzlikine A, Rotter C, Rago B, Poe J, Christoffersen C, Thomas VH, et al. Effect of chitosan glutamate, carbomer 974P, and EDTA on the in vitro Caco-2 permeability and oral pharmacokinetic profile of acyclovir in rats Effect of intestinal enhancer on acyclovir absorption. Drug Dev Ind Pharm. 2009;35:1082–91.

115. Shah P, Jogani V, Mishra P, Mishra AK, Bagchi T, Misra A. In vitro assessment of acyclovir permeation across cell monolayers in the presence of absorption enhancers. Drug Dev Ind Pharm. 2008;34:279–88.

116. De Miranda P, Blum MR. Pharmacokinetics of acyclovir after intravenous and oral administration. J Antimicrob Chemother. 1983;12:29–37.

117. Al-Yamani MJMS, Al-Khamis KI, El-Sayed YM, Bawazir SA, Al-Rashood KA, Gouda MW. Comparative bioavailability of two tablet formulations of acyclovir in healthy volunteers. Int J Clin Pharmacol Ther. 1998;36:222–6.

118. Laskin OL, Longstreth JA, Saral R, de Miranda P, Keeney R, Lietman PS. Pharmacokinetics and tolerance of acyclovir, a new anti-herpesvirus agent, in humans. Antimicrob Agents Chemother. 1982;21:393–8.

119. Cheng Y, Vapurcuyan A, Shahidullah M, Aleksunes LM, Pelis RM. Expression of organic anion transporter 2 in the human kidney and its potential role in the tubular secretion of guanine-containing antiviral drugs. Drug Metab Dispos. 2012;40:617–24.

120. Tanihara Y, Masuda S, Sato T, Katsura T, Ogawa O, Inui K ichi. Substrate specificity of MATE1 and MATE2-K, human multidrug and toxin extrusions/H+-organic cation antiporters. Biochem Pharmacol. 2007;74:359–71.

121. Takeda M, Khamdang S, Narikawa S, Kimura H, Kobayashi Y, Yamamoto T, et al. Human organic anion transporters and human organic cation transporters mediate renal transport of prostaglandins. J Pharmacol Exp Ther. 2002;300:918–24.

122. Shu Y, Brown C, Castro R, Shi R, Lin E, Owev R, et al. Effect of Genetic Variation in the Organic Cation Transporter 1, OCT1, on Metformin Pharmacokinetics. Clin Pharmacol Ther. 2008;83:273–80.

123. Koepsell H. The SLC22 family with transporters of organic cations, anions and zwitterions. Mol Aspects Med. 2013;34:413–35.

124. Califf RM. Clinical trials bureaucracy: Unintended consequences of well-intentioned policy. Clin Trials. 2006;3:496–502.

125. Pasqualetti G, Gori G, Blandizzi C, Del Tacca M. Healthy volunteers and early phases of clinical experimentation. Eur J Clin Pharmacol. 2010;66:647–53.

126. El-Massik MA, Abdallah OY, Galal S, Daabis NA. Towards a universal dissolution medium for carbamazepine. Drug Dev Ind Pharm. 2006;32:893–905.

127. Lake OA, Olling M, Barends DM. In vitro/in vivo correlations of dissolution data of carbamazepine immediate release tablets with pharmacokinetic data obtained in healthy volunteers. Eur J Pharm Biopharm. 1999;48:13–9.

128. Lee H, Park SA, Sah H. Surfactant effects upon dissolution patterns of carbamazepine immediate release tablet. Arch Pharm Res. 2005;28:120–6.

129. Ruiz-Picazo A, Gonzalez-Alvarez M, Gonzalez-Alvarez I, Bermejo M. Effect of Common Excipients on Intestinal Drug Absorption in Wistar Rats. Mol Pharm. 2020;17:2310–8.

130. Rege BD, Yu LX, Hussain AS, Polli JE. Effect of Common Excipients on Caco-2 Transport of Low-Permeability Drugs. J Pharm Sci. 2001;90:1776–86.

131. Rege BD, Kao JPY, Polli JE. Effects of nonionic surfactants on membrane transporters in Caco-2 cell monolayers. Eur J Pharm Sci. 2002;16:237–46.

132. Vaithianathan S, Raman S, Jiang W, Ting TY, Kane MA, Polli JE. Biopharmaceutic Risk Assessment of Brand and Generic Lamotrigine Tablets. Mol Pharm. 2015;12:2436–43.

133. Yuen KH, Peh KK, Billa N, Chan KL, Toh WT. Bioavailability and pharmacokinetics of acyclovir tablet preparation. Drug Dev Ind Pharm. 1998;24:193–6.

134. Lennernäs H, Lindahl A, Van Peer A, Ollier C, Flanagan T, Lionberger R, et al. In vivo predictive dissolution (IPD) and biopharmaceutical modeling and simulation: Future use of modern approaches and methodologies in a regulatory context. Mol Pharm. 2017;14:1307–14.

135. Schaeffeler E, Hellerbrand C, Nies AT, Winter S, Kruck S, Hofmann U, van der Kuip H, Zanger UM, Koepsell H SM. Schaeffeler E, Hellerbrand C, Nies AT, Winter S, Kruck S,

Hofmann U et al. DNA methylation is associated with downregulation of the organic cation transporter OCT1 (SLC22A1) in human hepatocellular carcinoma. Genome Med. 2011;3:82.

Chapter 6. Appendixes

APPENDIX 1 (PUBLICATION #1).

BIOWAIVER MONOGRAPH FOR IMMEDIATE-RELEASE SOLID ORAL DOSAGE FORMS: CARBAMAZEPINE

APPENDIX 2 (PUBLICATION #2).

IN VITRO PREDICTION OF IN VIVO ABSORPTION OF IBUPROFEN FROM SUSPENSIONS THROUGH RATIONAL CHOICE OF DISSOLUTION CONDITIONS

APPENDIX 3 (PUBLICATION #3).

THE EFFECT OF CHITOSAN ON THE BIOACCESIBILITY AND INTESTINAL PERMEABILITY OF ACYCLOVIR

APPENDIX 4 (PUBLICATION #4).

PREDICTING PHARMACOKINETICS OF MULTISOURCE ACYCLOVIR ORAL PRODUCTS THROUGH PHYSIOLOGICALLY BASED BIOPHARMACEUTICS MODELING

Journal of Pharmaceutical Sciences 110 (2021) 1935-1947

Contents lists available at ScienceDirect

Journal of Pharmaceutical Sciences

journal homepage: www.jpharmsci.org

Review

Biowaiver Monograph for Immediate-Release Solid Oral Dosage Forms: Carbamazepine

Mauricio A. García [a], Rodrigo Cristofoletti [b], Bertil Abrahamsson [c], Dirk W. Groot [d], Alan Parr [e], James E. Polli [f], Mehul Mehta [g], Vinod P. Shah [h], Tajiri Tomakazu [i], Jennifer B. Dressman [j, **], Peter Langguth [a, *]

[a] *Pharmaceutical Technology and Biopharmaceutics, Institute of Pharmaceutical and Biomedical Sciences, Johannes Gutenberg University, Mainz, Germany*
[b] *Center for Pharmacometrics and Systems Pharmacology, Department of Pharmaceutics, College of Pharmacy, University of Florida, Orlando, FL, USA*
[c] *Pharmaceutical Development, AstraZeneca R&D, Mölndal, Sweden*
[d] *RIVM (National Institute for Public Health and the Environment), Bilthoven, the Netherlands*
[e] *BioCeutics LLC, Cary, NC, USA*
[f] *Department of Pharmaceutical Sciences, School of Pharmacy, University of Maryland, Baltimore, MD, USA*
[g] *Division of Clinical Pharmacology, Centre for Drug Evaluation and Research, United States Food and Drug Administration, Silver Spring, MD, USA*
[h] *International Pharmaceutical Federation (FIP), The Hague, the Netherlands*
[i] *Pharmaceutical Science & Technology Laboratories, Astellas Pharma Inc, Ibaraki, Japan*
[j] *Fraunhofer Institute of Translational Medicine and Pharmacology, ITMP, Institute of Pharmaceutical Technology, Johann Wolfgang Goethe University, Frankfurt am Main, Germany*

ARTICLE INFO

Article history:
Received 29 December 2020
Revised 28 January 2021
Accepted 3 February 2021
Available online 18 February 2021

Keywords:
Carbamazepine
Biowaiver
Solubility
Permeability
Biopharmaceutics classification system (BCS)
Dissolution
IVIVC
Narrow therapeutic index

ABSTRACT

Literature relevant to assessing whether BCS-based biowaivers can be applied to immediate release (IR) solid oral dosage forms containing carbamazepine as the single active pharmaceutical ingredient are reviewed. Carbamazepine, which is used for the prophylactic therapy of epilepsy, is a non-ionizable drug that cannot be considered "highly soluble" across the range of pH values usually encountered in the upper gastrointestinal tract. Furthermore, evidence in the open literature suggests that carbamazepine is a BCS Class 2 drug. Nevertheless, the oral absolute bioavailability of carbamazepine lies between 70 and 78% and both *in vivo* and *in vitro* data support the classification of carbamazepine as a highly permeable drug. Since the therapeutic and toxic plasma level ranges overlap, carbamazepine is considered to have a narrow therapeutic index. For these reasons, a BCS based biowaiver for IR tablets of carbamazepine cannot be recommended. Interestingly, in nine out of ten studies, USP dissolution conditions (900 mL water with 1% SLS, paddle, 75 rpm) appropriately discriminated among bioinequivalent products and this may be a way forward to predicting whether a given formulation will be bioequivalent to the comparator product.

Introduction

Carbamazepine is commonly used to prevent seizure episodes in patients diagnosed with epilepsy, as well as to relieve the pain associated with trigeminal neuralgia. The World Health Organization (WHO) includes immediate release (IR) tablets containing carbamazepine as an anticonvulsant/antiepileptic drug in lists of essential medicines (EML) for both adults and children.[1–3] Additionally, the 21st edition of WHO EML for adults also recommends carbamazepine IR tablets as a treatment for behavioral disorders.[2]

A Biowaiver Monograph based on the available literature is presented for carbamazepine. The purpose and scope of these monographs have been previously discussed in detail.[4] To date, more than 45 biowaiver monographs have been published, which are all available on-line at www.fip.org/bcs_monographs.[5] Briefly, these aim to summarize and evaluate all data relevant for the

* Corresponding author. Pharmaceutical Technology and Biopharmaceutics, Institute of Pharmaceutical and Biomedical Sciences, Johannes Gutenberg University, Staudingerweg 5, 55099 Mainz, Germany.
** Corresponding author. Institute of Pharmaceutical Technology, Johann Wolfgang Goethe University, Frankfurt am Main, Germany.
E-mail addresses: dressman@em.uni-frankfurt.de (J.B. Dressman), langguth@uni-mainz.de (P. Langguth).

https://doi.org/10.1016/j.xphs.2021.02.019
0022-3549/

decision as to whether IR oral dosage forms containing the active pharmaceutical ingredient (APIs) could be approved according to the BCS-Biowaiver methodology, rather than having to undergo a pharmacokinetic evaluation of bioequivalence with a comparator formulation in a clinical study. APIs which are listed on the WHO EML,[2] have priority for this evaluation, since they are used in many countries where a clinical study might be onerous. The BCS-based biowaiver methodology, by contrast to pharmacokinetic-based bioequivalence studies, enables products to be evaluated using dissolution testing in order to assess bioequivalence, thus enabling new medicines to be brought to market more quickly and at less expense. However, the guidances[1,6–8] that have been issued to regulate the application of the BCS-based biowaiver must be followed to apply the BCS-based biowaiver methodology, with consideration not only of the solubility and permeability elements of the BCS but also wider clinical questions such as whether the API has a wide or narrow therapeutic index (NTI) and whether the benefits of applying the BCS-based biowaiver approach outweighs any potential risks associated with its application.

In the present monograph, the risk of waiving *in vivo* bioequivalence (BE) studies, by *in vitro* studies, in the approval of new and/or reformulated carbamazepine drug products manufactured as IR solid oral dosage forms is assessed.

Methods

Published information was obtained from PubMed, up to October 2020, and through the International Pharmaceutical Abstracts. Key words used were: carbamazepine, indications, therapeutic index, solubility, polymorphs, partition coefficient, permeability, absorption, distribution, metabolism, excretion, bioavailability, bioequivalence, dissolution, IVIVC, and excipients. Whenever appropriate, original literature based on the references in any given report was consulted.

General Characteristics

The chemical structure of carbamazepine is shown in Fig. 1. According the IUPAC nomenclature, its name is 5*H*-dibenz[*b,f*]azepine-5-carboxamide.[9,10] However, it can be also found under the chemical name: 5H-Dibenz[b,f]azepin-5-carbamide. Carbamazepine molecular formula is $C_{15}H_{12}N_2O$, its molecular weight (MW) is 236.3 g/mol and it is registered under the Chemical Abstracts Service (CAS) number: 298-46-4.[10] Visually, carbamazepine corresponds to white to yellowish-with crystalline powder that melts between 189 and 193 °C. The powder is very slightly soluble in water, freely soluble in dichloromethane and sparingly soluble in either acetone or ethanol 96%.[9]

Therapeutic Indication &Therapeutic Index

Carbamazepine is indicated in the prophylactic treatment of different types of epilepsy (partial and generalized tonic-clonic seizures), as well as to relieve pain related to trigeminal neuralgia.[11,12] The mechanisms of action have not yet been fully understood. However, a decrease of polysynaptic responses together with the blockage of post-tetanic potentiation seem to be involved in the prevention of seizures. This would depress the action potential in both the thalamus and polysynaptic reflexes (by binding to voltage-dependent sodium channels).[11,13]

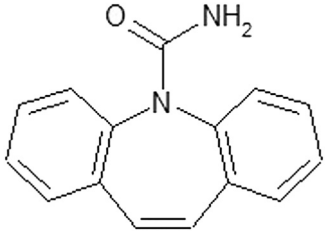

Fig. 1. Chemical structure of carbamazepine.

Conventionally, the therapeutic range for serum carbamazepine levels has been defined as 4–12 μg/mL.[14,15] However, diverse attempts to correlate either therapeutic or adverse effect with plasma concentrations have led to contradictory outcomes.[16,17] Newly diagnosed patients became seizure free at plasma concentrations lower than 8 μg/mL, although seizure control in certain individuals was also seen at plasma levels as low as 1.7,[16] or even at 1.2 μg/mL.[14,18] By contrast, Lesser et al. reported that around 50% of patients with intractable seizures responding to treatment showed plasma concentrations from 9.7 to 12.5 μg/mL, whereas practically the same plasma levels were found in patients whose epilepsy was not well controlled. Furthermore, the authors showed that serum concentrations of patients with and without adverse effects ranged between 7–12.3 and 9.4–17.2 μg/mL, respectively.[19]

Common adverse effects related to carbamazepine encompass central nervous system, hematologic, gastrointestinal and cutaneous symptoms.[15,20,21] A systematic review of diverse clinical studies indicated that somnolence, gastrointestinal symptoms and rash showed the highest incidences (26, 29 and 32%, respectively) in patients treated with 200–2000 mg.[22]

Consistently, adverse reactions have been detected within the range 5.9–8.3 μg/mL,[23,24] similar to the serum concentrations at which carbamazepine is used for the treatment of epilepsy. For instance, mean plasma levels at steady state (C_{ss}) of 6.52 μg/mL were reported after three weeks of treatment with 200 mg of the reference product three times a day.[25] Although that value must therefore considered to be within the therapeutic range, adverse effects have been reported at plasma levels at and above 5.9 μg/mL.[23,24]

With respect to cutaneous symptoms, the appearance of toxic epidermal necrolysis and Stevens-Johnson syndrome have both been related to carbamazepine. The risk of these events is estimated ten-fold higher in Asian than Caucasian populations, very likely due to a variant in the HLA-B gene (HLA-B*1502).[11] With respect to hematologic adverse effects, aplastic anemia and agranulocytosis have been associated with the use of this drug.

Interestingly, Olling et al. demonstrated that adverse effects (dizziness, fatigue, drowsiness, among others) occurred in a single dose BE trial at a dose of two 200 mg IR carbamazepine tablets. In this report, C_{max} of drug products ranged from 2.6 to 3.5 μg/mL, whereby faster absorbing formulations tended to evoke a higher occurrence of adverse effects.[26] Tothfalusi et al. further confirmed those findings by introducing a PK/PD model with the data already published by Olling et al. Good correlations between the partial AUC (AUCP) parameter of various bioinequivalent products and incidences of adverse events were observed.[17] However, it may be difficult to generalize these findings, since overlaps between therapeutic and toxic doses have been consistently reported in the literature.

Carbamazepine poisoning has been reported to occur after exposure to doses over 1400 mg, and it was mainly characterized by neurologic symptoms, namely, altered mental status, decreased consciousness, and recurrent seizures. Additionally, systemic consequences such as respiratory depression, hypotension and dysrhythmias have been observed.[15] Fatal outcomes have been associated after ingesting above 20 g orally.[15,21]

Given the therapeutic range from 4 to 12 μg/mL,[14] a therapeutic index of 3 can be calculated. Nevertheless, this value may actually

overestimate the reality since: i) therapeutic and toxic doses overlap, and ii) the therapeutic range of individuals could be even narrower.[22] Therefore, carbamazepine is considered to be a narrow therapeutic index (NTI) drug. This classification is further supported by the FDA in its draft guidance on carbamazepine, which considered these arguments, together with the need for therapeutic monitoring and low-to-moderate within subject variability.[27]

Dose, Dosage Forms and Strengths

Initially, carbamazepine 200 mg IR tablets twice daily are recommended in the treatment of epilepsy. Doses should be gradually increased by up to 200 mg weekly, leading to a regime of 200 mg three- or even four-times daily. Individual titration of the patient is also suggested, although typical maintenance doses consist of 800–1200 mg daily.[11,12] In special cases, daily doses as high as 1600 mg can be used.[11] Even though daily doses of 300–1400 mg have shown efficacy in seizure control,[23,28] no clear correlation has been observed between dose administered and efficacy.[20,22] On the other hand, 100 mg b.i.d. is recommended in the palliative treatment of trigeminal neuralgia, which can be increased up to 400–800 mg daily as maintenance doses.[11]

Carbamazepine drug products with market authorizations (MA) encompass intravenous (IV) solutions 200 mg/20 mL, oral suspensions (100 mg/5 mL), chewable tablets (100, 200 mg), immediate release tablets (100, 200, 300, 400 mg), extended release capsules (100, 200, 300 mg) and extended release tablets (100, 200, 400 mg).[29] Among them, only few presentations are listed in both the adult and pediatric WHO EML. Carbamazepine is stated as an anticonvulsant/antiepileptic medicine in both the 7th (children) and 21st (adults) EML when formulated as oral liquid (100 mg/5 mL), chewable tablets (100, 200 mg) and (scored) tablets (100, 200 mg).[2,3] This latter dosage form was also included in the EML as a treatment of bipolar disorders in adults.[2] In turn, the carbamazepine monograph in the U.S. Pharmacopeia (USP) includes oral suspensions (100 mg/5 mL), chewable tablets (100 mg), immediate release tablets (200 mg) and extended release tablets (100, 200, 400 mg).[10]

Physicochemical Properties

Polymorphs & Hydrates

Four anhydrous polymorphs and two dihydrates of carbamazepine have been extensively characterized.[30–33] According to the unified nomenclature proposed by Grzesiak et al., triclinic and trigonal polymorphs (forms I and II, respectively) share very similar crystal packing,[31,33] and needle-like morphology.[34,35] On the other hand, the P-monoclinic and C-monoclinic forms (III and IV, respectively) are also related to each other.[31] Similar to Forms I and II, carbamazepine dihydrate (DH) displays a needle-like form.[36,37] However the DH can be easily distinguished from either Form I or II given that the former exhibits a molecular weight approx. 13% higher at the same content of carbamazepine than the anhydrous forms.[34]

Power X-ray diffraction (PXRD) and differential scanning calorimetry (DCS) are powerful tools for discriminating among carbamazepine polymorphs.[31,33] Form I shows characteristic peaks in PXRD between 7.9 and 9.4 [2θ°], as well as several others at 12.3, 13.2, 19.9 and 22.9 [2θ°]. As for DCS, the scan of Form I shows just one endotherm in the range 189–191 °C, corresponding to its melting range.[30,31] This melting range can be also observed for the DH, and both Forms II and III. Nevertheless, these latter polymorphs showed additional endotherms before the peak, at 191 °C, which are not observed for form I. Flicker et al. characterized four different marketed products of IR carbamazepine, finding that Forms I and III were the most prevalent.[38]

Solubility

Numerous carbamazepine solubility data have been reported in the literature.[39–47] Given the biopharmaceutic aim of this monograph, Table 1 summarizes solubility data obtained at body temperature, i.e. at 37 °C. The presence of 0.5 or 1% sodium lauryl sulfate (SLS) increases carbamazepine solubility by approx. five- or ten-fold, respectively. The solubility of carbamazepine appears to be insensitive to effects of either buffer or pH. The Dose/Solubility ratio in SLS-free media was always reported to be higher than 580 mL (based on the highest strength in the WHO EML: 200 mg).[1] However, this ratio may be even larger if either the highest clinical

Table 1
Solubility of Carbamazepine in Different Media at Temperature 37 °C.

Media	pH	Sodium Lauryl Sulfate (SLS %)	Solubility (mg/mL)	D/S[a] (mL)	Reference (Ref)
Unbuffered		Absence			
Water	–	–	0.24	833[b]	44
Water	–	–	0.24	833[b]	40
Buffered		*Absence*			
HCl 0.1 N	1	–	0.34	588[b]	43
HCl 0.1 N	1	–	0.26	782[b]	46
SGF	1.2	–	0.24	849[b]	46
FaSSIF	6.5	–	0.24	847[b]	47
SIF	6.8	–	0.24	841[b]	46
HIF	6.5–7.5	–	0.28	707[b]	47
Unbuffered		*Presence*			
Water	–	0.5	1.50	133	44
Water	–	0.5	1.29	155	46
Water	–	1	2.94	68	46
Water	–	1	2.50	80	44
Water	–	1	2.04	98	43
Buffered		*Presence*			
Phosphate buffer	4	0.5	1.30	133	44
Phosphate buffer	6.8	0.5	1.40	154	44
Phosphate buffer	4	1.0	2.40	83	44
Phosphate buffer	6.8	1.0	2.40	83	44

SGF, Simulated gastric fluid; SIF, Simulated intestinal fluid; FaSSIF, Fasted state simulated intestinal fluid; HIF, Human intestinal fluid.
[a] For 200 mg = the highest tablet strength in the WHO Essential Medicines List, 21st Ed.
[b] Outside the critical limit of <250 mL.

dose or highest strength in the market (400 mg) are considered. As a result of its poor aqueous solubility, many attempts to increase carbamazepine solubility by applying diverse technologies such as co-crystals can be found in the literature.

Partition Coefficient

Calculated partition coefficient (CLogP) values of 1.98,[42] 2.28,[48] and 2.25,[49] have been reported using different computational approaches. Consistently, a LogP of 2.93 has been estimated by atomic contributions-based methods.[42] By contrast, a partition coefficient of 1.51 determined by shake flask methods was slightly lower than the computational values.[49] Overall, the literature suggests a higher affinity for lipids versus the aqueous phase.

pKa

Two relatively high pKa values have been published by two different authors (11.83 and 14),[49,50] probably belonging to the equilibrium $R{-}NH_2 \leftrightarrow R{-}NH^- + H^+$. Therefore, no ionization is expected for carbamazepine within the physiological pH range. This is in good agreement with the lack of pH-dependence of carbamazepine's solubility within the physiologically relevant pH range (Table 1).

Pharmacokinetic Properties

Absorption and Bioavailability

Faigle and Feldmann administered gelatin capsules containing ^{14}C-labeled carbamazepine orally to two healthy subjects. The authors found that 72% of the dose was recovered in the urine, while the remaining 28% was recovered in the feces.[51] Two decades later, Gérardin et al. prepared in-house IV solutions to study the absolute BA of 2% of ^{15}N-labeled suspensions in two healthy volunteers. Using this approach, absolute BA values of 100.1 and 102.3% were obtained by analyzing the ^{15}N-labeled carbamazepine contained in the orally administered product.[52] This apparent discrepancy might be explained by the biliary excretion of oxidative metabolites (see below). In fact, more than half of the amount present in feces was in form of metabolites.[51,53]

Recently, an IV carbamazepine formulation was developed using β-cyclodextrin to overcome solubility problems, and the formulation was approved by the U.S. Food and Drug Administration (FDA).[54] Marino et al. infused 100 mg of this IV formulation containing ^{13}C–^{15}N-labeled carbamazepine into 92 epilepsy patients treated with oral carbamazepine products. They were able to determine carbamazepine concentrations in plasma from both formulations simultaneously through the quantification of both the label and the mass of carbamazepine (using liquid chromatography coupled to mass spectrometry, LC-MS). In that study, the absolute BA at the steady-state (BA_{ss}) was found to be 78 ± 24%, independent of patients' gender.[55] It is worth noting that Gérardin et al. labeled the orally administered carbamazepine,[52] while Marino et al. labeled the IV drug.[55] This implies that BA determined by Gérardin et al. accounted for both the parent drug and metabolites, whereas Marino et al. accounted only for the parent carbamazepine from the orally administered dose, as this was quantified by LC-MS.

In another study, Tolbert et al. switched the treatment of epilepsy patients from their typical oral carbamazepine to an IV infusion, whose dose corresponded to 70% of their total oral daily dose.[56] By comparing the area under the plasma concentration-time curve (AUC) from the IV infusion and oral administration, authors observed that these values fell within the 90% confidence interval (CI) regardless of the infusion time. Moreover, the 30 min IV infusion was bioequivalent with the oral product in both AUC and maximum plasma concentration (C_{max}),[56] consistent with the BA of 78% reported by Marino et al.[55] Taken together, the literature suggests that the incomplete BA of carbamazepine (70–78%) might be principally related to first pass metabolism (see section Distribution, metabolism and excretion) rather than incomplete absorption.

The range of AUC values after oral administration of carbamazepine 200 mg IR tablets is around 120–190 μg*h/mL.[57,58] These values proportionally rise to 240–300 μg*h/mL when 400 mg are administered, suggesting linear pharmacokinetics within this dose range.[26] Linearity was further demonstrated over the range 50–600 mg.[59,60] Even though a slight disproportion was detected at lower doses (i.e. 50 and 100 mg),[58] this was almost negligible and may be attributable to nonlinear hepatic metabolism rather than nonlinear absorption.

The C_{max}, which is indirectly related to the absorption rate, seems to be more variable than AUC. For instance, values from 1.15 to 2.70 μg/mL were reported after the administration of 200 mg IR tablets to healthy subjects.[61,62] Nonetheless, the administration of two tablets of 200 mg caused the expected proportional increase in C_{max} (3.20–5.90 μg/mL). The absorption of oral solutions was faster than that of suspensions, which in turn was faster than for tablets.[60,63] This suggests that the *in vivo* performance of carbamazepine is to some extent dependent on the dosage form, and for solid dosage forms, potentially on the disintegration step and particle size.[63] Food also seems to have a modest influence carbamazepine absorption, since concomitant meal intake caused an increase of 20 and 25% in the AUC and C_{max}, respectively, although the effect was only statistically significant for C_{max}.[60]

Carbamazepine is slowly absorbed, showing a plasma peak at 24 h (T_{max}).[16,59] However, this value widely varied between 1.5 and 32 h (for the reference product), or 1–48 h (for many other IR formulations).[26] Carbamazepine's plasma-time curves display a plateau-like form when maximum concentrations were reached, in which several minor plasma peaks were identified.[26,60] This would be the most likely explanation for the above-mentioned erratic variation in T_{max}. This variation is perhaps amplified by carbamazepine's relatively long elimination half-life. Interestingly, this plateau-like behavior was not seen when carbamazepine was administered as an alcoholic oral solution,[58] suggesting that variability in C_{max} and T_{max} might be consequence of a limiting dissolution rate and a similarly rapid permeability along the gastrointestinal tract.

Permeability

Table 2 shows carbamazepine permeability values measured using a variety of experimental approaches.[64–71] Caco-2 and human permeability values were within the range of 10^{-5} to 10^{-4} cm/s, respectively. In both cases, carbamazepine permeabilities were higher than those of metoprolol, a high permeability reference compound.[64,71] Inter-study differences could be explained by different concentrations used, cell densities, presence or absence of collagen on *in vitro* membrane, and calculation methods, among other variables. Efflux ratio (ER) values were consistently reported as 0.78 to 1.27, regardless of the experimental set-up. Furthermore, the presence of verapamil, a well-known P-glycoprotein (P-gp) inhibitor, did not alter either carbamazepine permeability or its ER.[68] The absence of P-gp mediated transport was further confirmed by *in vitro* studies in seven different cell models, including over-expression systems.[72,73] Carbamazepine transport by breast cancer resistance protein (BCRP) was also assessed across transfected monolayers, where no differences between absorptive and secretory transport were found.[74] Overall, the evidence obtained with different *in vitro* experimental models agrees with both the high permeability and linear pharmacokinetics observed *in vivo*.

Table 2
In Vitro and *In Vivo* Permeability Data of Carbamazepine.

Method	Concentration (μM)	$P_{app,\ A\text{-}B}$ (cm/s,10^{-5})	ER	Ref
Caco-2	10	N.R.	0.78	69
	10–300	6.2	0.90	64
	25	14.4	0.84	67
	100	5.0	1.27	65
	1000	2.7	1.27	65
	N.R.	20.9	N.R.	70
PAMPA	100–200	1.2	N.R.	68
		$P_{app,\ M\text{-}S}$		
Mice intestine Ussing Chamber	200	1.5[a]	0.93	66
	+ Verapamil 200 μM	1.4[a]	1.03	66
Human intestinal double-balloon		P_{eff} (cm/s,10^{-4})		
	N.R.	4.3		71

$P_{app,\ A\text{-}B}$, Apparent permeability in the apical-to-basolateral (absorptive) direction; $P_{app,\ M\text{-}S}$, Apparent permeability in the mucosa-to-serosa (absorptive) direction; P_{eff}, Effective permeability; ER, Efflux ratio calculated by dividing basolateral-to-apical apparent permeability ($P_{app,\ B\text{-}A}$) by $P_{app,\ A\text{-}B}$; N.R, Not reported.

Distribution, Metabolism and Excretion

Carbamazepine is widely distributed throughout the body. The plasma protein binding is approximately 75%, with slight inter-individual variation.[58] The apparent volume of distribution (Vd) ranged from 0.79 to 1.86 L/kg,[58,75] and it was found to be highly affected by other drugs.[58] Consistent with its lipophilicity and permeability, carbamazepine is also distributed into breast milk and able to cross the placental barrier.[59]

After oral administration of a single dose, carbamazepine plasma elimination half-life ($t_{1/2}$) was relatively long, around 34–38 h,[58] with approx. 75% of the dose being excreted with the urine. From this fraction, only 2% was eliminated as the parent drug.[16,59] Metabolism, therefore, plays an important role in carbamazepine elimination. Its only active metabolite is carbamazepine-10,11-epoxide, which is formed by the action of diverse isoforms of cytochrome P450 (e.g. 3A4 and 2C8).[76–78] The effect of the CYP 3A4 inhibitor, grapefruit juice, on carbamazepine pharmacokinetics was studied in 10 patients treated with oral carbamazepine by following the $AUC_{0\text{-}8}$, the minimum ($C_{min,ss}$) and the maximum ($C_{max,ss}$) steady-state concentrations. The authors found that the aforementioned parameters increased by 40.8, 39.2 and 40.4% respectively in patients who received carbamazepine co-administered with grapefruit juice. Considering the strong intestinal expression of CYP 3A4 and the interaction with grapefruit juice, the occurrence of first pass metabolism in the intestinal wall is plausible.[76] Drug-food interactions have also been reported in various research publications and study cases.[79–81] Therefore, the first pass extraction appears to be the main explanation for the reported absolute BA of between 70 and 78%.[55]

The epoxide metabolite is finally biotransformed into the *trans*-10,11-dihydroxy-10,11-dihydrocarbamazepine (*trans*-CBZ-diol), which is excreted by the kidney (21% of the dose).[16] However, since carbamazepine can induce its own metabolism,[16] this value may be even larger in chronically treated patients. Moreover, co-administration with inducers of drug metabolism, such as phenytoin, might have an even greater impact. For example, Eichelbaum et al. demonstrated that carbamazepine elimination half-life decreased to 12 h in patients receiving chronic treatment and to 8 h in patients co-medicated with phenytoin.[16,75]

Dosage Form Performance

Bioavailability and Bioequivalence

Several studies on carbamazepine comparative BA and BE for oral IR dosage forms were found in the literature (Table 3). Further, reports that contained both *in vitro* and *in vivo* comparative studies and correlations are shown in Table 4. The pharmacokinetic parameters for the reference product (usually Tegretol®) containing carbamazepine 200 mg were consistent between single dose studies, with AUC and C_{max} values lying in the range from 144 to 182 μg*h/mL and from 1.89 to 2.43 μg/mL, respectively. These ranges remained similarly narrow when two 200 mg IR Tegretol® tablets (400 mg of carbamazepine in total) were administered to volunteers (Tables 3 and 4).[26,43,50,82] By contrast, test (generic) products often showed wider variability than the reference. Although BE was demonstrated for some generic products, some other test formulations failed the BE test mainly due to the C_{max} parameter (Tables 3 and 4).

The statistical criteria applied to reach a BE decision varied among studies. While typical statistical tests such as the paired *t*-test and ANOVA were performed in studies conducted between 1979 and 1995,[57,83] the confidence intervals were calculated in more recent publications (Tables 3 and 4). Of note, two studies used an innovative parameter ('A') which depended on the absorption constant (K_a), elimination constant (K_e), mean residence time (MRT), t_{max} and $AUC_{0\text{-}inf}$.[84,85] Although the 'A' parameter was advantageous improving the accuracy of relative bioavailability calculations for two generic products,[84] it seems difficult to fully rely on it because of the dependency on modeling required to estimate kinetic rate constants.

Often, concerns arise around demonstration of BE for NTI drugs, such that further evidence (i.e. multiple dose studies) could be requested. Three studies containing both single dose and multiple dose comparative data were located.[25,57,86] Anttila et al. studied the bioequivalence of one carbamazepine brand against the reference product in either subjects (single dose) or patients (multiple doses). Even though the C_{max} obtained with the test product after the single dose experiment was significantly higher than the reference, there were no statistical differences between C_{ss} in patients.[57] Similarly, Yacobi et al. showed that the $C_{max,ss}$ and AUC from the generic product were indistinct from the reference in a multiple dose study conducted in healthy volunteers, even using the 90% CI limits: 0.9–1.1. The same formulation had not been declared BE in a previous single dose study because of the AUC parameter.[25] These findings support the sensitivity of the single dose experimental design to detect differences in the pharmacokinetic performance of two pharmaceutical alternatives, although steady state data are more representative of the actual clinical use of the drug.

Is There a Polymorphism Effect on BA?

Since diverse polymorphic forms are reported in the literature (see *physicochemical properties*), it is worthwhile to address their potential effect on carbamazepine oral performance. Anhydrous carbamazepine is converted into DH in aqueous solution such that

Table 3
Summary of Published Bioequivalence Studies on Carbamazepine Immediate Release Tablets in Fasted Humans.

Subjects (nº Females; Males)	Study Design	Drug Product (Manufacturer)	Dose (mg)	AUC (μg[e]h/mL)	C_{max} (μg/mL)	Criteria and Result	Ref
9 healthy volunteers (4; 5)	Single dose, two-period, crossover.	Tegretol® (Ciba Geigy Pharm)[d]	200	182[a]	2.43	Paired *t*-test. Not BEs (C_{max}, $p < 0.001$).	57
		Neurotol® (Lääke/Farmos Group)	200	190[a]	3.40		
12 healthy volunteers (0; 12)	Single dose, two-period, crossover, randomized.	Tegretol® (Novartis India Limited)[d]	200	129[b]	2.17	Paired *t*-test. Not BEs (C_{max} and 'A' parameter, see below).	85
		Zen	200	150[b]	3.10		
5 healthy volunteers (0; 5)	Single dose, three-period, crossover, randomized.	Tegretol[d]	200	145[a]	2.11	'A' parameter (function of: Ka, Ke, MRT, t_{max} and AUC). BEs.	84
		Temporol[e]	200	162[a]	2.49		
		Karazepin[e]	200	127[a]	1.71		
9 healthy volunteers	Single dose, two-period, crossover, randomized.	Tegretol®[d]	400	272[b]	5.61	ANOVA. BEs.	83
		Marzepine (ICN Galenika)[e]	400	260[b]	4.29		
6 patients (2; 4)	Multiple doses, two-period, crossover.	Tegretol® (Ciba Geigy Pharm)[d]	PDNA	NR	NR	Paired *t*-test on mean concentrations. BEs	57
		Neurotol® (Lääke/Farmos Group)[e]	PDNA	NR	NR		
18 epilepsy patients.	Multiple doses, Three-period (three weeks/period), crossover, double-blind, randomized, non-washout.	Tegretol (Ciba Geigy Pharm)[d]	PDNA	85.6	11.0	MANOVA and IC 90% (0.8−1.25). BEs, except Panital (AUC).	86
		Carmapine (Central-Poly)[e]		85.0	10.5		
		Carzepine (Condrugs)[e]		93.0	11.0		
		Panital (Pharmaland)		98.2	10.5		
32 healthy volunteers (0; 32)	Multiple doses, Two-period (11 days/period), crossover, fasted, open-label, randomized, non-washout.	Tegretol (Ciba Geigy Corp.)[d]	200 t.i.d.	153	7.10	ANOVA, IC 90% and IC 95% (0.9 −1.1). BEs	25
		Test (Taro Pharm. Ind. Ltd)[e]	200 t.i.d	156	7.11		
40 patients either seizure-free or with refractory seizures	Multiple doses, Two-period (90 days/period), crossover, double blind, randomized, non-washout.	Tegretol (Ciba Geigy Corp.)[d]	PDNA	0.61−1.87[c]	6.2−16.0	Paired *t*-test on AUC. BEs	104
		Epitol (Lemmon Co.)[e]	PDNA		6.7−15.9		
12 young (6.5−15 yo) seizure patients (3; 9)	Multiple doses, two-periods (six weeks/period), crossover, non-washout.	Tegretol (Ciba Geigy Corp.)[d]	100 or 200 (PDNA)	98.9	10.2	Paired *t*-test. BEs	105
		Test (Ethical Generics)[e]		97.4	9.91		

BEs, Bioequivalents; PDNA, Patient's dose not adjusted; NR, Not reported.
[a] $AUC_{0\text{-}inf}$.
[b] $AUC_{0\text{-}t}$.
[c] Minimum and maximum values for intra-patient AUC ratios.
[d] Reference Product.
[e] Bioequivalent formulation.

Table 4
Summary of Further Single Dose Bioequivalence Studies and Dissolution Conditions Attempting IVIVC for Carbamazepine Immediate Release Products.

Drug Product Manufacterer	Dose (mg)	$AUC_{0\text{-}inf}$ ($\mu g^{b}h/mL$)	C_{max} ($\mu g/mL$)	*In-Vitro* Method Used in the Correlation	Correlated Parameters	Other Significant Results	Ref
Ciba Geigy Pharmaceuticals.[a]	200	144	1.89	➢ Media: 900 mL SLS 1%.	➢ Fa vs Fd (30–90 min).		61
Pharmaceutical Basics: Batch 1[b]		80.9	1.15	➢ Apparatus: Paddle.	➢ $AUC_{0\text{-}inf}$ or C_{max} vs Fd (15–60 min)		
Pharmaceutical Basics: Batch 2[b]		154	2.69	➢ Speed: 75 rpm.			
Pharmaceutical Basics: Batch 3[b]		105	1.40				
Ciba Geigy Pharmaceuticals.[a]	200	157	1.95	➢ Media: 900 mL SLS 1%.	➢ Fa vs Fd (30–120 min).		102
Inwood		163	2.32	➢ Apparatus: Paddle.	➢ C_{max} or T_{max} vs Fd (5–30 min).		
Sidmak		159	2.30	➢ Speed: 75 rpm.			
Purepac[b]		163	2.34				
Formulation A	200	–	1.90	➢ Media: 900 mL SLS 1%.	➢ Correlation parameters obtained from *in vitro* and *in vivo* data from three formulations.	Plasma profile of the remaining formulation predicted from correlation parameters.	62
Formulation B		–	2.70	➢ Apparatus: Paddle.			
Formulation C		–	2.30	➢ Speed: 75 rpm.			
Formulation D		–	2.50				
Ciba Geigy Pharmaceuticals.[a]	400	296	4.24	➢ Media: 900 mL simulated USP intestinal fluid, pH = 7.5.	➢ AUC vs Fd (45–90 min)	Neither SLS 1% nor HCl 1 N datacorrelated with *in vivo* parameters.	97
Amstrong[b]		331[c]	5.98				
Wayne[b]		316[c]	4.81	➢ Apparatus: Paddle.			
Precimex[b]		368[c]	5.98	➢ Speed: 75 rpm.			
Ciba Geigy Pharmaceuticals.[a]	400	296	4.54	➢ Media: 900 mL SLS 1% or HCl 1 N.	➢ C_{max} vs $Fd_{1\%\ SLS}$ (20–100 min).	Correlations were also obtained with HCl 1 N, although worse than with SLS.	26,43
Pharmachemie[b]		246	3.29	➢ Apparatus: Paddle.			
Centrafarm[b]		294	5.90	➢ Speed: 75 rpm.			
Pharbita[b]		292	6.15				
Reference product	400	211	4.34	➢ Media: 900 mL water, SLS 0.5, SLS 1%, HCl 0.1 N, USP Acetate (pH 4.5), USP phosphate (pH 6.8).	➢ Fa vs Fd point to point (Level A)	Overall, acceptable correlations being SLS 1% the highest r.[2]	106
Galenika a.d.[b]	400	220	4.74	➢ Apparatus: Paddle.			
				➢ Speed: 75 rpm.			
Novartis.[a]	400	259	4.74	➢ Media: 900 mL SLS 0.5 or 1%.	➢ Plasma profile predicted from *in vitro* data and *in silico* modeling.	Dissolution in USP buffer 4.5, 6.8 and HCl 0.1 N were not consistent with *in vivo* results.	50
Formulation Test.	400	259	4.34	➢ Apparatus: Paddle.			
				➢ Speed: 75 rpm.			
Novartis (Bioeq. Study 1).[a]	400	238	3.20	➢ Media: 900 mL SLS 1%.	➢ *In vitro* vs *in vivo* dissolution time		82
Formulation Test 1		238	3.40	➢ Apparatus: Paddle.	➢ Fa vs Fd point to point (Level A).		
Novartis (Bioeq. Study 2).[a]		243	3.20	➢ Speed: 75 rpm.			
Formulation Test 2[b]		230	2.90				
Novartis[a]	400	355	4.00	➢ Media: 900 mL water; 1% SLS.	➢ *In vitro* vs *in vivo* dissolution time		103
Test Formulation	400	389	5.14	➢ Apparatus: II.	➢ Fa vs Fd point to point (Level A).		
				➢ Speed: 75 rpm.			

Fd, Fraction dissolved; Fa, Fraction absorbed.
[a] Reference Product.
[b] Bioequivalent formulation.
[c] $AUC_{0\text{-}120}$.

the crystallization of this latter form seems to be the kinetic rate-limiting step in dissolution when the concentration exceeds the thermodynamic solubility. Nonetheless, after grinding the solid material, a decrease in the interconversion times was observed. This was associated with a change in the rate-limiting step to the dissolution of the anhydrous form.[37] All in all, it can be expected that the DH is the most prevalent form in suspensions because of the solution-mediated transformation. Further, the conversion rates of diverse forms of carbamazepine have been reported. Typically, faster conversion of Form I into DH was demonstrated, in comparison with Form III.[34,35,87] The intrinsic dissolution rate (IDR) of Form III was only slightly faster than Form I, less than 1.1-fold higher.[34,36,87] Most of the studies, however, agreed that anhydrous polymorphs dissolved between 1.6- and 2.3-fold faster than the less soluble DH carbamazepine.[34,36,87,88] Conversely, one report showed that amorphous dissolution was slower than the DH in a flow-through apparatus, using HCl 0.1 N as media. In this report, the authors also observed an increment in dissolution rate of the anhydrous form in presence of the wetting agent polysorbate 80. The enhanced dissolution rate was accompanied by a decrease in the crystal length, hence their findings were explained in the light of the anhydrous form having a higher tendency to crystal growth in HCl media.[89]

The presence and effect of polymorphs were studied in four marketed products. The IDR of products in which Forms I and III prevailed displayed the fastest IDR, although the differences were negligible compared to the slowest of those drug products (<1.15-fold). Meanwhile, the formulation that contained carbamazepine Form IV showed an IDR 1.8-fold slower than the fastest drug product.[38]

The oral performance of diverse polymorphs was studied in dogs, where the BA of Form III, I and DH in dogs were 69, 48 and 33%, respectively, compared to the oral solution. These results likewise indicate that the BA of Form III was 1.4 or 2.1-fold greater than Form I or DH, respectively.[34] Given that this behavior was not reflected in the *in vitro* dissolution experiment, the authors suggested that discrepancies might be due to disparities in rates of conversion.[34,35,87] Yet, the situation in humans is dissimilar. In this regard, Kahela et al. administered 200 mg of either anhydrous carbamazepine or DH in hard gelatin capsules to healthy volunteers. The *in vitro* dissolution results differed between the two formulations, but no differences were found in AUC and C_{max} parameters.[89] Likewise, Elqidra et al. prepared IR tablets containing 200 mg of different carbamazepine polymorphs, which were compared to the reference product, Tegretol®. The authors found that AUC and C_{max} values of drug product 1 (containing Form I), 2 (containing bulk carbamazepine), and 3 (the reference) were statistically insignificantly different from another.[90]

Excipients and Manufacturing Effects on BA

Table 5 displays the excipients present in IR carbamazepine 200 mg tablets with a market authorization (MA) in diverse countries. Besides carbamazepine 200 mg tablets, some companies

Table 5
Excipients Present in Carbamazepine IR Tablets 200 mg with Marketing Authorization (MA) in Diverse ICH and Associated Countries and the Minimal and Maximal Excipient Amount Present per Dosage Unit in Solid Oral Drug Products with MA in US.

Excipient	Drug Products[a], by Country[b] That Granted the MA[c]	Range Present in Solid Oral Dosage Form with MA in US (mg)[d]
Carmellose sodium	AU (1), CA (8), DE (12,13), ES (18), NL (23,26), UK (28), US (30)	3–160
Croscarmellose sodium	BR (3–7), DE (14,16), US (29,32,34)	9–165
Cellulose, hydroxypropyl	CN (11), JP (21,22)	0.4–198
Cellulose, ethyl	US (34)	2–292
Cellulose, methyl	NL (24)	3–184
Cellulose, microcrystalline	AU (1,2), BR (3–7), CA (8–10), DE (12–17), ES (18,19), JP (20–22), NL (25,26), UK (27,28), US (29,30)	27–1553
Silicon dioxide	AU (1,2), BR (4–6), CA (8,9), CN (11), DE (12,14–17), ES (18,19), NL (25,26), UK (27,28), US (30–34)	3–139
Gelatin	DE (13), NL (23), US (33)	2–756
Glycerin	US (33,34)	1–249
Hypromellose	JP (20), US (31)	1.2–537
Lactose	BR (5), US (34)	33–2500
Magnesium stearate	AU (1,2), BR (3–7), CA (8–10), CN (11), DE (12–17), ES (18,19), JP (20–22), NL (23–26), UK (29–34)	0.2–401
Povidone	BR (3–7), CA (10), DE (17)	0.5–240
Sodium laurylsulphate	BR (6), CA (10), DE (17)	0.3–148
Sodium starch glycolate	AU (2), CA (10), DE (15), ES (19), NL (25), UK (27), US (31,34)	2.4–876
Starch	BR (5,7), CN (11), DE (17), JP (20,21), NL (23, 24), US (31,33)	0.4–1000
Starch, hydroxypropyl	JP (22)	–
Starch, pregelatinized	AU (2), NL (24,25), UK (27), US (31,32)	32–453
Stearic acid	US (33)	5–72
Talc	AU (2), JP (21), NL (24,25), UK (27)	2–1000

[a] Manufacturers: 1: Novartis Pharmaceuticals Australia Pty Ltd.; 2: Alphapharm Pty Ltd.; 3: EMS S/A.; 4: Cristália Prod. Quím. Farm. Ltda.; 5: Brainfarma Indústria Química e Farmacêutica S.A.; 6: Laboratorio Teuto S/A.; 7: Sanval Comércio e Indústria Ltd.; 8: TARO PHARMACEUTICALS INC.; 9: NOVARTIS PHARMACEUTICALS CANADA INC.; 10: TEVA CANADA LIMITED; 11: Beijing Novartis Pharma Ltd.; 12: HEUMANN PHARMA GmbH; 13: RATIOPHARM GmbH; 14: NOVARTIS PHARMA GmbH; 15: 1 A Pharma GmbH; 16: Aristo Pharma GmbH; 17: neuraxpharm Arzneimittel GmbH; 18: Novartis Farmacéutica, S.A.; 19: Laboratorios Normon, S.A.; 20: Sun Pharma; 21: Kyowa Pharmaceutical Industry; 22: Fujinaga Pharm; 23: Apotex Europe B.V.; 24: Centrafarm B.V.; 25: Mylan B.V; 26: Novartis Pharma B.V.; 27: Mylan; 28: Novartis Pharmaceuticals UK Ltd.; 29: APOTEX INC ETOBICOKE SITE; 30: TARO PHARMACEUTICAL INDUSTRIES LTD; 31: TORRENT PHARMACEUTICALS LTD; 32: UMEDICA LABORATORIES PRIVATE LTD; 33: NOVARTIS PHARMACEUTICALS CORP; 34: TEVA PHARMACEUTICALS USA INC.

[b] Countries: AU: Australia; BR: Brazil; CA: Canada; CN: China, DE: Germany, ES: Spain, JP: Japan, NL: the Netherlands, UK: United Kingdom, US: United states.

[c] Therapeutic Goods Administration (TGA). Available at: https://www.tga.gov.au. Accessed May 05, 2020.; ANVISA (Brazilian Health Regulatory Agency). Available at: www.anvisa.gov.br Accessed May 26, 2020.; Health Canada. Available at: www.hc-sc.gc.ca. Accessed May 11, 2020.; China Food and Drug Administration (CFDA). Available at: http://en.nhc.gov.cn. Accessed May 04, 2020.; Bundesinstitut für Arzneimittel und Medizinprodukte (BfArM). Available at: https://www.pharmnet-bund.de. Accessed May 04, 2020.; Spanish Agency for Medicines and Health Products. Available at: www.aemps.es. Accessed May 11, 2020.; Pharmaceuticals and Medical Devices Agency (PMDA). Available at: https://www.pmda.go.jp/english/. Accessed May 04, 2020.; Medicines Evaluation Board. Available at: www.cbg-meb.nl. Accessed May 11, 2020.; Electronic medicines compendium. Available at: www.medicines.org.uk/emc. Accessed May 06, 2020.; National Institute of Health. US National Library of Medicine. Available at: www.dailymed.nlm.nih.gov. Accessed May 06, 2020.

[d] U.S. Food and Drug Administration. Available at: https://www.fda.gov/drugs/drug-approvals-and-databases/inactive-ingredients-database-download. Accessed August 27, 2020.

also manufacture IR tablets containing 100, 300 or 400 mg, although the qualitative composition declared is the same.

Being a poorly aqueous soluble drug, the presence of SLS in IR tablets may enhance carbamazepine's oral performance by increasing either the wettability or solubility.[44] In this monograph we found three generic products that declared SLS in their qualitative composition (Table 5). As mentioned above, carbamazepine is a highly permeable drug with almost complete absorption. Therefore, if any SLS effect will occur, this will most likely be reflected in the C_{max} parameter.

The quantitative amount of SLS in solid oral dosage forms with a MA in the United States ranges from 0.3 to 148 mg. However, the upper limit may not be representative for a 200 mg carbamazepine formulation, since this would imply an extremely high relative amount of SLS in those formulations. Considering that these three generic products were granted with a MA in their respective countries (and thus, it is very likely that bioequivalence has been previously demonstrated), we believe that SLS amounts in carbamazepine IR tablets may be near or even below the lower limit reported by the FDA's inactive ingredient database (Table 5).

Besides carbamazepine IR tablets, chewable tablets have also been developed and are currently available in the market.[29] The clinical pharmacokinetic performance of chewable relative to IR tablets was studied in adults and young populations. Chan et al. carried out a single dose, three-period, crossover study in six healthy volunteers who were administered the IR product, chewable tablets swallowed as a whole (SW) and chewable tablets chewed for 30 s before swallowing (CHW). Among these treatments, only CHW failed the BE study (95% CI, >20%) due to the C_{max} (4.19 μg/mL), which was 1.25-fold greater than the reference (3.36 μg/mL). However, the IR and CHW treatments were compared once again in a multiple doses study conducted in ten healthy volunteers, where no significant differences between C_{ss} (4.9–5.0 μg/mL) were found.[91] Likewise, another multiple dose, two-period, crossover study conducted in young epileptic patients (6–14 yr) displayed that $C_{max,ss}$, C_{ss} and AUC were not different between the IR and the chewable product.[92] In that study no information was given about whether the chewable tablets were swallowed as a whole or chewed.

The effect of particle size on BA has also been investigated. Dam et al. measured carbamazepine plasma profiles in epileptic patients after the administration of two tablets manufactured with either small (test product, in average 2–3 μm) or large (reference product, in average 100–150 μm) particle sizes. The authors found that C_{max} of the carbamazepine product with the large particle size was just 75% of that of the product with the small particle size.[93] Therefore, it is plausible that discrepancies in particle sizes could explain outcomes in some studies that have been unable to demonstrate BE.

Dissolution and IVIVC

Dissolution conditions for carbamazepine according to the U.S. Pharmacopeia (USP) 42nd edition are 900 mL of water containing 1% of sodium laurylsulfate (SLS 1%) as the dissolution medium, in USP type II apparatus (paddle) at a rotational speed of 75 rpm.[10,94] However, the specifications depend on the product. Pharmacopeial Test 1 applies only to 100 mg chewable tablets and is thus out of the scope of this manuscript. For IR tablets two different specifications are listed: Test 2: 45–75% of drug dissolved within 15 min, and no less than 75% after 60 min; or Test 3: 60–85% of drug dissolved within 15 min, and no less than 75% after 60 min.

Mittapalli et al. studied six IR marketed drug products containing 200 mg of carbamazepine tablets under different conditions. All six formulations met USP criteria when the USP conditions were applied, however the SLS-containing media were not able to distinguish among formulations.[45] Instead, the authors obtained more discriminating dissolution profiles when experiments were carried out in SLS-free HCl 0.1 N media. However, the clinical relevance of these findings is unclear because no *in vivo* data were reported.[45] Using the USP type IV apparatus, Medina et al. were able to discriminate better between five different marketed drug products than was possible with the USP monograph method.[95] Here too, the lack of *in vivo* data makes it impossible to draw conclusions about the biorelevance of the results.

Overall, Table 4 shows that USP dissolution conditions resulted in the best biorelevance for carbamazepine IR tablets. Nine out of ten studies achieved good correlations and/or predictions of plasma-time profiles from *in vitro* dissolution data using the pharmacopeial conditions. Replacing SLS by an acidic medium (HCl 1 N) also displayed good correlation,[43,96] but did not show superiority over the SLS 1% medium.[43] Examples for successful correlations obtained with SLS 1% are shown in Fig. 2. The performance of different SLS concentrations has also been assessed where one report showed that SLS 0.5% enabled successful prediction of plasma-time profiles,[50] while other work displayed the best predictions with SLS 0.1%.[63] Conversely, only one study reported that neither SLS nor HCl media correlated well with AUC parameter.[97]

The results from the literature agree that best correlations were obtained when using fraction dissolved (Fd) within 30–90 min. However, the choice of the *in vivo* parameter for establishing the correlation (Fa, AUC, C_{max}) was diverse, as shown in Fig. 2 and Table 4. Of note, some good correlations were also found with Fd at 5 min, although this might be irrelevant as this timeframe is shorter than the gastric emptying time (around 15 min).[43]

Discussion

Solubility

The highest strength of carbamazepine as an IR solid dosage recommended in the EML is 200 mg. Regulatory FDA guidance recommend the use of USP buffers within the pH range 1.2–6.8 (chloride, acetate or phosphate) to assess drug solubility.[7] However other buffers can be used whenever justified.[1,6] Considering the lack of physiologically relevant ionization, carbamazepine's solubility should not be dependent on the type of buffer. Table 1 shows that carbamazepine solubility was insensitive to pH and any other biorelevant content (i.e. bile components present in simulated media). Table 1 also reports D/S ratio values, which reflect the volume of medium needed to dissolve the respective dose strength. The D/S ratio ranged from 588 to 849 mL, respectively and thus is 2.4- to 3.4-fold higher than the cut off volume of 250 mL stipulated by the regulators.[7] Consistently, Amidon et al. reported a D/S ratio of 769 mL, implying that a dose number (Do) of around 3 can be obtained for a dose of 200 mg.[39] This number is even greater when the highest recommended single clinical dose, 400 mg, is considered, as required by the regulatory guidances.[2,6] Therefore, carbamazepine can be unequivocally classified as a “not highly soluble” drug according to the BCS.

Permeability

Different methodologies can be used to assess drug permeability. An API is considered highly permeable if the extent of its absorption (using the Fa parameter) is equal or higher than 85%, provided its stability in the gastrointestinal tract. The guidances recommend conducting either mass balance in humans or absolute BA experiments as a first preference to classify the API permeability. In the literature, both mass balance and BA studies are available and these consistently suggest that oral carbamazepine bioavailability is around 70–80%.[51–53,55] However, it is very likely that this range

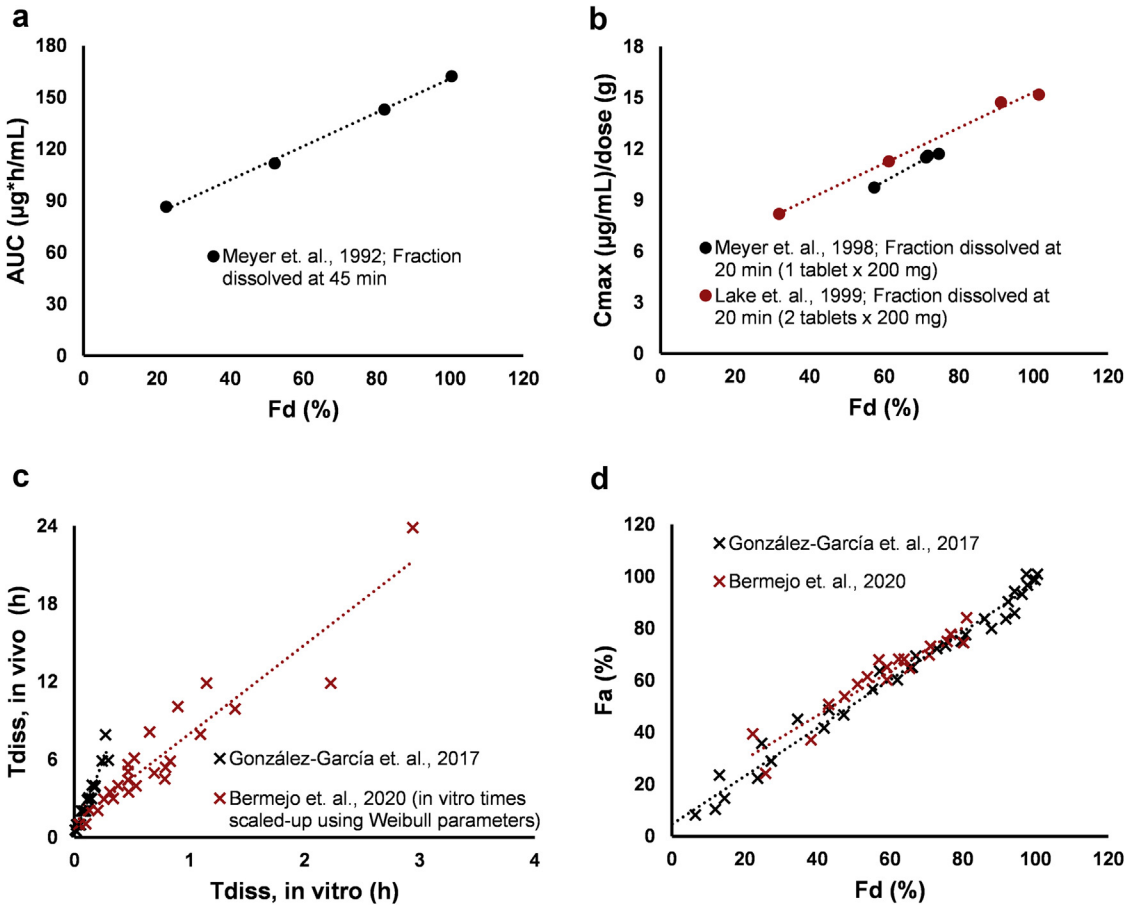

Fig. 2. Examples of level C (upper panels, circles) and level A (lower panels, crosses) IVIVC found in literature using 900 mL of SLS 1% in the USP type II apparatus at 75 rpm. Data was digitalized from Ref.[61] (a),[43,102] (b),[82,103] (c and d) with PlotDigitalizer 2.6.8 (Free Software Foundation, Inc., Boston, MA). C_{max} values in panel B were normalized by carbamazepine's dose utilized in each study (g) in order to allow data comparison. Differences between correlations in panel C may be consequence of the scaling step carried out in Bermejo and coauthors' study (red crosses).

underestimates the true absorption, as the first pass extraction seems to play an important role in carbamazepine oral disposition. In fact, the oral BA of carbamazepine in patients increased by 40% when it was co-administered with grapefruit juice (which contains CYP3A4 inhibitors) compared to co-administration with water.[76]

The BCS framework was developed using human permeability data obtained with intestinal perfusion techniques which allow direct permeability assessment. The effective permeability of carbamazepine was measured as 4.3×10^{-4} cm/s, 3.3-fold larger than the high permeability marker, metoprolol.[71] Such a study provides confirmatory evidence to classify carbamazepine as a highly permeable drug. Consistently, several surrogate *in vitro* experiments shown in Table 2 point toward the same conclusion. The FDA and the recently published ICH M9 guidances permit the use of *in vitro* Caco-2 cell experiments as a surrogate method to assess drug permeability.[7,8] Therefore, the good agreement between *in vivo* and *in vitro* observations published in the literature on carbamazepine provides additional support for the regulatory decision of including cell monolayer experiments as a surrogate tool for permeability evaluation.

The classification of carbamazepine as "highly permeable" is also in line with its molecular structure (Fig. 1) and reported LogP values. Indeed, carbamazepine is currently listed in both guidances as a high permeability model drug.[7,8] Moreover, *in vivo* linearity within the dose range 50–600 mg was demonstrated,[59,60] and supported by *in vitro* bidirectional studies in presence or absence of inhibitors that confirmed the null role of intestinal transporters (i.e. P-gp and BCRP).

BCS Classification

In 1995, Amidon et al. used carbamazepine as an example of a low solubility API (Do = 3).[39] Thereafter, many publications supported its classification as a BCS class 2.[42,98–100] For instance, Kasim et al. classified the drugs in the WHO list of essential medicines according to the BCS framework. The authors used LogP values indirectly accounting for permeability, which resulted in a Class 2 classification.[42] However, regulatory guidances do not consider descriptors of lipophilicity (i.e. LogP, LogD) in assessing drug permeability.[1,6,7] Regarding the evidence found, data from both *in vivo* and *in vitro* experiments lead to high permeability classification. Indeed, the FDA guidance lists carbamazepine as a model drug of high permeability.[7] Furthermore, the several examples of successfully achieved IVIVC demonstrate that carbamazepine dissolution, and not the permeation, would be the rate limiting step in its oral absorption.[43,50,62,63,82,96] Considering the whole body of evidence collected, carbamazepine can be classified as a BCS Class 2 drug.

Surrogate Techniques for In Vivo *BE Testing*

Given that carbamazepine dissolution appears to control carbamazepine absorption rate from IR products, a dissolution test may be an appropriate surrogate assay and thus a valuable tool for predicting the outcome of a BE study. This would be meaningful only if a high probability of detecting bioinequivalence by this method is demonstrated.[101]

IVIVCs were achieved in two studies that used SLS-free media: HCl 0.1 N and Simulated USP intestinal fluid at pH 7.5, respectively. However, the potential of using SLS-free buffers remains controversial. For instance, the absence of relevant pKa led to assume that the pH would not play a significant role in dissolution and solubility. Actually, water, as well as other aqueous buffers in the pH range 1.2−6.8, were unable to discriminate between bioinequivalent formulations.[50] In contrast, SLS not only increased the solubility of carbamazepine (Table 1), but also its dissolution,[44,46] suggesting a need to assess the concentration of SLS in the dissolution media. In this regard, several reports of successful IVIVC found in the literature endorse the use of SLS 1% as a suitable dissolution media for IR solid oral products containing carbamazepine.[26,43,50,61,62,82,102] As shown in Table 4, the USP conditions (900 mL SLS 1%, apparatus II, 75 rpm) appears to be sufficiently discriminating in terms of detecting a failure to meet bioequivalence. Nine out of the ten studies found in the literature achieved successful IVIVCs by using the USP conditions.[26,43,50,61,62,82,102] These data strongly support the application of this method as a surrogate technique. It is plausible that the usefulness of SLS 1% as *in vitro* dissolution media relies on the high carbamazepine solubility in this media (Table 1), which provides an improved sink for carbamazepine similar to the one *in vivo* cause by its high intestinal permeability (Table 2). Lastly, although certain changes in the dissolution media and apparatus have been proposed to detect some differences that the USP method did not pick up (see section *Dissolution and IVIVC*), these approaches have not been verified with *in vivo* data yet.

In summary, pharmacopeial dissolution conditions appear to be useful not only for quality control purposes, but also a promising way forward to establishing meaningful IVIVCs for solid oral IR dosage forms containing carbamazepine. The most appropriate absorption parameters (AUC, C_{max}, Fa) to correlate against Fd over the dissolution timeframe of 5−100 min are still to be standardized. Thus, a generally applicable method with regulatory impact does not exist yet. Therefore, further definition of the parameters to be used for establishing meaningful correlations would be necessary before enabling the USP method to function as an *in vitro* surrogate technique for BE studies.

Risk of Bioinequivalence Caused by Excipients and/or Manufacturing

The risk of bioinequivalence of oral solid IR dosage forms has been reported to be intrinsically high for BCS class 2 drug products, due to their physicochemical properties, as well as the formulation and its solubilization principles. Given the existence of diverse carbamazepine forms, the potential influence of polymorphism in the clinical performance becomes an attractive topic for research. The most prevalent polymorphs in tablets were forms I and III, which are transformed into DH in aqueous solution (form I faster than III).[38] Nevertheless, the actual implications of this interconversion in the carbamazepine oral performance are still not clear.

As member of the BCS class 2 group, excipients modifying carbamazepine solubility and dissolution (i.e. surfactants) would be of concern. The risk of a false positive BE decision would remain high as long as the discrimination capacity of the applied test is poor. Diverse excipients, including SLS, were found in carbamazepine IR tablets with a MA (Table 5). However, there is still uncertainty regarding the excipient amounts and processes involved in the manufacture of those products. In one of the aforementioned IVIVC studies, the USP test was discriminating enough to establish a proper IVIVC even though the qualitative composition of the bioinequivalent formulations was different.[43] This example provides evidence of the ability of the USP method to assess the risk of inequivalence due to differences in excipients and/or manufacturing processes. Meanwhile, the substantial evidence of carbamazepine formulations failing to meet BE requirements (Tables 3 and 4) suggests that the risk of a carbamazepine product to fail bioequivalence testing is high.

Patient's Risks Associated with Bioinequivalence

Regulators have the responsibility of approving generic drug products based on evidence of BE. Therefore, the risk of a failure detecting bioinequivalence merits to be assessed also in terms of efficacy and safety. Hence, the approval of a non-bioequivalent product could negatively impact not only the efficacy of treatment, but also the patient's safety. This risk should thus be deemed as high.

Conventional *in vivo* BE studies are usually conducted on a single dose manner; thus, it could be argued that this experiment might overestimate the actual clinical relevance of the formulation tested applying such a study design. Yet, the fact that carbamazepine is an NTI compound supports its classification as presenting a high risk for the BCS-Biowaiver approach to bioequivalence.

Conclusions

Various carbamazepine polymorphs and hydrates have been reported; however, they appear to have a negligible impact on the *in vivo* performance in humans. Carbamazepine displays a pH-independent poor aqueous solubility at the highest strength/clinical doses. Additionally, even though the extent of absorption does not seem to meet the guidance requirements for high permeable drugs, it is very likely that this was caused by the first pass effect rather than poor drug dissolution/permeability. Direct permeability measurements in *in vivo* and various *in vitro* models support this conclusion. In consequence, carbamazepine can be classified as a BCS class 2 drug. Further, the overlapping therapeutic and toxic plasma concentrations lead us to consider carbamazepine as a NTI drug. Taken together, both the BCS and NTI classification suggest that a biowaiver of the *in vivo* BE test is not recommended for carbamazepine IR drug products according to current regulatory guidances.

Nevertheless, several successful examples of IVIVC agreed that the USP dissolution conditions (900 mL water 1% SLS, apparatus II and 75 rpm) were sufficiently discriminative between bioinequivalent products. Further research on choosing the adequate correlation parameters, stressing test sensitivity and defining acceptance ranges, as well as risk assessment on efficacy and safety, is needed to determine whether the *in vitro* USP method can provide a surrogate technique for *in vivo* BE studies. Currently however, a biowaiver for carbamazepine cannot be recommended and the bioequivalence of immediate solid oral dosage forms of carbamazepine should be assessed in an appropriately designed clinical pharmacokinetic study.

Aknowledgments

MAG received financial support from the Agencia Nacional de Investigación y Desarrollo (ANID), Becas de doctorado en el extranjero, nº 72180466. The contributions of Dirk Barends to this manuscript are gratefully acknowledged.

References

1. WHO. *World Health Organization, WHO Technical Report Series, No 937. Annex 8. Proposal to Waive In Vivo Bioequivalence Requirements for WHO Model List of Essential Medicines Immediate-Release, Solid Oral Dosage Forms*. World Health Organization; 2006. http://apps.who.int/medicinedocs/documents/s19640en/s19640en.pdf. Accessed August 5, 2018.

2. WHO. *21st Edition World Health Organization. WHO Model List of Essential Medicines*. twentieth ed. World Health Organization; 2019. https://www.who.int/medicines/publications/essentialmedicines/en. Accessed August 5, 2018.
3. WHO. *7th Edition World Health Organization. WHO Model List of Essential Medicines for Children*. twentieth ed. World Health Organization; 2019. https://www.who.int/medicines/publications/essentialmedicines/en. Accessed August 5, 2018.
4. Vogelpoel H, Welink J, Amidon GL, et al. Biowaiver monographs for immediate release solid oral dosage forms based on biopharmaceutics classification system (BCS) literature data: verapamil hydrochloride, propranolol hydrochloride, and atenolol. *J Pharm Sci*. 2004;93(8):1945-1956.
5. FIP. International pharmaceutical Federation. Biopharmaceutics classification system (BCS). http://www.fip.org/bcs_monographs; 2009. Accessed January 24, 2019.
6. EMA. *European Medicines Agency, Committee for Medicinal Products for Human Use (CHMP). Guideline on the Investigation of Bioequivalence*. London, UK: European Medicines Agency; 2010. http://www.ema.europa.eu/docs/en_GB/document_library/Scientific_guideline/2010/01/WC500070039.pdf. Accessed November 27, 2019.
7. FDA. *Food and Drug Administration, U.S. Department of Health and Human Services. Center for Drug Evaluation and Research (CDER). Guidance for Industry. Waiver of In Vivo Bioavailability and Bioequivalence Studies for Immediate-Release Solid Oral Dosage forms Based on a Biopharmaceutics Classification System*. MD, USA: Food and Drug Administration; 2017. https://www.fda.gov/downloads/Drugs/Guidances/ucm070246.pdf. Accessed November 27, 2019.
8. ICH. *International Council for Harmonization. Committee for Medicinal Products for Human Use (CHMP). ICH M9 Guideline on Biopharmaceutics Classification System-Based Biowaivers, Setp 5*. Amsterdam, The Netherlands: European Medicines Agency; 2020. https://www.ema.europa.eu/en/documents/scientific-guideline/ich-m9-biopharmaceutics-classification-system-based-biowaivers-step-5_en.pdf. Accessed October 20, 2020.
9. Pharmacopeia E. *European Pharmacopeia 9.0*. Carbamazepine Monograph; 2017.
10. Pharmacopeia US. *USP 42 - NF 37. The United States Pharmacopeia*. 42 ed. Rockville, MD: The United States Pharmacopeial Convention, Inc; 2019.
11. Novartis. *Tegretol (carbamazepine USP)*. East Hanover, NJ: Food and Drug Administration U.S; 2009. https://www.accessdata.fda.gov/drugsatfda_docs/label/2009/016608s101,018281s048lbl.pdf. Accessed November 26, 2018.
12. Bauer. *Applied Clinical Pharmacokinetics*. second ed. US: McGraw-Hill; 2008.
13. Maan JS, Saadabadi A. Carbamazepine. In: *StatPearls [Internet]*. Treasure Island, FL: StatPearls Publishing; 2018. https://www.ncbi.nlm.nih.gov/books/NBK482455/. Accessed November 15, 2018.
14. Bialer M, Levy RH, Perucca E. Does carbamazepine have a narrow therapeutic plasma concentration range? *Ther Drug Monit*. 1998;20(1):56-59.
15. Ghannoum M, Yates C, Galvao TF, et al. Extracorporeal treatment for carbamazepine poisoning: systematic review and recommendations from the EXTRIP workgroup. *Clin Toxicol*. 2014;52(10):993-1004.
16. Bertilsson L, Tomson T. Clinical pharmacokinetics and pharmacological effects of carbamazepine and carbamazepine-10,11-epoxide. An update. *Clin Pharmacokinet*. 1986;11(3):177-198.
17. Tothfalusi L, Speidl S, Endrenyi L. Exposure-response analysis reveals that clinically important toxicity difference can exist between bioequivalent carbamazepine tablets. *Br J Clin Pharmacol*. 2008;65(1):110-122.
18. Callaghan N, O'Callaghan M, Duggan B, Feely M. Carbamazepine as a single drug in the treatment of epilepsy. A prospective study of serum levels and seizure control. *J Neurol Neurosurg Psychiatry*. 1978;41(10):907-912.
19. Lesser RP, Pippenger CE, Luders H, Dinner DS. High-dose monotherapy in treatment of intractable seizures. *Neurology*. 1984;34(6):707-711.
20. Chadwick D. Safety and efficacy of vigabatrin and carbamazepine in newly diagnosed epilepsy: a multicentre randomised double-blind study. Vigabatrin European Monotherapy Study Group. *Lancet*. 1999;354(9172):13-19.
21. Schmidt S, Schmitz-Buhl M. Signs and symptoms of carbamazepine overdose. *J Neurol*. 1995;242(3):169-173.
22. Greenberg RG, Melloni C, Wu H, et al. Therapeutic index estimation of antiepileptic drugs: a systematic literature review approach. *Clin Neuropharmacol*. 2016;39(5):232-240.
23. Brodie MJ, Richens A, Yuen AW. Double-blind comparison of lamotrigine and carbamazepine in newly diagnosed epilepsy. UK Lamotrigine/Carbamazepine Monotherapy Trial Group. *Lancet*. 1995;345(8948):476-479.
24. Reunanen M, Dam M, Yuen AW. A randomised open multicentre comparative trial of lamotrigine and carbamazepine as monotherapy in patients with newly diagnosed or recurrent epilepsy. *Epilepsy Res*. 1996;23(2):149-155.
25. Yacobi A, Zlotnick S, Colaizzi JL, et al. A multiple-dose safety and bioequivalence study of a narrow therapeutic index drug: a case for carbamazepine. *Clin Pharmacol Ther*. 1999;65(4):389-394.
26. Olling M, Mensinga TT, Barends DM, Groen C, Lake OA, Meulenbelt J. Bioavailability of carbamazepine from four different products and the occurrence of side effects. *Biopharm Drug Dispos*. 1999;20(1):19-28.
27. FDA. *Food and Drug Administration, U.S. Draft Guidance on Carbamazepine*. Food and Drug Administration; 2011. https://www.fda.gov/downloads/Drugs/GuidanceComplianceRegulatoryInformation/Guidances/UCM270381.pdf. Accessed February 5, 2019.
28. Mattson RH, Cramer JA, Collins JF. A comparison of valproate with carbamazepine for the treatment of complex partial seizures and secondarily generalized tonic-clonic seizures in adults. The Department of Veterans Affairs Epilepsy Cooperative Study No. 264 Group. *N Engl J Med*. 1992;327(11):765-771.
29. FDA. Food and Drug Administration, U.S. Department of Health and Human Services. Center for Drug Evaluation and Research (CDER). In: *Orange Book: Approved. DRUG Products with Therapeutic Equivalence Evaluations; 2018*. MD, USA: Food and Drug Administration; 2018. https://www.accessdata.fda.gov/scripts/cder/ob/index.cfm. Accessed October 20, 2020.
30. Behme RJ, Brooke D. Heat of fusion measurement of a low melting polymorph of carbamazepine that undergoes multiple-phase changes during differential scanning calorimetry analysis. *J Pharm Sci*. 1991;80(10):986-990.
31. Grzesiak AL, Lang M, Kim K, Matzger AJ. Comparison of the four anhydrous polymorphs of carbamazepine and the crystal structure of form I. *J Pharm Sci*. 2003;92(11):2260-2271.
32. Lang M, Kampf JW, Matzger AJ. Form IV of carbamazepine. *J Pharm Sci*. 2002;91(4):1186-1190.
33. Roberts RJ, Rowe RC. Influence of polymorphism on the Young's modulus and yield stress of carbamazepine, sulfathiazole and sulfanilamide. *Int J Pharm*. 1996;129:79-94.
34. Kobayashi Y, Ito S, Itai S, Yamamoto K. Physicochemical properties and bioavailability of carbamazepine polymorphs and dihydrate. *Int J Pharm*. 2000;193(2):137-146.
35. Tian F, Zeitler JA, Strachan CJ, Saville DJ, Gordon KC, Rades T. Characterizing the conversion kinetics of carbamazepine polymorphs to the dihydrate in aqueous suspension using Raman spectroscopy. *J Pharm Biomed Anal*. 2006;40(2):271-280.
36. Deng J, Staufenbiel S, Bodmeier R. Evaluation of a biphasic in vitro dissolution test for estimating the bioavailability of carbamazepine polymorphic forms. *Eur J Pharm Sci*. 2017;105:64-70.
37. Murphy D, Rodriguez-Cintron F, Langevin B, Kelly RC, Rodriguez-Hornedo N. Solution-mediated phase transformation of anhydrous to dihydrate carbamazepine and the effect of lattice disorder. *Int J Pharm*. 2002;246(1-2):121-134.
38. Flicker F, Eberle VA, Betz G. Variability in commercial carbamazepine samples–impact on drug release. *Int J Pharm*. 2011;410(1-2):99-106.
39. Amidon GL, Lennernas H, Shah VP, Crison JR. A theoretical basis for a biopharmaceutic drug classification: the correlation of in vitro drug product dissolution and in vivo bioavailability. *Pharm Res (N Y)*. 1995;12(3):413-420.
40. Beig A, Miller JM, Dahan A. Accounting for the solubility-permeability interplay in oral formulation development for poor water solubility drugs: the effect of PEG-400 on carbamazepine absorption. *Eur J Pharm Biopharm*. 2012;81(2):386-391.
41. Ikinci G, Capan Y, Senel S, Dalkara T, Hincal AA. Formulation and in vitro/in vivo investigation of carbamazepine controlled-release matrix tablets. *Pharmazie*. 1999;54(2):139-141.
42. Kasim NA, Whitehouse M, Ramachandran C, et al. Molecular properties of WHO essential drugs and provisional biopharmaceutical classification. *Mol Pharm*. 2004;1(1):85-96.
43. Lake OA, Olling M, Barends DM. In vitro/in vivo correlations of dissolution data of carbamazepine immediate release tablets with pharmacokinetic data obtained in healthy volunteers. *Eur J Pharm Biopharm*. 1999;48(1):13-19.
44. Lee H, Park SA, Sah H. Surfactant effects upon dissolution patterns of carbamazepine immediate release tablet. *Arch Pharm Res (Seoul)*. 2005;28(1):120-126.
45. Mittapalli PK, Suresh B, Hussaini SS, Rao YM, Apte S. Comparative in vitro study of six carbamazepine products. *AAPS PharmSciTech*. 2008;9(2):357-365.
46. El-Massik MA, Abdallah OY, Galal S, Daabis NA. Towards a universal dissolution medium for carbamazepine. *Drug Dev Ind Pharm*. 2006;32(7):893-905.
47. Soderlind E, Karlsson E, Carlsson A, et al. Simulating fasted human intestinal fluids: understanding the roles of lecithin and bile acids. *Mol Pharm*. 2010;7(5):1498-1507.
48. Obata K, Sugano K, Saitoh R, et al. Prediction of oral drug absorption in humans by theoretical passive absorption model. *Int J Pharm*. 2005;293(1-2):183-192.
49. Scheytt T, Mersmann P, Lindstädt R, Heberer T. 1-octanol/water partition coefficients of 5 pharmaceuticals from human medical care: carbamazepine, clofibric acid, diclofenac, ibuprofen, and propyphenazone. *Water Air Soil Pollut*. 2005;165:3-11.
50. Kovacevic I, Parojcic J, Homsek I, Tubic-Grozdanis M, Langguth P. Justification of biowaiver for carbamazepine, a low soluble high permeable compound, in solid dosage forms based on IVIVC and gastrointestinal simulation. *Mol Pharm*. 2009;6(1):40-47.
51. Faigle JW, Feldman F. Pharmacokinetic data of carbamazepine and its major metabolites in man. In: Schneider H, Janz D, Gardner-Thorpe C, Meinardi H, Sherwin AL, eds. *Clinical Pharmacology of Anti-epileptic Drugs*. Berlin, Heidelberg: Springer; 1975.
52. Gerardin A, Dubois JP, Moppert J, Geller L. Absolute bioavailability of carbamazepine after oral administration of a 2% syrup. *Epilepsia*. 1990;31(3):334-338.
53. Schneider HJD, Gardner-Thorpe C, Meindardi H, Sherwin AL. *Clinical Pharmacology of Anti-epileptic Drugs*. New Yor, Heldelberg, Berlin: Springer-Verlag; 1975.
54. Lundbeck. *U.S. FDA Approves Carnexiv™ (Carbamazepine) Injection as Intravenous Replacement Therapy for Oral Carbamazepine Formulation*. Copenhagen, DK: H. Lundbeck A/S; 2016. https://investor.lundbeck.com/static-files/9ebea97f-f286-4a6c-a61f-6bed362c2e39. Accessed November 26, 2018.

55. Marino SE, Birnbaum AK, Leppik IE, et al. Steady-state carbamazepine pharmacokinetics following oral and stable-labeled intravenous administration in epilepsy patients: effects of race and sex. *Clin Pharmacol Ther*. 2012;91(3):483-488.
56. Tolbert D, Cloyd J, Biton V, et al. Bioequivalence of oral and intravenous carbamazepine formulations in adult patients with epilepsy. *Epilepsia*. 2015;56(6):915-923.
57. Anttila M, Kahela P, Panelius M, Yrjana T, Tikkanen R, Aaltonen R. Comparative bioavailability of two commercial preparations of carbamazepine tablets. *Eur J Clin Pharmacol*. 1979;15(6):421-425.
58. Rawlins MD, Collste P, Bertilsson L, Palmer L. Distribution and elimination kinetics of carbamazepine in man. *Eur J Clin Pharmacol*. 1975;8(2):91-96.
59. Bertilsson L. Clinical pharmacokinetics of carbamazepine. *Clin Pharmacokinet*. 1978;3(2):128-143.
60. Levy RH, Pitlick WH, Troupin AS, Green JR, Neal JM. Pharmacokinetics of carbamazepine in normal man. *Clin Pharmacol Ther*. 1975;17(6):657-668.
61. Meyer MC, Straughn AB, Jarvi EJ, Wood GC, Pelsor FR, Shah VP. The bioinequivalence of carbamazepine tablets with a history of clinical failures. *Pharm Res (N Y)*. 1992;9(12):1612-1616.
62. Veng-Pedersen P, Gobburu JV, Meyer MC, Straughn AB. Carbamazepine level-A in vivo-in vitro correlation (IVIVC): a scaled convolution based predictive approach. *Biopharm Drug Dispos*. 2000;21(1):1-6.
63. Zhang X, Lionberger RA, Davit BM, Yu LX. Utility of physiologically based absorption modeling in implementing quality by design in drug development. *AAPS J*. 2011;13(1):59-71.
64. Alsenz J, Haenel E. Development of a 7-day, 96-well Caco-2 permeability assay with high-throughput direct UV compound analysis. *Pharm Res (N Y)*. 2003;20(12):1961-1969.
65. Faassen F, Vogel G, Spanings H, Vromans H. Caco-2 permeability, P-glycoprotein transport ratios and brain penetration of heterocyclic drugs. *Int J Pharm*. 2003;263(1-2):113-122.
66. Fortuna A, Alves G, Falcao A, Soares-da-Silva P. Evaluation of the permeability and P-glycoprotein efflux of carbamazepine and several derivatives across mouse small intestine by the Ussing chamber technique. *Epilepsia*. 2012;53(3):529-538.
67. Kratz JM, Teixeira MR, Koester LS, Simoes CM. An HPLC-UV method for the measurement of permeability of marker drugs in the Caco-2 cell assay. *Braz J Med Biol Res*. 2011;44(6):531-537.
68. Krstic M, Popovic M, Dobricic V, Ibric S. Influence of solid drug delivery system formulation on poorly water-soluble drug dissolution and permeability. *Molecules*. 2015;20(8):14684-14698.
69. Owen A, Pirmohamed M, Tettey JN, Morgan P, Chadwick D, Park BK. Carbamazepine is not a substrate for P-glycoprotein. *Br J Clin Pharmacol*. 2001;51(4):345-349.
70. Patil SR, Kumar L, Kohli G, Bansal AK. Validated HPLC method for concurrent determination of antipyrine, carbamazepine, Furosemide and phenytoin and its application in assessment of drug permeability through caco-2 cell monolayers. *Sci Pharm*. 2012;80(1):89-100.
71. Winiwarter S, Bonham NM, Ax F, Hallberg A, Lennernas H, Karlen A. Correlation of human jejunal permeability (in vivo) of drugs with experimentally and theoretically derived parameters. A multivariate data analysis approach. *J Med Chem*. 1998;41(25):4939-4949.
72. Dickens D, Yusof SR, Abbott NJ, et al. A multi-system approach assessing the interaction of anticonvulsants with P-gp. *PLoS One*. 2013;8(5):e64854.
73. Luna-Tortos C, Fedrowitz M, Loscher W. Several major antiepileptic drugs are substrates for human P-glycoprotein. *Neuropharmacology*. 2008;55(8):1364-1375.
74. Cerveny L, Pavek P, Malakova J, Staud F, Fendrich Z. Lack of interactions between breast cancer resistance protein (bcrp/abcg2) and selected antiepileptic agents. *Epilepsia*. 2006;47(3):461-468.
75. Eichelbaum M, Ekbom K, Bertilsson L, Ringberger VA, Rane A. Plasma kinetics of carbamazepine and its epoxide metabolite in man after single and multiple doses. *Eur J Clin Pharmacol*. 1975;8(5):337-341.
76. Garg SK, Kumar N, Bhargava VK, Prabhakar SK. Effect of grapefruit juice on carbamazepine bioavailability in patients with epilepsy. *Clin Pharmacol Ther*. 1998;64(3):286-288.
77. Kerr BM, Thummel KE, Wurden CJ, et al. Human liver carbamazepine metabolism. Role of CYP3A4 and CYP2C8 in 10,11-epoxide formation. *Biochem Pharmacol*. 1994;47(11):1969-1979.
78. Mesdjian E, Seree E, Charvet B, et al. Metabolism of carbamazepine by CYP3A6: a model for in vitro drug interactions studies. *Life Sci*. 1999;64(10):827-835.
79. Bonin B, Vandel P, Vandel S, Kantelip JP. Effect of grapefruit intake on carbamazepine bioavailability: a case report. *Therapie*. 2001;56(1):69-71.
80. Dresser GK, Spence JD, Bailey DG. Pharmacokinetic-pharmacodynamic consequences and clinical relevance of cytochrome P450 3A4 inhibition. *Clin Pharmacokinet*. 2000;38(1):41-57.
81. Mochizuki K, Hamano Y, Miyama H, Arakawa K, Kobayashi T, Imamura H. Successful treatment of a case with concurrent ingestion of carbamazepine overdose and grapefruit juice. *Acute Med Surg*. 2016;3(1):36-38.
82. Gonzalez-Garcia I, Mangas-Sanjuan V, Merino-Sanjuan M, et al. IVIVC approach based on carbamazepine bioequivalence studies combination. *Pharmazie*. 2017;72(8):449-455.
83. Popovic J, Mikov M, Jakovljevic V. Pharmacokinetics of carbamazepine derived from a new tablet formulation. *Eur J Drug Metab Pharmacokinet*. 1995;20(4):297-300.
84. Kayali A, Tuglular I, Ertas M. Pharmacokinetics of carbamazepine. Part I: a new bioequivalency parameter based on a relative bioavailability trial. *Eur J Drug Metab Pharmacokinet*. 1994;19(4):319-325.
85. Revankar SN, Desai ND, Bhatt AD, et al. Comparison of absorption rate and bioavailability of two brands of carbamazepine. *J Assoc Phys India*. 1999;47(7):699-702.
86. Silpakit O, Amornpichetkoon M, Kaojarern S. Comparative study of bioavailability and clinical efficacy of carbamazepine in epileptic patients. *Ann Pharmacother*. 1997;31(5):548-552.
87. Savolainen M, Kogermann K, Heinz A, et al. Better understanding of dissolution behaviour of amorphous drugs by in situ solid-state analysis using Raman spectroscopy. *Eur J Pharm Biopharm*. 2009;71(1):71-79.
88. Zhou Y, Chu W, Lei M, Li J, Du W, Zhao C. Application of a continuous intrinsic dissolution-permeation system for relative bioavailability estimation of polymorphic drugs. *Int J Pharm*. 2014;473(1-2):250-258.
89. Kahela P, Aaltonen R, Lewing E, Anttila M, Kristoffersson E. Pharmacokinetics and dissolution of two crystalline forms of carbamazepine. *Int J Pharm*. 1983;14(1):103-112.
90. Elqidra R, Ünlü N, Çapan Y, Sahin G, Dalkara T, Hincal AA. Effect of polymorphism on in vitro-in vivo properties of carbamazepine conventional tablets. *J Drug Deliv Sci Technol*. 2004;14(2):147-153.
91. Chan KK, Sawchuk RJ, Thompson TA, et al. Bioequivalence of carbamazepine chewable and conventional tablets: single-dose and steady-state studies. *J Pharm Sci*. 1985;74(8):866-870.
92. Cornaggia C, Gianetti S, Battino D, et al. Comparative pharmacokinetic study of chewable and conventional carbamazepine in children. *Epilepsia*. 1993;34(1):158-160.
93. Dam M, Christiansen J, Kristensen CB, Helles A, Jaegerskou A, Schmiegelow M. Carbamazepine: a clinical biopharmaceutical study. *Eur J Clin Pharmacol*. 1981;20(1):59-64.
94. Shah VP, Konecny JJ, Everett RL, McCullough B, Noorizadeh AC, Skelly JP. In vitro dissolution profile of water-insoluble drug dosage forms in the presence of surfactants. *Pharm Res (N Y)*. 1989;6(7):612-618.
95. Medina JR, Salazar DK, Hurtado M, Cortes AR, Dominguez-Ramirez AM. Comparative in vitro dissolution study of carbamazepine immediate-release products using the USP paddles method and the flow-through cell system. *Saudi Pharm J*. 2014;22(2):141-147.
96. Kaneniwa N, Umezawa O, Watari N, Kawakami K, Asami H, Sumi M. [Bioavailability and dissolution test of commercial carbamazepine tablets]. *Yakugaku Zasshi*. 1984;104(1):83-90.
97. Jung H, Milán RC, Girard ME, León F, Montoya MA. Bioequivalence study of carbamazepine tablets: in vitro/in vivo correlation. *Int J Pharm*. 1997;152(1):37-44.
98. Bonlokke L, Hovgaard L, Kristensen HG, Knutson L, Lindahl A, Lennernas H. A comparison between direct determination of in vivo dissolution and the deconvolution technique in humans. *Eur J Pharm Sci*. 1999;8(1):19-27.
99. Lobenberg R, Amidon GL. Modern bioavailability, bioequivalence and biopharmaceutics classification system. New scientific approaches to international regulatory standards. *Eur J Pharm Biopharm*. 2000;50(1):3-12.
100. Sethia S, Squillante E. In vitro-in vivo evaluation of supercritical processed solid dispersions: permeability and viability assessment in Caco-2 cells. *J Pharm Sci*. 2004;93(12):2985-2993.
101. Kubbinga M, Langguth P, Barends D. Risk analysis in bioequivalence and biowaiver decisions. *Biopharm Drug Dispos*. 2013;34(5):254-261.
102. Meyer MC, Straughn AB, Mhatre RM, Shah VP, Williams RL, Lesko LJ. The relative bioavailability and in vivo-in vitro correlations for four marketed carbamazepine tablets. *Pharm Res (N Y)*. 1998;15(11):1787-1791.
103. Bermejo M, Meulman J, Davanco MG, Carvalho PO, Gonzalez-Alvarez I, Campos DR. In vivo predictive dissolution (IPD) for carbamazepine formulations: additional evidence regarding a biopredictive dissolution medium. *Pharmaceutics*. 2020;12(6).
104. Oles KS, Penry JK, Smith LD, Anderson RL, Dean JC, Riela AR. Therapeutic bioequivalency study of brand name versus generic carbamazepine. *Neurology*. 1992;42(6):1147-1153.
105. Hartley R, Aleksandrowicz J, Bowmer CJ, Cawood A, Forsythe WI. Dissolution and relative bioavailability of two carbamazepine preparations for children with epilepsy. *J Pharm Pharmacol*. 1991;43(2):117-119.
106. Homsek I, Parojcic J, Cvetkovic N, Popadic D, Djuric Z. Biopharmaceutical characterization of carbamazepine immediate release tablets. In vitro-in vivo comparison. *Arzneim Forsch*. 2007;57(8):511-516.

APPENDIX 2 (PUBLICATION #2).

IN VITRO PREDICTION OF IN VIVO ABSORPTION OF IBUPROFEN FROM SUSPENSIONS THROUGH RATIONAL CHOICE OF DISSOLUTION CONDITIONS

European Journal of Pharmaceutics and Biopharmaceutics 149 (2020) 229–237

Contents lists available at ScienceDirect

European Journal of Pharmaceutics and Biopharmaceutics

journal homepage: www.elsevier.com/locate/ejpb

Research paper

In vitro prediction of *in vivo* absorption of ibuprofen from suspensions through rational choice of dissolution conditions

Michael Hofmann[a,1], Mauricio A. García[a,1], Jozef Al-Gousous[a], Alejandro Ruiz-Picazo[b], Florian Thieringer[c], Mai A. Nguyen[a], Wiking Månsson[d], Peter R. Galle[c], Peter Langguth[a,*]

[a] Johannes Gutenberg-Universität, Staudingerweg 5, 55128 Mainz, Germany
[b] Miguel Hernandez University, Alicante 03550, Spain
[c] I. Medizinische Klinik und Poliklinik, Universitätsmedizin der Johannes Gutenberg-Universität Mainz, Langenbeckstraße 1, 55131 Mainz, Germany
[d] Bioperm AB, Tullgatan 1A, SE-223 54 Lund, Sweden

ARTICLE INFO

Keywords:
Dissolution
Bicarbonate
Buffer
Intestine
Biowaivers

ABSTRACT

Two ibuprofen suspension formulations were investigated for their dissolution in various bicarbonate, phosphate and acetate buffers. Phosphate and acetate gave faster release than bicarbonate at comparable molarities. Nevertheless, mass transport modelling using the reversible non-equilibrium (RNE) approach enabled the calculation of phosphate molarities that gave good matches to physiological bicarbonate in terms of ibuprofen dissolution. This shows that developing surrogate buffers for bicarbonate that are devoid of the technical difficulties associated with the bicarbonate-CO_2 systems is possible. In addition, the intestinal dissolution kinetics of the tested suspensions were determined by applying compartmental pharmacokinetic modelling to plasma profiles that were previously obtained for these suspensions in an *in vivo* study performed on healthy human volunteers. The *in vitro* dissolution profiles in bicarbonate compared reasonably well with the profiles representing the *in vivo* intestinal dissolution kinetics of the tested suspensions when applied to healthy human volunteers in a pharmacokinetic study. This shows the possible potential toward extending biowaivers so that they include BCS class IIa compounds.

1. Introduction

Pharmaceutical industry routinely uses dissolution methodologies for quality control and drug product development purposes. From a regulatory perspective, the dissolution test is also used to assess for the possibility of obtaining biowaivers for immediate release solid dosage forms of BCS class I and III drugs. Given that biowaivers are beneficial and advantageous in terms of cost, time and ethics (through reduction of experiments on human subjects), the possibility of extending them to additional BCS class II is an attractive option [1]. Typically, the *in vivo* performance of a BCS II compound is mainly determined by the *in vivo* dissolution within the gastrointestinal tract (GIT), supposedly the rate-limiting step for the systemic appearance. Thus, an inadequate *in vitro* dissolution methodology that is not sufficiently discriminative might result in a false positive bioequivalence decision (i.e. increased consumer risk) [2]. Therefore, the development of biopredictive and robust dissolution methods is a major need to make such an extension feasible [1,2].

The extension for biowaivers to BCS class II weak acids (BCS IIa) has already been vastly debated in the pharmaceutical field, because theoretically, the higher intestinal pHs should raise their solubility after leaving the stomach. However, there is still a concern regarding to the *in vitro* detection of bioinequivalence, as shown by experimental evidence. Álvarez et al. investigated the *in vitro* dissolution of many bioinequivalent tablets containing 600 mg of ibuprofen using the following pharmacopoeial media: (1) hydrochloric acid (pH 1.2, ionic strength 130 mM); (2) acetate (pH 4.5, ionic strength 540 mM); and (3) phosphate (pH 6.8, ionic strength 70 mM). None of these experimental conditions were capable to discriminate between any of the tests and their references [3]. On the other hand, the possibility of over-discriminating *in vitro* dissolution methodologies may negatively impact the pharmaceutical industry [4], where the *in vivo* performance of innovator, as well as generics, BCS II-containing drug products can be misjudged during the early development stages (i.e. increased producer

* Corresponding author at: Institut für Pharmazeutische und Biomedizinische Wissenschaften, Abteilung Pharmazeutische Technologie und Biopharmazie, Johannes Gutenberg-Universität, Staudingerweg 5, 55128 Mainz, Germany.
E-mail address: langguth@uni-mainz.de (P. Langguth).
[1] Equal first authors.

https://doi.org/10.1016/j.ejpb.2020.02.009
Received 14 December 2019; Received in revised form 7 February 2020; Accepted 21 February 2020
Available online 26 February 2020
0939-6411/

risk).

These two scenarios emphasize the need for biopredictive *in vitro* methods. One possible approach to increase biopredictability is reduction of buffer molarities in order to match the typically slower dissolution *in vivo*. For instance, Tsume et al. demonstrated that *in vitro* dissolution of ibuprofen tablets in phosphate 10 mM was slower compared to 50 mM at a starting pH of 6.0 [5]. According to Mooney's stagnant film-based dissolution model, those findings can be explained by the lower ability of more diluted buffers to counter the acidifying effect of the dissolving ibuprofen on the boundary layer pH (owing to reduced buffer capacity) [6]. In this regard, the significance of the chemical nature of the buffer must also be considered. Physiologically, the species buffering the proximal small intestine is bicarbonate at a concentration of 8 ± 6 mM [7]. As a matter of fact, the use of bicarbonate 11.5 mM accounted for *in vivo* differences observed in the aforementioned study by Álvarez et al. [3,8]. In order to explain these observations, the complex physical chemistry governing the buffering action by bicarbonate should be taken into account. This complexity is associated with the relatively slow interconversion between carbonic acid and carbon dioxide [9]. This causes the effective pKa of bicarbonate in the boundary layer to be much lower than the potentiometrically determined value of 6.35, which under intestinal conditions weakens its ability to buffer the boundary layer against incoming ionizable solute. To account for this complexity, a mass transport model termed the "reversible non-equilibrium" (RNE) model was developed [9].

Additionally, developing biopredictive dissolution methods needs reliable estimates of the *in vivo* dissolution rates as a validation standard. One approach to obtain an *in vivo* dissolution profile is to deconvolute the pharmacokinetic profile using an oral solution as a weighing function [10]. This approach, while often useful for extended release dosage forms, suffers from some limitations. For instance, the gastric emptying rate is often not satisfactorily separated from the dissolution rate due to the high variability in gastric emptying, incomplete solid oral dosage form disintegration in the stomach and/or differences between the gastric emptying kinetics of solids and liquids. In addition to the possibility of precipitation in some cases, namely poorly soluble weakly acidic drugs being precipitated by gastric acid. Bypassing the stomach by intubation combined with the infusion of a suspension at a controlled rate is an elegant albeit technically complex way of overcoming such issues. Along these lines, our laboratory studied the PK of ibuprofen after the intraduodenal infusion of either an ibuprofen solution or suspensions with different particle sizes [11].

The aim of this work is the development of a biopredictive method for the dissolution of ionizable BCS class II compounds. Dissolution of ibuprofen particles from either small (SA) and large (SB) particle size suspensions was tested in phosphate, acetate and bicarbonate. The Mooney and the RNE models were used to estimate the surface pH and to calculate the equivalent buffer concentrations in order to develop surrogate buffers. Finally, a modeling methodology is described to deconvolute recently published clinical data after intraduodenal administration of the same formulations. The so generated *in vivo* dissolution profiles were used to support the biorelevance of the *in vitro* methodologies presented here.

2. Materials and methods

2.1. Materials

Reagents used in formulations' manufacturing were acquired from different sources. Ibuprofen 25 and 70, as well as Povidone (PVP) K 90, were obtained from BASF (BTC Europe GmbH - BASF, Germany). Polysorbate (Tween) 80 and sodium chloride were purchased from Fagron (Fagron GmbH & Co. KG, Germany). Potassium Sorbate was bought from Euro-OTC (Euro OTC Pharma GmbH, Germany). Tygon® LFL pumping tubes (OD 4.47 mm, ID 2.79 mm) were purchased from IDEX (Ismatec, IDEX Health and Science, Germany), whilst tube connectors from Carl Roth (Carl Roth GmbH & Co. KG, Germany). Likewise, all buffer reagents (sodium acetate, sodium bicarbonate, monobasic sodium phosphate, dibasic sodium phosphate, sodium chloride, hydrochloric acid and sodium hydroxide) and supplies for dissolution experiments (syringes and filters) were obtained from Carl Roth GmbH, too.

2.2. Formulations

Ibuprofen suspensions were manufactured as described by Hofmann et al. [11]. Briefly, the formulations were typically prepared one or two days before dissolution experiments. Proper amounts of PVP K 90, sodium chloride, tween 80 and potassium sorbate were placed into a glass beaker, filled with deionized water up to 250 g and stirred (vehicle). Afterwards, 400 mg of either ibuprofen 25 (small particle size) or 70 (large particle size) were added to the vehicle and stirred overnight. Finally, the median particle sizes (d50) were verified in the Universal Liquid Module of a Laser Diffraction Particle Size analyzer LS 13 320 (Beckman Coulter, IN, United States). Suspension A (SA) and suspension B (SB) showed d50 values of 58.3 ± 4.7 and 128.6 ± 7.0 μm, respectively.

2.3. In vitro dissolution

Ibuprofen dissolution was studied in diverse dissolution media, namely phosphate, acetate and bicarbonate at concentrations of either 5 or 15 mM on basis of the molarity of their respective conjugate base. In addition, dissolution experiments were also carried out in phosphate media at 1 and 2 mM. A pH of 6.0 and ionic strength of 154 mM (equal to that of physiological saline) were reached by adjusting the buffers' conjugate acid molarities and amounts of sodium chloride, respectively, for each media. Owing to the volatility of dissolved CO_2, continuous sparging of CO_2/air to maintain the concentration of the conjugate acid was required. Gas flow was adjusted until pH = 6.0 and kept for at least 15 min before starting the experiment. This flow was subsequently maintained along the experiment regardless any eventual fluctuation of the pH as consequence of drug dissolution.

All dissolution experiments were conducted in a USP type II apparatus PTW S III (Pharma Test, Germany) at 50 rpm and 37 °C. Because pumping the coarse suspension was found to slightly but significantly reduce the particle size (apparently through mechanical fracture of some of the largest particles as explained in the Supplementary Material), it was passed through the pump (Ismatec, IDEX Health and Science, Germany) before starting the dissolution experiment to mimic the *in vivo* conditions. The experiment started after adding 20 ml of either SA or SB to 900 ml of dissolution media (n = 3). The pH was monitored in one of the vessels during the whole experiment. Samples of 5 ml were taken after 2.5, 5, 10, 15, 20, 30, 45, 60, and 90 min, and filtered through 45 μm-filters. Volumes withdrawn were not re-filled but taken into account for the calculation of the fraction dissolved. The dissolved amounts of ibuprofen were determined spectrophotometrically at λ_{max} = 225.3 nm using a UV 6300 PC double beam spectrophotometer (VWR International, LLC, PA, US).

2.4. Surface pH and equivalent buffer molarities

The recently published RNE model was used to estimate the pH on the surface of a solid particle of ibuprofen (pH_0) in bicarbonate buffer, while the Mooney model was used to estimate the phosphate concentration that would give the same surface pH [9]. The required physico-chemical constants for bicarbonate buffer and ibuprofen were taken from the Al-Gousous et al. work [9], those for phosphate were taken from the work of Sheng et al. [12], with the phosphate pKa being corrected for the influence of ionic strength (pKa = 6.8 at an ionic strength of 0.154 M).

As for the boundary layer thickness, which influences the surface pH in bicarbonate but not in phosphate, a rough estimate was obtained from the plots in the work of Sugano [13]. Based on average particle radii of 32 and 57 μm for the fine and coarse suspensions respectively, the boundary layer thickness was estimated to lie, on average, in the range ~17 to 22 μm. Therefore, 20 μm was taken as an estimate to be used for calculating the surface pH in bicarbonate.

2.5. In vivo model

2.5.1. Software

Berkeley Madonna version 8.3.18 (University of California, Department of Molecular and Cellular Biology, Berkeley, CA 94720, United States) was used for solving the differential equations. Further data analysis was done with Microsoft® Excel® 2016 MSO.

2.5.2. Clinical data

The clinical data used to assess the intraluminal dissolution of ibuprofen suspensions was obtained from a previous work [11]. Briefly, ibuprofen formulations were directly infused into the duodenal region of nine fasted healthy human volunteers at predefined infusion rates to mimic gastric emptying (half-life 12 min). The study phases are encoded as follows: Study Phase A (SPA): 400 mg/250 ml solution, Study Phase B (SPB): 400 mg/250 ml suspension with small particles (SA) and Study Phase C (SPC): 400 mg/250 ml suspension with large particles (SB).

2.5.3. Modeling strategy

Two models were developed and used for the fits and predictions. Briefly, a solution model (SM) was used to obtain individual pharmacokinetic rate constants [absorption rate constant (k_a), transport rate constants between central and peripheral compartment (k_{12} and k_{21}), elimination rate constant (k_{10})], and the individual volume of distribution in the central compartment ($V_{central}$). These were used as input for a Diphasic Dissolution Model (DPDM) for suspensions in order to obtain the individual dissolution rates. Both models used the Runge-Kutta 4 (RK4) integration method, a start time of 0 h, a stop time of 10 h and a default dt interval of 0.02. As for general assumptions, no precipitation was considered for the model due to the physicochemical properties as well as no significant degradation alongside the transport of the drug through the gastrointestinal tract. Furthermore, no change of the k_a was assumed for this work.

2.5.4. Solution model

Scheme 1 is describing the sequence of events that were considered after dosing a solution. Compartments in this model were the infusion reservoir (inf res), the intestine, the central compartment and the peripheral compartment. The model used the following rate constants: infusion rate constant (k_{inf}), absorption rate constant (k_a), intercompartmental transfer rate constants (k_{12} and k_{21}), elimination rate constant (k_{10}). k_{inf} was set to a gastric emptying half-life of 12 min according the clinical study. The datasets of 7 volunteers were imported and used for the fit of k_a, k_{12}, k_{21}, k_{10} and $V_{central}$. The differential equations are given in the supplementary material.

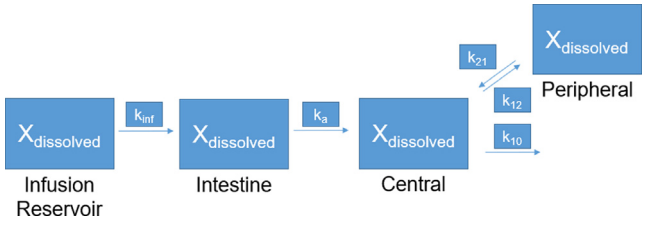

Scheme 1. Solution Model describing the sequence of events after intestinal infusion of a solution. Each Box represents either a compartment (large box) or a rate constant (small box).

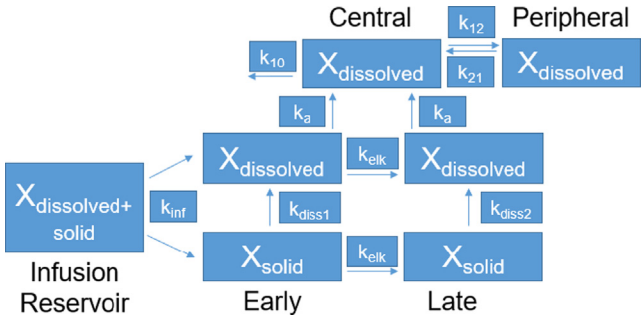

Scheme 2. Diphasic Dissolution Model describing the sequence of events after intestinal infusion of a suspension. Each box represents a compartment (large box) or a rate constant (small box).

2.5.5. Diphasic dissolution model (DPDM)

Scheme 2 describes the sequence of events that were considered after dosing a suspension. Compartments in this model were the infusion reservoir, the intestinal dissolution and absorption compartment where the dissolution is divided into early and late dissolution phases, and the central and peripheral systemic compartments. The model used the following rate constants: k_{inf}, k_a, k_{12}, k_{21}, k_{10}, the rate constant for the change from early to late dissolution **k**inetics (k_{elk}), and dissolution rate constants for each dissolution phase (k_{diss1}, k_{diss2}). The DPDM used the individual fitted values of k_a, k_{12}, k_{21}, k_{10} and $V_{central}$ obtained by the SM for each respective volunteer. The datasets of 7 volunteers for SPB and 4 volunteers for SPC were imported and used for the fit of k_{diss1}, k_{diss2} and k_{elk}. The differential equations are given in the supplementary material.

2.5.6. In vivo equivalent dissolution

To describe the *in vivo* dissolution kinetics of the solid fraction of the SA and SB, *in vivo* equivalent dissolution (IVED) profiles were calculated. Individual k_{diss1}, k_{diss2} and k_{elk} were obtained by the procedure explained above and used as input. The differential equation system for the models can be solved using Laplace Transform and applying partial fractions theorem to give an algebraic expression that describes the overall dissolution kinetics (Eq. (1)) [14].

$$Q_{diss} = D \times \left[1 - e^{-(k_{diss1}+k_{elk})*t} - \frac{k_{elk} * e^{-k_{diss2}*t}}{(k_{elk} + k_{diss1} - k_{diss2})} - \frac{k_{elk} * e^{-(k_{diss1}+k_{elk})*t}}{(k_{diss2} - k_{diss1} - k_{elk})}\right] \quad (1)$$

Where Q_{diss} is the amount dissolved at time (t) and D is the dose.

3. Results and discussion

3.1. In vitro dissolution of ibuprofen suspensions

Fig. 1 shows ibuprofen dissolution from SA and SB in the different dissolution media studied. Overall, dissolution rates in media with lower molarities (5 mM, solid lines) were slower than in more concentrated media (15 mM, dashed lines), consistent with a dissolution process controlled by the concentration of buffer's conjugate base [5,6]. Overall, the fastest profiles were obtained in phosphate media, where ibuprofen was very rapidly dissolved (100% in less than 15 min) regardless of the formulation or the buffer molarity (Fig. 1A). Furthermore, no differences between profiles of SA and SB were observed.

Similarly, the complete dissolution of SA and SB was also very fast in acetate 15 mM, with little discrimination between the dissolution profiles (Fig. 1B, dashed lines). Conversely, the dissolution of SB was

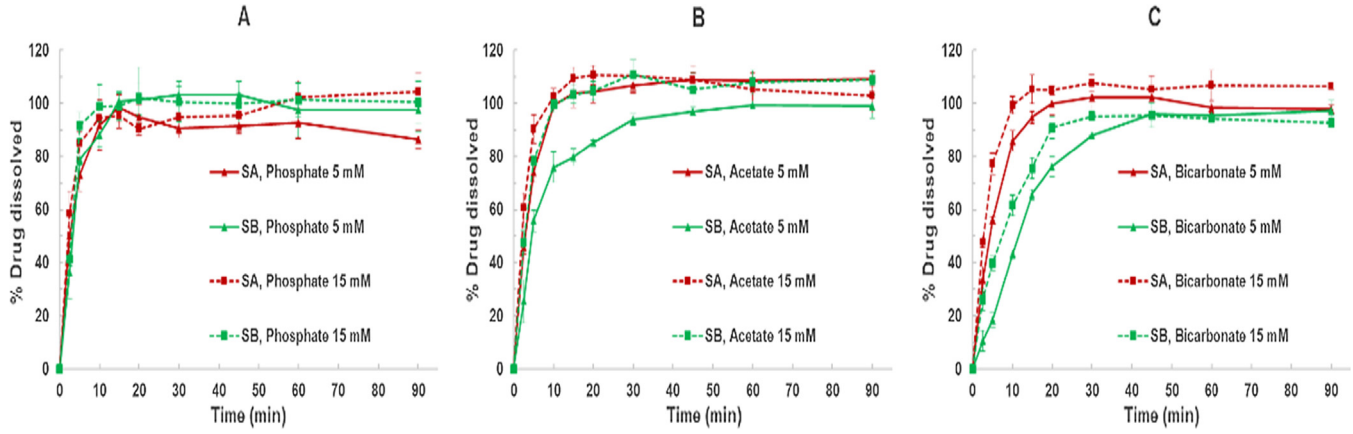

Fig. 1. *In vitro* dissolution of ibuprofen from either suspension A (SA, red) or B (SB, green) in phosphate (A), acetate (B) and bicarbonate media (C) at concentrations of 5 (solid lines) or 15 mM (dashed lines). The error bars represent the standard deviation (n = 3). The concentrations represent the conjugate base molarities. The % Drug dissolved represents that of the solid fraction of the suspension (For interpretation of the references to color in this figure legend, the reader is referred to the web version of this article.)

slower in acetate 5 mM, allowing it to be visibly distinguished from SA (Fig. 1B, solid lines). As a matter of fact, complete dissolution of SB in the latter media did not occur before 45 min. Interestingly, this dissolution profile seems rather closer to those seen in bicarbonate media (Fig. 1C), in which the slowest dissolution rates were observed. Consistently, the slower dissolution rates caused by bicarbonate media were accompanied by an improvement in the discrimination between SA and SB curves at both of the investigated buffer molarities (Fig. 1C) [8,15].

Motivated by these findings, the pH_0 values in bicarbonate were estimated by using the RNE model (Table 1) [9]. As anticipated, pH_0 values were smaller than the initial bulk pH (6.0) as a consequence of the acidic microclimate created by the dissolution of the acidic drug. Even though a slight decrease in the bulk pH was observed throughout the experiment in bicarbonate, no values below 5.95 were recorded which can be explained by the phase-heterogeneous nature of bicarbonate buffer in bulk [16]. The Mooney model predicted that phosphate concentrations of 1 and 2 mM are required to resemble the results in bicarbonate media at 5 and 15 mM, respectively (Table 1). This means that phosphate molarities initially chosen (5 and 15 mM) were too high to result in a pH_0 comparable to that of bicarbonate.

As for the calculated acetate concentrations, their use would have been problematic since already at 5 mM acetate, a pH shift of 0.3 units was observed due to the poor bulk buffering capacity. However, it is of note that that the molarity equivalent to 15 mM bicarbonate is almost triple that equivalent to 5 mM bicarbonate. This stands in contrast to the doubling observed in phosphate. The explanation is related to the pKa of acetate (4.62 at 0.154 M ionic strength) being closer to the effective pKa of bicarbonate in the boundary layer (4.27; calculated using the RNE model assuming a 20 μm-thick boundary layer).

Therefore, 1 and 2 mM phosphate buffers were chosen for the next step. Fig. 2 shows the ibuprofen dissolution in phosphate at the equivalent concentrations (solid lines) and their comparison with dissolution profiles in bicarbonate (dashed lines). Firstly, the dissolution profiles at the equivalent phosphate concentrations (1 and 2 mM) were considerably slower than at the higher phosphate molarities shown in Fig. 1A. This was especially observed for SB. Both equivalent phosphate concentrations were capable of discriminating between SA and SB and tended to provide a rather good match to bicarbonate. Consistent with our previous findings, the slower dissolution rate associated with lower molarities led to better discrimination between dissolution curves. These observations were in good agreement with ibuprofen dissolution in bicarbonate media (Fig. 2 and Table 2). The numerical evaluation of the match between the bicarbonate results and those in the equivalent phosphate buffers (shown in Table 2) was done using the difference factor (f_1) specified by the FDA [17]. f_1 was chosen for it represents an average percent error for the points up to the first timepoint after both products' reaching 85% dissolution [17,18]. This makes averaging this value mathematically meaningful. Thus, the overall "prediction error" was calculated by calculating a grand average f_1 value weighted by the number of points included in calculating the f_1 factor for each bicarbonate-phosphate pair as shown in the equation below:

$$\textit{Weighted grand average } f_1 \text{ value} = \frac{\sum_{i=1}^{N} (f_{1i} \times n_i)}{\sum_{i=1}^{N} n_1} \quad (2)$$

where n is the number of datapoints included in the f_1 calculation for the ith comparison. N is the number of comparisons (bicarbonate-phosphate pairs).

This matching could be even further improved if computational work dealing with the dissolution of each size fraction of the suspended particles and with the particle size distribution change during dissolution were undertaken. Particularly because, as found by Salehi et al. [19], the surface pH of smaller particles could be lower than that of larger particles (for an acidic drug). This is because the boundary layer thickness tends to decrease with particle size [13], and, as shown by the RNE model [9], the effective pKa of bicarbonate decreases with decreasing boundary layer thickness, which leads to decreased surface pH of an acidic solute like ibuprofen. It is for this reason that the surface pH could also change as the particle size distribution changes during dissolution, which can, for polydisperse powders/suspensions, be pretty unstraightforward instead of, for instance, having a continuous decrease in the mean particle size [20] even in the presence of sink conditions.

The particle sizes used in our particular case were in a range where the size-dependence of the boundary layer thickness is not very strong. For this reason, using a rather rough approximation for the boundary layer thickness resulted in acceptably accurate calculation of equivalent phosphate molarity without the need for extensive computing with the entire particle size distributions and their evolution as a function of time. However, such work will be necessary in other cases, not to

Table 1
Surface pH (pH_0) values at given bicarbonate molarities and respective equivalent buffer concentrations (conjugate base molarities).

Bicarbonate concentration	pH_0	Equivalent concentration (mM)	
		Phosphate	Acetate
5 mM	5.09	1.0	2.9
15 mM	5.31	2.0	8.3

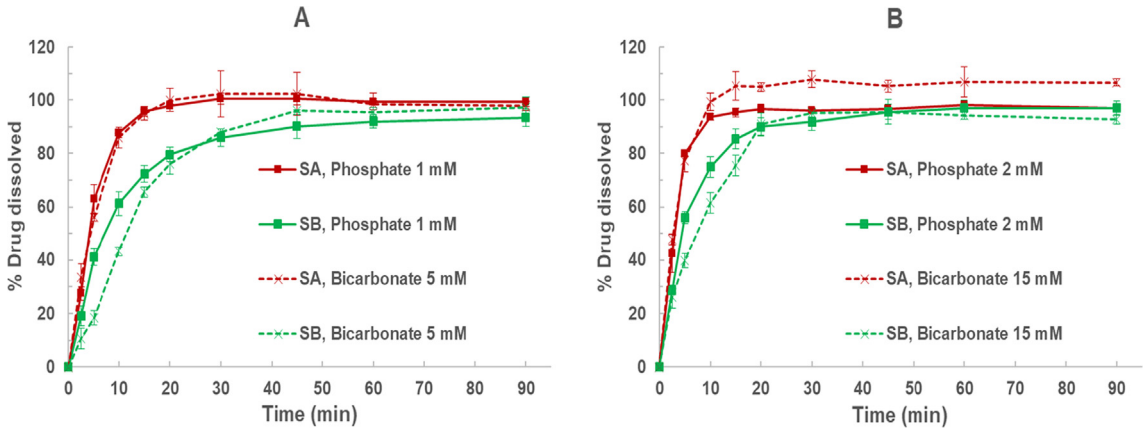

Fig. 2. *In vitro* dissolution of SA (red) and SB (green) in phosphate media (solid lines) at the equivalent concentrations of 1 (Panel A) and 2 mM (Panel B). To better comparison, suspensions dissolution in the corresponding bicarbonate media (Panel A: 5 mM; Panel B: 15 mM) are also depicted as dashed lines. The error bars represent the standard deviation (n = 3). The concentrations represent the conjugate base molarities. The % Drug dissolved represents that of the solid fraction of the suspension. (For interpretation of the references to color in this figure legend, the reader is referred to the web version of this article.)

Table 2
Comparison of dissolution profiles in bicarbonate and equivalent phosphate buffers.

Reference buffer	Surrogate buffer	Suspension	f_1 (%)	Number of dissolution time points included
5 mM bicarbonate	1 mM phosphate	A	8.42	3
		B	20.45	6
15 mM bicarbonate	2 mM phosphate	A	6.05	3
		B	14.40	5
Weighted grand average f_1 value between curves in surrogate and reference buffers			14.01	

mention that it could further improve the matches obtained in this study. All in all, the rather good match between bicarbonate and phosphate dissolution profiles for both SA and SB at the respective equivalent concentrations demonstrates the importance of performing a meaningful mechanistic and physicochemical analysis before selecting the proper biorelevant dissolution media.

Previously, Álvarez et al assessed the possibility of biowaiver for BCS IIa drugs by studying *in vitro* dissolution of bioinequivalent ibuprofen 600 mg tablets under diverse dissolution conditions [3]. None of the buffers investigated in that study proved to be biopredictive. When the dissolution was tested under WHO specifications, very rapid dissolution was only achieved in pharmacopoeial phosphate media pH 6.8 (70 mM), although no discrimination between formulations was observed. Even though only around 25% of ibuprofen was dissolved in pharmacopoeial acetate pH 4.5 (540 mM), the plateau was also rapidly reached within 20 min without making any distinction between formulations. In a further attempt to detect potential bioinequivalence, the authors decreased the rotational speed to 50 rpm in order to slow down the dissolution process. However, dissolution profiles were displaced to the right without any improvement in discrimination [3]. In light of our results, it is very likely that the aforementioned observations can be explained by the tremendously high capacities of the buffers used. As a matter of fact, additional supposedly biorelevant acetate buffers (pHs: 5.0, 5.5 and 6.0) were tested in the same study, but no major improvement in discriminatory power was achieved. For instance, the acetate buffer pH 6.0 was prepared at a final ionic strength of 1290 mM [3], probably because of an excessive buffer concentration in order to maintain the bulk pH throughout the whole experiment. However, the extremely high concentration used may have elevated the surface pH and, subsequently, accelerate ibuprofen dissolution [6]. This showcases a major dilemma in biopredictive drug dissolution testing: while bicarbonate exhibits a low buffer capacity in the boundary layer owing to its low effective pKa there, its buffering capacity in bulk is high owing to its phase-heterogeneous nature restricting the accumulation or (in the case of base dissolution) depletion of the systems conjugate acid. For this reason, it could come to situations where a dilute buffer that is sufficiently weak to simulate bicarbonate in the boundary layer would be prone to saturation with the drug, while a buffer that keeps the pH of the medium constant would buffer the boundary layer too strongly. In the present work, this dilemma was circumvented by adding only 20 ml of suspension in each experiment (approximately 26 mg of solid ibuprofen), which however would more often than not be unacceptable in an industrial quality control setting. Potential solutions for this problem could be using a pH-stat system to control the pH, introducing an organic phase as sink for dissolved ibuprofen. Another option would be using bicarbonate, however this would be restricted by the required sparging and continuous pH monitoring introducing several technical difficulties. For example, the buffer would inapplicable to disintegration testers and reciprocating cylinder apparatuses. In addition, foaming in the presence of surfactants could sometimes make the addition of bile salts impossible as observed by Sheng et al. [12].

3.2. Modeling the PK of ibuprofen formulations

3.2.1. Oral solution

In order to assess the biorelevance of these findings, a deconvolution approach was applied to the *in vivo* data published previously. Ibuprofen solution (SPA), as well as the aforementioned SA (SPB) and SB (SPC), were administered intraduodenally to healthy subjects and plasma concentrations were followed over time. Table 3 shows the pharmacokinetic parameters calculated for the solution. The obtained k_a indicates that ibuprofen is rapidly absorbed. As for the disposition parameters, $V_{central}$ values agreed well with the average of 4.8 and 5.0 L reported by Martin et al., after intravenous (IV) administration of 200 and 400 mg, respectively [21]. Martin et al. used an instantaneous IV bolus injection model to estimate the $V_{central}$ while the solution was injected slowly over 3 min. This might result in an overestimation of the $V_{central}$ due to the unaccounted initial distribution. Taking this together

Table 3
Pharmacokinetic parameters obtained after fitting the SPA data with the oral solution model for 7 healthy human volunteers.

Parameter	k_a (h^{-1})	k_{12} (h^{-1})	k_{21} (h^{-1})	k_{10} (h^{-1})	$V_{central}$ (L)
Arithmetic mean	9.75	2.98	2.31	0.90	3.81
Standard deviation	5.63	1.10	0.92	0.14	0.97

with the well-known high plasma protein binding [21], our $V_{central}$ value of 3.8 L can be considered as an accurate estimation.

Likewise, the model-dependent clearance ($Cl = k_{10} \times V_{central}$) was 54.41 ± 8.21 ml/min, comparable with the 56.2 ± 15.9 and 58.2 ± 15.6 ml/min for the 200 and 400 mg doses respectively reported in Martin's study. The volume of the peripheral compartment estimated by Martin et al. (5.4 and 5.1 L for 200 and 400 mg, respectively) suggests that the value of k_{12} is slightly higher or similar than k_{21}, which is consistent with our estimates. Conversely, an average k_{21} to k_{12} ratio of 5.9 was published by Wagner et al. after administering an oral solution of ibuprofen. This value was tremendously higher than the 0.78 found in the present work [22]. This discrepancy is most probably because of the gastric emptying and/or possible precipitation of ibuprofen in the acidic stomach. Hence, the fitting of plasma profiles by using a first-order absorption may result in an oversimplification of overall absorption process. This situation emphasizes the value of infusing a liquid formulation directly into the duodenum over the typical approach.

One major caveat to using oral solution data without an IV reference is related to the absolute bioavailability. Here it was assumed to be 100%, which is supported by comparing the solution $AUC_{0\text{-inf}}$ data to IV data in literature. In the study of Chassard et al. [23], where 5 mg of ibuprofen per kg body mass (approx. 359 mg based on the published body weights) were administered to healthy human volunteers, the $AUC_{0\text{-inf}}$ of the solution was found to be very similar (only 5% lower) compared to the $AUC_{0\text{-inf}}$ observed in the SPA. Similar results were also obtained when comparing against the IV data of Martin et al., with the dose-normalized intravenous $AUC_{0\text{-inf}}$ being ~6% lower for the 400 mg dose and ~3% lower for the 200 mg dose compared to the oral solution in this study [21]. The AUC of the solution is slightly higher than that from the IV administration in the cited studies indicating that the solution in this study was virtually 100% bioavailable. A possible source of error could be potential flip-flop between k_a and the hybrid distribution rate macro-constant alpha. However, calculations (see supplementary material table 1) done based on the equations of Benet [24] showed that if such a flip-flop occurred, the values of $V_{central}$ would be even lower than the plasma volumes. This shows that the used k_a values are appropriate. In this regard, the calculated alpha value is 5.84 h^{-1} and beta (elimination rate hybrid macro-constant) is 0.35 h^{-1}. The discrepancy between the alpha value and the one of 7.56 h^{-1} for the 200 mg dose and 10.94 h^{-1} for the 400 mg dose, respectively, reported by Martin et al is most probably owing to Martin et al. fitting data obtained from a slow injection over 3 min using a model assuming an instantaneous injection bolus. Based on these k_a values and assuming a luminal radius (r) value of 1.75 cm [25], an estimate for the P_{eff} value can be calculated with Eq. (3) [26]:

$$k_a = P_{eff} * \frac{2}{r} \tag{3}$$

The resulting value is 23.70 × 10^{-4} cm/s, indicating that the permeation of ibuprofen might be controlled by the unstirred water layer (UWL). This can be shown as follows: If the resistance to mass transfer of ibuprofen were assumed to be negligible in the epithelium relative to the UWL, the obtained permeability coefficient would be equal to the diffusion coefficient for ibuprofen (7.93 × 10^{-6} cm^2/s) [15] divided by the thickness of the UWL. Given the estimated P_{eff}, the thickness of this layer would be 33.5 μm. With unstirred water layer thickness estimates of around 40 μm being reported [27], such a value indicates that even near total control of ibuprofen permeation by diffusion through the UWL could be plausible. Actually, this very high estimate for ibuprofen permeability is supported by the work of Zakeri-Milani et al. where comparatively high permeability value for ibuprofen was obtained by perfusion in rats [28].

3.2.2. Oral suspensions

The pharmacokinetic parameters shown in Table 3 were used to calculate the *in vivo* dissolution profiles for SA and SB. The plasma profiles for each subject after receiving either SA (SPB) or SB (SPC) were fitted using the parameter values obtained from their own solution profile. As shown in Fig. 3, the used models provided very good fits for the experimental plasma concentration-time profiles and serves as validation. The dissolution kinetics of the suspensions were intended to be estimated as accurately as possible with the least possible amount of assumptions such as particle shape, the exact buffer concentrations, intestinal transit and motility. In a first attempt, the simple monophasic first order dissolution model was tried. However, this analysis underfitted the observed data, likely because of an oversimplification of the dissolution process. Alternatively, the widely used Weibull model not only resulted in under-fitting, but also it led to an artefactual lack of time-invariance. This could be related to the suspensions being administered by infusion instead of a single bolus administration. The

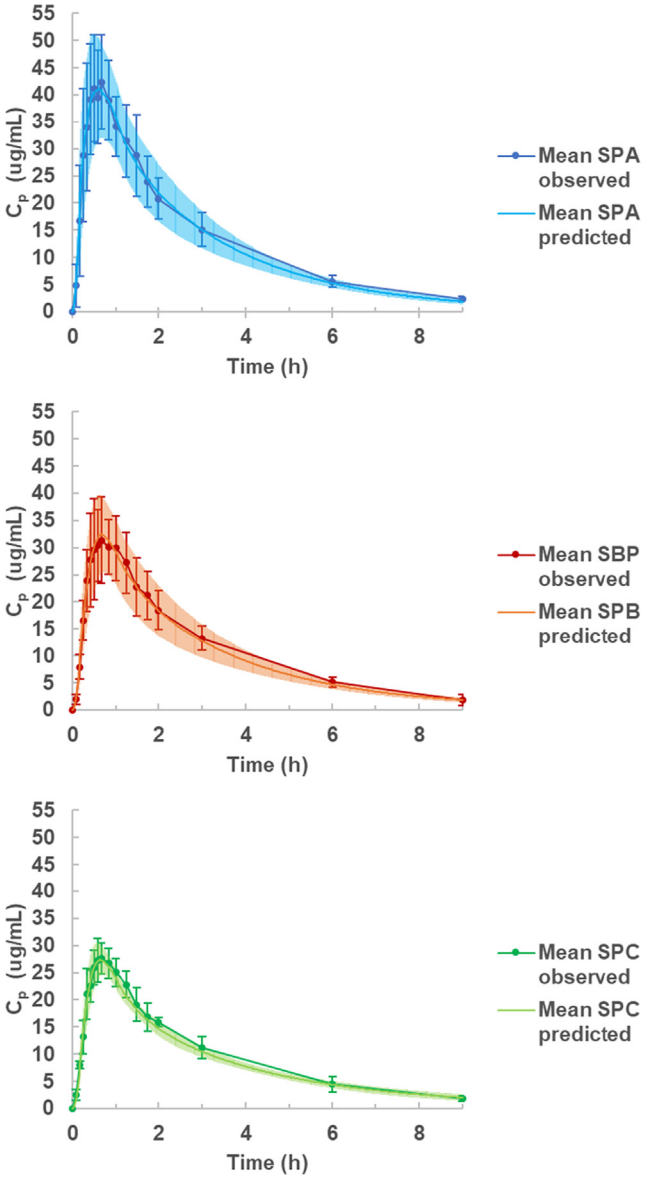

Fig. 3. Mean predicted and observed plasma concentration – time profiles of ibuprofen formulations after direct intestinal intubation and an infusion rate mimicking a 12 min half-life of gastric emptying. Curves depict arithmetic mean and standard deviation. Dark color depicts observed, bright color predicted values. Top : SPA, n = 7, ibuprofen solution. Middle: SPB, n = 7, ibuprofen suspension small particles. Bottom: SPC, n = 4, ibuprofen suspension large particles.

differential equation describing the dissolution rate contains a time term as follows:

$$\frac{dX_{dissolved}}{dt} = \frac{b * t^{b-1}}{a^b} * X_{solid} \quad (4)$$

where a and b are the scale and time factors, respectively. This results in suspension particles reaching the duodenum at later times being subjected to different dissolution kinetics than those arriving earlier. This lack of time invariance would be forced by the model without any mechanistic basis. Ultimately, the DPDM used in this work, as shown in Fig. 3, seems to properly account for the complexity of the *in vivo* dissolution behavior along the GIT as evidenced by the fits of the plasma concentration profiles shown in the mentioned figure. In other words, this empirical model with two different dissolution phases and the first order kinetics of transfer from the first phase two the second managed to fit the overall dissolution process and the change in dissolution kinetics owing to changing intestinal environment during transit [29,30] as well as the changing particle size distribution during the dissolution process.

One potential caveat in our modelling approach is the assumption of a constant k_a value. However, the apparently very high and UWL-limited P_{eff} suggests that ibuprofen is probably absorbed at the tips of the microvilli [25]. Therefore, the permeability along the small intestine is not expected to change dramatically. In fact, permeability values of ketoprofen, a similar compound that is apparently not as highly permeable, were similar in jejunum and ileum [25]. On the other hand, a colonic k_a of 1–2 h^{-1} was reported after administering a rectal solution of ibuprofen. However, given the very slow dissolution calculated for times after one hour, the effect of the changing permeability following ileocecal transit is not expected to be large [31].

The presented *in vivo* dissolution kinetics (as shown by the IVED-curves, Fig. 4) differ from those obtained using a recently published mechanistical deconvolution model, where the dissolution was considerably slower [32]. One potential reason for that was that the *in vivo* data used in that publication were obtained for an 800 mg tablet formulation. Even though the particle size of that formulation was not specified, it may be higher than that in our suspensions. Possible ibuprofen particle fusion due to partial melting during compression makes this explanation plausible [33]. Secondly, the oral solution data (from the aforementioned Wagner et al. study) in which they base the k_a estimation might still be controversial. As explained above, the lack of consideration of both an eventual gastric precipitation of the oral solution and unknown gastric emptying (which might not be a perfect match to the gastric emptying model applied in the cited work), increase the uncertainty of their approach. On the other hand, the method here showed allows to obtain individual estimates of k_a, which in turn improves the reliability on the dissolution kinetics.

3.3. Comparison of in vitro and in vivo dissolution results

The mean IVED profiles are depicted in Fig. 4. The dissolution rate of SA was faster than that of SB (Fig. 4A and C). The same was also observed when only the volunteers that attended both SPB and SPC were directly compared (Fig. 4B and D). In this latter case, the dissolution rate of SA is more clearly visually discriminated from that of SB, with clear separation between the profiles being observed almost from the beginning. But for the case presented in Fig. 4A and C, the profiles were almost identical up to ~20 min. This indicates that, for the moment, the small number of volunteers makes it premature to draw definitive conclusions. Nonetheless, it can be said that the IVED profiles seem not to contradict the validity of the *in vitro* dissolution profiles obtained in bicarbonate, with at least one *in vitro* profile largely lying (up to at least 80% dissolution) within less than one standard deviation from the IVED curve for each suspension (Fig. 5). 5 mM

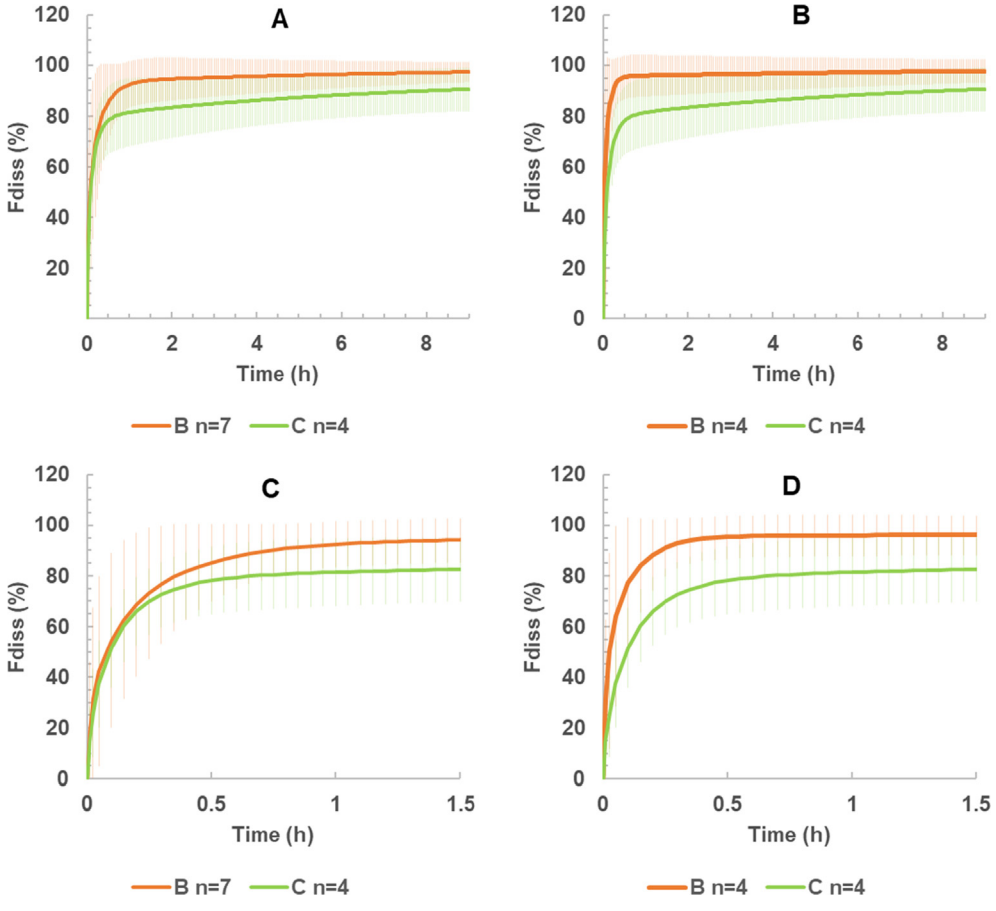

Fig. 4. Arithmetic mean *in vivo* equivalent dissolution (IVED) – time profiles for the solid fraction of the SA (orange) and SB (green). On the panel A, the profiles calculated for all volunteers that participated in the corresponding study phase are shown. On the panel B, the profiles for the four volunteers who attended both study phases are shown. The error bars represent the standard deviation. Panels C and D represent a zoom in of the profiles depicted in panels A and B, respectively. (For interpretation of the references to color in this figure legend, the reader is referred to the web version of this article.)

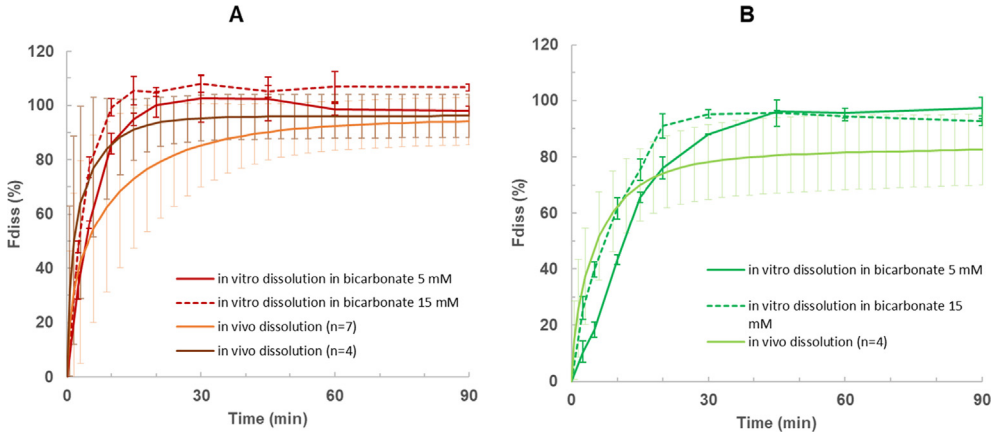

Fig. 5. Overlay of *in vitro* and IVED curves for SA (panel A) and SB (panel B). Red and green lines show *in vitro* dissolution in bicarbonate buffer (n = 3) either at 5 (solid lines) or 15 mM (dashed lines). In panel A, orange and brown lines show IVED profiles with n = 7 or n = 4, respectively (the 4 volunteers who took both suspensions). In panel B, the light green line shows the IVED profile. Error bars represent standard deviations. (For interpretation of the references to color in this figure legend, the reader is referred to the web version of this article.)

bicarbonate gave the closest profile to the IVED of SA (with a tendency to overestimate the *in vivo* profile) while 15 mM bicarbonate gave a profile lying closer to the IVED curve for SB (with a tendency toward underestimating the *in vivo* profile). The contrast between the IVED profiles for SA when all the 7 volunteers were averaged vs averaging only the 4 who took both suspensions, showcases the aforementioned variability considerations. Given that both over- and underestimations were seen, it is likely that these misestimations of IVED are explained by random error related to the low statistical power of the sample as a result of the low number of volunteers combined with the high variability in *in vivo* parameters like, for example, intestinal bicarbonate levels (~73% relative standard deviation observed [7]). Therefore, while it can be said that this study indicates that extending biowaivers to include BCS Class II drugs (at least the weak acids among them) is possible, further higher-powered *in vivo* studies and investigating the influence of other factors like agitation rate and presence of bile salts should be undertaken before making any definitive statement in this regard.

4. Conclusion

Both phosphate and acetate failed to match bicarbonate, when used at the same molarities, because of differences in effective pKa in the boundary layer. Because of this difference was lower for acetate, the resulting discrepancy with bicarbonate was also lower. However, using mass transport modelling for surface pH calculation enabled the determination of phosphate buffer molarities (surrogate buffers) that provided matched bicarbonate fairly well in terms of dissolution performance. The dissolution profiles in bicarbonate and the phosphate-based surrogate buffers compared reasonably well with the *in vivo* dissolution profiles of the tested suspensions in human volunteers. This shows that mechanistic investigations of dissolution processes could enable the extension of biowaivers to BCS class IIa compounds.

Declaration of Competing Interest

The authors declare that they have no known competing financial interests or personal relationships that could have appeared to influence the work reported in this paper.

Acknowledgments

This work has received support from the Innovative Medicines Initiative Joint Undertaking (http://www.imi.europa.eu) under grant agreement no. 115369, resources of which are composed of financial contribution from the European Union's Seventh Framework Programme (FP7/2007-2013) and EFPIA companies' in kind contribution. The authors acknowledge partial financial support to ERASMUS Programme. ARP received an ERASMUS + Practice grant (ERASMUS + 2018/2019). MAG is granted by the Agencia Nacional de Investigación y Desarrollo (ANID), Becas de doctorado en el extranjero, Becas Chile, no 72180466.

Appendix A. Supplementary material

Supplementary data to this article can be found online at https://doi.org/10.1016/j.ejpb.2020.02.009.

References

[1] H. Lennernas, A. Lindahl, A. Van Peer, C. Ollier, T. Flanagan, R. Lionberger, A. Nordmark, S. Yamashita, L. Yu, G.L. Amidon, V. Fischer, E. Sjogren, P. Zane, M. McAllister, B. Abrahamsson, In vivo predictive dissolution (IPD) and biopharmaceutical modeling and simulation: future use of modern approaches and methodologies in a regulatory context, Mol. Pharm. 14 (2017) 1307–1314.
[2] M. Kubbinga, P. Langguth, D. Barends, Risk analysis in bioequivalence and biowaiver decisions, Biopharm. Drug Dispos. 34 (2013) 254–261.
[3] C. Alvarez, I. Nunez, J.J. Torrado, J. Gordon, H. Potthast, A. Garcia-Arieta, Investigation on the possibility of biowaivers for ibuprofen, J. Pharm. Sci. 100 (2011) 2343–2349.
[4] I.E. Shohin, J.I. Kulinich, G.F. Vasilenko, G.V. Ramenskaya, Interchangeability evaluation of multisource Ibuprofen drug products using biowaiver procedure, Indian J. Pharm. Sci. 73 (2011) 443–446.
[5] Y. Tsume, P. Langguth, A. Garcia-Arieta, G.L. Amidon, In silico prediction of drug dissolution and absorption with variation in intestinal pH for BCS class II weak acid drugs: ibuprofen and ketoprofen, Biopharm. Drug Dispos. 33 (2012) 366–377.
[6] K.G. Mooney, M.A. Mintun, K.J. Himmelstein, V.J. Stella, Dissolution kinetics of carboxylic acids II: effect of buffers, J. Pharm. Sci. 70 (1981) 22–32.
[7] J.G. Banwell, S.L. Gorbach, N.F. Pierce, R. Mitra, A. Mondal, Acute undifferentiated human diarrhea in the tropics. II. Alterations in intestinal fluid and electrolyte movements, J. Clin. Invest. 50 (1971) 890–900.
[8] B.J. Krieg, In vivo predictive dissolution: analyzing the impact of bicarbonate buffer and hydrodynamics on dissolution, in: College of Pharmacy, University of Michigan, 2015, pp. 117–135.
[9] J. Al-Gousous, N. Salehi, G.E. Amidon, R.M. Ziff, P. Langguth, G.L. Amidon, Mass transport analysis of bicarbonate buffer: effect of the CO2-H2CO3 hydration-dehydration kinetics in the fluid boundary layer and the apparent effective pKa controlling dissolution of acids and bases, Mol. Pharm. 16 (2019) 2626–2635.
[10] P. Langguth, Angewandte Biopharmazie und Pharmakokinetik in der Arzneimittelentwicklung, in: P. Langguth, G. Fricker, H. Wunderli-Allenspach (Eds.), Biopharmazie, Wiley-VCH Verlag GmbH & Co. KGaA, Weinheim, 2004, pp. 242–247.
[11] M. Hofmann, F. Thieringer, M.A. Nguyen, W. Mansson, P.R. Galle, P. Langguth, A novel technique for intraduodenal administration of drug suspensions/solutions with concurrent pH monitoring applied to ibuprofen formulations, Eur. J. Pharm. Biopharm. 136 (2019) 192–202.
[12] J.J. Sheng, D.P. McNamara, G.L. Amidon, Toward an in vivo dissolution methodology: a comparison of phosphate and bicarbonate buffers, Mol. Pharm. 6 (2009) 29–39.
[13] K. Sugano, Theoretical comparison of hydrodynamic diffusion layer models used for dissolution simulation in drug discovery and development, Int. J. Pharm. 363 (2008) 73–77.
[14] L.Z. Benet, J.S. Turi, Use of general partial fraction theorem for obtaining inverse Lapace transforms in pharmacokinetic analysis, J. Pharm. Sci-Us 60 (1971) 1593–2000.
[15] B.J. Krieg, S.M. Taghavi, G.L. Amidon, G.E. Amidon, In vivo predictive dissolution: transport analysis of the CO2 bicarbonate in vivo buffer system, J. Pharm. Sci.-Us 103 (2014) 3473–3490.

[16] J. Al-Gousous, K.X. Sun, D.P. McNamara, B. Hens, N. Salehi, P. Langguth, M. Bermejo, G.E. Amidon, G.L. Amidon, Mass transport analysis of the enhanced buffer capacity of the bicarbonate-CO2 buffer in a phase-heterogenous system: physiological and pharmaceutical significance, Mol. Pharm. 15 (2018) 5291–5301.
[17] FDA, Guidance for Industry: Dissolution Testing of Immediate Release Solid Oral Dosage Forms, 1997.
[18] J.W. Moore, H.H. Flanner, Mathematical comparison of dissolution profiles, Pharm. Technol. 20 (1996) 64–74.
[19] N. Salehi, J. Al-Gousous, G. Amidon, G. Amidon, R. Ziff, Mechanistic mass transport modeling of ionizable drug dissolution under in vivo-relevant buffer and hydrodynamical conditions, in: AIChE Annual Meeting Orlando, 2019.
[20] S.E. LeBlanc, H.S. Fogler, Dissolution of powdered minerals: the effect of polydispersity, Aiche J. 35 (1989) 865–868.
[21] W. Martin, G. Koselowske, H. Toberich, T. Kerkmann, B. Mangold, J. Augustin, Pharmacokinetics and absolute bioavailability of ibuprofen after oral administration of ibuprofen lysine in man, Biopharm. Drug Dispos. 11 (1990) 265–278.
[22] J.G. Wagner, K.S. Albert, G.J. Szpunar, G.F. Lockwood, Pharmacokinetics of ibuprofen in man IV: absorption and disposition, J. Pharmacokinet. Biopharm. 12 (1984) 381–399.
[23] D. Chassard, A. Geneteau, V. Gualano, M. Brault, Bioequivalence study of two Ibuprofen formulations administered intravenously in healthy male volunteers, Clin. Drug Invest. 24 (2004) 739–747.
[24] L.Z. Benet, General treatment of linear mammillary models with elimination from any compartment as used in pharmacokinetics, J. Pharm. Sci. 61 (1972) 536–541.
[25] D. Dahlgren, C. Roos, A. Lundqvist, B. Abrahamsson, C. Tannergren, P.M. Hellström, E. Sjögren, H. Lennernäs, Regional intestinal permeability of three model drugs in human, Mol. Pharm. 13 (2016) 3013–3021.
[26] D. Dahlgren, C. Roos, E. Sjögren, H. Lennernäs, Direct in vivo human intestinal permeability (P-eff) determined with different clinical perfusion and intubation methods, J. Pharm. Sci.-Us 104 (2015) 2702–2726.
[27] M.D. Levitt, J.K. Furne, A. Strocchi, B.W. Anderson, D.G. Levitt, Physiological measurements of luminal stirring in the dog and human small bowel, J. Clin. Invest. 86 (1990) 1540–1547.
[28] P. Zakeri-Milani, H. Valizadeh, H. Tajerzadeh, Y. Azarmi, Z. Islambolchilar, S. Barzegar, M. Barzegar-Jalali, Predicting human intestinal permeability using single-pass intestinal perfusion in rat, J. Pharm. Pharm. Sci. 10 (2007) 368–379.
[29] D.M. Mudie, G.L. Amidon, G.E. Amidon, Physiological parameters for oral delivery and in vitro testing, Mol. Pharm. 7 (2010) 1388–1405.
[30] M. Bermejo, B. Hens, J. Dickens, D. Mudie, P. Paixão, Y. Tsume, K. Shedden, G.L. Amidon, A mechanistic physiologically-based biopharmaceutics modeling (PBBM) approach to assess the in vivo performance of an orally administered drug product: from IVIVC to IVIVP, Pharmaceutics 12 (2020) 74.
[31] M.G. Eller, C. Wright, A.A. Dellacoletta, Absorption kinetics of rectally and orally-administered ibuprofen, Biopharm. Drug Dispos. 10 (1989) 269–278.
[32] A. Yu, M.J. Koenigsknecht, B. Hens, J.R. Baker, B. Wen, T.L. Jackson, M.P. Pai, W. Hasler, G.L. Amidon, D. Sun, Mechanistic deconvolution of oral absorption model with dynamic gastrointestinal fluid to predict regional rate and extent of GI drug dissolution, AAPS J. 22 (2019) 3.
[33] V.N. Le, P. Leterme, A. Gayot, M.P. Flament, Influence of granulation and compaction on the particle size of ibuprofen–development of a size analysis method, Int. J. Pharm. 321 (2006) 72–77.

APPENDIX 3 (PUBLICATION #3).

THE EFFECT OF CHITOSAN ON THE BIOACCESIBILITY AND INTESTINAL PERMEABILITY OF ACYCLOVIR

European Journal of Pharmaceutics and Biopharmaceutics 136 (2019) 147–155

Contents lists available at ScienceDirect

European Journal of Pharmaceutics and Biopharmaceutics

journal homepage: www.elsevier.com/locate/ejpb

Research paper

The effect of chitosan on the bioaccessibility and intestinal permeability of acyclovir

Marlies Kubbinga[a,b,c], Patrick Augustijns[d], Mauricio A. García[b], Christian Heinen[b], Heleen M. Wortelboer[e], Miriam Verwei[e,f], Peter Langguth[b,*]

[a] National Institute for Public Health and the Environment, Bilthoven, the Netherlands
[b] Institute of Pharmacy and Biochemistry, Johannes Gutenberg University, Mainz, Germany
[c] Medicines Evaluation Board, Utrecht, the Netherlands
[d] Drug Delivery and Disposition, KU Leuven, Department of Pharmaceutical and Pharmacological Sciences, Belgium
[e] TNO Zeist, the Netherlands
[f] TNO Triskelion, Zeist, the Netherlands

ARTICLE INFO

Keywords:
Acyclovir
Chitosan
Caco-2
Intestinal tissue segments
TNO gastro-Intestinal Model (TIM-1)

ABSTRACT

Chitosan is object of pharmaceutical research as a candidate permeability enhancer. However, chitosan was recently shown to reduce the oral bioavailability of acyclovir in humans. The effect of chitosan on two processes determining the oral bioavailability of acyclovir, bioaccessibility and intestinal absorption, was now investigated. Acyclovir's bioaccessibility was studied using the dynamic TNO gastro-Intestinal Model (TIM-1). Four epithelial models were used for permeability experiments: a Caco-2 cell model in absence and presence of mucus and both rat and porcine excised intestinal segments. Study concentrations of acyclovir (0.8 g/l) and chitosan (1.6 g/l and 4 g/l) were in line with those used in the aforementioned human study. No effect of chitosan was measured on the bioaccessibility of acyclovir in the TIM-1 system. The results obtained with the Caco-2 models were not in line with the *in vivo* data. The tissue segment models (rat and porcine intestine) showed a negative trend of acyclovir's permeation in presence of chitosan. The Ussing type chamber showed to be the most biopredictive, as it did point to an overall statistically significantly reduced absorption of acyclovir. This model thus seems most appropriate for pharmaceutical development purposes, in particular when interactions between excipients and drugs are to become addressed.

1. Introduction

Chitosan is an unbranched binary heteropolysaccharide consisting of the two units N-acetyl-D-glucosamine and D-glucosamine, obtained by partial deacetylation of the natural product chitin [1–3]. Besides its employment as a conventional excipient (e.g. filler, disintegrant, release modifier), chitosan has been tested as a candidate drug bioavailability modulator. Several studies has showed that chitosan is able to enhance the permeability of diverse low permeability compounds, such as acyclovir, or other hydrophilic markers mannitol and fluorescein isothiocyanate dextran 4000 [4–8]. Particularly, chitosan salts increased the *in vitro* permeability of acyclovir across Caco-2 monolayers and the oral absorption of acyclovir in the rat at concentrations varying from 0.1% to 3% [9,10]. However, the data from those *in vitro* and animal experiments were not confirmed by human data tested at identical dose levels.

The mechanism for permeation enhancement is postulated to occur through an interaction of the positively charged chitosan molecules and negative charges in the cavity of the epithelial tight junctions resulting in opening of these tight junctions [8,11,12]. However, the presence of different anions along the gastrointestinal tract might change in the *in vivo* situation. For instance, both polyanionic macromolecules, heparin and mucin, has demonstrated to interact with chitosan decreasing its absorption enhancement effect [13,14]. Furthermore, luminal contents as bile salts may also provide an additional potential source of interactions [11,15].

A recent study in healthy human volunteers performed by the authors showed how chitosan hydrochloride actually reduced the

Abbreviations: AUC, area under the curve; C_{max}, maximum concentration; DD, degree of deacetylation; FD4, fluorescein isothiocyanate-dextran; GI, gastrointestinal; MW, molecular weight; P_{app}, apparent permeability; PBPK, physiologically-based pharmacokinetic; Rf, transsegmental electrical resistance; TEER, transepithelial electrical resistance; T_{max}, time at which C_{max} is reached

* Corresponding author at: Pharmaceutical Technology and Biopharmaceutics, Johannes-Gutenberg University Mainz, Staudingerweg 5, 55128 Mainz, Germany.
E-mail address: langguth@uni-mainz.de (P. Langguth).

https://doi.org/10.1016/j.ejpb.2019.01.021
Received 30 July 2018; Received in revised form 9 January 2019; Accepted 21 January 2019
Available online 22 January 2019
0939-6411/

bioavailability of 200 mg acyclovir when orally administered at a concentration of 0.16% or 0.4% (1.6 g/l or 4 g/l; given as 400 mg and 1000 mg chitosan hydrochloride respectively in 250 ml water) [16]. Although apparent inconsistent results emerge from the human and preclinical studies, data are often difficult to compare as the characteristics of the applied chitosan (molecular weight, degree of deacetylation (DD), salt form), as well as the test compounds and dose levels differ between studies. In the current work, we used five different *in vitro* methods to study effect of chitosan on acyclovir absorption. As a highlight, all experiments were performed with chitosan of the same or very similar quality at identical dose levels as applied in the human study. These studies improve the understanding of chitosan's effects on two kinetic processes underlying the oral bioavailability of the high solubility and low permeability model drug acyclovir (BCS class III, [17]). In addition, this research allows evaluation of the different intestinal permeability models for pharmaceutical development or biowaiver purposes.

2. Materials and methods

2.1. Materials

Chitosan hydrochloride was obtained from Heppe Medical GmbH, Halle, Germany. The following characteristics applied: DD 92.7%; viscosity 4–5 mPa s at 1% in water at 20 °C for TIM-1 studies and Ussing type rat model and DD 93.05%, viscosity 5.9 mPa s at 1% in water at 20 °C for Caco-2 and the inTESTine. Zovirax 200 mg dispersible tablets (GlaxoSmithKline, UK) were purchased in the Netherlands. Acyclovir was obtained from Fagron (Fagron, The Netherlands). For the Caco-2 studies, Hanks' balanced salt solution (HBSS), Dulbecco's modified Eagle's medium (DMEM), 10,000 IU/ml penicillin and 10,000 µg/ml streptomycin, nonessential amino acid medium (100×) and 4-(2-hydroxyethyl)-1-piperazineethanesulfonic acid (HEPES) were obtained from Lonza (Verviers, Belgium). Fetal bovine serum (FBS) was purchased from Biological Industries (Beit Haemek, Israel). 2-(N-morpholino)ethanesulfonic acid (MES) was obtained from Sigma–Aldrich (St. Louis, MO, United States). For rat ligated loop studies, ketamin (Ketavet, Pfizer, Germany), and xylazin (Rompun, Bayer, Germany) were obtained via the Pharmacy of the Medical Center of the Johannes Gutenberg University, Mainz, Germany. For the InTESTine study, ^{14}C-Antipyrine (55 mCi/mmol) was purchased from American Radiolabeled Chemicals Inc. (St. Louis, Missouri, United States). ^{3}H-Atenolol (1.79 Ci/mmol), and ^{14}C-acyclovir (440 mCi/mmol) were purchased from Moravek biochemicals Inc. (Brea, California, United States). All other chemicals were purchased at Sigma-Aldrich, Schnelldorf, German.

2.2. TIM-1 model

The *in vitro* dynamic TIM-1 system (TNO Triskelion, The Netherlands) consists of one gastric compartment and three intestinal compartments (duodenum, jejunum and ileum) connected with valves simulating the gastric and small intestinal passage of food and pharmaceutical products. The TIM-1 systems, previously well described [18–20], have a simulated pyloric sphincter for controlled gastric emptying of liquids and solids (particles less than 3–5 mm) with specific settings for fasted and fed conditions. The conditions in the compartments are computer-controlled via pH electrodes, temperature and pressure sensors. The secretions into the gastric compartment consist of artificial saliva with electrolytes, α-amylase and gastric juice with hydrochloric acid, pepsin and lipase. In the small-intestinal compartments, the secretion fluids consist of bicarbonate, electrolytes, pancreatic juice with digestive enzymes, and bile.

The TIM-1 studies were performed with acyclovir (0.8 g/l) in absence or presence of chitosan (1.6 and 4.0 g/l) to provide information on the effect of chitosan on the bioaccessibility (i.e. availability for absorption) of acyclovir during gastrointestinal passage. Preparation of the dispersions containing Zovirax tablets in presence and absence of the two levels of chitosan took place in line with the instructions applied during the human study [16]: a total volume of 250 ml water was introduced in the gastric compartment. The model conditions simulated the fasted state including gastric pH profile, enzyme levels, gastric emptying etc. A gastric emptying half-time of 20 min (default fasted state) was used for the three conditions (acyclovir in absence of chitosan, in presence of 1.6 g/l or in presence of 4.0 g/l chitosan). The jejunum and ileum compartments were connected with dialysis membranes (cut-off 5 kDa) to remove the released and water-dissolved compounds. Jejunum and ileum dialysate samples were collected every 30 min during the first three hours and every 60 min during the next 2 h till a total of five hours. The amount of acyclovir in these dialysate samples was considered as the fraction available for absorption from the upper gastrointestinal tract, i.e. the bioaccessible amount, within a given time period. In addition, ileum effluent was sampled every hour. These ileum effluent samples provide information on the non-bioaccessible fraction during transit through the upper GI tract, and which will enter the colon. After five hours, the experiments were ended and the residues were collected to be able to calculate the mass balance of acyclovir in each individual TIM-1 experiment. All samples were stored at or below −18 °C until analysis.

2.3. Caco-2 cell permeation studies (n = 3 wells)

Caco-2 cells were obtained from American Type Culture Collection (Manassas, VA) and were grown in DMEM^{+} at 37 °C in an atmosphere of 5% CO_2 and 90% relative humidity. Cells were passaged every 3–4 days (at 80–90% confluence) at a split ratio of 1:6. For transport experiments, cells were seeded at a density of 90,000 cells/cm^2 on Costar Transwell membrane inserts (3 µm pore diameter, 12 mm diameter; Corning Inc., Corning, NY, United States) and were used for experiments 17–18 days after seeding. Only monolayers with transepithelial electrical resistance (TEER) values higher than 400 Ω * cm^2 were used for transport studies.

Caco-2 cell culture medium consisted of DMEM supplemented with 10% FBS, 1% nonessential amino acids, 100 IU/ml penicillin and 100 µg/ml streptomycin (DMEM^{+}).

Transport medium consisted of HBSS containing 25 mM glucose and was buffered with 10 mM MES to pH 6.0 (donor compartment) or with 10 mM HEPES to pH 7.4 (acceptor compartment).

Three conditions were tested in absence or presence of mucus: 0.8 g/l acyclovir, 0.8 g/l acyclovir + 1.6 g/l chitosan and 0.8 g/l acyclovir + 4 g/l chitosan based on the concentrations for chitosan which effects have been described previously [9,10,16]. The mucus used as a protective barrier in the Caco-2 assay consisted of type III mucin derived from porcine stomach dissolved in HBSS^{+} pH 6.0. Mucus was used in a concentration of 50 mg/ml [21].

Prior to the transport study, Caco-2 cells were washed twice with pre-warmed HBSS^{+} pH 7.4 and placed in a shake incubator (Thermostar, BMG Labtech, Offenburg, Germany) at 37 °C and 300 rotations per minute (rpm) for 30 min. After the pre-incubation, 100 µl of mucus were applied to the apical compartment of the transwell plates for the corresponding conditions; in the basolateral compartment fresh HBSS^{+} pH 7.4 was added. The transport experiment was initiated by adding 0.5 ml of the corresponding incubation medium at pH 6.0 to the donor compartment. Plates were incubated in the shake incubator at 300 rpm for 2 h at 37 °C. 200 µl samples were taken from the basolateral compartment at t = 15, 30, 45, 60, 90 and 120 min and were replaced by fresh buffer. 10 µl apical samples were taken at t = 0 and 120 min and diluted 100× in HBSS^{+} pH 7.4. Samples were analyzed immediately. Monolayer integrity after the transport experiment was confirmed by comparing the measured TEER at t = 0 min with the TEER at t = 120 min.

2.4. Ussing-type chamber permeation studies using rat jejunal segments (5–6 rats)

Rats were purchased from Charles River (Sulzfeld, Germany). Rat excised jejunal segments were obtained and permeation studies in an Ussing-type chamber were performed as described by Heinen et al. 2013 [22]. On the apical side, a 5 ml Krebs-Ringer-Bicarbonate-Buffer (KRB) containing MES at pH 6.0 was used. Same three conditions mentioned above were tested. Samples of 600 µl were taken at 30, 60, 90 and 120 min from the acceptor chamber, each replaced with fresh KRB buffer and at 0 and 120 min from the donor chamber. Similar as Caco-2 experiments, transsegmental electrical resistance (Rf) was measured at both the beginning and end of each experiment assessing the integrity of the tissue. Acyclovir permeability experiments were performed in the presence of chitosan (0, 1.6, and 4.0 g/l). Additional electrical resistance measurements were performed at higher chitosan concentrations up to 50.0 g/l.

2.5. Porcine excised segment InTESTine permeation studies (2 individual studies each with 4 replicates)

Porcine excised jejunal segments were obtained from healthy pigs, mounted in a newly developed InTESTine™ system, and permeability studies were performed as described by Westerhout et al. [23]. On the apical side, a 1 ml pre-warmed (37 °C) Krebs-Ringer Bicarbonate buffer (containing 10 mM glucose, 25 mM HEPES, 15 mM sodium bicarbonate, 2.5 mM calcium chloride, pH 7.4, and saturated with oxygen using a 95%/5% O_2/CO_2 mixture by gassing for 120 min, further indicated as KRB-HEPES) dose solutions containing 10 µM acyclovir (containing [^{14}C]-acyclovir, 2 kBq/ml) in the absence and presence of chitosan (0, 1.6, 4.0 g/l) and 50 µM fluorescein isothiocyanate-dextran (FD4) as a membrane integrity marker was used. The basolateral compartment contained 7.5 ml pre-warmed KRB buffer (37 °C). In parallel, the permeability of ^{3}H-atenolol and ^{14}C-antipyrine (both 10 µM) was determined in the absence and presence of chitosan as a control for the permeability of a low and high permeability marker, respectively. The InTESTine samples were taken from both the apical and basolateral compartment after a pre-incubation time of 45 min in order to measure the linear phase of the transport over 60 min incubation. Recovery of active substance compared to added quantity at the beginning of the study was determined at the end of the studies by determination of the mass balance. It was previously shown that intestinal permeability of a wide range of compounds is comparable between (adult) human and porcine intestinal tissue [23].

2.6. Analytical methods

2.6.1. Acyclovir by HPLC-Fluorescence Detection (TIM-1)

Acyclovir in ileum and jejunum dialysate, ileum effluent and residue samples from the TIM-1 experiment was analyzed by HPLC (Jasco PU-980, Jasco, Germany) with fluorescence detection (Shimadzu, RF-551, Shimadzu, Germany) (excitation wavelength 260 nm, emission wavelength 375 nm). A Waters Sunfire 150 × 3.0 mm 3.5 µm column was used at ambient conditions, with an injection volume of 10 µl. A gradient elution method was applied involving solvent A (0.1% formic acid in acetonitrile) and solvent B (0.1% formic acid in purified water) at a flow rate of 0.6 ml/min. Solvent A and B were used in a ratio of 99:1 during the first 5 min, followed by 2 min of 100% solvent B. The run time of 14 min was completed using the 99:1 ratio again. Low, middle and high QC samples in two TIM matrices were analyzed in duplo in parallel with the samples. Linearity was demonstrated in a range of 25 µg/ml to 250 µg/ml ($R^2 \geq 0.998$). Regarding precision, intraday variation coefficients per concentration level varied from 0.03 to 5.1%, which is acceptable considering the complex matrix. The results for accuracy showed for QC low (25 µg/ml) an average deviation of +15% in both matrices. Considering that the deviation varied from +5% to +23% and that the results for overall recovery are limited to 110%, a correction factor was not applied. The mean QC middle (100 µg/ml) and high (250 µg/ml) showed an average deviation of the nominal values of −1% and 4%, respectively. LOQ was set at 25 µg/ml while LOD was 10 µg/ml.

2.6.2. Acyclovir by HPLC-UV (Caco-2)

Acyclovir concentration in media samples from the Caco-2 cell experiments were analyzed by HPLC consisting of a Waters 600 pump and a Waters 717 auto injector (Waters, Milford, MA). For chromatographic separation a Waters Novapak C18 column under radial compression was used. UV absorbance was monitored using a Waters 2487 detector at 254 nm. The observed peaks were integrated using Empower Pro (Empower 2) software. The mobile phase consisted of a 25 mM acetate buffer (pH 3.5) (95%)/methanol (5%) and a flow rate of 1 ml/min was applied. Retention time of acyclovir was 6.0 min. The calibration curve of acyclovir was linear over the concentration range of 0.12–1000 µM. The assessment of repeatability at concentrations of 250, 25, 2.5 and 0.25 µM resulted all in RSD's below 2.5%. Samples from the acceptor compartment were not diluted; the 10 µl samples from the apical department were diluted with 990 µl HBSS+ pH 7.4. The injection volume amounted to 50 µl. LOQ was set at 0.12 µM and LOD was 0.05 µM, respectively.

2.6.3. Acyclovir by HPLC-UV (Ussing-type chamber)

Acyclovir concentration in media samples from Ussing-type chamber experiments were determined using isocratic HPLC with UV detection at 254 nm (equipment see above). A Lichrospher 10 RP 18 (5 µm), 250-4 column was used for chromatographic separation, at 40 °C and ~133 bar. The mobile phase consisted of 10 mM acetic acid and acetonitrile (95:5; V/V) and a flow rate of 1 ml/min was applied (retention time acyclovir ~4.6 min). Linearity was demonstrated in a range of 0.050 µg/ml to 50.0 µg/ml acyclovir. Intraday precision resulted in RSD values < 5.5% for concentrations ≥0.50 µg/ml and < 11% for the lower concentrations. Interday precision resulted in RSD values < 5.5% for concentrations ≥0.10 µg/ml and 13% for the lowest concentration of 0.050 µg/ml. Samples from the acceptor compartment were not diluted; 10 µl of the samples from the apical department were diluted with 390 µl buffer. Injection volumes were 50 µl.

2.6.4. Liquid scintillation counting (InTESTine)

Concentrations of radioactive labeled compounds in The InTESTine samples were measured on a Tri-Carb 3100TR Liquid Scintillation counter (LSC, Perkin Elmer, Boston, Massachusetts, United States) after adding scintillation liquid (Ultima Gold, Perkin Elmer Inc., Boston, Massachusetts, United States) to samples of the InTESTine experiments.

2.6.5. Fluorescence spectrophotometry (InTESTine)

FD4 levels in media samples from both the apical and basolateral compartments of the InTESTine system were determined using a FLUOstar OPTIMA fluorescence spectrometer (BMG Labtech, Ortenberg, Germany) at excitation wavelength 490 nm and emission wavelength 520 nm.

2.7. Data analysis

2.7.1. Bioaccessibility

The amount of acyclovir in each sample collected during the TIM-1 experiment was calculated by multiplying the measured concentration by the total volume of the individual samples collected in the time periods. The bioaccessibility of acyclovir is given as percentage of the intake dose of acyclovir and expressed as the mean and range of duplicate TIM-1 experiments. The mass balance (recovery) was calculated as the sum of the bioaccessible fraction (ileum and jejunum), the ileum effluent and the residues in the system after ending the experiments.

2.7.2. Apparent permeability

The apparent permeability coefficient (P_{app}) was calculated based on the linear part of the curves according to the following equation:

$$P_{app} = dQ/dt * 1/A * C_0$$

where Q is the amount of drug appearing in the acceptor compartment as a function of time (t), A is the surface area of the Transwell membrane (1.13 cm^2) or the exposed surface of the intestinal segment in the Ussing-type chamber (0.67 cm^2), or InTESTine system (0.79 cm^2), and C_0 is the initial drug concentration in the donor (apical) compartment.

2.8. Statistical analysis

The TIM-1-results for cumulative bioaccessibility were compared using unpaired t-tests at each time point. Differences were considered statistically significant when $p < 0.05$.

Statistical analysis of the permeation studies was performed using GraphPad Prism 6.03. The mean P_{app} values obtained from the Caco-2 study, Ussing-type chamber and InTESTine experiments were compared with the references using one-way ANOVA and Dunnett's multiple comparison test. P-values below 0.05 were considered significant at a confidence level of 95%.

3. Results

3.1. Bioaccessibility in TIM-1

Fig. 1 shows the jejunal, ileal and total bioaccessible fractions of acyclovir tested in absence (reference) and presence of chitosan (1.6 g/l and 4.0 g/l). The total bioaccessibility of the high solubility compound acyclovir tested under fasted state conditions in TIM-1 was found to be high, as values above 90% were measured. No effect of chitosan on the bioaccessibility of acyclovir was observed. Equal bioaccessible fractions were measured in the TIM-1 runs in absence of chitosan (93.6% ± 0.9%, mean ± range expressed as % of intake, n = 2); in presence of 1.6 g/l chitosan (90.6% ± 6%, mean ± range, n = 2) and in presence of 4.0 g/l chitosan (93.2% ± 3.2%, mean ± range, n = 2), respectively. Overall recovery of acyclovir in the six TIM-1 runs was 108.6% ± 5.1% (mean ± rsd; n = 6).

Values above 100% could be related to possible overestimation of the acyclovir content at low concentrations as observed in the analysis of the low QC samples (in contrast to the mid and high levels).

3.2. Intestinal permeability

Table 1 shows an overview of the results of the intestinal permeability of acyclovir measured in results of the five different models. The mean relative effect on the absorption is reflected by the ratio of test versus reference condition. The p-values indicate the statistical significance of the observed effect compared to the reference.

3.3. Caco-2 cell permeation studies

Monolayer integrity was measured through the TEER values, see Table 2. In absence of chitosan, the monolayer integrity was well preserved in both absence and presence of a mucus layer. In the unmodified model, the addition of 1.6 g/l and 4 g/l chitosan resulted in a complete loss of monolayer integrity after 120 min of incubation. Due to this loss of barrier function, the transport of acyclovir from apical to the basolateral compartment increased at these conditions. This effect was confirmed in a second study at the University of Mainz with the same test substances at the same concentrations following the same study protocol (data not shown): a reduction of TEER values to 2–3% of the original value was found in presence of chitosan, accompanied by a

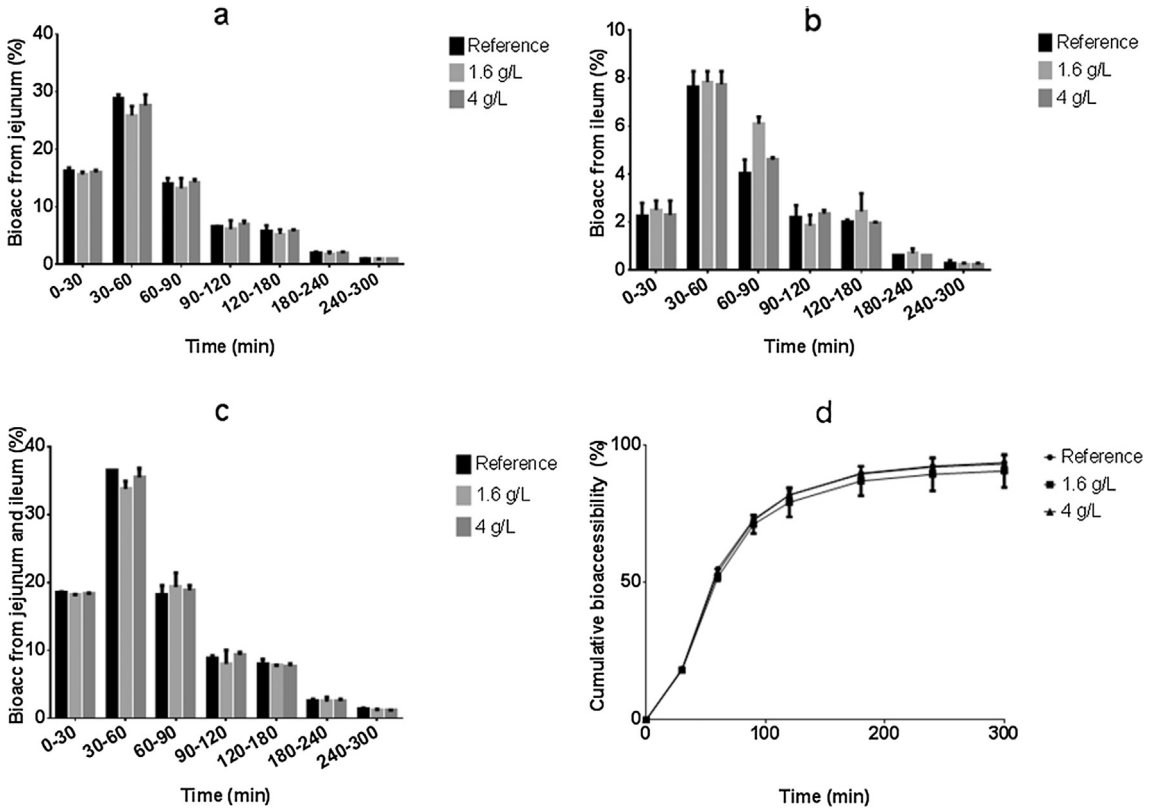

Fig. 1. Bioaccessibility of acyclovir in absence (reference) or presence of chitosan (1.6 and 4.0 g/l) as measured in TIM-1 in hourly time intervals. a. jejunal bioaccessibility (% of intake, mean ± range, n = 2); b. ileal bioaccessibility (% of intake, mean ± range, n = 2); c. total bioaccessibility (=sum of jejunum and ileum; % of intake, mean ± range, n = 2); d. cumulative total bioaccessibility (% of intake, mean ± range, n = 2).

Table 1
Apparent permeability values (P_{app}) of acyclovir in the presence of chitosan as measured in different permeability models.

Model and concentration chitosan hydrochloride[#]		Permeation of acyclovir		Significant result			
Caco-2	Nr of inserts	P_{app} in 10^{-6} cm/s (sd)	Ratio test vs reference	$p < 0.05$, ANOVA + Tukey multiple comparison	$p < 0.05$, ANOVA + Dunnett's multiple comparison	*t*-test individual values compared to reference, Bonferroni correct alpha ($p = 0.05/3 = 0.02$)	*t*-test individual values
0 g/l	3	0.17 (0.01)					
1.6 g/l	3	21 (1.08)	124	y	y	y	y
4 g/l	3	24 (1.31)	143	y	y	y	y
Caco-2 + mucus	Nr of inserts	P_{app} in 10^{-6} cm/s (sd)	Ratio				
0 g/l	3	0.12 (0.01)					
1.6 g/l	3	0.13 (0.003)	1.08	n	n	n	n
4 g/l	3	0.28 (0.15)	2.33	n	n	n	n
Ussing type	Nr of segments (rat)	P_{app} in 10^{-6} cm/s (sd)	Ratio				
0 g/l	5	7.4 (1.5)					
1.6 g/l	5	5.4 (0.9)	0.73	n	y	n	y
4 g/l	5	6.2 (1.0)	0.84	n	n	n	n
InTESTine	Nr of segments (pig)[$]	P_{app} in 10^{-6} cm/s (sd)	Ratio				
0 g/l	8	0.54 (0.10)					
1.6 g/l	8	0.49 (0.15)	0.91	n	n	n	n
4 g/l	8	0.38 (0.13)	0.70	n	n	n	y

[#] All conditions included 0.8 g/l acyclovir.
[$] From two pigs, each 4 slices.

Table 2
Effect of acyclovir and the addition of chitosan on monolayer integrity of Caco-2 cells as measured in the absence and presence of mucus.

Concentration chitosan hydrochloride (g/l)	TEER (0 min) (%)	TEER (120 min) (%)	SD (%)	RSD (%)
Caco-2				
0	100	115.0	6.0	5.3
1.6	100	4.1	0.2	5.9
4	100	2.8	0.5	18.4
Caco-2 + mucus				
0	100	124.5	2.4	1.9
1.6	100	132.4	1.6	1.2
4	100	55.7	27.8	49.9

30- to 40-fold increase in acyclovir's permeability.

In absence of chitosan, P_{app} values of acyclovir in the Caco-2 system in absence and presence of mucus were comparable. This indicates that the mucus layer had no influence on the permeation of acyclovir. When 1.6 g/l chitosan was added in the apical compartment of the Caco-2 model in presence of a mucus layer, the monolayer integrity was maintained during the experiment. Addition of 4 g/l chitosan showed that the monolayer integrity was partly compromised after 120 min, which was accompanied by increased variation in TEER results (Table 2). In presence of mucus, 1.6 g/l chitosan resulted in a P_{app} value (i.e. $0.13 * 10^{-6}$ cm/s) similar to the reference value (i.e. $0.12 * 10^{-6}$ cm/s). Increasing the concentration of chitosan to 4 g/l led to an elevated P_{app} value (i.e. $0.28 * 10^{-6}$ cm/s) compared to the reference conditions, although this difference was not statistically significant.

3.4. Rat jejunal tissue mounted in the Ussing-type chamber

Two concentrations of chitosan hydrochloride (1.6 g/l and 4 g/l) were applied in the Ussing type chamber with rat intestinal segments to test their effect on the permeability of acyclovir (0.8 g/l). The results were compared with acyclovir alone (reference). At the end of all incubations, the transsegmental electrical resistance (Rf) values decreased during the experiment as presented in Table 3. The Rf decreased by 20% in absence of chitosan, however this effect was attenuated by the co-incubation with chitosan either at 1.6 or 4.0 g/l (Table 3). A relatively high P_{app} value for the permeability of acyclovir in absence of chitosan was found (i.e. $7.4 * 10^{-6}$ cm/s) in the Ussing type chamber with rat intestinal segments. This mean P_{app} was reduced by both concentrations of chitosan, which was statistically significant only for 1.6 g/l chitosan in the donor solution.

3.5. Porcine intestinal tissue

The permeability of acyclovir, atenolol and antipyrine was measured across jejunal porcine tissue mounted in the InTESTine system. The tissue was subjected to the same test concentrations with respect to chitosan used in the rat tissue Ussing-type chamber experiments. Recovery of all compounds based upon media alone were > 95%. FD4 leakage remained below 1% indicating no effect of the test solutions on intestinal integrity. The P_{app} values of acyclovir, atenolol, and antipyrine in the absence of chitosan were $0.54 * 10^{-6}$, $0.46 * 10^{-6}$, and $6.58 * 10^{-6}$ cm/s, respectively. Low concentrations of chitosan (1.6 and 4 g/l) showed a negative trend on the absorption of acyclovir across porcine jejunal segments mounted in the InTESTine system, although not statistically significantly different from the control incubations. The permeability of the paracellular transport marker atenolol enhanced with higher concentrations of chitosan from $0.46 * 10^{-6}$ cm/s up to > $1 * 10^{-6}$ cm/s at 30 and 50 g/l (data not shown). No effect of chitosan was observed on the permeability of the transcellular transport marker antipyrine, which varied in the range of $6–9 * 10^{-6}$ cm/s (data not shown).

Table 3
Effect of acyclovir and the addition of chitosan on monolayer integrity of rat intestinal tissue as mounted in Ussing-type chamber.

Concentration chitosan hydrochloride (g/l)	Rf (0 min) (%)	Rf (120 min) (%)	SD (%)	RSD (%)
0	100	79.7	6.6	8.3
1.6	100	97.3	5.6	5.8
4	100	88.2	6.6	7.5
10	100	128.5	13.0	10.1
30	100	45.9	15.0	32.7
50	100	8.4	3.6	43.3

4. Discussion

Excipients such as chitosan may exert their effect on oral bioavailability through modulation of different elements of the absorption process including the dissolution of the active substance from the dosage form, the gastrointestinal transit process and interactions in the intraluminal compartment or at the permeation site. In this study, two of these individual processes were investigated using different *in vitro* techniques that could provide a mechanistic understanding of previously obtained *in vivo* observations [16]. Chitosan decreased both acyclovir's mean area under the plasma concentration-time curve (AUC_{0-12} and $AUC_{0-\infty}$) and maximal plasma concentration (C_{max}) following concomitant oral intake of 400 and 1000 mg chitosan (administered as 1.6 and 4.0 g/l in water) in humans (Table 4). Meanwhile, the T_{max} of acyclovir increased significantly for the treatment combinations with chitosan; however, the effect was statistically significant for the 1000 mg of chitosan co-administration only. Overall, the negative effect of chitosan on acyclovir's absorption was variable between the human subjects but statistically significant [16].

In the human study, the test products were dissolved prior to use and as such, an effect of chitosan on dissolution of acyclovir from the dosage form can be ruled out [16]. In the present study, various *in vitro* intestinal models were used to investigate whether chitosan has an effect on the bioaccessibility and intestinal permeability of acyclovir at the same dose levels as applied in the human study. The selected models have previously been described as tools to study the individual processes underlying oral bioavailability and identify the critical process(es) hampering the oral bioavailability of a specific compound. Based on its physico-chemical properties and available data, acyclovir was previously classified as a BCS III compound indicating that intestinal permeability, not solubility, is the rate limiting process in oral bioavailability [17].

Table 4
Oral bioavailability data of acyclovir as measured in humans [16].

C_{max} (mg/ml)		Ratio[#]
Reference Zovirax 200	0.37 ± 0.21	
Ref + 400 mg chitosan	0.21 ± 0.09*	0.56
Ref + 1000 mg chitosan	0.24 ± 0.26*	0.63
$AUC_{0-\infty}$ (mg·h/ml)		
Reference Zovirax 200	1.53 ± 0.63	
Ref + 400 mg chitosan	1.13 ± 0.42	0.74
Ref + 1000 mg chitosan	1.07 ± 0.05*	0.70
T_{max} (h)		
Reference Zovirax 200	1.2 ± 0.4	
Ref + 400 mg chitosan	1.5 ± 0.9	1.25
Ref + 1000 mg chitosan	1.8 ± 0.9*	1.50

[#] Ratio of absolute values of test vs reference.
* $p < 0.05$ comparing 90% confidence intervals of the ratio of test and reference product.

The TIM-1 system simulating the human physiological conditions in the stomach and the three parts of the small intestine is an *in vitro* tool mainly used to study biorelevant dissolution. Since acyclovir tablets were dissolved before the administration, this tool was applied to investigate the effect of chitosan rather on the bioaccessibility of acyclovir than on its dissolution (Fig. 1). A high bioaccessibility of acyclovir was measured (> 90%) in absence and presence of chitosan which indicates a large fraction of the acyclovir dose added to the gastric compartment appears to be available for absorption irrespective of the presence of chitosan. These observations are in line with acyclovir's high solubility, 2.33 mg/ml at biorelevant pH [17,24]. Luminal interactions affecting both acyclovir and chitosan might possibly explain the *in vivo* results. For instance, an interaction of chitosan with bile acids in the gut lumen, reducing the solubility of acyclovir was hypothesized [15,16]. Nevertheless, no effect of chitosan on the bioaccessibility of acyclovir was observed in this study, suggesting that it is highly unlikely that luminal interactions may affect the oral bioavailability of acyclovir.

The current set-up of the TIM-1 experiments simulated the average human adult fasted state conditions concerning enzyme levels, pH values, transit times, etc. Gastric emptying time was fixed and identical in the TIM-1 runs testing the three applied experimental conditions. Even though the computer-controlled TIM-1 system allows changes in gastric emptying time to study the effect of chitosan on this specific parameter, it was not tested in the current study. In fact, 5 mg/kg of chitosan, corresponding to 1.4 g/l, did not delay gastric emptying of several drugs with different absorption/physicochemical characteristics. Furthermore, even higher chitosan amounts (7 g/l) had also no effect on residence time of the low permeability cephalexin [11]. The recently performed human study showed an increased T_{max} value at 4 g/l chitosan, however associated with high interindividual variability.

Chitosan is thought to act as a potential permeability modulator through interaction with the tight junctions between the epithelial cells, resulting in redistribution of cytoskeletal F-actin and translocation of tight junction proteins ZO-1 and occludin from the membrane to the cytoskeleton [8,25]. Smith et al. showed activation of PKC-dependent signal transduction pathways using a Caco-2 model [12]. Although, the mucus layer was also reported to play a role in the access of chitosan to the epithelial membrane and the subsequent effect on the paracellular permeation route [14]. Therefore, the effect of chitosan causing a change in permeation of acyclovir was tested in four different permeability models with and without a mucus layer. As described in methods, the chitosan effect was assessed in buffered solutions (pH = 6.0) preventing that the polymer precipitates. Selection of this pH also resembles the proximal small intestinal pH (5.9–6.3) [26] and also because this allows the comparison with previous studies (pH = 5.5–6.2) [4,6,9,10].

In the unmodified human intestinal Caco-2 cell model, chitosan concentrations enhanced the permeability of acyclovir 124- and 143-fold, respectively (Table 1). This was caused by the disruption of the monolayer integrity by the reduction of the TEER values as it is shown in Table 2 and several other studies [7,9,10,27]. Although the reference Caco-2 P_{app} in this study was slightly lower than some previously reported values [9,10,28], this does not fully explain the relatively large increase in presence of chitosan. For instance, Merzlikine et al. showed an enhancement on acyclovir Caco-2 permeability of only approx. 10-fold by co-administrating even much higher chitosan concentrations (10–30 g/l) than those used in the present work [9]. However, the chitosan tested in that study had a lower degree of deacetylation (DD = 75–90%) compared to the one used in the present study (DD = 93.05%). It has been proposed that chitosan positive charges are critical for binding to membrane proteins and to exert its subsequent permeability enhancer effect [5,8]. Considering that chitosan exhibits a pKa around 6.3–6.5 [29,30], the charge density of polymer molecules will mainly depend on DD at the studied pH (=6.0). Therefore, discrepancies regarding to the magnitude of the enhancing effect could be related to the physicochemical characteristics of chitosan. In fact, Shah et al. showed that similar concentrations (1–5 g/l) of chitosan (DD = 85%) only enhanced acyclovir Caco-2 P_{app} 5.8–10.2-fold, accompanied by a TEER reduction of 46.6–58.5% [10]. Consistently, chitosan displayed a much greater TEER reduction in this study (Table 2), which could be also due to the high deacetylation degree. Finally, both the low pH of the current study, applied to overcome precipitation of chitosan, and the general interlaboratory variability of the Caco-2 system [31,32], may also contribute to explain the differences found.

The modified Caco-2 model with mucus demonstrated that the disruptive effect of chitosan on the integrity of the epithelial cells is much lower in presence of mucus [14,33]. Both TEER values and acyclovir's permeation were less affected than in the unmodified model when 1.6 g/l chitosan was added, suggesting that the mucus layer prevented damage to cell monolayer integrity and consequential increased permeation of acyclovir. The higher concentration of chitosan (4 g/l) caused reduced monolayer integrity accompanied by an elevated permeation of acyclovir, although this was not statistically significant. Likewise, such reduction of monolayer integrity was not accompanied by an increase in acyclovir P_{app}. Therefore, in the presence of mucus, no effect of chitosan (1.6 and 4.0 g/l) on the absorption of acyclovir was detected in this modified Caco-2 cell model.

Rat intestine mounted in an Ussing chamber has shown to be a useful model in predicting human intestinal absorption too, although differences in transporter expression and metabolic characteristics apply as well [34–36]. Even though apparently larger permeability values were observed in this model (Table 1), they were comparable with P_{app} of other low permeability compounds across rat jejunum mounted in this same experimental set-up [36]. Permeability of acyclovir was statistically significantly reduced in presence of a concentration of 1.6 g/l chitosan, while the reduction remained a non-significant trend at 4.0 g/l. The Rf values decreased during the experiment and the limited reduction in presence of chitosan suggested a stabilizing effect (Table 3). Interactions of chitosan with mucus may again explain these observations. The mucus production of intestinal tissue segments in the Ussing-type chamber is enhanced by the experimental conditions [22], as was also observed in the present study. Charge interactions of chitosan in the mucus-producing model may neutralize the reactivity of chitosan and prevent an absorption enhancing effect.

Acyclovir permeability through porcine intestine was slightly lower than previously reported for other low permeability compounds by using this same system [23], consistent with its classification as BCS class III [17]. The results of same concentrations of chitosan (1.6 and 4 g/l) suggested a negative effect on the absorption of acyclovir across porcine jejunal segments mounted in the InTESTine system (Table 1). However, neither the negative nor the positive effect were statistically significantly different from the reference. The effect of chitosan on paracellular transport marker compound atenolol was in line with that for acyclovir, which confirmed an effect of chitosan on the paracellular absorption route. The absence of an effect of chitosan on transport of antipyrine confirmed the absence of an effect on the transcellular route and of a non-specific effect on the mucus barrier (data not shown).

Despite of the chitosan effect has been already studied in diverse *in vitro* systems, they do not necessarily resemble the true anatomic intestinal lining due to the lack of a mucus layer. Especially the differences in protective mucus layer and tight junctions are of relevance, as the modulation of membrane transport by cationic chitosan is postulated to occur through an interaction with negative charges in the cavity of the tight junctions [8]. In this line, Schipper et al. studied the permeability of the well-known permeability marker mannitol through HT29-H mucus-secretory cells in presence of chitosan. As expected, chitosan co-administration increased mannitol P_{app} when the mucus layer was removed. However, the presence of a mucus layer prevented such enhancement through unwashed cells [14]. In the present study,

three out of four permeability experiments were performed in mucus containing set-ups. Consistently, the expected enhancing effect of chitosan on acyclovir P_{app} in all mucus containing models was at least prevented. Furthermore, acyclovir permeability across rat and pig intestinal tissues was decreased when co-incubated, being statistically significant in rat at 1.6 g/l of chitosan, in good agreement with the *in vivo* situation. The protective effect of mucus on barrier integrity was also observed in electrical resistance measurements, where mucus-containing models maintained TEER and Rf values in presence of chitosan (Tables 2 and 3). Fluorescence microscopy experiments showed that highly deacetylated chitosan did not reach the membrane of mucus-secreting cells [14]. Although mucus displayed similar magnitudes of protective effect for different types of chitosan (DD and MW), it is still possible that the interaction depends on those physicochemical features. A key factor of this present work is that the same chitosan from the clinical trial was used. Therefore, the chitosan mucus interaction could provide an explanation for controversial bioavailability estimates obtained from different *in vitro* models for the human situation.

Being a polycation, chitosan might bind to any other polyanion present in the system studied. For example, the enhancing chitosan effect observed in Caco-2 cells was reverted by addition of heparin, demonstrating the un-specificity of such ionic interaction [8]. Acyclovir tablets studied here declare the presence of sodium starch glycolate, a polyanion with pKa 4.8, likely charged at biorelevant pHs. Hence, a possible excipient-excipient interaction can be speculated. Nevertheless, clear solutions were observed when tablets were dissolved in water, regardless of the presence of chitosan [16]. Moreover, acyclovir mass balance > 90% after TIM-1 experiment (Fig. 1), suggests that even when an excipient-excipient interaction occurred, it would not affect the amount of acyclovir available for absorption. On the other hand, the chitosan effect could be also attenuated by slightly alkaline media because of its low solubility above its pKa [30]. However, experimental media were well-buffered 0.5 units below the chitosan pKa, which was enough to achieve the needed solutions before running permeability experiments. In contrast, precipitation was observed after sample addition to Caco-2 cells supplemented with mucus, suggesting a direct interaction of chitosan with the mucus, rather than other possible causes, thus reducing the available concentration of the modulator in solution. Taken together, the results presented here provide additional evidence supporting the protective role of mucus, and suggest that its presence in the *in vivo* GI tract might have prevented chitosan to exert an overall enhancing effect on the bioavailability of acyclovir. The presence of a mucus layer thus seems an important factor in determining the biorelevance of permeation models and might also be considered for other excipients effects on intestinal permeability, in particular when they are positively charged.

Our human study showed a relatively high intra-individual and interindividual variability of the absorption of acyclovir itself, which augmented in presence of chitosan. Both increased and decreased AUC and C_{max} values were observed when acyclovir was co-administered with chitosan. Moreover, four out of twelve volunteers showed a higher AUC in presence of one of the two doses of chitosan and a lowered AUC in presence of the other dose [16]. Further evaluation of potential intra- and interindividual differences in physiological processes in the absorption of acyclovir and the potential effect of chitosan on these processes, may thus be relevant. Integration of different *in vitro* datasets in a PBPK model can also be helpful in this perspective and will be the subject of a follow-up study.

The observed results on bioaccessibility and intestinal permeability could also be important in the context of biowaiving. Based on human studies with acyclovir and cimetidine, Vaithianathan et al. recently proposed widened biowaiver possibilities for changes in the content of 12 common excipients combined with BCS class III substances [37]. In the current case of potential excipient chitosan, the contrary can be concluded. The unmodified Caco-2 cell model showed a loss of membrane integrity, which has no correlation to the *in vivo* human situation. The mucus-containing Caco-2 model showed a non-significant positive trend, which is not line with the *in vivo* data. These models thus seem unsuitable to replace *in vivo* testing. The trends observed for the tissue segment models (rat and porcine intestine) were negative. Among the models explored in the present study, the Ussing type chamber showed to be the most biopredictive as it did point to an overall statistically significantly reduced absorption of acyclovir. This model thus seems most appropriate for pharmaceutical development purposes. However, it is not considered suitable to fully exempt from *in vivo* testing e.g. for biowaiver purposes. An *in vivo* pharmacokinetic study is needed to determine the magnitude of the clinical effect on AUC and C_{max} and its consequential relevance for drug absorption.

5. Conclusion

This study presents for the first time a comparison of various preclinical intestinal permeability models run under comparative conditions with the aim of testing the predictive power of each model. The overall *in vivo* effects of chitosan pointed to a reduced rate and extent of the absorption of acyclovir. Acyclovir's bioaccessibility in TIM-1 was not affected by chitosan; this model thus confirmed absence of intraluminal interactions hampering the solubility and availability for absorption of acyclovir. Chitosan's influence on intestinal permeability of acyclovir differed per model. The results obtained with the Caco-2 models were not in line with the *in vivo* data. The tissue segment models (rat and porcine intestine) showed a negative trend of acyclovir's permeation in presence of chitosan. The Ussing type chamber showed to be the most biopredictive of models studied, as it did point to an overall statistically significantly reduced absorption of acyclovir. This model thus seems most appropriate for pharmaceutical development purposes. As a follow-up, PBPK modelling is currently applied to more specifically correlate the outcome of the models to the *in vivo* data. In absence of an established correlation, *in vivo* pharmacokinetic studies remain necessary to determine the actual clinical effect of chitosan on the absorption of acyclovir.

Acknowledgements

The authors wish to thank Dr. Dirk Barends for initializing this project; unfortunately, Dirk passed away before the results became available. The authors thank Maria Teresa Sendra Todo who performed supportive Caco-2 experiments and analyzed the samples of the rat studies. The work of Evelijn Zeijdner, Joost Westerhout, and other TNO colleagues on the TIM-1 and porcine intestinal InTESTine studies is gratefully acknowledged. These studies were performed as a part of the RIVM Biothree project, for which FIP kindly provided seed funding. This work has received support from the Innovative Medicines Initiative Joint Undertaking (http://www.imi.europa.eu) under grant agreement n° 115369. Part of the data described in this paper were also reported in the thesis of Christian Heinen. C.H. is currently employed at F. Hoffmann-La Roche Ltd., Basel, Switzerland. M.K. is employed at the MEB of the Netherlands, but the views presented here do not necessarily reflect the opinion of the Board.

References

[1] J. Synowiecki, N.A. Al-Khateeb, Production, properties, and some new applications of chitin and its derivatives, Crit. Rev. Food Sci. Nutr. 43 (2003) 145–171.
[2] F. Tajdini, M.A. Amini, N. Nafissi-Varcheh, M.A. Faramarzi, Production, physiochemical and antimicrobial properties of fungal chitosan from *Rhizomucor miehei* and *Mucor racemosus*, Int. J. Biol. Macromol. 47 (2010) 180–183.
[3] T. Wu, S. Zivanovic, F.A. Draughon, W.S. Conway, C.E. Sams, Physicochemical properties and bioactivity of fungal chitin and chitosan, J. Agric. Food. Chem. 53 (2005) 3888–3894.
[4] M. Ates, M.S. Kaynak, S. Sahin, Effect of permeability enhancers on paracellular permeability of acyclovir, J. Pharm. Pharmacol. 68 (2016) 781–790.
[5] A.F. Kotze, M.M. Thanou, H.L. Luebetaen, A.G. de Boer, J.C. Verhoef,

H.E. Junginger, Enhancement of paracellular drug transport with highly quaternized N-trimethyl chitosan chloride in neutral environments: in vitro evaluation in intestinal epithelial cells (Caco-2), J. Pharm. Sci. 88 (1999) 253–257.
[6] A. Masuda, Y. Goto, Y. Kurosaki, T. Aiba, In vivo application of chitosan to facilitate intestinal acyclovir absorption in rats, J. Pharm. Sci. 101 (2012) 2449–2456.
[7] P. Opanasopit, P. Aumklad, J. Kowapradit, T. Ngawhiranpat, A. Apirakaramwong, T. Rojanarata, S. Puttipipatkhachorn, Effect of salt forms and molecular weight of chitosans on in vitro permeability enhancement in intestinal epithelial cells (Caco-2), Pharm. Dev. Technol. 12 (2007) 447–455.
[8] N.G. Schipper, S. Olsson, J.A. Hoogstraate, A.G. deBoer, K.M. Varum, P. Artursson, Chitosans as absorption enhancers for poorly absorbable drugs 2: mechanism of absorption enhancement, Pharm. Res. 14 (1997) 923–929.
[9] A. Merzlikine, C. Rotter, B. Rago, J. Poe, C. Christoffersen, V.H. Thomas, M. Troutman, A. El-Kattan, Effect of chitosan glutamate, carbomer 974P, and EDTA on the in vitro Caco-2 permeability and oral pharmacokinetic profile of acyclovir in rats, Drug Dev. Ind. Pharm. 35 (2009) 1082–1091.
[10] P. Shah, V. Jogani, P. Mishra, A.K. Mishra, T. Bagchi, A. Misra, In vitro assessment of acyclovir permeation across cell monolayers in the presence of absorption enhancers, Drug Dev. Ind. Pharm. 34 (2008) 279–288.
[11] M. Nadai, C. Tajiri, H. Yoshizumi, Y. Suzuki, Y.L. Zhao, M. Kimura, Y. Tsunekawa, T. Hasegawa, Effect of chitosan on gastrointestinal absorption of water-insoluble drugs following oral administration in rats, Biol. Pharm. Bull. 29 (2006) 1941–1946.
[12] J.M. Smith, M. Dornish, E.J. Wood, Involvement of protein kinase C in chitosan glutamate-mediated tight junction disruption, Biomaterials 26 (2005) 3269–3276.
[13] N.G. Schipper, K.M. Varum, P. Artursson, Chitosans as absorption enhancers for poorly absorbable drugs. 1: influence of molecular weight and degree of acetylation on drug transport across human intestinal epithelial (Caco-2) cells, Pharm. Res. 13 (1996) 1686–1692.
[14] N.G. Schipper, K.M. Varum, P. Stenberg, G. Ocklind, H. Lennernas, P. Artursson, Chitosans as absorption enhancers of poorly absorbable drugs. 3: influence of mucus on absorption enhancement, Eur. J. Pharm. Sci.: Off. J. Eur. Fed. Pharm. Sci. 8 (1999) 335–343.
[15] C.A. Heinen, S. Reuss, G.L. Amidon, P. Langguth, Ion pairing with bile salts modulates intestinal permeability and contributes to food-drug interaction of BCS class III compound trospium chloride, Mol. Pharm. 10 (2013) 3989–3996.
[16] M. Kubbinga, M.A. Nguyen, P. Staubach, S. Teerenstra, P. Langguth, The influence of chitosan on the oral bioavailability of acyclovir – a comparative bioavailability study in humans, Pharm. Res. 32 (2015) 2241–2249.
[17] J. Arnal, I. Gonzalez-Alvarez, M. Bermejo, G.L. Amidon, H.E. Junginger, S. Kopp, K.K. Midha, V.P. Shah, S. Stavchansky, J.B. Dressman, D.M. Barends, Biowaiver monographs for immediate release solid oral dosage forms: aciclovir, J. Pharm. Sci. 97 (2008) 5061–5073.
[18] J. Brouwers, B. Anneveld, G.J. Goudappel, G. Duchateau, P. Annaert, P. Augustijns, E. Zeijdner, Food-dependent disintegration of immediate release fosamprenavir tablets: in vitro evaluation using magnetic resonance imaging and a dynamic gastrointestinal system, Eur. J. Pharm. Biopharm.: Off. J. Arbeitsgemeinschaft fur Pharmazeutische Verfahrenstechnik e.V 77 (2011) 313–319.
[19] P.A. Dickinson, R. Abu Rmaileh, L. Ashworth, R.A. Barker, W.M. Burke, C.M. Patterson, N. Stainforth, M. Yasin, An investigation into the utility of a multicompartmental, dynamic, system of the upper gastrointestinal tract to support formulation development and establish bioequivalence of poorly soluble drugs, AAPS J. 14 (2012) 196–205.
[20] M. Minekus, P. Marteau, R. Havenaar, J.H.H. Huis in't Veld, Multicompartmental dynamic computer-controlled model simulating the stomach and small intestine, Altern. Lab. Anim. 23 (1995) 197–209.
[21] B. Wuyts, D. Riethorst, J. Brouwers, J. Tack, P. Annaert, P. Augustijns, Evaluation of fasted state human intestinal fluid as apical solvent system in the Caco-2 absorption model and comparison with FaSSIF, Eur. J. Pharm. Sci.: Off. J. Eur. Fed. Pharm. Sci. 67 (2015) 126–135.
[22] C. Heinen, S. Reuss, S. Saaler-Reinhardt, P. Langguth, Mechanistic basis for unexpected bioavailability enhancement of polyelectrolyte complexes incorporating BCS class III drugs and carrageenans, Eur. J. Pharm. Biopharm.: Off. J. Arbeitsgemeinschaft fur Pharmazeutische Verfahrenstechnik e.V 85 (2013) 26–33.
[23] J. Westerhout, E. van de Steeg, D. Grossouw, E.E. Zeijdner, C.A. Krul, M. Verwei, H.M. Wortelboer, A new approach to predict human intestinal absorption using porcine intestinal tissue and biorelevant matrices, Eur. J. Pharm. Sci.: Off. J. Eur. Fed. Pharm. Sci. 63 (2014) 167–177.
[24] A.H. Shojaei, B. Berner, L. Xiaoling, Transbuccal delivery of acyclovir: I. In vitro determination of routes of buccal transport, Pharm. Res. 15 (1998) 1182–1188.
[25] V. Dodane, M. Amin Khan, J.R. Merwin, Effect of chitosan on epithelial permeability and structure, Int. J. Pharm. 182 (1999) 21–32.
[26] M. Koziolek, M. Grimm, D. Becker, V. Iordanov, H. Zou, J. Shimizu, C. Wanke, G. Garbacz, W. Weitschies, Investigation of pH and temperature profiles in the GI tract of fasted human subjects using the Intellicap((R)) system, J. Pharm. Sci. 104 (2015) 2855–2863.
[27] P. Shah, V. Jogani, P. Mishra, A.K. Mishra, T. Bagchi, A. Misra, Modulation of ganciclovir intestinal absorption in presence of absorption enhancers, J. Pharm. Sci. 96 (2007) 2710–2722.
[28] B.D. Rege, L.X. Yu, A.S. Hussain, J.E. Polli, Effect of common excipients on Caco-2 transport of low-permeability drugs, J. Pharm. Sci. 90 (2001) 1776–1786.
[29] Q.Z. Wang, X.G. Chen, N. Liu, S.X. Wang, C.S. Liu, X.H. Meng, C.G. Liu, Protonation constants of chitosan with different molecular weight and degree of deacetylation, Carbohydr. Polym. 65 (2006).
[30] C.K.S. Pillai, W. Paul, C.P. Sharma, Chitin and chitosan polymers: chemistry, solubility and fiber formation, Prog. Polym. Sci. 34 (2009) 641–678.
[31] C.A. Larregieu, L.Z. Benet, Drug discovery and regulatory considerations for improving in silico and in vitro predictions that use Caco-2 as a surrogate for human intestinal permeability measurements, AAPS J. 15 (2013) 483–497.
[32] D.A. Volpe, Variability in Caco-2 and MDCK cell-based intestinal permeability assays, J. Pharm. Sci. 97 (2008) 712–725.
[33] P. He, S.S. Davis, L. Illum, In vitro evaluation of the mucoadhesive properties of chitosan microspheres, Int. J. Pharm. 166 (1998) 75–89.
[34] H. Lennernäs, Human jejunal effective permeability and its correlation with preclinical drug absorption models, J. Pharm. Pharmacol. 49 (1997) 627–638.
[35] E. Sjogren, B. Abrahamsson, P. Augustijns, D. Becker, M.B. Bolger, M. Brewster, J. Brouwers, T. Flanagan, M. Harwood, C. Heinen, R. Holm, H.P. Juretschke, M. Kubbinga, A. Lindahl, V. Lukacova, U. Munster, S. Neuhoff, M.A. Nguyen, A. Peer, C. Reppas, A.R. Hodjegan, C. Tannergren, W. Weitschies, C. Wilson, P. Zane, H. Lennernas, P. Langguth, In vivo methods for drug absorption – comparative physiologies, model selection, correlations with in vitro methods (IVIVC), and applications for formulation/API/excipient characterization including food effects, Eur. J. Pharm. Sci.: Off. J. Eur. Fed. Pharm. Sci. 57 (2014) 99–151.
[36] A.L. Ungell, S. Nylander, S. Bergstrand, A. Sjoberg, H. Lennernas, Membrane transport of drugs in different regions of the intestinal tract of the rat, J. Pharm. Sci. 87 (1998) 360–366.
[37] S. Vaithianathan, S.H. Haidar, X. Zhang, W. Jiang, C. Avon, T.C. Dowling, C. Shao, M. Kane, S.W. Hoag, M.H. Flasar, T.Y. Ting, J.E. Polli, Effect of common excipients on the oral drug absorption of biopharmaceutics classification system class 3 drugs cimetidine and acyclovir, J. Pharm. Sci. 105 (2016) 996–1005.

APPENDIX 4 (PUBLICATION #4).

PREDICTING PHARMACOKINETICS OF MULTISOURCE ACYCLOVIR ORAL PRODUCTS THROUGH PHYSIOLOGICALLY BASED BIOPHARMACEUTICS MODELING

Journal of Pharmaceutical Sciences 111 (2022) 262–273

Contents lists available at ScienceDirect

Journal of Pharmaceutical Sciences

journal homepage: www.jpharmsci.org

Pharmacokinetics, Pharmacodynamics and Drug Transport and Metabolism

Predicting Pharmacokinetics of Multisource Acyclovir Oral Products Through Physiologically Based Biopharmaceutics Modeling

Mauricio A. García[a], Michael B. Bolger[b], Sandra Suarez-Sharp[b], Peter Langguth[a,*]

[a] Johannes Gutenberg-Universität, Staudingerweg 5, 55099 Mainz, Germany
[b] Simulations Plus, Inc., 42505 10th St. West, Lancaster, CA, United States

ARTICLE INFO

Article history:
Received 13 August 2021
Revised 13 October 2021
Accepted 13 October 2021
Available online 20 October 2021

Keywords:
PBPK
PBBM
Dissolution
BCS
Bioequivalence
OCT
Population PKs

ABSTRACT

Highly variable disposition after oral ingestion of acyclovir has been reported, although little is known regarding the underlying mechanisms. Different studies using the same reference product (Zovirax ®) showed that C_{max} and AUC were respectively 44 and 35% lower in Saudi Arabians than Europeans, consistent with higher frequencies of reduced-activity polymorphs of the organic cation transporter (OCT1) in Europeans. In this study, the contribution of physiology (*i.e.*, OCT1 activity) to the oral disposition of acyclovir immediate release (IR) tablets was hypothesized to be greater than dissolution. The potential role of OCT1 was studied in a validated physiologically-based biopharmaceutics model (PBBM), while dissolution of two Chilean generics (with demonstrated bioequivalence) and the reference product was assessed *in vitro*. The PBBM suggested that OCT1 activity could partially explain population-related pharmacokinetic differences. Further, dissolution of generics was slower than the regulatory criterion for BCS III IR products. Remarkably, virtual bioequivalence (incorporating *in vitro* dissolution into the PBBM) correctly and robustly predicted the bioequivalence of these products, showcasing its value in support of failed BCS biowaivers. These findings suggest that very-rapid dissolution for acyclovir IR products may not be critical for BCS biowaiver. They also endorse the relevance of cross-over designs in bioequivalence trials.

Introduction

The pharmaceutical industry and regulators share the quest of reducing the cost, time and number of *in vivo* trials in the development/approval of generic drug products around the world. The biopharmaceutics classification system (BCS) was a major breakthrough, because it allowed the introduction of biowaivers for highly soluble active pharmaceutical ingredients (APIs) formulated as rapidly dissolving immediate release (IR) solid oral dosage forms. Physiologically based pharmacokinetic (PBPK) models have further broadened the opportunities of utilizing additional methodologies to understand and predict drug disposition and bioequivalence of drug products. Recently, the concept of physiologically based biopharmaceutics modeling (PBBM) was introduced to account for the interaction between physiology and formulations. This framework is particularly important to understand subject-to-subject and formulation variability in oral bioavailability and its impact on the clinical exposure of a given drug product.[1] While parameters like gastrointestinal fluid volumes and luminal contents are of concern for poorly soluble drugs (*e.g.* BCS II), the passive and carrier mediated permeability across biological membranes are rather more critical for poorly permeable drugs (*e.g.* BCS III).

Acyclovir is a poorly permeable drug with variable oral bioavailability (F) between 10–30%.[2] It has aqueous solubility of

Abbreviations: ADH, Alcohol dehydrogenase; ALDH, Aldehyde dehydrogenase; API, Active Pharmaceutical Ingredient; AUC, Area under the curve; BCS, Biopharmaceutics classification system; BMI, Body mass index; BWt, Body weight; CI, confidence inverval; C_{max}, Maximum concentration; CMMG, 9-carboxymethoxymethylguanine; F, Bioavailability; Fa, Fraction absorbed; Fel,u, Fraction eliminated unchanged in urine; Fm, Fraction metabolized; ICH, International council for harmonisation; IR, Immediate release; IV, Intravenous; IVIVC, In vivo in vitro correlation; K_m, Michaelis-Menten constant; MATE, multidrug and toxin compound extrusion transporter; OAT, Organic anion transporter; OCT, Organic cation transporter; P_{app}, Apparent permeability; P_{eff}, Effective permeability; P_{para}, Paracellular permeability; P_{trans}, Transcellular permeability; PBBM, Physiologically based biopharmaceutics model; PBPK, Physiologically based pharmacokinetic model; PE, Prediction error; PStc, Permeability surface area product; SIF, Simulated intestinal fluid; SGF, Simulated gastric fluid; SNP, Single nucleotide polymorphism; SpecPStc, Specific permeability surface area product; V_{max}, Maximum rate.

* Corresponding author at: Pharmaceutical Technology and Biopharmaceutics, Institute of Pharmaceutical and Biomedical Sciences, Johannes Gutenberg University, Staudingerweg 5, 55099 Mainz, Germany.
E-mail address: langguth@uni-mainz.de (P. Langguth).

https://doi.org/10.1016/j.xphs.2021.10.013
0022-3549/

2.3 mg/ml at pH = 5.8 and exhibits linear oral pharmacokinetics in the dose range 200–400 mg[3]. In fact, its absorption is not expected to be solubility-limited at these doses (Do < 1).[2] However, large within-study coefficients of variability (CVs) of 30–40% have been reported at these lower doses.[4,5] The variability does not appear to be necessarily related to the dosage form, because both the C_{max} and AUC after an oral solution were reportedly not different from acyclovir IR capsules at 200 mg in a single-dose cross-over study.[3] In addition, its variable bioavailability is accentuated between different populations. For instance, the C_{max} and the AUC of the reference product (Zovirax® IR tablets 400 mg) were respectively 44 and 35% lower in Saudi Arabians,[6] compared to Europeans.[5] Other studies conducted in different populations showed C_{max} and AUC values lying between those above mentioned.[7] Interestingly, the generic products tested in those publications were found to be bioequivalent to the reference in the respective populations.

Even though the variable oral bioavailability of acyclovir is well-known, there is a paucity of evidence in identifying the physiological mechanisms underlying this observation. Acyclovir absorption seems to be governed by passive processes,[8] with significant contribution of paracellular absorption.[9,10] Nonetheless, both transporters and enzymes play a major role in its distribution, metabolism and elimination. After an intravenous (IV) infusion, acyclovir is rapidly distributed in more than one compartment and eliminated mainly through the urine.[5,11,12] In fact, acyclovir was identified as a substrate of the organic anion transporter (OATs),[13,14] and the multidrug and toxin compound extrusion (MATE) transporter,[15] respectively located in the basolateral and apical membrane of the renal epithelium. Further, acyclovir is metabolized into 9-carboxymethoxymethylguanine (CMMG),[16,17] due to the action of the alcohol/aldehyde dehydrogenase (ALDH/ADH) system.[2,17,18] Moreover, acyclovir is also transported by the human organic cation transporter (OCT1),[14] which mediates its hepatic uptake prior to biotransformation. This latter transporter has also shown a large extent of polymorphism, especially in European ethnicity.[19] For example, the frequencies of the non-synonymous single nucleotide polymorphs (SNPs) R61C, G401S and G465R are the highest in Europeans, while they are completely absent in Asians, Africans, and other ethnicities.[19–22] The activity of the aforementioned polymorphs was impaired compared to wild-type in *in vitro* cation uptake assays.[19] Moreover, their impact on pharmacokinetics was also demonstrated in humans, where the C_{max} and AUC of metformin (another BCS III, OCT1-substrate) were 20–50% higher in subjects expressing those SNPs.[23] Therefore, the role of OCT1 polymorphism in explaining acyclovir variable bioavailability cannot be ruled out.

The aim of this study was to use the PBBM framework to identify the contributions of physiological (*i.e.* OCT1 activity) and formulation (*i.e.* product dissolution) factors to acyclovir's variable disposition following oral administration and assess their potential biopharmaceutic implications. Gastroplus® software was used to develop a complete PBPK model for acyclovir that included the main mechanisms underlying its pharmacokinetics. The OCT1 V_{max} was varied to account for differences between ethnicity of populations. In addition, the *in vitro* dissolution of two Chilean acyclovir 200 mg IR generics (with *in vivo* bioequivalence demonstrated) and the reference (Zovirax® 200 mg IR) was studied at biorelevant pHs.[24,25] Finally, the validated PBBM was used to assess the bioequivalence decision on virtual populations with different physiologies. The model robustly predicted the bioequivalence of the products, even though they did not meet the approved dissolution acceptance criterion. Instead, the clinical performance of BCS class III drug products seems to be more critically impacted by variations on physiological factors rather than small variations beyond the threshold for rapidly dissolving criterion (*i.e.*, 15 min).[26]

Experimental Section

Materials and Software

Acyclovir powder (purity < 99%) was purchased from Sigma-Aldrich (Merck KGaA, Germany). Hydrochloric acid 37% v/v was bought from VWR International (LLC, PA, US). Sodium chloride, potassium dihydrogen phosphate and all supplies for dissolution experiments (syringes and 80 μm-filters) from Carl Roth (Carl Roth & Co. KG, Germany). Two Chilean generics IR oral tablets containing acyclovir 200 mg from Laboratorio Chile S.A. (Generic A) and Mintlab Co. S. A. (Generic B),[25,27] plus Zovirax® 200 mg IR tablets (Reference) were acquired from local pharmacies. Modeling and simulations were carried out in GastroPlus® V. 9.8.1 (Simulations Plus, Inc., Lancaster, CA). Digitalization of literature data was performed with Digit 1.0.4 (Simulations Plus, Inc., Lancaster, CA), while RNA expression data was digitalized with ImageJ 1.46r (National Institute of Health, Bethesda, MD).

PBPK Model After Intravenous Administration

Data on acyclovir intravenous (IV) pharmacokinetics reported by Laskin et al.[11] was utilized to build the PBPK model. A female American subject, 66 years old, body weight (BWt) 64 Kg was created in the Population Estimates for Age-Related (PEAR™) physiology module to match the body measurements reported in the study for American malignancy patients that received a one-hour infusion of 10 mg/Kg. Acyclovir physicochemical parameters were mostly taken from the available literature, otherwise predicted by ADMET Predictor 10.0 (Table 1). The Poulin extracellular method was used to calculate the extracellular fluid/plasma concentration ratio (Kp) for all permeability-limited tissues.[28] All tissues were treated as permeability-limited with a specific PStc = 9.9×10^{-5} ml/s/ml tissue resulting in liver PStc = 0.082 ml/s for a 74 kg male subject. Other physiological considerations when building the model are briefly described below:

a) Acyclovir's low permeability through biological membranes suggests that slow passive diffusion may limit its tissue distribution,[8,29] hence all tissues were treated as permeability-limited. As previously described, one single permeability surface area product (PStc), also called specific PStc (SpecPStc, with units of ml/s/ml of tissue), was assumed in order to decrease the number of estimations.[30] The PStc for each tissue was, thereafter, calculated from the SpecPStc and cellular volumes of the respective tissue.
b) Organic anion transporters (OATs) share a similar tissue distribution, mainly in the basolateral membrane of tissue epithelia mediating the uptake of substrates into cells.[31,32] Therefore, the isoform with the highest affinity for acyclovir (hOAT2) was chosen to account for OATs-mediated transport from blood into the kidney.[13] Likewise, the hOCT1 mediates the basolateral uptake into hepatocytes.[14] Lastly, hMATE1 effluxes substrates into both the renal lumen and the bile, through the apical membrane of tubule cells and the canicular membrane of hepatocytes, respectively. Given that acyclovir is a substrate of these transporters,[13–15] they were all taken into account to model acyclovir disposition. *In vitro* K_m previously reported for humans isoforms were used as input,[13–15] while the *in vivo* V_{max} values were optimized against clinical observations (see below).[11]
c) The fraction metabolized (Fm) of acyclovir following an IV infusion was found to vary between 8 and 15%,[17] although values up to 19% have been reported,[16] as well. The main metabolite is 9-carboxymethoxymethylguanine (CMMG),[2,17] which is formed after a two-step oxidation where both the alcohol (ADH) and aldehyde dehydrogenase (ALDH) are involved 0.[33] Acyclovir

Table 1
Summary of input parameters used in acyclovir simulations.

Physicochemical parameter	Value	PBPK parameter		Value
log P[2]	−1.57	SpecPStc (ml/s/ml)[e]		1.0×10^{-4}
pKa base[2]	2.27	OAT2	K_m (μM)[13]	94
pKa acid[2]	9.25		V_{max} (mg/s/mg Trans)[e]	0.092
$S_{pH=5.8}$ (mg/ml)[47]	2.33	OCT1	K_m (μM)[14]	151
Fup (%)[16]	84.6		V_{max} (mg/s/mg Trans)[e]	0.016
Blood:plasma ratio[a]	1.07		V_{max} (mg/s/mg Trans)[f]	0.035
D (cm^2/s, 10^{-6})[a]	8.9	MATE1	K_m (μM)[15]	2640
Hydrodynamic radius (Å)[a]	4.74		V_{max} (mg/s/mg Trans)[e]	0.016
Mean projected radius (Å)[a]	5.06	ADH1	K_m (μM)[35]	155
Human P_{eff} (cm/s, 10^{-4})[b]	0.22		V_{max} PBPK (mg/s/mg Enz)[e]	9.34×10^{-8}
Human P_{eff} (cm/s, 10^{-4})[c]	0.31		MW (g/mol)[54]	82,000
Human P_{eff} (cm/s, 10^{-4})[d]	0.29		Liver exp (mg Enz/g tissue)[34]	9.62
			Kidney exp (mg Enz/g tissue)[18]	0.32

[a] Predicted (ADMET Predictor 10.0).
[b] Converted from Caco-2 experiments.
[c] Converted from rat intestine Ussing chamber experiments.
[d] Refined value. Utilized to run all simulations unless otherwise specified.
[e] Optimized with Laskin et al. IV data after a 10 mg/Kg dose (See methods).
[f] Increased to account for different OCT1 activities due to potential polymorphism (See methods).

metabolism was assumed to be a consequence of only the ADH1 isoform, as this showed the highest expression in the human liver.[34] Given the lack of information on acyclovir affinity for these enzymes, the affinity of a chemically similar compound (K_m=155 μM) was used and assumed to be the same for acyclovir.[35] Quantitative ADH1 liver expression (9.62 mg of ADH1/g of liver)[34] was converted into enzyme expression amounts (pmol/mg cytosolic protein) by using both the enzyme molecular weight and the scaling factor= 80 mg of cytosolic protein per gram of liver included in the software. Renal expression was set to 0.32 mg of ADH1/g of kidney based on published findings.[18] The ADH1 V_{max} was optimized to match observed clinical data, as described below.[11,17]

d) The fraction of acyclovir eliminated urinary unchanged (Fel,u) after 72 h seems to be dose-independent and was found to vary from 30 to 69%, with a mean of 60%.[12] Most of the parent drug was excreted in urine during the first eight hours.[12] Acyclovir was found to be accumulated in the kidney, with approximately ten-fold higher concentration than the plasma, as determined in post-mortem patients that received acyclovir therapy before passing away.[33,36]

The permeability-limited model created was used to optimize the uncertain parameters: SpecPstc, OAT2 V_{max}, OCT1 V_{max}, MATE1 V_{max} and ADH1 V_{max} (Hooke & Jeeves method, weighting to $1/\hat{y}^2$). The initial estimates were 2×10^{-4} ml/s/ml, 0.1 mg/s/mg transporter (OAT2), 0.03 mg/s/mg transporter (OCT1), 0.03 mg/s/mg transporter (MATE1) and 8×10^{-7} mg/s/mg enzyme (ADH1), respectively. The sum of squared deviation between the simulated and observed plasma concentration *vs.* time profile after the IV infusion of 10 mg/Kg reported by Laskin et al.[11] was used as the objective function in fitting the parameters. As additional objective constraints, the kidney concentrations were assumed to be ten-fold higher than the plasma,[36] and the cumulative unchanged urinary fraction assumed to be 60%.[12] The parameters were simultaneously optimized to match the plasma concentration profile, kidney concentration profile, urinary excretion, observed C_{max} and AUC. After the optimization, the ADH1 V_{max} was manually increased to match the Fm to ~10% as reported in the literature.[17] The model was validated by simulating the IV plasma concentrations and hypothetical kidney profiles with further acyclovir doses (2.5, 5.0 and 15 mg/Kg). Urinary data reported by de Miranda et al.[12] for a dose of 5.0 mg/Kg in individuals with similar characteristics as those in the Laskin et al.[11] study, was also used for model validation. External validation was carried out on IV data reported by Vergin et al.,[5] who studied both the IV and oral pharmacokinetics of acyclovir (See below).

Model for Gastrointestinal Transit and Absorption

The gastrointestinal physiology was described by the Advanced Compartmental Absorption and Transit (ACAT™) model. This was supplemented with regional expression of ADH1 enzyme (Table S-1, Supp. Material).

To the best of our knowledge, the effective jejunal permeability (P_{eff}) of acyclovir in humans has not been determined experimentally. Therefore, the human P_{eff} was estimated from in-house apparent permeabilities (P_{app}) from two *in vitro* experiments, namely Caco-2 monolayers and rat jejunum mounted on an Ussing chamber. While the *in vitro* Caco-2 P_{app} (0.17×10^{-6} cm/s) was translated into human P_{eff} with the calibration included in the software, the construction of a correlation was needed for rat intestine Ussing chamber P_{app} (7.4×10^{-6} cm/s). The correlation equation was built with experimental P_{app} reported by Ungell et al.,[37] and it was based on the best fit equation (P_{eff} (x 10^4) cm/*s* = $10^{(-0.3226+1.449 * \log[Papp\ (x\ 10\text{^}5)\ cm/s])}$. For instance, for a P_{app} value = 7.4×10^{-6} cm/s, then the simulation P_{eff} = 0.31 (10^4, cm/s) = $10^{(-0.3226+1.449 * \log[0.74])}$. The final P_{eff} was refined to a value in between the human P_{eff} estimated from the respective correlations. Acyclovir's paracellular permeability (P_{para}) was calculated with the He, Zhimim model included in Gastroplus®.[38] This parameter is already considered in the P_{eff} value, such that P_{eff}–P_{para}= P_{trans} (transcellular permeability).

Physiological Differences Between Populations

Studies Selection and Population Modeling

Studies using acyclovir 200 mg are scarce, therefore three bioequivalence studies on healthy subjects orally administered with the reference product (Zovirax® IR tablets 400 mg) were chosen. Since the reference product 400 mg showed very rapid *in vitro* dissolution (>85% in 15 min in HCl 0.1 N, USP type 2 apparatus at 50 rpm, data not shown), inter-studies differences in C_{max} and AUC parameters for the reference product are most likely related to the interaction between the API and the given population. Populations in these studies were modeled as healthy subjects using the PEAR physiology, matching the observed mean age and body measurements, when possible. Dosage form in each model was set to "IR Tablet", while the remaining parameters were the same as detailed in Table 1, unless otherwise specified.

Firstly, the Vergin et al.[5] paper was selected because it showed the highest C_{max} and AUC acyclovir plasma profiles among the studies found in the literature. This pharmacokinetic behavior was expected due to the higher frequency of lower activity OCT1 variant transporters in the European population (See below). The German test products (Heuman® IR Tablets 200 and 400 mg, Heuman Pharma GmbH, Germany) were compared to the reference product at the respective doses in Europeans. Furthermore, acyclovir was administered intravenously in this study (10 min infusion, 250 mg IV), which served as external validation of the disposition model (See above). The products were tested in two cross-over studies (study-i: test 200 mg po, reference 250 mg IV infusion (10 min) and reference 200 mg po; and study-ii: the test 400 mg po and the reference 400 mg po). Eight volunteers in study i, participated also in study ii. Subjects gender ratio was 50:50 female:male in both cases, mean ages were 26 and 25 year old (in each study, respectively). A healthy 26 years old female was used to model an average participant from study i, while a 25 years old male was used to model a subject from study ii. Typical healthy subjects' body measurements (73–74 Kg and 24–28 BMI) were assumed in both cases. Gender had no meaningful effect on the simulation metrics (Table S-2).

Secondly, the Al-Yamani et al.[6] work was chosen given that the lowest acyclovir plasma profiles were found in this publication. The test product (Clovir® IR tablets 400 mg, Saudi Pharmaceutical Industries and Medical Appliances Corp., Saudi Arabia) was compared to the reference in a crossover design on healthy males. Subjects were in average 36 years old, 78 Kg and 174 cm. Even though the ethnicity was not defined, the subjects were most likely Saudi Arabians, based on the origin of the test product, the affiliations of the authors and the hospital that authorized the study protocol.

Finally, the Yuen et al.[7] study was picked because the plasma profiles presented were in between the above-mentioned publications. Male volunteers received either two tablets of the test (Avorax 200 mg, Xepa-Soul Pattinson Manufacturing, Malaysia) or the reference in a crossover design. The trial was performed on Malaysian population with mean age 35 years old and 67 Kg. Since the height of the subjects was not reported, the body mass index (BMI) was assumed 21.5, as calculated by the PEAR module.

Modeling Inter-Studies Variabilities and Parameter Sensitivity

Given that abundant polymorphism has been reported for the human OCT1, we hypothesized that discrepancies in C_{max} and AUC between studies may be mechanistically explained by differences in OCT1 activity. Reduced-activity OCT1 polymorphs, R61C (33% activity), G401S (12% activity) and G465R (12% activity), were more frequent in Europeans, while their prevalence in other populations was negligible.[19–22] To the best of our knowledge, the relative activities of diverse OCT1 polymorphs transporting acyclovir have not been investigated yet. Therefore, the reported relative uptakes (transport activities) of the cationic substrate MPP^+ were used to estimate the reduction in activity in Europeans.[19] The mean relative MPP^+ uptake from the seven OCT1 polymorphs found in Europeans was 59%. Considering this value as a rough estimate, the OCT1 V_{max} was increased to account for differences between the Vergin et al. and Al-Yamani et al. studies. A final OCT1 V_{max} increase of 55% was chosen on the basis of visual matching of Al-Yamani et al.'s plasma profiles.

Acknowledging that the variation of other parameters optimized may also simulate the lowered plasma profiles reported by Al-Yamani et al., the sensitivity to the V_{max} of OAT2 and ADH1 in matching the mentioned profiles was also studied by using the optimization module (Hooke & Jeeves method, weighting function: unity). Sensitivity was assessed as the folds of change between the initial and the optimized parameters, such that the lower the value, the higher the sensitivity to that parameter (Results in Supp. Material).

Dissolution Experiments

Dissolution of acyclovir tablets was studied in USP type II apparatus PTW S III (Pharma Test, Germany) at 50 rpm. The tablet was added into 900 ml of a non-containing enzymes simulated gastric fluid (SGF, pH 1.2) or simulated intestinal fluid (SIF, pH 6.5), prewarmed at 37 °C (n = 3). Samples were withdrawn at 5, 10, 15, 20, 30 and 45 min, filtered and analyzed in a UV 6300 PC double beam spectrophotometer (VWR International, LLC, PA, US) at λ_{abs}=250 nm. Generic products A and B were both demonstrated bioequivalent to the reference by comparative bioavailability studies.

Virtual Bioequivalence Trials

Two virtual populations were created by the PEAR physiology module with different OCT1 V_{max} to account for variabilities on OCT1 activity due to putative polymorphism. Sample size was calculated to n = 36,[27] assuming a conservative intra-individual CV= 30%.[4] A reduced-OCT1 activity population was built on the basis of the Vergin et al. study: female/male= 50:50 and age= 19–36 years old.[5] Body dimensions predicted by the software were assumed. On the other hand, the creation of a population with normal-OCT1 activity was based on the Al-Yamani et al. publication: only males, age= 21–50 years old, BWt= 62–92 Kg and BMI= 24–26.[6] P_{eff} variability was set to 25% to simulate the observed outcomes.[5] The virtual bioequivalence trial was performed on each virtual population in a fasted, single dose, three-period (two generics plus the reference product), cross-over design. In addition, plasma profiles obtained from the reference arm in populations with either reduced or normal-OCT1 activity were also compared to explore the effect of a parallel design. Drug product *in vitro* dissolution profiles were directly incorporated into the model.[1,39] Bioequivalence between the reference and either Chilean generic product was established through comparison of the ratio of geometric means for both C_{max} and AUC, such that the 90% confidence interval (CI 90%) falls within the 80–125%.

Results

PBPK Development and Validation

The input parameters utilized in all simulations are depicted in Table 1. The optimized SpectPstc was similar to the previously optimized value (2×10^{-4} ml/s/ml) for ganciclovir,[30] an analog drug which closely resembles acyclovir molecular structure. Optimized V_{max} values for all transporters were comparable and much higher than the ADH1 V_{max}, suggesting that interplay of transporters is a greater contributor to acyclovir disposition than its metabolism. As expected, simulated plasma and renal excretion curves matched the observed profiles used to construct the model (Fig. 1). The model was validated by simulating acyclovir plasma concentrations for different doses, such that it predicted the Fel,u between 54.8 and 63.3%, consistent with *in vivo* observations.[12] Simulated Fm ranged from 7.1 to 18.3% in good agreement with values published for a single dose IV infusion.[16,17] The very same parameters predicted the plasma profiles observed in the Vergin et al.[5] study (external validation), in which acyclovir was administered intravenously, as well (Fig. S-3 and Table S-2). Therefore, identical values for each parameter were used to simulate the oral administration of acyclovir 200 and 400 mg IR tablets (reference product) reported in the said study (Fig. 2).

The human P_{eff} was estimated from acyclovir P_{app} across Caco-2 monolayers (0.17×10^{-6} cm/s) and rat jejunum-Ussing chamber (7.4×10^{-6} cm/s), previously reported.[29] After conversion into human permeability, P_{eff} were 0.22 and 0.31×10^{-4} cm/s, respectively (Table 1). In spite of the closeness of these estimates, oral acyclovir simulations showed that the model is highly sensitive to this

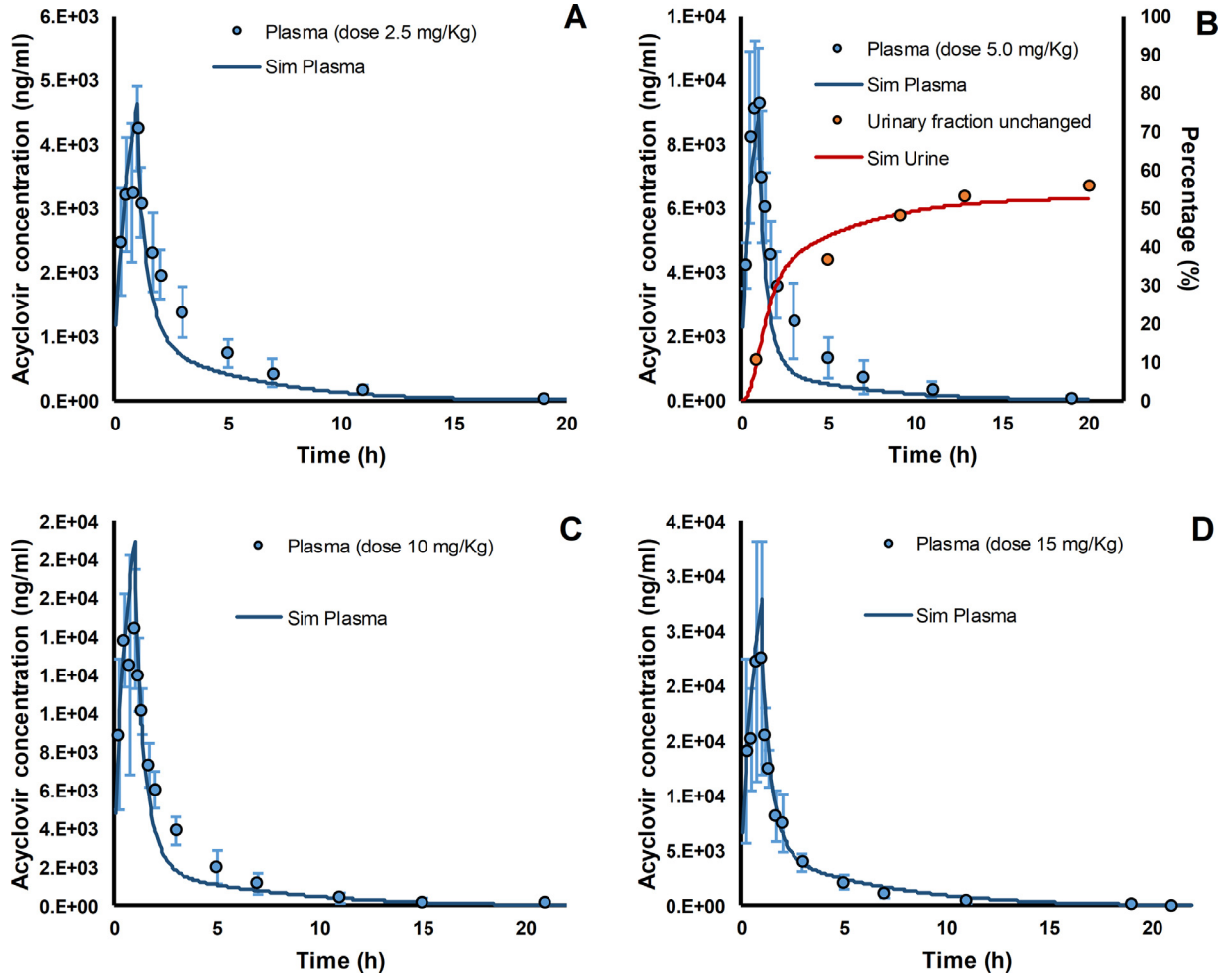

Figure 1. Model validation for IV infusion (1 h) at doses 2.5 (A), 5.0 (B), 10 (C) and 15 mg/Kg (D). Observed mean plasma profiles (dots) and error bars (standard deviations) were reported by Laskin et al..[11] Urinary fraction unchanged (orange dots) was taken from de Miranda et al.,[12] who administered the same dose to subjects with comparable characteristics to those in the Laskin et al. study..[11]

parameter (Fig. 2, dashed lines), as expected for a BCS III API. Caco-2-converted-P_{eff} underpredicted both acyclovir strengths, while rat-jejunum-converted-P_{eff} overpredicted only the 400 mg strength. Hence, P_{eff} was refined to an in between value (0.29×10^{-4} cm/s), giving acceptable simulations of the mean observed data at both strengths (Fig. 2, blue lines). Validation of P_{eff} is depicted by the acceptable matches between observed and simulated C_{max} and AUC at different strengths (Fig. 2 and Table 2).

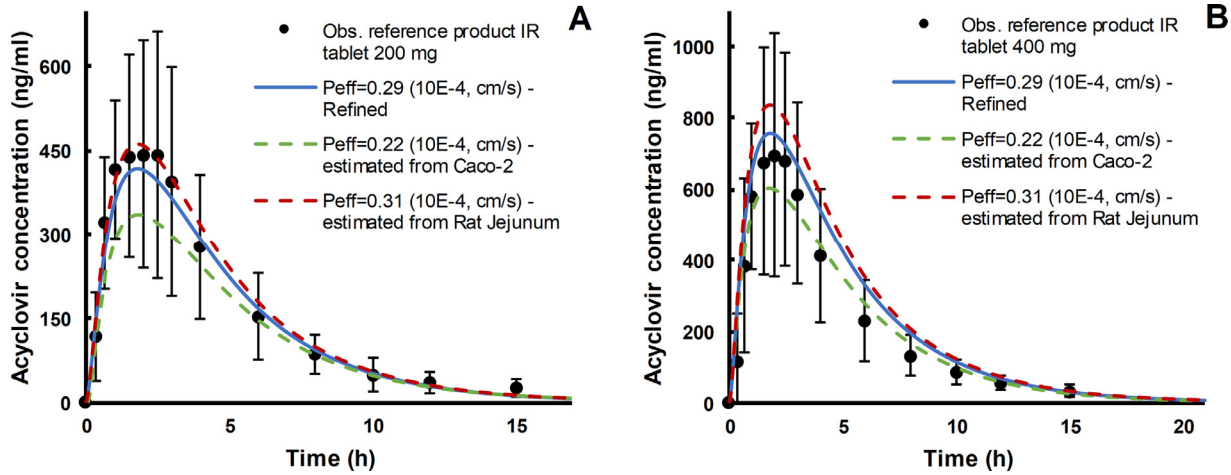

Figure 2. Effect of the P_{eff} on the simulation of acyclovir oral profiles (black dots) reported by Vergin et al. for the reference product (IR tablets) at 200 (A) and 400 mg (B). Simulated profiles obtained with P_{eff} converted from Caco-2 and rat jejunum-Ussing chamber are shown in dashed lines, green and red, respectively. Simulations utilizing the refined P_{eff} are shown in blue lines.

Table 2
Mean observed and simulated pharmacokinetic parameters for the reference product in subjects from different populations.

Study and dose	OCT1 V_{max}[a]	C_{max} (ng/ml)				AUC (μg*h/ml)			
		Obs	Sim	Sim/Obs ratio	PE (%)	Obs	Sim	Sim/Obs ratio	PE (%)
Vergin et al. 200 mg	0.016	525	417	0.81	−19	2.63	2.38	0.90	−9.5
Vergin et al. 400 mg		800	755	0.95	−5.0	3.92	4.54	1.16	16
Al-Yamani et al. 400 mg	0.035	455	443	0.98	−2.2	2.54	2.99	1.18	18
Yuen et al. 400 mg		594	495	0.83	−17	3.10	3.14	1.01	1.3

[a] OCT1 V_{max} values are given in mg/s/Trans.

The Role of OCT1

In an attempt to mechanistically explain the pharmacokinetic inter-studies differences observed in the literature, the initial estimate for OCT1 V_{max} was increased to simulate the lowered profiles reported by Al-Yamani et al. in Saudi Arabians.[6] The increase of this parameter from 0.016 to 0.035 mg/s/mg of transporter (by 2.2-fold) was able to produce acceptable simulations of acyclovir profiles in this population (Fig. 3, red lines). Moreover, the application of the latter value for OCT1 V_{max} resulted in a reasonably good prediction for Malaysian population (external validation),[7] as well (Fig. 3, blue lines). In addition, the effect of modifying either OAT2 or ADH1 V_{max} on matching the data reported by Al-Yamani et al. was also studied. While OAT2 V_{max} needed a 6.4-fold increase to match the observed data, the variation of ADH1 was never able to accurately simulate the plasma profile (Table S-4). Hence, the sensitivity to the V_{max} of different proteins ranked: OCT1>OAT2>>>ADH1. The results suggest that OCT1 relative activities could, at least partially, explain the discrepancies evidenced between populations. Thus, the V_{max} value of 0.035 mg/s/mg of transporter obtained with this approach may be interpreted as the normal activity situation, while the 0.016 mg/s/mg as a scenario with reduced-OCT1 activity due to polymorphism (See discussion). A similar two-fold difference in V_{max} between the reduced activity polymorph (R61C) and the reference OCT1 transporter has been observed with the model substrate MPP^+.[19] Table 2 summarizes the validation of the oral disposition model, including mean observed and simulated pharmacokinetic parameters for each study and their respective statistics. All simulations met the standard bioequivalence criteria against observed data (0.8–1.25).[1]

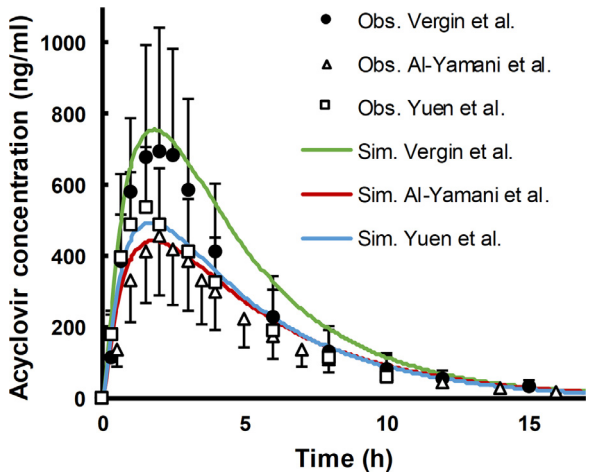

Figure 3. Effect of the OCT1 V_{max} on simulating acyclovir plasma concentrations reported by Vergin et al.[5] (dots), Al-Yamani et al.[6] (triangules) and Yuen et al.[6](squares) after the oral administration of the reference product (Zovirax® 400 mg). Error bars represent the standard deviation. Simulations were run with OCT1 V_{max} = 0.016 (green) or 0.035 mg/s/mg of transporter (red and blue).

Dissolution of Multisource Acyclovir Oral Products

The *in vitro* dissolution of two *in vivo* bioequivalent multisource acyclovir 200 mg IR tablets plus the reference (Zovirax® 200 mg) was studied in compendial media mimicking gastrointestinal pHs (Fig. 4). Dissolutions were overall faster in SGF (Fig. 4A) than SIF (Fig. 4B), consistent with acyclovir weak ionization (Table 1). The reference exhibited very fast dissolution regardless of the media, while the generics showed slower profiles. Even though generic product B was somehow faster than generic A in reaching complete dissolution, the dissolution from product A seems to be faster at earlier timepoints. In SGF, acyclovir dissolution for drug products A and B was rapid (*i.e.* >85% at 30 and 20 min, respectively). On the other hand, > 85% of dissolution was observed at 30 min for product B in SIF, while acyclovir dissolution from generic A did not exceed the 85% before 45 min. All f2 values were below 50 (data not shown). Further, no critical excipients with potential effect on the permeability was identified (Table 3). Overall, the multisource generics did not fulfill the dissolution requirement to apply for a BCS-biowaiver according to both Chilean and ICH current guidance.[24,26]

Simulating the Clinical Performance of Multisource Acyclovir Oral Products in Virtual Populations

In vitro dissolution profiles were input directly into the validated model to conduct virtual bioequivalence trials on two populations with either reduced- or normal-OCT1 activity. The oral profiles reported by Vergin et al.[5] for the reference product 200 mg were used to validate the virtual populations. Fig. 5 shows that the created population resembles the clinical data, even if the slowest dissolution profile for the reference (in SIF media) is used as input. In fact, pharmacokinetic parameters from observed and simulated populations were not statistically different after applying the bioequivalence metrics (Table 4). On the other hand, Chilean generics were bioequivalent to the reference in a cross-over design, since C_{max} and AUCs were within the accepted ranges, regardless of the population (Fig. 6A, B and C vs Fig. 6D, E and F). Even though the slower dissolutions in SIF tended to cause geometric mean ratios slightly below 1 (Fig. 6, squares), the 90% confidence intervals were still within the acceptance ranges (dashed red lines). Interestingly, the reference product was not bioequivalent to itself when comparing two populations with different OCT1 activities in a parallel design (Fig. 7). The differences between populations ranged, indeed, from 40 to 60% (Table 5), consistent with the cited studies.[5,6]

Discussion

The variable oral bioavailability for a low permeable drug is commonly associated with the contribution of active processes to the total mass transport, such as transporters and/or enzymes. Consequently, alterations in the expression of these proteins, their affinities and/or activity (*e.g.*, polymorphism and/or patients) may play a significant role in subject-to-subject variability. In addition, the

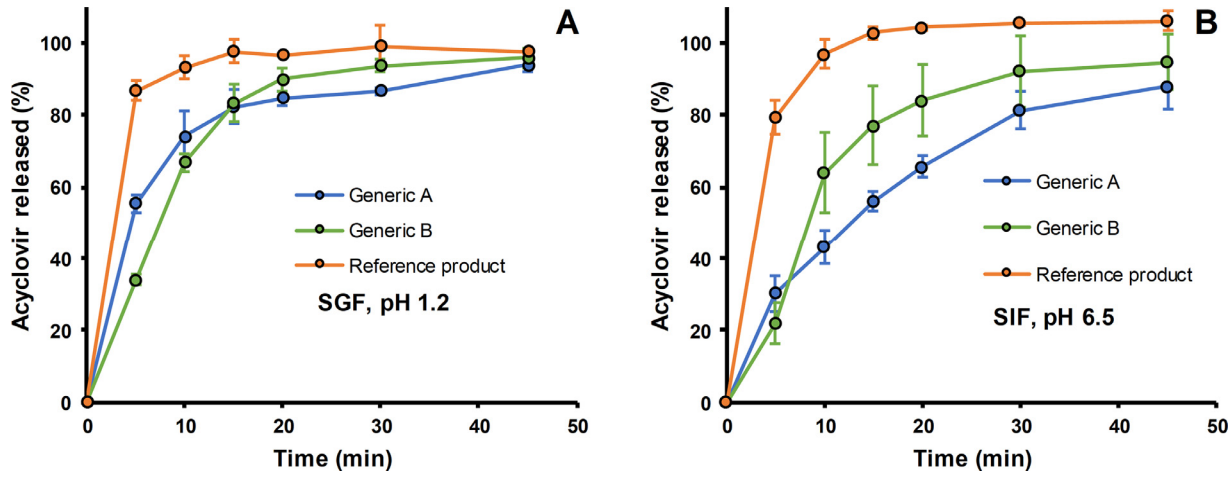

Figure 4. Acyclovir dissolution from generic A (blue), generic B (green) and the reference product (orange) in 900 ml of SGF (A) or SIF (B) utilizing the USP type II apparatus at 50 rpm and 37 °C (n = 3). Error bars show standard deviations.

Table 3
List of excipients declared for each acyclovir product used in this study.

Excipient	Reference	Generic A	Generic B
Microcrystalline cellulose	Yes	Yes	Yes
Magnesium Aluminum silicate	Yes	–	–
Sodium starch glycolate	Yes	Yes	Yes
Povidone	Yes	Yes	Yes
Magnesium stearate	Yes	Yes	Yes
Hypromellose	Yes[a]	–	–
Titanium dioxide	Yes[a]	–	–
Macrogol	Yes[a]	–	–

[a] Excipient included in the film coating.

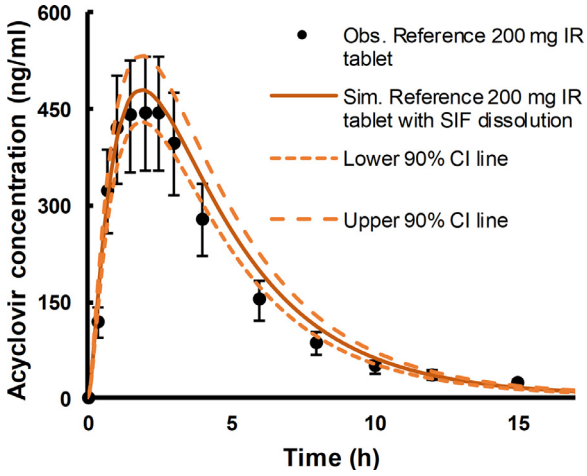

Figure 5. Comparison between mean observed acyclovir plasma profiles after the oral administration of the reference product IR tablets 200 mg (black dots) and simulated profiles using *in vitro* dissolution of the reference in SIF media on the virtual population (orange line). The bioequivalence limits (0.8–1.25) are shown for the observed data (error bars), while the lower and upper 90% confidence intervals (90% CI) for the simulated population are shown in dashed lines.

manufacture of solid oral dosage forms and drug product composition may affect its dissolution, which could be another source of variability. The PBBM framework was recently introduced to understand these complex interactions through evidence-based simulations. In this work, the PBBM approach was applied to acyclovir IR tablets to evaluate the impact of the OCT1 transporter (as a physiological variable) on the disposition of different multisource acyclovir products and its biopharmaceutic implications.

Mechanistically Understanding Acyclovir Disposition

The first goal of this work was the development and validation of a PBPK model for acyclovir. The IV studies chosen to develop the model included subjects with well characterized body compositions, who were administered with different doses.[11] The estimation of multiple parameters was needed, hence the Fm, Fel,u and kidney concentration profiles were added as additional constraints. Even though the assumptions made to set the constraints were based on data from different studies,[12,17,36] the subjects in those publications shared comparable characteristics with the population studied in the Laskin et al. publication (American patients with malignancy and comparable body measurements). The development of this model using data from healthy subjects would have been extremely difficult, as much of the information needed to set the constraints is much scarcer in volunteers than in patients. This is not the first PBPK model for acyclovir,[40,41] although it is the first in including important features to understand its disposition/elimination, such as a permeability-limited distribution model and the role of the OCT1 in the

Table 4
Comparison between observed (Vergin et al.) and simulated (using dissolution profiles in either SGF or SIF media) pharmacokinetic parameters for the reference product in population with reduced-OCT1 activity.

	SGF		SIF	
Pharmacokinetic parameter	Geometric mean ratio (sim/obs)	90% Confidence intervals	Geometric mean ratio (sim/obs)	90% Confidence intervals
C_{max}	0.92	0.85–1.01	0.93	0.85–1.02
AUC_{0-t}	1.03	0.94–1.12	1.04	0.95–1.13
AUC_{0-inf}	1.00	0.92–1.09	1.01	0.93–1.10

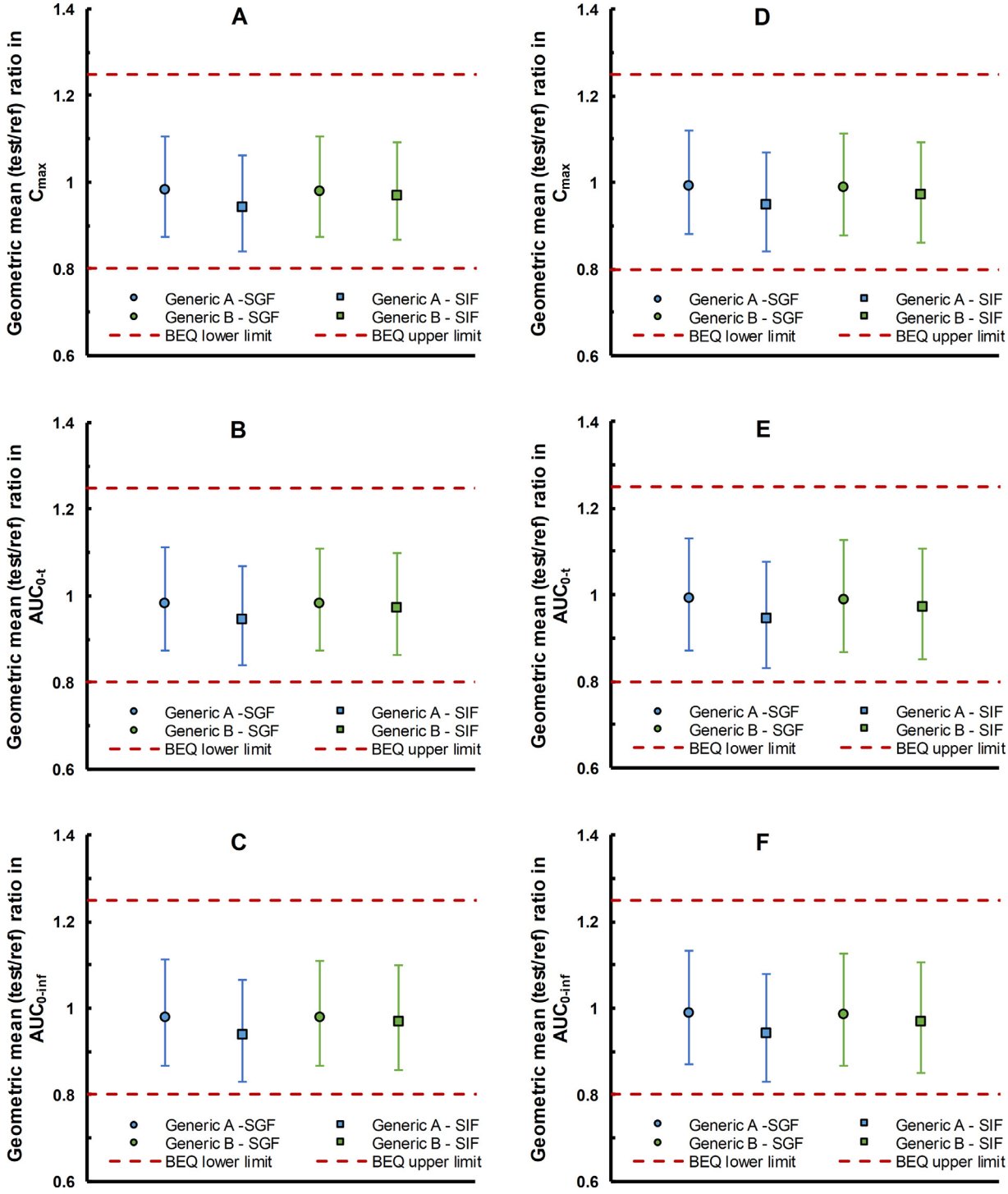

Figure 6. Results from virtual bioequivalence studies on 36 subjects with either reduced- (A, B and C) or normal-OCT1 activity (D, E and F). Each panel shows the geometric mean (test/reference) ratio for C_{max} (A and D), $AUC_{0\text{-}t}$ (B and E) and $AUC_{0\text{-}inf}$ (C and F) of the generic product A (blue) or B (green). Simulations were run with either SGF (circles) or SIF media (squares). Error bars show the 90% CI and dashed red lines the bioequivalence limits from 0.8 to 1.25.

liver. Nonetheless, the disposition model was not only validated for different IV doses (Fig. 1), but it also predicted the IV profile reported by Vergin et al.[5] in healthy subjects (Fig. S-3). It is noteworthy that the prediction of plasma profiles of volunteers utilizing models created with patient's data may not necessarily work in every situation (further discussed below). In the previously published model, acyclovir metabolism was attributed to the ALDH, which handles the second oxidation step, instead of the first oxidative step by ADH1.[40] In the present model, it was decided to include only ADH1 because acyclovir disappearance from the plasma was more important than the formation of metabolites for the aims of this study. Further, the role of ALDH on acyclovir clinical pharmacokinetics is still debatable, as no clear relation was found between three ALDH2 polymorphs and acyclovir pharmacokinetic parameters, C_{max} and $AUC_{0\text{-}inf}$.[42] One caveat of introducing ADH1-mediated metabolism was the lack of information on acyclovir's affinity. That is why the K_m was taken

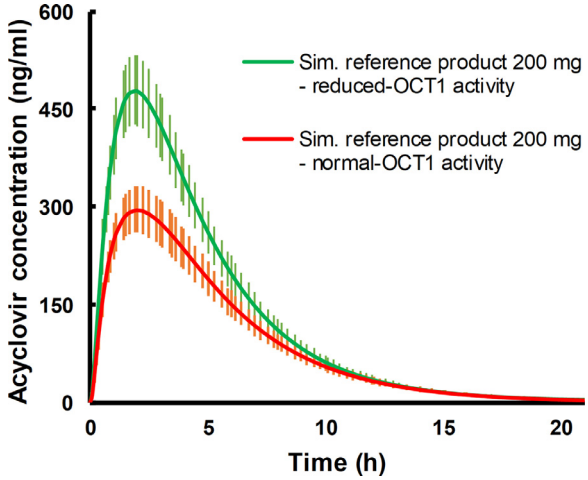

Figure 7. Simulated plasma profiles in a population with reduced-OCT1 activity (green) and normal-OCT1 activity (red) after administering the reference product 200 mg, using SGF dissolution data. Error bars represent the 90% confidence intervals (90% CI).

from *in vitro* affinity studies of other substrates with alcohol functions in human liver homogenates.[35] MHET molecular structure was the most similar to acyclovir among the studied compounds, hence MHET K_m was assumed. In the same study, the K_m for both benzyl alcohol and piperonyl alcohol were lower than for furfuryl alcohol and MHET,[35] suggesting that perhaps the presence of heteroatoms in aromatic nucleus could decrease the affinity. Considering the latter, it is possible that the K_m assumption overestimates acyclovir true affinity for ADH1. Another caveat was the assumption on ADH1 gut expression, as the relative amounts were taken from studies in rat tissues. Even though rat expression patterns were suggested comparable to humans,[43] the relevance of this caveat seems to be limited as the model predicts negligible pre-absorptive metabolism. Even more important, acyclovir plasma levels were practically insensitive to changes in ADH1 V_{max} in the model, due to the cytosolic location of ADH1 and the setting of a permeability-limited distribution model (Fig. S-4).

The estimates of P_{eff} using *in vitro* P_{app} from Caco-2 and Ussing chamber experiments resulted in relatively close predictions of acyclovir oral profiles (Fig. 2). Thus, further refinement was needed to obtain a P_{eff} that predicts across doses. One possible explanation for these mispredictions could be the use of non-in-house data in developing calibrations. Still, there was only little difference between the P_{eff} calculated from Ussing chamber and from Caco-2 (1.4-fold, Table 1), suggesting that mispredictions were a consequence of the high sensitivity to P_{eff} rather than the P_{app}-to-P_{eff} conversion method. By using the refined P_{eff}, the model was able to accurately predict the oral F (obs. and pred., 32.3 and 31.5%, respectively) and Fel,u after an oral dose (obs. and pred. 17.6 and 21.8%, respectively).[5] The accuracy in these predictions highlights the relevance of setting several constraints (based on clinical evidence) when fitting key physiological parameters, such as transporters V_{max}. As expected for a BCS III drug, the model predicted an incomplete fraction absorbed (Fa) of 37%, with a significant paracellular contribution (10% of the total administered mass) and passive transcellular (27%), pointing out the importance of taking into account both absorption mechanisms for molecules like acyclovir. In fact, the refined P_{eff} was closer to Ussing chamber than Caco-2 calculated P_{eff} (Table 1). This might be explained by the leakier paracellular transport in rat jejunum Ussing chamber set-up compared to Caco-2 cells,[44] resembling better the paracellular route in the upper gastrointestinal absorption site. Therefore, these results emphasize the value of considering diverse sources of *in vitro* evidence (*i.e.*, Caco-2 and rat intestine-Ussing chamber experiments)[29] when dealing with uncertain parameters in PBBM/PBPK modeling, such as permeability.

OCT1 Polymorphism as a Source of Variability on Acyclovir Oral Bioavailability

In single-dose bioequivalence studies, both Vergin et al. and Al-Yamani et al. administered the reference product (Zovirax® 400 mg IR tablet) to fasted healthy subjects. Interestingly, acyclovir C_{max} and AUC were respectively 44 and 35% lower in Saudi Arabians (Al-Yamani et al.) than in Europeans (Vergin et al.) (Table 2 and Fig. 3).[5,6] In order to account for this discrepancy, the model was used to test the hypothesis of OCT1 polymorphism being one of the causes for inter-studies discrepancies. The frequencies of the reduced-activity variants R61C, G401S and G465R are the highest in Europeans compared to other ethnicities,[19] while they have not been found in Saudi Arabians.[20,22] The clinical importance of these polymorphs has been previously reported for another BCS III API with similar characteristics to acyclovir, *i.e.* metformin. Among others, these drugs share an incomplete gastrointestinal absorption (Fa= 40–60% for metformin), the usage of the paracellular pathway and the affinity for the OCT1 transporter. Shu et al. found that metformin C_{max} and AUC were 20–50% higher in Caucasian subjects expressing the OCT1 polymorphs R61C, G401S and G465R than in volunteers expressing the wild-type transporter.[23] In the present work, it was found that an increase of 55% in the OCT1 V_{max} used to simulate Vergin et al. profiles was able to simulate the lower plasma concentrations observed in Saudi Arabians (the contributions of other possible mechanisms are discussed below). Likewise, the plasma curves reported in Malaysians were also predicted by the incremented OCT1 V_{max} (0.035 mg/s/mg of transporter) value, consistent with the very low frequency of reduced-OCT1 activity polymorphs in South Asians.[20,21] Interestingly, the OCT1 V_{max} used to predict plasma concentrations in Europeans, 0.016 mg/s/mg of transporter, was obtained from the model developed with American patients with malignancy (Fig. 1). The reduction on OCT1 activity may also be associated with pathological conditions. In fact, hepatocellular cancer decreased the expression and, consequently, the activity of the OCT1 carrier in the liver.[45] This may provide an explanation on why the V_{max} for reduced-OCT1 activity resulted in good simulations for these two cases. In contrast, the normal-OCT1 activity caused lower plasma concentrations of acyclovir (Fig. 2), due to its greater liver uptake after oral absorption. Noteworthy, the rise of the OCT1 V_{max} resulted in an increase of the biliary

Table 5
Comparison of simulated pharmacokinetic parameters for the reference product between a population with reduced-activity (RA) for OCT1 and another with normal-OCT1 activity (NA), using dissolution profiles in either SGF or SIF media.

	SGF		SIF	
Pharmacokinetic parameter	Geometric mean ratio (RA/NA)	90% confidence intervals	Geometric mean ratio (RA/NA)	90% confidence intervals
C_{max}	1.62	1.44–1.83	1.61	1.43–1.81
AUC_{0-t}	1.43	1.27–1.63	1.42	1.25–1.61
AUC_{0-inf}	1.42	1.25–1.61	1.41	1.24–1.60

excretion rather than metabolism, due to the higher contribution of MATE1-mediated transport compared to ADH1-mediated metabolism (Table 1). The involvement of hepatic extraction as a source of variability is further supported by classic pharmacokinetic analysis. For instance, acyclovir total clearance (Cl_{tot}) of 16.7 L/h can be calculated from the de Miranda et al. publication, where the mean observed Fel,u was 60%.[12] Assuming the mean Fel,u and a hepatic plasma flow around 25 L/h (acyclovir blood:plasma ratio ~1), the calculated hepatic extraction is 27%. Nevertheless, if the highest (85%) and lowest (30%) Fel,u reported in literature are considered,[12,17] the calculated hepatic extraction ranges from 10 to 47%, respectively. This calculation supports that OCT1-mediated hepatic extraction may be a major contributor to acyclovir variability, accounting for up to 37% of population differences. Even though this latter number might be even higher when dealing with different ethnicities, other concomitant mechanisms cannot be ruled out to explain the inter-studies discrepancy. Acyclovir tubular active secretion was suggested to occur mainly through the hOAT2 transporter, due to the highest affinity and capacity of this isoform.[13] However, acyclovir is also a substrate of the kidney basolateral isoforms hOAT1 and hOAT3.[13,14] The OATs transporters are thought to be critical in eliminating metabolic products, hence the low frequency of polymorphs reported for OAT2 and the overlapped substrate specificity among OATs isoforms.[46] Therefore, the active tubular secretion is unlikely to explain inter-population differences. Instead, the high sensitivity to permeability (Fig. 2) and transit time (Fig. S-5) suggests these factors are more likely explanations for the unaccounted inter-subject variability. Yet, further research is needed to understand the population-related variables that affect P_{eff} and how to account for them in mechanistic modeling.

Limited Relevance of Very Rapid Dissolution on Clinical Performance of Multisource Acyclovir Oral Products

In order to assess the role of formulation variants, the dissolution of two acyclovir generics with Chilean bioequivalence certification to the reference product was studied in two pharmacopeial media resembling extreme cases for acyclovir. On the one hand, SGF pH 1.2 media does not only simulate the gastric environment, but also promotes acyclovir dissolution, as its solubility rises to over 3.5 mg/ml below pH 2.0[47]. On the other hand, SIF was chosen to resemble upper small intestinal conditions were acyclovir absorption takes place. A pH 6.5 was preferred over 6.8 because this minor reduction leads to solubility values closer to the minimum solubility of 2.33 mg/ml,[2,47] while still mimicking the intestinal luminal pH. As anticipated, dissolution profiles were slightly faster in gastric conditions (SGF), regardless of the drug product. It is possible that acyclovir dissolution from the reference was aided by the disintegrant agent, magnesium aluminum silicate, which was absent in both generics. Interestingly, the initial dissolution of generic A was consistently faster than generic B at both pHs, although the latter product reached complete dissolution at earlier times. This behavior suggests differences in the dissolution mechanisms between the generic products. The slower initial dissolution from generic B may be associated with a slower dosage form disintegration, while the shorter time to reach complete drug release may relate to a faster dissolution of solid particles in this formulation. Differences in tablet porosity and particle size distribution of raw materials between the generics may underlie this observation.

Gastrointestinal dissolution of tablets is expected to be slower than in typical *in vitro* dissolution set-ups, since both the volume of luminal fluids and concentrations of buffering species are lower under *in vivo* conditions.[48] Therefore, a method to convert *in vitro* into hypothetical *in vivo* dissolution is often required to incorporate dissolution data in PBPK models. The development of an IVIVC for highly soluble drugs is theoretically possible, if the dissolution rate is slower than its permeation.[49] However, the scarcity of examples suggest that dissolution rate must be very slow to become the rate limiting step (*e.g.* extended release dosage forms). In fact, Davanço et al. recently reviewed systematically up to 50 IVIVC studies, finding no examples of successful correlation for BCS III IR dosage forms.[50] Alternatively, the Z-factor has been successfully utilized to incorporate the pH-dependent dissolution of the BCS II, ibuprofen.[39] However, this method accelerated acyclovir dissolution profiles to a point where complete dissolution was achieved before 10 min (not shown), such that all simulations overlapped. Therefore, *in vitro* dissolutions were used as direct input in simulations, as it has been previously suggested for BCS III APIs.[39] Both acyclovir weak ionization (pKa=2.27) and the strength studied (Do=0.34) further supported this decision.[2] Remarkably, the PBBM robustly predicted the bioequivalence decision made by the Chilean authority (Fig. 6), even though the generic products did not meet the BCS-biowaiver criteria for dissolution. The irrelevance of rapid dissolution was recently reported using a similar *in silico* PBBM approach for the BCS I, bisoprolol.[51] It is noteworthy that generic A resulted bioequivalent to the reference even when using the dissolution in SIF media as input (Fig. 6), where >85% of the dose was dissolved only after 45 min (Fig. 4). This finding was in good agreement with previous *in vitro* and *in vivo* evidence reported for ranitidine IR tablets, another BCS III API. In that work, the ranitidine formulation with the slowest dissolution displayed an *in vitro* profile comparable to acyclovir generic A (>85% after 45 min), much slower than the fastest ranitidine formulation (>85% in 15 min). Similar to the present study, both ranitidine formulations showed overlapping plasma curves and similar pharmacokinetic parameters after a single dose bioequivalence study in volunteers.[49,52] Hence, the dissolution safe space for BCS III IR oral solid dosage forms seems to be wider than biowaiver specifications, as long as dissolution is completely achieved within the absorption window. The model here presented was further used in an attempt to suggest the range of dissolution for acyclovir IR oral products, in which bioequivalence is expected (See supp. Materials for details). The reference dissolution profile in SIF was able to be stretched without significantly altering neither C_{max} nor AUC. From experimental data, it was clear that dissolution of 85% of the labeled amount in 45 min did not impact the bioequivalence decision. This was in good agreement with conclusions from the approach combining time-scaled theoretical profiles together with the validated PBPK (85% of the labeled amount in 46 min, Supp. Material). Thus, a low risk of bio-inequivalence is suggested for acyclovir IR oral products provided more than 85% of the dose is dissolved in 45 min. The findings presented in this study are consistent with the conservative spirit of regulatory guidances. Furthermore, they showcase the potential of the PBBM approach in early development, as formulations may be erroneously discarded after not meeting the *in vitro* dissolution expectations.

Being acyclovir a poorly permeable drug, this study did not consider P_{eff} alterations because the mechanisms underlying subject-to-subject variability are not fully understood yet. It is true that excipients can alter the intestinal permeability and/or transit time, which may be crucial for drugs like acyclovir.[53] However, both the qualitatively similar composition and the lack of potential critical excipients in the three formulations studied do not justify any alterations of P_{eff} in the present model (Table 3). Nonetheless, this factor may be more decisive than very rapid dissolution in bio-inequivalence of BCS III and further research in combining acyclovir *in vitro* permeability from these formulations and PBPK modeling to assess the effect of excipients is encouraged. Instead, we explored physiological variability by altering the OCT1 activity to account for potential inter-population differences in polymorphism. Results showed that the bioequivalence decision robustly stands regardless of the population, as acyclovir generics were bioequivalent to the reference product in both reduced- (Fig. 6A, B and C) and normal-OCT1 activity populations (Fig. 6D, E and

F). By contrast, the pharmacokinetics between populations were significantly different, although they were administered with the same drug product (Fig. 7). Therefore, careful attention should be paid when making conclusions in terms of the clinical impact of formulation effects for drug products containing BCS class III drug substances meeting the criterion for rapidly dissolving. As such, whenever *in vivo* bioequivalence studies are required for this kind of drug products, randomized cross-over studies must be considered to avoid wrong interpretations which may be confounded by carrier-mediated variability. Furthermore, the findings presented here do not only endorse the cross-over study design, but also throw some warnings about potential over-discriminations associated with the parallel study design, especially for drug products containing BCS III APIs (as needed when *e.g.*, dissolution criterion is not met). Current debates on PBBM development favor the simplicity of modeling due to their higher interpretability. Nonetheless, our model allowed to unveil inter-population differences by accounting for acyclovir transporters, while still being able to predict bioequivalence of the products. The population-related differences would have been invisible otherwise.

Conclusion

The development and validation of a PBBM for acyclovir was carried out in this work, which allowed the modeling of population variability by considering different OCT1 activities. The multisource acyclovir products studied did not meet the very-rapid dissolution criterion as per BCS class III framework. However, the PBBM robustly predicted their bioequivalence, regardless of the virtual population used. The results showed the limited relevance of very rapid dissolution for IR dosage forms containing BCS III APIs like acyclovir and emphasized the importance of a cross-over design. Overall, this manuscript demonstrated the power of the PBBM approach in predicting the clinical performance of multisource acyclovir products and showcased the potential of simulations in saving time and gaining confidence moving towards *in vivo* studies, provided the model is correctly constructed.

Declaration of Competing Interest

The authors declare the following financial interests/personal relationships which may be considered as potential competing interests: Michael B. Bolger and Sandra Suarez-Sharp are currently employed at Simulations Plus, Inc., developer of Gastroplus® software.

Acknowledgements

The authors would like to thank Dr. Jozef Al-Gousous for the insightful discussions. MAG received financial support from the Agencia Nacional de Investigación y Desarrollo (ANID), Becas de doctorado en el extranjero, nº 72180466. MBB and SSS currently work at Simulations Plus, Inc., developer of Gastroplus®.

Supplementary materials

Supplementary material associated with this article can be found in the online version at doi:10.1016/j.xphs.2021.10.013.

References

1. Parrott N, Suarez-Sharp S, Kesisoglou F, et al. Best practices in the development and validation of physiologically based biopharmaceutics modeling. a workshop summary report. *J Pharm Sci*. 2021;110(2):584–593. https://doi.org/10.1016/j.xphs.2020.09.058.
2. Arnal J, González-álvarez I, Bermejo M, et al. Biowaiver monographs for immediate release solid oral dosage forms: aciclovir. *J Pharm Sci*. 2012;101(7):2271–2280.
3. De Miranda P, Blum MR. Pharmacokinetics of acyclovir after intravenous and oral administration. *J Antimicrob Chemother*. 1983;12(SUPPL. B):29–37. https://doi.org/10.1093/jac/12.suppl_b.29.
4. Kubbinga M, Nguyen MA, Staubach P, Teerenstra S, Langguth P. The influence of chitosan on the oral bioavailability of acyclovir - a comparative bioavailability study in humans. *Pharm Res*. 2015;32(7):2241–2249. https://doi.org/10.1007/s11095-014-1613-y.
5. Vergin H, Kikuta C, Mascher H, Metz R. Pharmacokinetics and bioavailability of different formulations of aciclovir. *Arzneimittelforschung*. 1995;45(4):508–515.
6. Al-Yamani MJMS, Al-Khamis KI, El-Sayed YM, Bawazir SA, Al-Rashood KA, Gouda MW. Comparative bioavailability of two tablet formulations of acyclovir in healthy volunteers. *Int J Clin Pharmacol Ther*. 1998;36(4):222–226.
7. Yuen KH, Peh KK, Billa N, Chan KL, Toh WT. Bioavailability and pharmacokinetics of acyclovir tablet preparation. *Drug Dev Ind Pharm*. 1998;24(2):193–196. https://doi.org/10.3109/03639049809085607.
8. Meadows KC, Dressman JB. Mechanism of acylovir uptake in rat jejunum. *Pharm Res*. 1990;7(3):299–303.
9. Ates M, Kaynak MS, Sahin S. Effect of permeability enhancers on paracellular permeability of acyclovir. *J Pharm Pharmacol*. 2016;68(6):781–790. https://doi.org/10.1111/jphp.12551.
10. Avdeef A. Leakiness and size exclusion of paracellular channels in cultured epithelial cell monolayers-interlaboratory comparison. *Pharm Res*. 2010;27(3):480–489. https://doi.org/10.1007/s11095-009-0036-7.
11. Laskin OL, Longstreth JA, Saral R, de Miranda P, Keeney R, Lietman PS. Pharmacokinetics and tolerance of acyclovir, a new anti-herpesvirus agent, in humans. *Antimicrob Agents Chemother*. 1982;21(3):393–398. https://doi.org/10.1128/AAC.21.3.393.
12. de Miranda P, Whitley RJ, Blum MR, et al. Acyclovir kinetics after intravenous infusion. *Clin Pharmacol Ther*. 1979;26(6):718–728. https://doi.org/10.1002/cpt1979266718.
13. Cheng Y, Vapurcuyan A, Shahidullah M, Aleksunes LM, Pelis RM. Expression of organic anion transporter 2 in the human kidney and its potential role in the tubular secretion of guanine-containing antiviral drugs. *Drug Metab Dispos*. 2012;40(3):617–624. https://doi.org/10.1124/dmd.111.042036.
14. Takeda M, Khamdang S, Narikawa S, et al. Human organic anion transporters and human organic cation transporters mediate renal transport of prostaglandins. *J Pharmacol Exp Ther*. 2002;300(3):918–924. https://doi.org/10.1124/jpet.301.1.293.
15. Tanihara Y, Masuda S, Sato T, Katsura T, Ogawa O, Inui K. Substrate specificity of MATE1 and MATE2-K, human multidrug and toxin extrusions/H+-organic cation antiporters. *Biochem Pharmacol*. 2007;74(2):359–371. https://doi.org/10.1016/j.bcp.2007.04.010.
16. de Miranda P, Good SS, Krasny HC, Connor JD, Laskin OL, Lietman PS. Metabolic fate of radioactive acyclovir in humans. *Am J Med*. 1982;73(1 PART 1):215–220. https://doi.org/10.1016/0002-9343(82)90094-8.
17. de Miranda P, Good SS, Laskin OL, Krasny HC, Connor JD, Lietman PS. Disposition of intravenous radioactive acyclovir. *Clin Pharmacol Ther*. 1981;30(5):662–672. https://doi.org/10.1038/clpt.1981.218.
18. Gunness P, Aleksa K, Bend J, Koren G. Acyclovir-induced nephrotoxicity: the role of the acyclovir aldehyde metabolite. *Transl Res*. 2011;158(5):290–301. https://doi.org/10.1016/j.trsl.2011.07.002.
19. Shu Y, Leabman MK, Feng B, et al. Evolutionary conservation predicts function of variants of the human organic cation transporter, OCT1. *Proc Natl Acad Sci U S A*. 2003;100(10):5902–5907. https://doi.org/10.1073/pnas.0730858100.
20. Phan L, Jin Y, Zhang H, et al. *ALFA: Allele Frequency Aggregator*. Bethesda, MD: National Center for Biotechnology Information, U.S. National Library of Medicine; 2020. Available at: www.ncbi.nlm.nih.gov/snp/docs/gsr/alfa/. Accessed 7 June 2021.
21. Makhtar SM, Husin A, Baba AA, Ankathil R. Genetic variations in influx transporter gene SLC22A1 are associated with clinical responses to imatinib mesylate among Malaysian chronic myeloid leukaemia patients. *J Genet*. 2018;97(4):835–842. https://doi.org/10.1007/s12041-018-0978-9.
22. Hakooz N, Jarrar YB, Zihlif M, Imraish A, Hamed S, Arafat T. Effects of the genetic variants of organic cation transporters 1 and 3 on the pharmacokinetics of metformin in Jordanians. *Drug Metab Pers Ther*. 2017;32(3):157–162. https://doi.org/10.1515/dmpt-2017-0019.
23. Shu Y, Brown C, Castro R, et al. Effect of genetic variation in the organic cation transporter 1, OCT1, on metformin pharmacokinetics. *Clin Pharmacol Ther*. 2008;83(2):273–280. doi:1 0.1038/sj.clpt.6100275.
24. Instituto De Salud Pública De SeguridadS.De. Chile Bioexención de los estudios de. 2007. Available at: https://www.ispch.cl/sites/default/files/guia_tec_g_biof02.pdf. Accessed November 8, 2021.
25. SeguridadS.De.RES. EX. 6836/13: NO HA Lugar Al Protocolo De Estudio In Vitro Para Demostrar Equivalencia Terapeutica Del Producto Farmac eutico Aciclovir Comprimi- dos 200 Mg,.000538, 1–2. (Visited on August 2021). 2014. Available at: https://www.ispch.cl/sites/default/files/resolucion/2014/02/image2014-02-17-152819.pdf. Accessed November 8, 2021.
26. Council I, Harmonisation FOR, Technical OF, et al. International Council For Harmonisation Of Technical Requirements For Pharmaceuticals For Human Use Biopharmaceutics Classification System-Based. 2019. Available at: https://www.ema.europa.eu/en/documents/scientific-guideline/ich-m9-biopharmaceutics-classification-system-based-biowaivers-step-5_en.pdf. Accessed November 8, 2021.
27. Estudios de SeguridadS.De. Biodisponibilidad Comparativa con Producto de Referencia (R) para establecer Equivalencia Terapéutica Año 2007. 2007:1–51. Available at: https://www.ema.europa.eu/en/documents/scientific-guideline/ich-

m9-biopharmaceutics-classification-system-based-biowaivers-step-5_en.pdf. Accessed November 8, 2021.
28. Poulin P, Theil FP. Prediction of pharmacokinetics prior to *in vivo* studies. 1. Mechanism-based prediction of volume of distribution. *J Pharm Sci*. 2002;91(1):129–156. https://doi.org/10.1002/jps.10005.
29. Kubbinga M, Augustijns P, García MA, et al. The effect of chitosan on the bioaccessibility and intestinal permeability of acyclovir. *Eur J Pharm Biopharm*. 2019;136:147–155. https://doi.org/10.1016/j.ejpb.2019.01.021.
30. Lukacova V, Goelzer P, Reddy M, Greig G, Reigner B, Parrott N. A physiologically based pharmacokinetic model for ganciclovir and its prodrug valganciclovir in adults and children. *AAPS J*. 2016;18(6):1453–1463. https://doi.org/10.1208/s12248-016-9956-4.
31. Shen H, Lai Y, Rodrigues AD. Organic anion transporter 2: an enigmatic human solute carrier. *Drug Metab Dispos*. 2017;45(2):228–236. https://doi.org/10.1124/dmd.116.072264.
32. Koepsell H. The SLC22 family with transporters of organic cations, anions and zwitterions. *Mol Aspects Med*. 2013;34(2–3):413–435. https://doi.org/10.1016/j.mam.2012.10.010.
33. De Miranda P, Good SS. Species differences in the metabolism and disposition of antiviral nucleoside analogues: 1. Acyclovir. *Antivir Chem Chemother*. 1992;3(1):1–8. https://doi.org/10.1177/095632029200300101.
34. Chiang CP, Lai CL, Lee SP, et al. Ethanol-metabolizing activities and isozyme protein contents of alcohol and aldehyde dehydrogenases in human liver: phenotypic traits of the ADH1B*2 and ALDH2*2 variant gene alleles. *Pharmacogenet Genomics*. 2016;26(4):184–195. https://doi.org/10.1097/FPC.0000000000000205.
35. Kassam JP, Tang BK, Kadar D, Kalow W. *In vitro* studies of human liver alcohol dehydrogenase variants using a variety of substrates. *Drug Metab Dispos*. 1989;17(5):567–572.
36. Wade JC, Hintz M, McGuffin RW, Springmeyer SC, Connor JD, Meyers JD. Treatment of cytomegalovirus pneumonia with high-dose acyclovir. *Am J Med*. 1982;73(1 PART 1):249–256. https://doi.org/10.1016/0002-9343(82)90100-0.
37. Ungell AL, Nylander S, Bergstrand S, Sjöberg Å, Lennernäs H. Membrane transport of drugs in different regions of the intestinal tract of the rat. *J Pharm Sci*. 1998;87(3):360–366. https://doi.org/10.1021/js970218s.
38. He Z. Theoretical effects of molecular dimension and configuration on effective diffusion coefficient of macromolecules in microporous membranes. *Trans Tianjin Univ*. 1995;1(1):42–47.
39. Jamei M, Abrahamsson B, Brown J, et al. Current status and future opportunities for incorporation of dissolution data in PBPK modeling for pharmaceutical development and regulatory applications: Orbito consortium commentary. *Eur J Pharm Biopharm*. 2020;155(August):55–68. https://doi.org/10.1016/j.ejpb.2020.08.005.
40. Liu XI, Momper JD, Rakhmanina N, et al. Physiologically Based Pharmacokinetic Models to Predict Maternal Pharmacokinetics and Fetal Exposure to Emtricitabine and Acyclovir. *J Clin Pharmacol*. 2020;60(2):240–255. https://doi.org/10.1002/jcph.1515.
41. Lukacova V, Bolger MB, Woltosz WS. Prediction of acyclovir pharmacokinetics in pediatrics populations using a physiologically based pharmacokinetic (PBPK) model. *AAPS Annual Meeting*. 2014:W5306.
42. Hara K, Suyama K, Itoh H, Nagashima S. Influence of ALDH2 genetic polymorphisms on aciclovir pharmacokinetics following oral administration of valaciclovir in Japanese end-stage renal disease patients. *Drug Metab Pharmacokinet*. 2008;23(5):306–312. https://doi.org/10.2133/dmpk.23.306.
43. Vaglenova J, Martínez SE, Porté S, Duester G, Farrés J, Parés X. Expression, localization and potential physiological significance of alcohol dehydrogenase in the gastrointestinal tract. *Eur J Biochem*. 2003;270(12):2652–2662. https://doi.org/10.1046/j.1432-1033.2003.03642.x.
44. Lozoya-Agullo I, Gonzalez-Alvarez I, Zur M, et al. Closed-loop doluisio (Colon, Small Intestine) and single-pass intestinal perfusion (Colon, Jejunum) in rat—biophysical model and predictions based on Caco-2. *Pharm Res*. 2018;35(1). https://doi.org/10.1007/s11095-017-2331-z.
45. Schaeffeler E, Hellerbrand C, Nies AT, et al. DNA methylation is associated with downregulation of the organic cation transporter OCT1 (SLC22A1) in human hepatocellular carcinoma. *Genome Med*. 2011;3(12):82. https://doi.org/10.1186/gm298.
46. Cropp CD, Yee SW, Giacomini KM. Genetic variation in drug transporters in ethnic populations. *Clin Pharmacol Ther*. 2008;84(3):412–416. https://doi.org/10.1038/clpt.2008.98.
47. Shojaei AH, Berner B, Li X. Transbuccal delivery of acyclovir: I. *In vitro* determination of routes of buccal transport. *Pharm Res*. 1998;15(8):1182–1188. https://doi.org/10.1023/A:1011927521627.
48. Mudie DM, Murray K, Hoad CL, et al. Quantification of gastrointestinal liquid volumes and distribution following a 240mL dose of water in the fasted state. *Mol Pharm*. 2014;11(9):3039–3047. https://doi.org/10.1021/mp500210c.
49. Langguth P, Fricker G, Wunderli-Allenspach H. *Biopharmazie*. Weinheim, Germany: Wiley-VCH Verlag GmbH & Co. KGaA; 2004.
50. Davanço MG, Campos DR, Carvalho PO. *In vitro – in vivo* correlation in the development of oral drug formulation: a screenshot of the last two decades. *Int J Pharm*. 2020;580:(March) 119210. https://doi.org/10.1016/j.ijpharm.2020.119210.
51. Macwan JS, Fraczkiewicz G, Bertolino M, Krüger P, Peters SA. Application of physiologically based biopharmaceutics modeling to understand the impact of dissolution differences on *in vivo* performance of immediate release products: the case of bisoprolol. *CPT Pharmacometrics Syst Pharmacol*. 2021;10(6):622–632. https://doi.org/10.1002/psp4.12634.
52. Polli JE. In vitro-in vivo relationships of several “immediate” release tablets containing a low permeability drug. In: Young D, Devane J, Butler J, eds. *In Vitro-in Vivo Correlations. Advances in Experimental Medicine and Biology*. Boston, MA: Springer; 1997. doi:https://doi.org/10.1007/978-1-4684-6036-0_17.
53. Vaithianathan S, Haidar SH, Zhang X, et al. Effect of common excipients on the oral drug absorption of biopharmaceutics classification system class 3 drugs cimetidine and acyclovir. *J Pharm Sci*. 2016;105(2):996–1005. https://doi.org/10.1002/jps.24643.
54. Brändén C-I. Structure of horse liver alcohol dehydrogenase: I. Structural symmetry and conformational changes. *Arch Biochem Biophys*. 1965;112(2):215–217.